Separation, Purification and Application of Bioactive Compounds from Pigmented Rice Bran

A Thesis Submitted for the Award of the Degree

of

DOCTOR OF PHILOSOPHY

by

Amit Baran Das

Department of Chemical Engineering

Indian Institute of Technology Guwahati

Guwahati-781 039, India

October 2020

Separation, Purification and Application of Bioactive Compounds from Pigmented Rice Bran

A Thesis Submitted for the Award of the Degree

of

DOCTOR OF PHILOSOPHY

by

Amit Baran Das

(Roll No. 136107040)

Department of Chemical Engineering

Indian Institute of Technology Guwahati

Guwahati-781 039, India

October 2020

Department of Chemical Engineering

Indian Institute of Technology Guwahati, Assam, India

STATEMENT

I hereby declare that the matter embodied in this thesis is the result of investigations carried out by me in the Department of Chemical Engineering, Indian Institute of Technology Guwahati and Department of Food Engineering and Technology, Tezpur University Assam, India under the supervision of **Prof. Chandan Das** and **Prof. Vaibhav Vasant Goud.**

In keeping with the general practice of reporting scientific observations, due acknowledgement has been made wherever the work described is based on the findings of other investigations.

Guwahati

October 2020 Signature

Department of Chemical Engineering

Indian Institute of Technology Guwahati, Assam, India

CERTIFICATE

It is certified that the work contained in this thesis entitled "**Separation, Purification and Application of Bioactive Compounds from Pigmented Rice Bran**" by Mr. Amit Baran Das (Roll No. 136107040) for the award of Ph.D. degree, is a record of bonafide research carried out by him at the Department of Chemical Engineering, Indian Institute of Technology Guwahati, under our guidance and supervision. The work embodied in this thesis has not been submitted to any other University or Institute for the award of any other degree or diploma.

Dr. Chandan Das
Professor
Department of Chemical Engineering
Indian Institute of Technology Guwahati

Date:

Dr. Vaibhav Vasant Goud
Professor
Department of Chemical Engineering
Indian Institute of Technology Guwahati

Date:

ACKNOWLEDGEMENTS

It is my great privilege to sincerely thank the persons who have supported me to complete my Doctoral Dissertation.

First and foremost, I take this opportunity to express my deep sense of respect and gratitude to my thesis supervisors, **Prof. Chandan Das** and **Prof. Vaibhav Vasant Goud**, for providing inspiration and valuable guidance throughout the course. I am also indebted to them for their constant suggestions and encouragement. It has really been a remarkable experience working with them.

I would like to acknowledge my sincere gratitude to my doctoral committee members, **Prof. Mihir Kumar Purkait** and **Prof. G. Pugazhenthi**, Department of Chemical Engineering and **Prof. Selvaraju Narayanasamy**, Department of Biosciences and Bioengineering. Their intuitive revision of my work, valuable advice, and constructive suggestions during my research progress kept the flow of my research work in the right direction.

I would like to acknowledge my sincere gratitude to **Dr. Animes Kr. Golder** for his valuable suggestions and continuous encouragement during my research work.

I also thank **Prof. Anugrah Singh**, Head of Department of Chemical Engineering for his administrative support. Furthermore, I would like to thank all the other Faculties and Staff members of the Department of Chemical Engineering for their invaluable support during my research.

I express my sincere gratitude to Honorable Vis-chancellor, Tezpur University for the kind permission and encouragement. I would like to thank my colleague **Prof. Charu Lata Mahanta**, **Prof. Sankar Chandra Deka**, **Dr. Manuj Kumar Hazarika**, **Dr.Brijesh Srivastava**, **Dr. Nandan Sit**, **Dr. Laxmikant S. Badwaik**, **Dr. Poonam Mishra**, **Dr. Dibyakanta Seth**, **Dr. Raj Kumar Duary**, **Dr. Kshirod Kumar Dash** and **Dr. Nishant Rachayya Swami Hulle,** for their continues support.

I am grateful to the Analytical Laboratory of the **Department of Chemical Engineering**. **Central Instruments Facility**, **IIT Guwahati, Department of Food Engineering and Technology** and **Sophisticated Analytical Instrumentation Centre at Tezpur University** for providing me the necessary support for sample analysis.

I would sincerely like to thank to my student **Ms. Laishram Basantarani,** and **Mrs Duyi Saymor** for whom I came to know about the pigmented rice.

I wish to thank our lab alumni **Dr. Mahesh Kumar Gagrai, Dr. Vijay Singh, Dr. Arijit Das, Dr. Sujoy Bose, and Dr. Kibrom Alebel Gebru, Dr. Raj Kumar Das, Dr. Venkatnarasimha Rao Chelli, Dr. Suman Saha, Mr. Sandup Tshering Bhutia, Mr. Rishiket Kundu,** and **Mr. Vishal Kumar Sandhwar** for lending their hands of support whenever needed. I thank all my lab members **Mr. Abhradip Pal, Mr. Abhishek Shukla, Ms. Sushma Chakraborty,** and **Ms. Aritra Das** for providing a co-operative research environment.

Finally, my wholehearted gratitude goes to my parents, **Mr. Bimal Kumar Das** and **Mrs. Chayya Das,** my elder brother **Dr. Asim Bikas Das**, Sister-in-law **Dr. Urmila Saxena** and my better-half **Mrs. Moumita Bera** whose blessings, love, wise advice and boundless patience to keep my morale high during the course of study.

Sincerely,

Amit Baran Das

TABLE OF CONTENT

Nomenclatures

A	Absorbance
A_o	Absorbance of control blank
A_s	Absorbance of sample extract
A_r	Redlich–Peterson isotherm constant (L/mg)
A_t	Koble–Corrigan isotherm constant (L mg/g)
A	Color value
a_w	Water activity
B	Koble–Corrigan isotherm constant (L/mg).
B	Color value
C	Concentration of monomeric anthocyanin (mg/L)
C_o	Initial concentration of anthocyanin in the extract (mg/L)
C_e	Equilibrium concentration of anthocyanin in the extract (mg/L).
C_d	Concentration of anthocyanin in the desorption solutions (mg/L)
C_5	Rice dough with 5 % microencapsulated anthocyanin
C_{10}	Rice dough with 10 % microencapsulated anthocyanin
C_{15}	Rice dough with 15 % microencapsulated anthocyanin
C_{20}	Rice dough with 20 % microencapsulated anthocyanin
D	Desorption ratio (%)
D_s	Peleg Constants
E	Adsorption ratio (%)
E_a	Activation energy (kJ/mol)
ΔG	Gibbs free energy change (kJ/mol)
ΔH	Enthalpy change (kJ/mol)
K	Degradation rate constant (1/min)
k_H	Consistency index for Herschel–bulkley model
k_M	Consistency index for Mizrahi-Berk model
k_{ref}	Frequency factor (per min)
k_1	Rate constant of the pseudo-first order model (1/min)
k_2	Rate constant of pseudo-second order models (g/mg min)
k_i	Intra-particle diffusion rate constant (g/mg $min^{0.5}$)
K_L	Equilibrium distribution coefficient
K_D	Hill constant (L/g)

K_R	Redlich–Peterson isotherm constant (L/g)
K_T	Toth isotherm constant (mg/g)
K_f	Freundlich constant (adsorption capacity)
L	Color value
L	Path length (cm)
M_w	Moisture content (kg/kg dry solid)
M_o	Monolayer moisture content (kg/kg dry solid)
M	Moisture content of the resin (% w/w)
$1/n$	Empirical constant (adsorption intensity)
q_e	Adsorption capacity at equilibrium (mg/g dry resin)
q_t	Concentration of anthocyanin absorbed at time t (mg/g)
q_e	Adsorption capacity of adsorbent (mg/g resin)
q_m	Maximum amount of adsorption(mg/g resin)
R	Ideal gas constant (8.314 J/mol K)
R_{ad}	Recovery percentage (%)
R^2	Coefficient of determination
ΔS	Entropy change (J/mol K)
T	Temperature (K)
$t_{1/2}$	Half-life (min)
T_o	Onset temperature (°C)
T_p	Peak temperature (°C)
W	Mass of the resin (g)
V_i	Volume of the crude extract (mL)
V_d	Volume of the desorption solution (mL);
V_i	Volume of the initial sample solution (mL);
X_1	Temperature for conventional extraction (°C)
X_2	Time for conventional extraction (min)
X_3	Solvent concentration for conventional extraction (%)
X_4	Solvent to solid ratio for conventional extraction (mL/g)
X_5	Temperature for ultrasound assisted extraction (°C)
X_6	pH for ultrasound assisted extraction
X_7	Solvent concentration (%) for ultrasound assisted extraction
X_8	Time for ultrasound assisted extraction (min)

X_9	Starch concentration (%)
X_{10}	Nozzel pressure during spray drying (MPa)
X_{11}	Drying temperature during spray drying (°C)
X_{12}	Barrel Temperature (°C)
X_{13}	Screw Speed (RPM)
X_{14}	Feed moisture (%)
Y_1	TPC from purple rice bran in acetone (mg GAE/100g)
Y_2	TPC from purple rice bran in ethanol (mg GAE/100g)
Y_3	TPC from black rice bran in acetone (mg GAE/100g)
Y_4	TPC from black rice bran in ethanol (mg GAE/100g)
Y_5	Total phenolic content in black rice bran (mg GAE/100g)
Y_6	Monomeric anthocyanin content in black rice bran (mg C3G/L)
Y_7	Total phenolic content in purple bran extract (mg GAE/100g)
Y_8	Monomeric anthocyanin content in purple bran extract (mg C3G/L)
Y_9	Encapsulation efficiency (%)
Y_{10}	Anthocyanin content (mg C3G/L)
Y_{11}	DPPH scavenging activity (%)
Y_{12}	True density (g/cm^3)
Y_{13}	Water activity

Greek letters

τ	Shear stress
σ_{0_H}	Yield stress for Herschel–bulkley model
σ_{0_M}	Yield stress for Mizrahi-Berk model
η_H	Flow behavior index for herschel–bulkley model
η_M	Flow behavior index for Mizrahi-Berk model
γ	Shear rate
ε	Molar absorptivity
Ψ	Intercept
β_0	Constant
β_j	Linear effects
β_{jj}	Quadratic effects
β_{ij}	Interaction effects

Abbreviations

RSM	Response surface methodology
AACC	American association of cereal chemists
ANN	Artificial neural network
C3G	Cyanidin-3-glucoside
TPC	Total Phenolic content
RCCD	Rotatable central composite design
DF	Dilution factor
DPPH	2, 2-diphenyl-1-picrylhydrazyl
GAE	Gallic acid equivalent
HR	Hausner ratio
SPSS	Statistical Package for the Social Sciences
MW	Cyanidin-3-glucoside molecular weight
P3G	Peonidin-3-glucoside
RMSE	Root mean square error
SME	Specific mechanical energy
WSI	Water solubility index
UAE	Ultrasound-assisted extraction

List of Figures

List of Tables

ABSTRACT

The investigation stated in the thesis was aimed to separate the anthocyanin from black and purple rice bran and used as a functional ingredient and pH indicator in the food system. In the initial study, to separate the anthocyanin from black and purple rice bran, the conventional extraction process was followed by the ultrasound assisted extraction process. In the conventional extraction process, acetone, ethanol, and water were used as extractants and optimized using four-factor rotatable central composite design (RCCD). The ethanol was found to be the most effective solvent to extract total phenolic content (TPC) from rice bran. The purple rice bran extract showed a promisingly higher amount of phytochemical content and antioxidant activity than the black rice bran extract. After the conventional extraction, the ultrasound-assisted extraction (UAE) process was used with a mixture of ethanol and water as extractant to enhance the extraction yield in terms of TPC and anthocyanin. The UAE of TPC and anthocyanin from black and purple rice bran was optimized using RCCD in terms of temperature, pH, extraction time and solvent concentration. The comparative analysis of the purple and black rice bran extract revealed higher anthocyanin (34.9 mg C3G/L) and TPC (2232 mg GAE/100 g) in the purple rice bran extractives than black rice bran (31.9 mg C3G/L and 1978.8 mg GAE/100 g). The HPLC analysis of purple rice bran extract showed the higher amount of α-tocopherol, cyanidin-3-glucoside, 4-hydroxybenzoic acid than black rice bran. As the purple rice bran extract indicated higher anthocyanin contain, thus in the further study only purple rice bran extract was used.

After extraction, the adsorption and desorption process was used as a non-thermal process to separate and concentrate anthocyanin from the crude extract of purple rice bran. The adsorption and desorption behavior of anthocyanin was investigated using amberlite XAD2, XAD4, XAD7, activated charcoal, and bentonite as adsorbents. Amberlite XAD7 showed higher adsorption/desorption capacities (1.9 mg/g and 1.8 mg/g) and recovery (41.5 %) of anthocyanin from bran extract over other adsorbents. The adsorption behavior of anthocyanin was better explained by pseudo-first order kinetics than pseudo-second order kinetics model. Adsorption isotherm behavior of anthocyanin on adsorbents was found to be homogeneous and more suitable for Langmuir, and Redlich–Peterson isotherm model. The adsorption mechanisms of anthocyanin on adsorbents followed the intra-particle diffusion model and indicated that XAD7 has a higher diffusion rate than the other adsorbents. The phytochemical profiling of the separated and concentrated bran extract was

investigated in terms of anthocyanins, cyanidin-3-glucoside (C3G), peonidin-3-glucoside (P3G) and phenolic acid content. After separation, the degradation behavior of anthocyanin, C3G, and P3G was investigated at various pH and temperature. The kinetics was investigated at a pH range of 2 to 8 and temperatures ranging from 60 to 90 °C. At pH 2 and 6, the anthocyanin, C3G, and P3G showed the lowest and highest degradation rate, respectively. During thermal degradation, the lowest rate of degradation for anthocyanin (3.46×10^{-4} /min), C3G (1.75×10^{-4} /min), and P3G (1.99×10^{-4} /min) was observed at 60 °C and the highest rate of degradation were observed at 90 °C. The effect of hydrocolloids such as carboxymethyl cellulose, xanthan gum, modified starch, and gum arabic on the stability of anthocyanin, C3G, and P3G was significant ($p \leq 0.05$). The modified starch showed the highest stability effect on anthocyanins and antioxidant activity in the aqueous medium.

After the degradation study, the thesis work aims to provide a stable anthocyanin powder through microencapsulation using modified rice starch as wall material. The microencapsulation was carried out in a spray dryer, and the process was optimized using RCCD. The optimum values of spray drying process parameters were 6.01 % of starch concentration, 168.8 °C inlet air temperature, and 4.96 MPa atomizer pressure. The thermal, crystallinity, and surface properties of the microcapsules were also comprehensively studied using DSC, XRD, FTIR, and scanning electron microscopy. The storage stability of microencapsulated anthocyanin showed higher stability at 4 °C than at 25 °C for 90 days. The release behavior of anthocyanin was also investigated at 2 and 7 pH. In addition, the effect of microencapsulate on the steady-shear and dynamic oscillatory rheology of the rice dough was investigated.

The developed microencapsulated anthocyanin was used in the food product as a functional ingredient. The rice-based extrudate was developed using microencapsulated anthocyanin and the storage study was investigated in terms of moisture sorption isotherm. The RCCD was used to optimize the extrusion process, and the optimized conditions were: screw speed 121 rpm (12.7 rad/s); barrel temperature 91.9 °C, and moisture content, 22.03 %. The antioxidant activity, solubility, and cooking properties of the extrudate were determined and compared with the native rice extrudate. The storage study of the extrudate was found to follow type III isotherm behavior according to the BET classification. The sorption isotherm was analyzed using several models, and the Caurie and Peleg models showed the best fit with the extrudate isotherm data.

In the end, a paper base pH-sensitive indicator was developed using anthocyanin. The efficiency of the indicator was studied with different buffer solutions of pH range 2 - 10. The indicator made with 150 mg/L anthocyanin concentration showed a distinct *L*, *a*, and *b* values of color. Further, the indicator was tested in different liquid foods and indicating a distinct color with respect to pH values. The degradation behavior of *a*-value (redness) of the indicator showed first-order kinetics behavior. At high-temperature storage conditions, the degradation rate constant of a-value was higher than the low-temperature storage condition.

INTRODUCTION

CHAPTER 1

INTRODUCTION

In this chapter, a brief summary of the various rice bran, phenolic compounds, and anthocyanins are presented. The chemical structure of various anthocyanins is reviewed and presented in this chapter. It also includes various extraction processes for total phenolics and anthocyanin from pigmented rice bran. The adsorption of bioactive compound specifically anthocyanin is described. To increase the retention of the anthocyanin during food processing, anthocyanin needs to protect from the processing factores such as temperature, pH, light, and oxygen. A detailed literature review on microencapsulation and spray drying process is also conducted. The development of the functional extrudate food product is reviewed extensively. This chapter also consists of the literature review on the application of anthocyanin as a pH indicator in the paper-based indicator. The knowledge gap of the investigation is discussed elaborately. The aims and movitavtion for this reserach work are also discussed in this chapter.

1.1. Rice bran

Rice bran is the most abundant by-product of the rice milling process. The hard outer layers of the rice grain are known as bran. It is a combination of aleurone and pericarp. The rice bran contains a high amount of oil (15–25 % v/w) and low moisture (6–7 % w/w) having a powdery consistency (Lakkakula et al., 2004). Rice bran is predominantly rich in dietary fibre, essential fatty acids, and significant quantities of starch, protein, vitamins, and dietary minerals. It also contains high amounts of phytochemicals, such as tocopherols, tocotrienols, oryzanols, vitamin B complex, and various phenolic compounds (Min et al., 2012). The bioactive compounds in rice bran have purported health benefits as well as antioxidant activity. Thus, rice bran is considered as a potential source of various high-value bioactive compounds for use as additives in foods, pharmaceuticals, and cosmetics (Lloyd et al., 2000). In some rice varieties, various types of pigments are concentrated in rice bran layer, resulting in pigmented rice with a different color. Pigmented rice is classified as black, red, purple, and green rice according to the color. These kinds of pigments are mainly due to the presence of phenolic compound such as anthocyanin and anthocyanidin (Paiva et al., 2014).

1.2. Pigmented rice bran

In some rice varieties, color-causing phytochemicals are concentrated in the pericarp and testa or in the bran part, resulting in rice with different colors. Pigmented rice bran is a potential source of various phytochemicals such as phenolic acid, anthocyanin, and anthocyanidin (Laokuldilok et al., 2011). These bioactive compounds have shown an important role in the prevention of diverse diseases such as cancer, cardiovascular diseases, detoxification, anti-proliferation, induction of apoptosis, anti-angiogenic activity; anti-inflammatory activity; inhibition of digestive enzymes; improvement of night vision as well as in the retardation of the aging process, and reducing the risk of degenerative disorders (Lila, 2004). Among the all pigmented rice bran, the purple and black rice bran are the most potent sources of various phytochemicals (Zhang et al., 2010).

The black and purple rice (*Oryza sativa L.*) is the most indigenous rice variety in India. These two varieties are mostly available in North-east India. Black and purple rice contain a high amount of bioactive compound as anthocyanins, in the bran (Pedro et al., 2016; Zhang et al., 2010). Both the rice bran are containing high amounts of cyanidin-3-O-glucoside, peonidin-3-O-glucoside, and cyanidin-3-O-gentiobioside (Shao et al., 2014; Zhang et al., 2010). Moreover, both the rice bran contains various type of phenolic acid (Catechin hydrate, Coumaric acid, Ferulic acid, Syringic acid, Vanillic acid, and gallic acid) and flavonoids (Zhang et al., 2010). This rice bran shows numerous antioxidant activities such as ferric reducing antioxidant power, Trolox equivalent antioxidant capacity and scavenging effect on the 1,1-diphenyl-2-picrylhydrazyl free radical (Wu et al., 2018; Zhang et al., 2010).

However, still, there is scanty of investigation on the phytochemical properties of the black and purple rice bran extract and use for human consumption. Therefore, to utilize the bioactive compounds as a food ingredient, there is a need to investigate the types of bioactive compounds and their properties.

1.3. Bioactive compounds

1.3.1. Phenolic compounds

Phenolic compounds are abundantly available bioactive compounds in nature. All the plant material, such as vegetable, nuts, seeds, cereals, vegetables, and fruits, are good sources of phenolic compounds. The most popular and widely available phenolic compounds in nature are anthocyanins, coumarins, flavonoids, and phenolic acids. These

plant-derived products have been suggested to be bioactive and involved in the prevention of oxidative stress, reducing free-radical related cellular damage, potentiating redox defense of the body, and contributing to the reduction of the risk of developing free-radical-related diseases (Laokuldilok et al., 2011). As a result, anthocyanins, coumarins, flavonoids, and phenolic acid are used as a functional ingredient in the food system. Abdel-Aal et al. (2006) and Pereira-Caro et al. (2013) reported that pigment rice bran specifically black and purple rice contains anthocyanins, carotenoids, and flavonol glycosides. Pedro et al. (2016) illustrated that black and purple rice bran is a good potential source of anthocyanin. The anthocyanin has some advantage over other bioactive compounds. Anthocyanins also act as pigments that give red, purple, and blue plants. In addition to that, anthocyanins acting as antioxidants and free radicals scavenger, offer anti-inflammatory, anti-viral, and anti-cancer benefits to the human body (Lila, 2004).

1.3.2. Anthocyanin

Anthocyanin is one of the most commonly used water-soluble bioactive compound. It has well established that anthocyanin has significant effect on the various diseases such as cardiovascular disease (Wallace, 2011), Alzheimer's diseases (Shih et al., 2010) low vision (Miyake et al., 2012) diabetes and obesity (Norberto et al., 2013). The vibrant colors of anthocyanin range from red to blue (Yoshida et al., 2009). The molecules of anthocyanin are considered as polyphenols that are typically extracted from the color parts of certain plants, including fruits, vegetables, flowers, leaves, and rice bran. As the anthocyanins have tremendous industrial and commercial values, thereby few researchers used engineered microorganisms to developed anthocyanin in the lab (Lim et al., 2015; Yan et al., 2008; Yan et al., 2005). Lim et al. (2015) modified the gene expression level of *Escherichia coli* to produce anthocyanin. They identified *E. coli* transporter proteins that were responsible for the uptake of catechin and secretion of cyanidin-3-O-glucoside. Yan et al. (2005) also modified the gene expression of *E. coli* using plant genes to produce anthocyanin. It was reported that *E. coli* cells containing the recombinant plant pathway, were able to take up either naringenin or eriodictyol and converted it to the corresponding glycosylated anthocyanin, pelargonidin-3-O-glucoside or cyaniding-3-O-glucoside. The recombinant *E. coli* strain produced 6.0 µg/L of cyaniding-3-glucoside and 5.6 µg/L pelargonidin-3-glucoside using naringenin and eriodictyol as precursors, respectively.

However, irrespective of sources, the color of anthocyanin is strongly dependent on the pH of the surrounding aqueous phase (Ekici et al., 2014). Moreover, due to a unique

molecular structure, the anthocyanin is very sensitive to the processing factor such as temperature, light, and oxygen.

Structurally, anthocyanins are glycosides and acyl-glycosides of anthocyanidins. The aglycones and flavylium (2-phenylbenzopyrilium) varied due to hydroxyl or methoxyl substitutions in their primary structures. The core of the anthocyanidin is flavylium having the typical C6-C3-C6 skeleton, which contains one heterocyclic benzopyran ring, one fused aromatic ring and one phenyl constituent (**Fig. 1.1**). Substitution with H, OH, and OCH_3 in the B ring produces six different anthocyanidins: pelargonidin, cyanidin, delphinidin, peonidin, petunidin, and malvidin (Wrolstad, 2004). Glycosidic substitution occurs at the 3 and/or 5 positions, and the mono, di or tri-saccharides may be acylated with aliphatic or cinnamic acids which leads to a considerable structural variation of anthocyanin (Holton and Cornish, 1995). In the cation form, anthocyanidins have two double bonds in the C ring, and hence it carries a positive charge (**Fig. 1.1**) (Castaneda-Ovando et al., 2009).

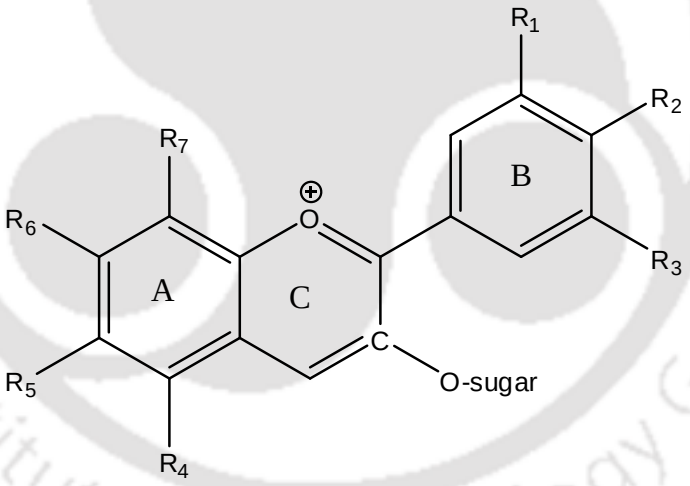

Fig. 1.1: The basic chemical structure of anthocyanin

Differences between individual anthocyanidins occurs due to (i) the number and position of hydroxyl (OH) groups in the structure, (ii) the degree of methylation of these OH groups, (iii) the nature, number, and location of sugars attached to the molecule, and (iv) the nature and number of aliphatic or aromatic acids attached to the sugar (Pojer et al., 2013) as shown in **Table 1.1**.

Table 1.1: Various anthocyanins and their groups

Anthocyanin	R_1	R_2	R_3	R_4	R_5	R_6	R_7
Aurantinidin	H	OH	H	OH	OH	OH	OH
Cyanidin	OH	OH	H	OH	OH	H	OH
Delphinidin	OH	OH	OH	OH	OH	H	OH
Europinidin	OCH_3	OH	OH	OH	OCH_3	H	OH
Luteolinidin	OH	OH	H	H	OH	H	OH
Malvidin	OCH_3	OH	OCH_3	OH	OH	H	OH
Pelargonidin	H	OH	H	OH	OH	H	OH
Peonidin	OCH_3	OH	H	OH	OH	H	OH
Petunidin	OH	OH	OCH_3	OH	OH	H	OH
Rosinidin	OCH_3	OH	H	OH	OH	H	OCH_3

Cultivar type and viticulture conditions significantly influence the proportion and amount of each anthocyanin. These factors are also influencing, the hue, and the color stability, which are directly affected by the hydroxylation and methylation pattern of the anthocyanidins (Siriwoharn et al., 2004). The extraction and separation process of anthocyanin from the plant material affect the hue and color stability as well as the bioactivity of anthocyanin. Thereby, there is a need to select a proper extraction and separation process, having less severity on anthocyanin structure.

1.4. Extraction of bioactive compounds

The effectiveness of bioactive compounds are dependents on the quality and quantity of the compounds. The qualitative and quantitative studies of bioactive compounds from plant materials mostly rely on the selection of proper extraction method (Azmir et al., 2013). Extraction is the first step of any bioactive compound study, which plays a crucial role in the result and outcome.

The extraction of bioactive compounds depends on several factors, such as the extraction technique, raw materials, extraction condition, and the extraction solvent. The extraction techniques can be classified into the conventional and non-conventional process (Meireles, 2008). Conventional techniques require organic solvents, temperature, and agitation for the extraction such as soxhlet, maceration, and hydrodistillation. Modern techniques or non-conventional techniques such as enzyme-assisted extraction, microwave-assisted extraction, supercritical fluid extraction, and ultrasound-assisted

extraction, are green or clean techniques due to less use of energy and organic solvent, which are beneficial to the environment (Soquetta et al., 2018).

1.4.1. Conventional extraction

The conventional extraction techniques are widely used for the extraction of bioactive compounds from plant materials. These techniques are based on the extracting efficiency of different solvents and the application of heat and/or mixing. To obtain bioactive compounds from plants, the existing classical techniques are (1) Soxhlet extraction, (2) Maceration, and (3) Hydrodistillation.

1.4.1.1. Soxhlet extraction

The Soxhlet extraction has widely been used for the extraction of valuable bioactive compounds from various natural sources. It is used as a model for the comparison of new extraction techniques. In this process, a wide range of solvent is used as extractant, which carries extracted solutes. Few researchers have applied the soxhlet extraction techniques to extract bioactive compounds, especially anthocyanin from various plant sources (Lapornik et al., 2005; Veggi et al., 2011). The rate and degree of extraction of anthocyanins from plant materials through soxhlet depends upon a number of factors such as types of solvent (ethanol, methanol, water), temperature, time and acid (HCl, citric, tartaric, formic, acetic, propionic) (Ameer et al., 2017). Though this process is widely used for the extraction, however, this technique requires long extraction time and large amounts of solvent (Heleno et al., 2016) which enhance the degradation of the bioactive compounds.

1.4.1.2. Maceration

In the maceration process, the sample is ground into smaller particles to increase the surface area for an efficient mixing with the solvent. During maceration, the continuous agitation makes the extraction process easier in two ways: by increasing the diffusion and removing the concentrated solution from the surface of the sample. However, this process requires a long extraction time to obtain bioactive compounds from plant sources (Azmir et al., 2013). Romero-Cascales et al. (2005) reported that the maceration process increases the rate of anthocyanin extraction from skins of Monastrell grapes. However, in this process the exhaustive bulk extractions can be time-consuming, taking from a few hours to several weeks, and consume large volumes of solvent. Thereby decreases the extraction efficiency of bioactive compounds.

1.4.1.3. Hydrodistillation

Hydrodistillation is performed with distilled water and is generally used to extract the volatile fraction from foods. Hydrodistillation extraction process usually takes 6–8 h without organic solvents. This technique involves three main physicochemical processes: hydro-diffusion, hydrolysis, and decomposition by heat. Due to the presence of heat, this process generally is not used for the extraction of the heat-sensitive compounds. Though Santana-Méridas et al. (2014) extracted various polyphenol, and antioxidant from the solid residue of *Rosmarinusofficinalis L.* using hydrodistillation process. Santana-Méridas et al. (2014) have identified various phenolic compounds such as carnosol, carnosic acid, cirsimaritin in extract having antioxidant and bioplaguicide activities. Hydrodistillation consumes high levels of energy and is time-consuming (Okoh et al., 2010). Moreover, it also involves a heating process, which restricts its application for the extraction of heat-sensitive bioactive compounds from plant material.

1.4.2. Non-conventional extraction techniques

The major challenges of conventional extraction are longer extraction time, high purity solvent, evaporation of the huge amount of solvent, low extraction selectivity and thermal decomposition of thermolabile compounds (Wang and Weller, 2006). To overcome these limitations, non-conventional extraction techniques are introduced. Some of the most promising non-conventional extraction techniques are enzyme-assisted extraction, microwave-assisted extraction, supercritical fluid extraction, pressurized liquid extraction, and ultrasound-assisted extraction. These include less hazardous chemical, energy efficiency, reduce derivatives, catalysis, less degradation, and less time (Vieira da Silva et al., 2016). Thereby, the non-conventional extraction techniques nowadays are commonly used for the extraction of bioactive compounds.

1.4.2.1. Enzyme-assisted extraction

Enzyme-assisted extraction methods are gaining more attention because of the eco-friendly feature of the extraction process (Puri et al., 2012). Enzymes have been used particularly for the treatment of plant material before conventional methods for extraction. Various enzymes such as cellulases, pectinases, and hemicellulase are often used to disrupt the structural integrity of the plant cell wall, thereby enhancing the extraction of bioactive compounds from plants. Xu et al. (2016) and Landbo and Meyer (2001) extracted anthocyanins from blueberry and black currant residue using enzyme-assisted extraction process. Xu et al. (2016) proposed that the enzyme-assisted extraction is more efficient than

existing extraction process and easy to scale-up for industrial application. Enzyme-assisted extraction is a non-thermal method which can increase oxidative stability and antioxidant activity of bioactive components (Nadar et al., 2018). However, it has numbers of disadvantage, such as separation of enzyme and cost-effective (Puri et al., 2012).

1.4.2.2. Microwave-assisted extraction

In the microwave-assisted extraction process, microwave energy is used to heat the solvent and reduce the size of the sample to increase the mass transfer rate of the solutes from the food matrix into the solvent (Delazar et al., 2012). The microwave energy causes molecular motion by the migration of ions and rotation of dipoles (Gujar et al., 2010). This process is generally influenced by solvent nature and volume, extraction time, microwave power, matrix characteristics, and temperature. Microwave-assisted extraction used to extract bioactive compounds more rapidly, and recovery efficiency is higher than conventional extraction processes (Chemat and Cravotto, 2012). Pap et al. (2013) extracted anthocyanin from black currant marc by microwave-assisted extraction and reported that there was a 20 % (v/v) increase in anthocyanin yield as compared to the conventional extraction process. Yang and Zhai (2010) optimized the microwave-assisted extraction of anthocyanins from purple corncob. They also suggested that microwave-assisted extraction was highly efficient and rapid in comparison with conventional solvent extraction. Nevertheless, microwave irradiation can accelerate the chemical reactions and can modify the chemical structures of the target compounds. Compared with ultrasonic-assisted and conventional extraction, apparatuses, and equipment of microwave-assisted extraction are more expensive, and their operation is more difficult in many cases (Zhang et al., 2011).

1.4.2.3. Supercritical fluid extraction

Supercritical fluids extraction has several advantages over the conventional extraction process, such as high dissolving power, higher diffusion coefficient, and easy to separate. Due to their low viscosity and relatively high diffusivity, supercritical fluids have high transport properties than liquids; thereby, it can diffuse easily through solid materials and give faster extraction rates. Moreover, the solvents generally used for the extraction are recognized as safe (da Silva et al., 2016). Few researchers were used supercritical fluids extraction process to extract anthocyanin from the various plant sources (Garcia-Mendoza et al., 2017; Maran et al., 2014; Paes et al., 2014). Garcia-Mendoza et al. (2017) and Paes et al. (2014) used supercritical fluids extraction process to extract anthocyanin from juçara and blueberry residues, respectively. They concluded that the supercritical fluids extraction

process had higher efficiency in extracting anthocyanin than pressurized liquids and conventional extraction process. Paula et al. (2014) extracted anthocyanins and luteolin from *Arrabidaeachica* using supercritical CO_2, ethanol, and water as solvents and demonstrated that pure supercritical CO_2 showed lowest extraction yield and with ethanol as co-solvent showed the highest yield. However, this process has a few disadvantages like the requirement of co-solvent, high operating pressure, higher capital, and operating costs (Wang and Weller, 2006).

1.4.2.4. Ultrasound-assisted extraction

Ultrasound-assisted extraction has been revealed to be an economically feasible technique for the extraction of heat-sensitive bioactive compounds (Chemat et al., 2017). According to Pingret et al. (2013) ultrasound has several advantages over conventional extraction processes such as higher diffusion, higher mass transfer, breakdown of plant cells, more solvent penetration, and capillary effects of ultrasound (Sono capillary Effect). The ultrasound-assisted extraction does not act with one mechanism but through different independent or combined mechanisms between fragmentation, erosion, capillarity, denaturation, and sonoporation. The efficiency of ultrasound-assisted extraction depends upon sonochemical effects, frequency, wavelength, amplitude, size of ultrasonic reactors, and medium parameters such as solvent type, temperature (Chemat et al., 2017). Few researchers extracted anthocyanin from various plant sources such as haskap berries (Jang and Xu, 2009), purple waxy corn (McGhie and Walton, 2007) mulberry (Jang and Xu, 2009) and red rose petals (McGhie and Walton, 2007) using ultrasound-assisted extraction. They also suggested that ultrasound-assisted extraction showed higher extraction yield than conventional extraction process. Moreover, the ultrasound-assisted extraction used as a continuous process in the industry for extraction (Pan et al., 2011). Thereby, ultrasound-assisted extraction is now gaining interest to extract the bioactive compound.

However, to further enhance the activity of extracted bioactive compounds, its need to separate specifically from undesirable components and concentrate using non-thermal process.

1.5. Adsorption of bioactive compounds

After extraction, further enhancing the activity of bioactive compounds, it needs to separate and concentrate more explicitly using non-thermal processing. The commonly used methods to separate the bioactive compound especially anthocyanin from aqueous

phases are adsorption (Brouillard and Delaporte, 1977) and membrane separation (Hossain et al., 2009). The adsorption is the most preferred method as compared to membrane separation, due to non-thermal and fewer maintenance in nature (Ruthven, 1984). Adsorption is a single step non-thermal way to separate and concentrate bioactive compounds, such as anthocyanin from the crude extract of plant sources with low energy and less maintenance costs (Choi et al., 2017). The adsorption process generally classified as physisorption and chemisorption. In physisorption, the adsorbate adheres to the surface only through Vander Waals interactions. Whereas, in chemisorption, a molecule adheres to the surface through the formation of a chemical bond (Rouquerol et al., 2013). The adsorption of bioactive compounds from plant sources considered as physisorption process (Puri et al., 2012). The adsorption process of bioactive compounds depends upon some factors such as the surface area of adsorbent, particle size, contact time, temperature, pH and solute properties (Scordino et al., 2004).

Therefore, the analysis of adsorption isotherm and kinetics are important parameters to understand the adsorption mechanisms of bioactive compounds. Adsorption isotherm descript the equilibrium relationship between the solute concentration in the liquid phase and that on the adsorbent's surface (Foo and Hameed, 2010). Whereas, adsorption kinetics describe the diffusion behavior, the adsorption rate of solute. For the isotherm study, Langmuir and Freundlich's isotherms are most commonly used isotherms to explain the adsorption process. Whereas pseudo-first-order (Chemat et al., 2017) and pseudo-second-order (Wang and Weller, 2006) kinetic models are most commonly used to explain the adsorption process. The Intra-particle diffusion (Pan et al., 2011) model also used to explain the rate-limiting step of an adsorption process.

The resin adsorption process is widely used to separate and concentrate bioactive compounds from crude extract (Zhang et al., 2010). In general, synthetic resins, namely, XAD16, XAD7, XAD4, and XAD2 were used by few researchers to separate bioactive compounds mainly anthocyanin from various plant sources (Brouillard and Delaporte, 1977; Chen et al., 2016; Jampani et al., 2014). Synthetic resins are able to adsorb phytochemical from aqueous solution through hydrophobic bonding and aromatic stacking and desorb in organic solvents, such as methanol or ethanol. Few- researchers have used different adsorbents for purification of anthocyanins from *Hibiscus sabdariffa* sp. (Chang et al., 2012), mulberry (Chen et al., 2016), blueberry (Buran et al., 2014), and red cabbage (Chandrasekhar et al., 2012) and many more as shown in **Table 1.2**.

However, the adsorption process of anthocyanin from pigmented rice bran, especially purple rice bran, has not been studied yet. Therefore, its need to investigate extensively to know the adsorption mechanisms, isotherm, and enhance the adsorption efficacy. Nevertheless, the anthocyanin is very much sensitive to processing factors such as temperature, pH, light, and oxygen, thereby its need to protect from the processing factors during.

Table 1.2: Adsorption of anthocyanin from various plant sources

Sources	Adsorbent	References
Wines	Yeast lees	Vasserot et al. (1997)
Mulberry	D3520, D4020, X-5, NKA-9, D101A, and AB-8	Xueming Liu et al. (2004)
Purple-fleshed potatoes	XAD-7HP, XAD-1180, XAD-4, XAD-1600, EXA-31, EXA-117, EXA-32, EXA-90, EXA-45, EXA-50, and EXA-118	Xuan Liu et al. (2007)
Hibiscus sabdariffa L.	AB-8, X-5, HPD-100, SP-207, XAD-4, LS-305A, DM-21, LS-610B, and LS-305	Chang et al. (2012)
red cabbage	XAD7HP, XAD4,IRC 80, IRC 120, and Dowex 50WX8	Chandrasekhar et al. (2012)
Blueberries	FPX66, XAD7HP, XAD4 XAD761, and XAD1180	Buran et al. (2014)
Jamun	XAD7HP, XAD4, IRC 86, IRC 120, Dowex 50xw8	Jampani et al. (2014)
Grape skin	Mesoporous silica	Kohno et al. (2014)
Mulberry	XAD-7HP, AB-8, HP-20, D-101, and X-5	Chen et al. (2016)
Blueberry	XAD-7HP	Wu et al. (2018)

1.6. Microencapsulation of bioactive compound through spray drying

To develop a stable and usable food ingredient from anthocyanin, several approaches are in consideration, such as microencapsulation, emulsion, and freeze-drying. For anthocyanin, microencapsulation method has been demonstrated and accepted by a few researchers (Ersus and Yurdagel, 2007; Kalusevic et al., 2017; Weber et al., 2017).

Microencapsulation is an efficient way to enhance the products' bioavailability and stability as well as managing the release of the active agent (Mahdavi et al., 2016). Shahidi and Han (1993) proposed six reasons for applying microencapsulation in food industry: to reduce the core reactivity with environmental factors; to decrease the transfer rate of core material to the outside environment; to promote easier handling; to control the release of the core material; to mask the core taste; and finally to dilute the core material when it should be used. There are various types of microencapsulation techniques, such as vibrational nozzle, centrifugal extrusion, spray drying, and co-crystallization (**Table 1.3**).

Table 1.3: Microencapsulation processes for anthocyanins

Process	**Wall Material**	**Anthocyanin source**	**References**
	Maltodextrin	Black carrots	Ersus and Yurdagel (2007)
	Maltodextrin	Corozo	Osorio et al. (2010)
Spray drying	Maltodextrin DE20 and hi-maize	Blueberry	Righi da Rosa et al. (2019)
	Maltodextrin, gum arabic, and skimmed milk powder.	Black soybean	Kalusevic et al. (2017)
Emulsion	Whey protein	Bilberry	Betz and Kulozik (2011)
Phase separation	Ethyl cellulose	Blueberry	li et al., (2009)
Gelation	Curdlan, pectin and sodium alginate	Blackberry	Ferreira et al., (2009)

The most commonly used technique is spray drying, due to its continuity in nature, low cost, and less time which can produce particles with good quality (Mahdavi et al., 2016). Spray drying involves making a homogenous mixture of the core material and wall material, which is then atomized inside a spray dryer (Nedovic et al., 2011). The dried particles tend to be spherical with an average diameter of 5-100 µm. Researcher had used spray drying techniques for microencapsulation of anthocyanin from various plant source such as black carrot (Ersus and Yurdagel, 2007), corozo (Osorio et al., 2010), pomegranate juice (Robert et al., 2010), grape juice (Zhang et al., 2007), *Opuntiastricta* fruit (Obón et

al., 2009) with maltodextrin, gum arabic, and soy protein isolate in different drying temperature.

For microencapsulation through the spray drying process, the selection of wall material is the primary step. The commonly used wall materials for anthocyanin encapsulations are maltodextrin, gum Arabic (Brouillard and Delaporte, 1977), skimmed milk powder (Hossain et al., 2009) and starches (Tonon et al., 2010). The carbohydrates, such as, maltodextrins and starches, have properties like good solubility and low viscosity at high solids contents which are highly desirable for an encapsulating agent. However, native starch is insoluble in cold water and, when heated with water it forms a paste-like texture with high viscosity, which limits its application for microencapsulation using spray drying. These limitations can be overcome by modification of native starches. Researchers were used modified starch as a wall material in for encapsulation of various bioactive compounds (Hoyos-Leyva et al., 2018; Lacerda et al., 2016; Tonon et al., 2010). However, the application of modified low amylose rice starch as a wall material in microencapsulation of anthocyanin from purple rice bran is scanty.

1.7. Ready to cook food product

The demand for ready-to-cook (RTC) food products has been increased over the last few years because of hectic lifestyles and rising income levels of consumers. Among RTC products, ready-to-cook breakfast cereals have gained market share because of the convenience and practicality claims associated with these products (Albertson et al., 2013). These products commonly consumed with milk, water or any other medium and are considered as a source of micronutrients as vitamins, dietary fiber, and minerals (Brennan et al., 2013). There is various type of processing technology used to developed RTC such as extrusion (Charutigon et al., 2008), flakes roller (Takhellambam et al., 2016) and cooking (Turkmen et al., 2005). Out of all the processing techniques, extrusion cooking is prefered over other food-processing techniques in terms of the continuous process with high productivity and significant nutrient retention, and short processing time (Singh et al., 2007).

Extrusion cooking is a technology that is widely used for the development of new food products. This process combines several unit operations including mixing, cooking, kneading, shearing, shaping, and forming. During the extrusion cooking, the major changes that may occur in the feed material are starch gelatinization, protein denaturation,

carbohydrate-lipid complex formation (such as, amylose-lipid) and degradation of heat and shear sensitive components such as vitamins, antioxidants, and pigments (Camire et al., 1990). These changes depend on the process conditions, e.g., types of the extruder, feed material, material moisture content, barrel temperature, and screw speed. However, due to high temperature and shear, the bioactive compounds are generally deteriorated during extrusion cooking. Therefore, the development of extrudate food enriches with bioactive compounds is a challenge for food technologist.

1.8. Functional ready to cook extrudate food

Presently, consumers demand nutritious food that provides health benefits. This situation has led to transformation of the food processing industry to ensure delivery of healthy foods to consumers recognized as "functional foods." Therefore, food extrusion studies have been focused on the development of functional food products using legumes, cereals, fruits, fruit extracts, and vegetables. In order to develop the ready-to-cook functional food products, bioactive ingredients are to be added with the feed mixtures before extrusion. However, the majority of these bioactive compounds are lost during the extrusion cooking due to their sensitivity towards processing conditions such as temperature, pressure, pH (Riaz et al., 2009). Considerable effort was made to improve the retention of bioactive compounds such as tannin, ascorbic acid, riboflavin (Anuonye et al., 2010), flavonols, total anthocyanins (White et al., 2010), D-limonene, betacyanin, and betaxanthin (Yuliani et al., 2006) in extrudate food as precursor, flavour, and functional ingredient. It is reported that after extrusion of *kiwi cha*, the level of total phenolic content decreases up to 80.3 % (w/v) (Repo-Carrasco-Valencia et al., 2009). Similarly, White et al. (2010) observed a significant loss (46-64 % w/v) in anthocyanin content after the development of cranberry pomace extrudates. Thereby, to retain the bioactive compound in the extrudate, the compounds may be used after encapsulation. Studies reported that the use of the molecular encapsulated bioactive compound in extrusion process enhances the retention of these components (Yuliani et al., 2006). Researchers have already developed the functional extrudate product with encapsulated bioactive compounds, such as betalains (Ruiz-Gutiérrez et al., 2015), D-limonene (Yuliani et al., 2006). However, no reports are available on the microencapsulated anthocyanin extrudate.

1.9. pH sensitivity of anthocyanin

Anthocyanins are the most commonly available water-soluble natural colorants, ranges from red to blue (Yoshida et al., 2009). The vibrant color of anthocyanins depends

on the pH of the surrounding liquid phase. For the change of pH, the anthocyanin structure transforms into various derivative and shows various color, as shown in **Fig. 1.2.** The change of pH causes, the rapid loss of a proton from the flavylium cation and generate various color compound such as quinonoidal-base structure with red, colorless carbinol pseudo-base, yellow colorchalcone structure (Brouillard and Delaporte, 1977; McGhie and Walton, 2007). Due to this unique characteristic, the anthocyanin is used as a natural pH-sensitive dye.

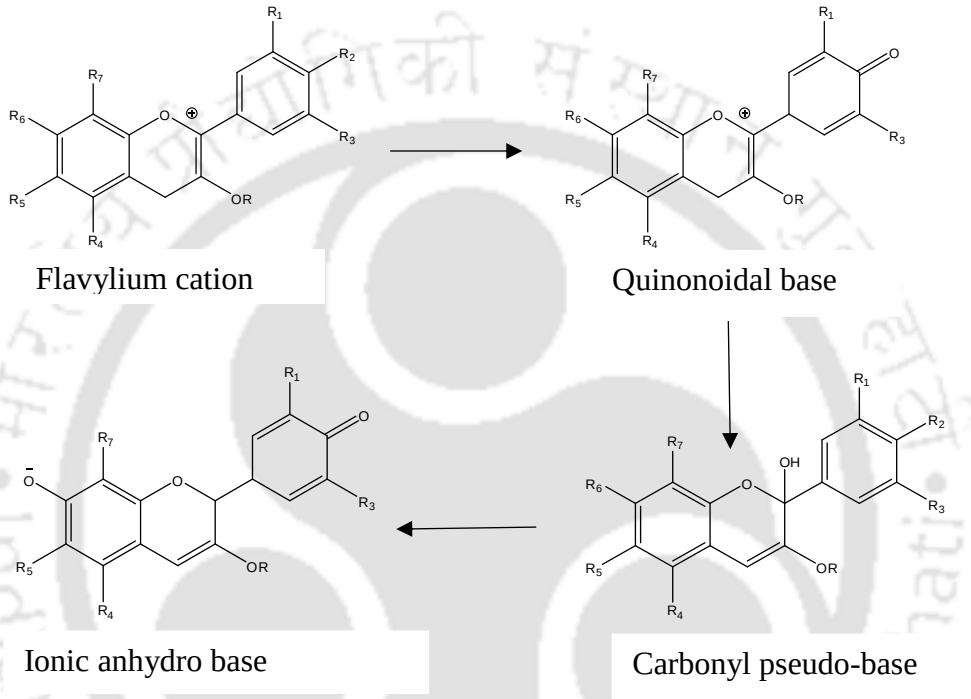

Fig. 1.2: Changes of anthocyanin structure in various pH

1.10. Anthocyanin based pH sensitive paper indicator

The measurement of pH is almost universal in the environmental, agricultural, food, cell culture, microbiology, biotechnology, and biomedical industries. Generally, in the food system pH is measured to monitor the food quality by using pH meter or litmus paper. However, there is a need for food compatible pH indicator from natural dye, and anthocyanin is the most widely available pH-sensitive dye. Hence, there is a need for a low-cost pH sensor with widely available natural dye, and anthocyanin is the most widely available pH-sensitive dye. Researchers have used the anthocyanin to develop pH-sensitive material for food quality control, as shown in **Table 1.4**. However, there is no pH-sensitive film with anthocyanin from purple rice bran.

Table 1.4: Biodegradable films with anthocyanin as pH indicator

Material	Use	References
Starch	To extend storage life of strawberries	García et al. (1998)
Cross-linked chitosan membrane	To monitor the quality of perishable food	Williams and Myers (2005)
Film on glass	To determine the of iron (III) in the liquaid system	Zhang et al. (2010)
Chitosan intelligent films	To monitor pH variations in the food system	Yoshida et al. (2014)
Agarose film Filter paper	Intelligent packaging application	Shukla et al. (2016)
Agar/potato starch	Intelligent packaging application	Choi et al. (2017)
Starch and polyvinyl alcohol	To monitor the freshness of fish	Zhai et al. (2017)
Hydrogel	To control the amount of refrigenatant in the refrigerator	Jung and Jeong (2018)
Cellulose-based paper	To monitor shrimp spoilage	Listyarini et al. (2018)

Recently, paper-based patterned solid-phase sensors (which are simple, portable, disposable, and inexpensive) have been developed to run multiple bioassays and controls simultaneously. These portable bio-sensing papers are extremely useful in remote settings and developing countries, where simple bioassays are essential in the first stages of detecting disease, and for monitoring environmental and toxins in the food system (Hossain et al., 2009). Therefore, demand for the paper sensor is increasing gradually. In the paper sensor, various type of paper was used as a substrate such as hydrophilic filter paper (Cai et al., 2014) Whatman no. 1 filter paper (Hossain and Brennan, 2011). However, filter paper as a substrate has many advantages such as power-free fluid transport via capillary action, high surface area to volume ratio that improves detection limits for colorimetric methods, cost-effective and portable and can store reagents in active form within the fiber network (Liana et al., 2012). For the pH indicator, anthocyanin from various plant sources such as purple sweet potato (Choi et al., 2017), red cabbage and rose (Shukla et al., 2016) and other (**Table 1.4**) was used for the development of the paper

sensor. However, there is scanty of literature on the pH-sensitive paper indicator using anthocyanin from purple rice bran for application in the food system.

1.11. Knowledge gap and objectives of the thesis

The diverse topography and climatic conditions of North east India make the region suitable for the production of a broad range of crops. Some of the crops are neither grown commercially on a large scale nor traded widely and termed as underutilized horticultural crops. These crops are cultivated, traded, and consumed locally. Apart from nutritive value, underutilized crops are more important for medicinal properties and famous for the retentive value in Ayurvedic medicine (Jang and Xu, 2009). The popularity of these horticultural crops is restricted within the locality, thereby the benefit of these crops also restricted which, however, can be enhanced to a greater extent through more utilization in term of a new food product. The black and purple rice (*Oryza sativa L.*) is the most important indigenous underutilized crops variety of North east India. Both the rice contents anthocyanin and proanthocyanidin compounds (Paiva et al., 2014). In comparison to brown rice bran, black and purple rice bran has higher phenolic content and antioxidant activities. Hence, the recovery of phenolic compounds from both the rice bran may provide commercial benefits in term of natural antioxidant. However, no attempt has been made to recover the TPC and anthocyanin from the black and purple rice bran.

To use the bioactive compounds in the food system, these bioactive compounds from rice bran need to be extracted using efficient and environmentally friendly extraction techniques. However, traditional methods, such as refluxing, boiling, and Soxhlet extraction, are time-consuming and have low extraction efficiency due to oxidation, hydrolysis, and ionization of the phenolic compounds. To supersede these difficulties, emerging technologies, especially ultrasound-assisted extraction (UAE) is applied and investigated for the extraction of bioactive compounds from plant sources. Ultrasound base extraction has been revealed to be an economically feasible technique for the extraction of heat-sensitive bioactive compounds. Although, UAE is not used for the above mentioned rice bran to extract the bioactive compounds, especially anthocyanins from bran.

After extraction, for further enhancing the activity of TPC and anthocyanin, it needs to separate and concentrate more explicitly using non-thermal processing. Membrane filtration, supercritical fluid extraction, vacuum evaporation, and adsorption are used for concentration of bioactive compounds from the plant sources. However, except adsorption,

all the above-mentioned process are sophisticated, complex with a high amount of energy requirement and high maintenance costs. Whereas, adsorption is a single step non-thermal way to concentrate bioactive compounds, namely, anthocyanin from the crude extract of plant sources with low energy and lesser maintenance costs. However, there is no information on adsorption and desorption behaviors of anthocyanin from purple rice bran. Moreover, there is no detailed study available in the literature on intra-particle diffusion of anthocyanin from purple rice bran on the various adsorbents.

The anthocyanin is sensitive compound, affected by environmental factors such as pH, light, heat, and oxygen. Thereby, its need to develop a stable anthocyanin for food processing., Several approaches are in consideration to develop a stable food ingredient from anthocyanin, such as encapsulation, emulsion, and freeze-drying. The most commonly used process is encapsulation, specifically microencapsulation. Microencapsulation may be an efficient way to enhance bioavailability of productand stability as well as managing the release of the active agent. For microencapsulation, the selection of wall material is the most important step. There are various types of wall material used as wall material for anthocyanins such as maltodextrin, gums, starch, and protein. However, the application of modified low amylose rice starch as wall material in microencapsulation of anthocyanin was scanty. Moreover, there is no information on microencapsulated anthocyanin incorporated extrudate food product.

Anthocyanin is a water-soluble pH-sensitive natural dye. With the change of pH anthocyanin changes the appearance, hence it is used as a pH indicator. Moreover, the demand for low cost environmental friendly pH sensor gradually increases for the food quality monitoring. The paper-based sensor has the potential to overcome the limitations. The paper sensor is widely used for the multiple bioassays and quality control of any liquid system. The pH-sensitive paper-based sensor with synthetic indicators is used extensively. However, the use of natural dye as a pH indicator in the paper sensor is limited. The anthocyanin from plant sources is used as a natural pH indicator in the food system. However, the use of anthocyanin from purple rice bran in the paper sensor is scanty.

Therefore, considering the above research gap, the objectives are formulated as follows:

Objectives of the thesis

1. To evaluate the extraction processes using solvent extraction technique for bioactive phytoconstituents (anthocyanin) from purple and black rice bran
2. To study the adsorption and desorption characteristics of anthocyanin extracted from purple rice bran and its degradation kinetics
3. To evaluate the microencapsulation process of anthocyanin and its effect on rice dough rheology
4. To develop functional food and paper based indicator from anthocyanin

References

Abdel-Aal, E.S.M., Young, J.C. and Rabalski, I., (2006). Anthocyanin Composition in Black, Blue, Pink, Purple, and Red Cereal Grains. *Journal of Agricultural and Food Chemistry, 54*(13), 4696-4704.

Mahdavi, S.A., Jafari, S.M., Assadpour, E. and Ghorbani, M. (2016). Storage stability of encapsulated barberry's anthocyanin and its application in jelly formulation. *Journal of Food Engineering, 181*, 59-66.

Albertson, A.M., Franko, D.L., Thompson, D.R., Tuttle, C. and Holschuh, N.M., (2013). Ready-to-eat cereal intake is associated with an improved nutrient intake profile among food insecure children in the United States. *Journal of Hunger & Environmental Nutrition, 8*(2), 200-220.

Ameer, K., Shahbaz, H.M. and Kwon, J.H. (2017). Green extraction methods for polyphenols from plant matrices and their byproducts: a review. *Comprehensive Reviews in Food Science and Food Safety, 16*(2), 295-315.

Anuonye, Julian C., Onuh, John O., Egwim, Evans, and Adeyemo, Samuel O. (2010). Nutrient and antinutrient composition of extruded acha/soybean blends. *Journal of Food Processing and Preservation, 34*(s2), 680-691.

Azmir, J., Zaidul, I.S.M., Rahman, M.M., Sharif, K.M., Mohamed, A., Sahena, F., Jahurul, M.H.A., Ghafoor, K., Norulaini, N.A.N. and Omar, A.K.M., (2013). Techniques for extraction of bioactive compounds from plant materials: A review. *Journal of Food Engineering, 117*(4), 426-436.

Betz, M. and Kulozik, U. (2011). Microencapsulation of bioactive bilberry anthocyanins by means of whey protein gels. *Procedia Food Science, 1*, 2047-2056.

Brennan, M.A., Derbyshire, E., Tiwari, B.K. and Brennan, C.S.,. (2013). Ready-to-eat snack products: the role of extrusion technology in developing consumer acceptable and nutritious snacks. *International Journal of Food Science & Technology, 48*(5), 893-902.

Brouillard, R. and Delaporte, B. (1977). Chemistry of anthocyanin pigments. 2. Kinetic and thermodynamic study of proton transfer, hydration, and tautomeric reactions of

malvidin 3-glucoside. *Journal of the American Chemical Society, 99*(26), 8461-8468.

Buran, T.J., Sandhu, A.K., Li, Z., Rock, C.R., Yang, W.W. and Gu, L., (2014). Adsorption/desorption characteristics and separation of anthocyanins and polyphenols from blueberries using macroporous adsorbent resins. *Journal of Food Engineering, 128*, 167-173.

Cai, L., Xu, C., Lin, S., Luo, J., Wu, M., and Yang, F. (2014). A simple paper-based sensor fabricated by selective wet etching of silanized filter paper using a paper mask. *Biomicrofluidics, 8*(5), 056504.

Camire, M.E., Camire, A. and Krumhar, K. (1990). Chemical and nutritional changes in foods during extrusion. *Critical Reviews in Food Science and Nutrition, 29*(1), 35-57.

Castaneda-Ovando, A., de Lourdes Pacheco-Hernández, M., Páez-Hernández, M.E., Rodríguez, J.A. and Galán-Vidal, C.A. (2009). Chemical studies of anthocyanins: A review. *Food chemistry, 113*(4), 859-871.

Chandrasekhar, J., Madhusudhan, M. C. and Raghavarao, K. S. M. S. (2012). Extraction of anthocyanins from red cabbage and purification using adsorption. *Food and Bioproducts Processing, 90*(4), 615-623.

Chang, X.L., Wang, D., Chen, B.Y., Feng, Y.M., Wen, S.H. and Zhan, P.Y. (2012). Adsorption and desorption properties of macroporous resins for anthocyanins from the calyx extract of roselle (*Hibiscus sabdariffa L.*). *Journal of Agricultural and Food Chemistry, 60*(9), 2368-2376.

Charutigon, C., Jitpupakdree, J., Namsree, P. and Rungsardthong, V. (2008). Effects of processing conditions and the use of modified starch and monoglyceride on some properties of extruded rice vermicelli. *LWT-Food Science and Technology, 41*(4), 642-651.

Chemat, F. and Cravotto, G. (2012). Microwave-assisted extraction for bioactive compounds: theory and practice (Vol. 4): Springer Science and Business Media.

Chemat, F., Rombaut, N., Sicaire, A.G., Meullemiestre, A., Fabiano-Tixier, A.S. and Abert-Vian, M., (2017). Ultrasound assisted extraction of food and natural

products. Mechanisms, techniques, combinations, protocols and applications. A review. *Ultrasonics Sonochemistry, 34*, 540-560.

Chen, Y., Zhang, W., Zhao, T., Li, F., Zhang, M., Li, J., Zou, Y., Wang, W., Cobbina, S.J., Wu, X. and Yang, L. (2016). Adsorption properties of macroporous adsorbent resins for separation of anthocyanins from mulberry. *Food Chemistry, 194*, 712-722.

Choi, I., Lee, J. Y., Lacroix, M., and Han, J. (2017). Intelligent pH indicator film composed of agar/potato starch and anthocyanin extracts from purple sweet potato. *Food Chemistry, 218*, 122-128.

da Silva, Rui P. F. F., Rocha-Santos, Teresa A. P., and Duarte, A. C. (2016). Supercritical fluid extraction of bioactive compounds. *TrAC Trends in Analytical Chemistry, 76*, 40-51.

Delazar, A., Nahar, L., Hamedeyazdan, S. and Sarker, S.D. (2012). Microwave-Assisted Extraction in Natural Products Isolation. In S. D. Sarker & L. Nahar (Eds.), *Natural Products Isolation* (pp. 89-115). Totowa, NJ: Humana Press.

Ekici, L., Simsek, Z., Ozturk, I., Sagdic, O. and Yetim, H. (2014). Effects of temperature, time, and pH on the stability of anthocyanin extracts: Prediction of total anthocyanin content using nonlinear models. *Food Analytical Methods, 7*(6), 1328-1336.

Ersus, S. and Yurdagel, U. (2007). Microencapsulation of anthocyanin pigments of black carrot (Daucus carota L.) by spray drier. *Journal of Food Engineering, 80*(3), 805-812.

Ferreira, Daniela S., Faria, Adelia F., Grosso, Carlos R.F., and Mercadante, Adriana Z. (2009). Encapsulation of blackberry anthocyanins by thermal gelation of curdlan. *Journal of the Brazilian Chemical Society, 20*(10), 1908-1915.

Foo, K. Y. and Hameed, B. H. (2010). Insights into the modeling of adsorption isotherm systems. *Chemical engineering journal, 156*(1), 2-10.

Garcia-Mendoza, M.D., Espinosa-Pardo, F.A., Baseggio, A.M., Barbero, G.F., Marostica, M.R., Rostagno, M.A. and Martinez, J. (2017). Extraction of phenolic compounds and anthocyanins from juçara (*Euterpe edulis Mart*.) residues using pressurized liquids and supercritical fluids. *The Journal of Supercritical Fluids, 119*, 9-16.

García, M. A., Martino, M. N. and Zaritzky, N. E. (1998). Plasticized starch-based coatings to improve strawberry (Fragaria× ananassa) quality and stability. *Journal of Agricultural and Food Chemistry, 46*(9), 3758-3767.

Gujar, J. G., Wagh, S. J., and Gaikar, V. G. (2010). Experimental and modeling studies on microwave-assisted extraction of thymol from seeds of Trachyspermum ammi (TA). *Separation and Purification Technology, 70*(3), 257-264.

Heleno, S.A., Diz, P., Prieto, M.A., Barros, L., Rodrigues, A., Barreiro, M.F. and Ferreira, I.C. (2016). Optimization of ultrasound-assisted extraction to obtain mycosterols from Agaricus bisporus L. by response surface methodology and comparison with conventional Soxhlet extraction. *Food Chemistry, 197*, 1054-1063.

Holton, T. A. and Cornish, E. C. (1995). Genetics and Biochemistry of Anthocyanin Biosynthesis. *The Plant Cell, 7*(7), 1071-1083.

Hossain, S. M. Z. and Brennan, J. D. (2011). β-Galactosidase-Based Colorimetric Paper Sensor for Determination of Heavy Metals. *Analytical Chemistry, 83*(22), 8772-8778.

Hossain, S.Z., Luckham, R.E., Smith, A.M., Lebert, J.M., Davies, L.M., Pelton, R.H., Filipe, C.D. and Brennan, J.D. (2009). Development of a Bioactive Paper Sensor for Detection of Neurotoxins Using Piezoelectric Inkjet Printing of Sol−Gel-Derived Bioinks. *Analytical Chemistry, 81*(13), 5474-5483.

Hoyos-Leyva, Javier D., Bello-Pérez, Luis A., Alvarez-Ramirez, J., and Garcia, Hugo S. (2018). Microencapsulation using starch as wall material: A review. *Food Reviews International, 34*(2), 148-161.

Jampani, C., Naik, A. and Raghavarao, K.S.M.S. (2014). Purification of anthocyanins from jamun (*Syzygium cumini L.*) employing adsorption. *Separation and Purification Technology, 125*, 170-178.

Jang, S. and Xu, Z. (2009). Lipophilic and Hydrophilic Antioxidants and Their Antioxidant Activities in Purple Rice Bran. *Journal of Agricultural and Food Chemistry, 57*(3), 858-862.

Jung, H. J, and Jeong, Y. W. (2018). Gas sensor, refrigerator having the gas sensor and method of controlling the refrigerator: Google Patents.

Kalušević, A., Lević, S., Čalija, B., Pantić, M., Belović, M., Pavlović, V., Bugarski, B., Milić, J., Žilić, S. and Nedović, V. (2017). Microencapsulation of anthocyanin-rich black soybean coat extract by spray drying using maltodextrin, gum Arabic and skimmed milk powder. *Journal of Microencapsulation, 34*(5), 475-487.

Kohno, Y., Haga, E., Yoda, K., Shibata, M., Fukuhara, C., Tomita, Y., Maeda, Y. and Kobayashi, K. (2014). Adsorption behavior of natural anthocyanin dye on mesoporous silica. *Journal of Physics and Chemistry of Solids, 75*(1), 48-51.

Lacerda, E.C.Q., de Araújo Calado, V.M., Monteiro, M., Finotelli, P.V., Torres, A.G. and Perrone, D. (2016). Starch, inulin and maltodextrin as encapsulating agents affect the quality and stability of jussara pulp microparticles. *Carbohydrate Polymers, 151*, 500-510.

Lakkakula, N.R., Lima, M. and Walker, T. (2004). Rice bran stabilization and rice bran oil extraction using ohmic heating. *Bioresource Technology, 92*(2), 157-161.

Landbo, A. K. and Meyer, A. S. (2001). Enzyme-Assisted Extraction of Antioxidative Phenols from Black Currant Juice Press Residues (Ribes nigrum). *Journal of Agricultural and Food Chemistry, 49*(7), 3169-3177.

Laokuldilok, T., Shoemaker, C.F., Jongkaewwattana, S. and Tulyathan, V. (2011). Antioxidants and Antioxidant Activity of Several Pigmented Rice Brans. *Journal of Agricultural and Food Chemistry, 59*(1), 193-199.

Lapornik, B., Prošek, M. and Wondra, A.G. (2005). Comparison of extracts prepared from plant by-products using different solvents and extraction time. *Journal of food engineering, 71*(2), 214-222.

Li, Y.C., Ma, Z.L., Zhang, L.H., Meng, X.J. And Yu, N., (2009). Study on the microencapsualtion of blueberry anthocyanins by ethyl cellulose [J]. *Science and Technology of Food Industry, 9*.

Liana, Devi D., Raguse, B., Gooding, J. Justin, and Chow, E. (2012). Recent Advances in Paper-Based Sensors. *Sensors, 12*(9), 11505.

Lila, M. A. (2004). Anthocyanins and Human Health: An In Vitro Investigative Approach. *Journal of Biomedicine and Biotechnology, 2004*(5), 306-313.

Lim, C. G., Wong, L., Bhan, N., Dvora, H., Xu, P., Venkiteswaran, S., and Koffas, M. A. (2015). Development of a Recombinant Escherichia coli Strain for Overproduction of the Plant Pigment Anthocyanin. A*pplied and Environmental Microbiology, 81*(18), 6276-6284.

Listyarini, A., Sholihah, W. and Imawan, C. (2018). A paper-based Colorimetric Indicator Label using Natural Dye for Monitoring Shrimp Spoilage. Paper presented at the IOP Conference Series: *Materials Science and Engineering*.

Liu, X., Xu, Z., Gao, Y., Yang, B., Zhao, J. and Wang, L., (2007). Adsorption Characteristics of Anthocyanins from Purple-fleshed Potato (*Solanum tuberosum Jasim*) Extract on Macroporous Resins. *International Journal of Food Engineering* (Vol. 3).

Liu, X., Xiao, G., Chen, W., Xu, Y. and Wu, J., (2004). Quantification and purification of mulberry anthocyanins with macroporous resins. *BioMed Research International, 2004*(5), 326-331.

Lloyd, J.B., Siebenmorgen, T.J., and Beers, K.W. (2000). Effects of Commercial Processing on Antioxidants in Rice Bran. *Cereal Chemistry, 77*(5), 551-555.

Maran, J. Prakash, Priya, B., and Manikandan, S. (2014). Modeling and optimization of supercritical fluid extraction of anthocyanin and phenolic compounds from Syzygium cumini fruit pulp. *Journal of Food Science and Technology, 51*(9), 1938-1946.

McGhie, T. K., and Walton, M. C. (2007). The bioavailability and absorption of anthocyanins: towards a better understanding. *Molecular Nutrition & Food Research, 51*(6), 702-713.

Meireles, M. and Angela, A. (2008). *Extracting bioactive compounds for food products: theory and applications*: CRC press.

Min, B., Gu, L., McClung, A.M., Bergman, C.J. and Chen, M.H. (2012). Free and bound total phenolic concentrations, antioxidant capacities, and profiles of proanthocyanidins and anthocyanins in whole grain rice (*Oryza sativa L.*) of different bran colours. *Food Chemistry, 133*(3), 715-722.

Miyake, S., Takahashi, N., Sasaki, M., Kobayashi, S., Tsubota, K., and Ozawa, Y. (2012). Vision preservation during retinal inflammation by anthocyanin-rich bilberry extract: cellular and molecular mechanism. *Lab Invest, 92*(1), 102-109.

Nadar, Shamraja S., Rao, P. and Rathod, V. K. (2018). Enzyme assisted extraction of biomolecules as an approach to novel extraction technology: A review. *Food Research International, 108,* 309-330.

Nedovic, V., Kalusevic, A., Manojlovic, V., Levic, S. and Bugarski, B. (2011). An overview of encapsulation technologies for food applications. *Procedia Food Science, 1*, 1806-1815.

Norberto, S., Silva, S., Meireles, M., Faria, A., Pintado, M. and Calhau, C. (2013). Blueberry anthocyanins in health promotion: A metabolic overview. *Journal of Functional Foods, 5*(4), 1518-1528.

Obón, J. M., Castellar, M. R., Alacid, M., and Fernández-López, J. A. (2009). Production of a red–purple food colorant from Opuntia stricta fruits by spray drying and its application in food model systems. *Journal of Food Engineering, 90*(4), 471-479.

Okoh, O. O., Sadimenko, A. P., and Afolayan, A. J. (2010). Comparative evaluation of the antibacterial activities of the essential oils of Rosmarinus officinalis L. obtained by hydrodistillation and solvent free microwave extraction methods. *Food Chemistry, 120*(1), 308-312.

Osorio, C., Acevedo, B., Hillebrand, S., Carriazo, J., Winterhalter, P. and Morales, A.L. (2010). Microencapsulation by spray-drying of anthocyanin pigments from corozo (*Bactris guineensis*) fruit. *Journal of Agricultural and Food Chemistry, 58*(11), 6977-6985.

Paes, J., Dotta, R., Barbero, G.F. and Martínez, J., (2014). Extraction of phenolic compounds and anthocyanins from blueberry (*Vaccinium myrtillus L.*) residues using supercritical CO2 and pressurized liquids. *The Journal of Supercritical Fluids, 95*, 8-16.

Paiva, F.F., Vanier, N.L., Berrios, J.D.J., Pan, J., de Almeida Villanova, F., Takeoka, G. and Elias, M.C. (2014). Physicochemical and nutritional properties of pigmented

rice subjected to different degrees of milling. *Journal of Food Composition and Analysis, 35*(1), 10-17.

Pan, Z., Qu, W., Ma, H., Atungulu, G.G. and McHugh, T.H. (2011). Continuous and pulsed ultrasound-assisted extractions of antioxidants from pomegranate peel. *Ultrasonics Sonochemistry, 18*(5), 1249-1257.

Pap, N., Beszédes, S., Pongrácz, E., Myllykoski, L., Gábor, M., Gyimes, E., Hodúr, C. and Keiski, R.L., (2013). Microwave-Assisted Extraction of Anthocyanins from Black Currant Marc. *Food and Bioprocess Technology, 6*(10), 2666-2674.

aula, J.T., Paviani, L.C., Foglio, M.A., Sousa, I.M., Duarte, G.H., Jorge, M.P., Eberlin, M.N. and Cabral, F.A., (2014). Extraction of anthocyanins and luteolin from Arrabidaea chica by sequential extraction in fixed bed using supercritical CO2, ethanol and water as solvents. *The Journal of Supercritical Fluids, 86*, 100-107.

Pedro, A.C., Granato, D. and Rosso, N.D. (2016). Extraction of anthocyanins and polyphenols from black rice (*Oryza sativa L.*) by modeling and assessing their reversibility and stability. *Food Chemistry, 191*, 12-20.

Pereira-Caro, G., Watanabe, S., Crozier, A., Fujimura, T., Yokota, T. and Ashihara, H. (2013). Phytochemical profile of a Japanese black–purple rice. *Food Chemistry, 141*(3), 2821-2827.

Pingret, D., Fabiano-Tixier, Anne-Sylvie, and Chemat, F. (2013). Ultrasound-assisted extraction. *Natural Product Extraction: Principles and Applications, 21*, 89.

Pojer, E., Mattivi, F., Johnson, D. and Stockley, C.S., (2013). The Case for Anthocyanin Consumption to Promote Human Health: A Review. *Comprehensive Reviews in Food Science and Food Safety, 12*(5), 483-508.

Puri, M., Sharma, D. and Barrow, C. J. (2012). Enzyme-assisted extraction of bioactives from plants. *Trends in Biotechnology, 30*(1), 37-44.

Repo-Carrasco-Valencia, R., Peña, J., Kallio, H., and Salminen, S. (2009). Dietary fiber and other functional components in two varieties of crude and extruded kiwicha (*Amaranthus caudatus*). *Journal of Cereal Science, 49*(2), 219-224.

Riaz, M. N, Asif, M. and Ali, R. (2009). Stability of vitamins during extrusion. *Critical Reviews in Food Science and Nutrition, 49*(4), 361-368.

da Rosa, J.R., Nunes, G.L., Motta, M.H., Fortes, J.P., Weis, G.C.C., Hecktheuer, L.H.R., Muller, E.I., de Menezes, C.R. and da Rosa, C.S. (2019). Microencapsulation of anthocyanin compounds extracted from blueberry (Vaccinium spp.) by spray drying: Characterization, stability and simulated gastrointestinal conditions. *Food Hydrocolloids, 89*, 742-748.

Robert, P., Gorena, T., Romero, N., Sepulveda, E., Chavez, J. and Saenz, C. (2010). Encapsulation of polyphenols and anthocyanins from pomegranate (Punica granatum) by spray drying. *International Journal of Food Science & Technology*, *45*(7), 1386-1394.

Romero-Cascales, I., Fernández-Fernández, J.I., López-Roca, J.M. and Gómez-Plaza, E. (2005). The maceration process during winemaking extraction of anthocyanins from grape skins into wine. *European Food Research and Technology, 221*(1-2), 163-167.

Rouquerol, J., Rouquerol, F., Llewellyn, P., Maurin, G. and Sing, K.S. (2013). *Adsorption by powders and porous solids: principles, methodology and applications*: Academic press.

Ruiz-Gutiérrez, M., Amaya-Guerra, C., Quintero-Ramos, A., Pérez-Carrillo, E., Ruiz-Anchondo, T., Báez-González, J. and Meléndez-Pizarro, C. (2015). Effect of extrusion cooking on bioactive compounds in encapsulated red cactus pear powder. *Molecules, 20*(5), 8875-8892.

Ruthven, D. M. (1984). *Principles of adsorption and adsorption processes*: John Wiley and Sons.

Santana-Méridas, O., Polissiou, M., Izquierdo-Melero, M.E., Astraka, K., Tarantilis, Petros A., Herraiz-Peñalver, D., and Sánchez-Vioque, R. (2014). Polyphenol composition, antioxidant and bioplaguicide activities of the solid residue from hydrodistillation of *Rosmarinus officinalis L*. *Industrial Crops and Products, 59*, 125-134.

Scordino, M., Di Mauro, A., Passerini, A. and Maccarone, E. (2004). Adsorption of Flavonoids on Resins: Cyanidin 3-Glucoside. *Journal of Agricultural and Food Chemistry, 52*(7), 1965-1972.

Shahidi, F., and Han, X. Q. (1993). Encapsulation of food ingredients. *Critical Reviews in Food Science and Nutrition, 33*(6), 501-547.

Shao, Y., Xu, F., Sun, X., Bao, J. and Beta, T., (2014). Identification and quantification of phenolic acids and anthocyanins as antioxidants in bran, embryo and endosperm of white, red and black rice kernels (*Oryza sativa L.*). *Journal of Cereal Science, 59*(2), 211-218.

Shih, P. H., Chan, Y. C., Liao, J. W., Wang, M. F., and Yen, G. C. (2010). Antioxidant and cognitive promotion effects of anthocyanin-rich mulberry (Morus atropurpurea L.) on senescence-accelerated mice and prevention of Alzheimer's disease. *The Journal of Nutritional Biochemistry, 21*(7), 598-605.

Shukla, V., Kandeepan, G., Vishnuraj, M.R. and Soni, A. (2016). Anthocyanins Based Indicator Sensor for Intelligent Packaging Application. *Agricultural Research, 5*(2), 205-209.

Singh, S., Gamlath, S. and Wakeling, L. (2007). Nutritional aspects of food extrusion: a review. *International Journal of Food Science & Technology, 42*(8), 916-929.

Siriwoharn, T., Wrolstad, R.E., Finn, C.E. and Pereira, C.B. (2004). Influence of Cultivar, Maturity, and Sampling on Blackberry (*Rubus L. Hybrids*) Anthocyanins, Polyphenolics, and Antioxidant Properties. *Journal of Agricultural and Food Chemistry, 52*(26), 8021-8030.

Soquetta, M.B., Terra, L.D.M. and Bastos, C.P. (2018). Green technologies for the extraction of bioactive compounds in fruits and vegetables. *CyTA - Journal of Food, 16*(1), 400-412.

Takhellambam, R.D., Chimmad, B.V. and Prkasam, J.N. (2016). Ready-to-cook millet flakes based on minor millets for modern consumer. *Journal of Food Science and Technology, 53*(2), 1312-1318.

Tonon, R.V., Brabet, C. and Hubinger, M.D., (2010). Anthocyanin stability and antioxidant activity of spray-dried açai (*Euterpe oleracea Mart.*) juice produced with different carrier agents. *Food Research International, 43*(3), 907-914.

Turkmen, N., Sari, F. and Velioglu, Y.S. (2005). The effect of cooking methods on total phenolics and antioxidant activity of selected green vegetables. *Food Chemistry, 93*(4), 713-718.

Vasserot, Y., Caillet, S., and Maujean, A. (1997). Study of Anthocyanin Adsorption by Yeast Lees. Effect of Some Physicochemical Parameters. *American Journal of Enology and Viticulture, 48*(4), 433-437.

Veggi, Priscilla C., Santos, Diego T., and Meireles, M. A. A. (2011). Anthocyanin extraction from Jabuticaba (*Myrciaria cauliflora*) skins by different techniques: economic evaluation. *Procedia Food Science, 1*, 1725-1731.

da Silva, B.V., Barreira, J.C. and Oliveira, M.B.P. (2016). Natural phytochemicals and probiotics as bioactive ingredients for functional foods: Extraction, biochemistry and protected-delivery technologies. *Trends in Food Science & Technology, 50*, 144-158.

Wallace, T. C. (2011). Anthocyanins in Cardiovascular Disease. *Advances in Nutrition, 2*(1), 1-7.

Wang, L. and Weller, C. L. (2006). Recent advances in extraction of nutraceuticals from plants. *Trends in Food Science & Technology, 17*(6), 300-312.

Weber, F., Boch, K. and Schieber, A. (2017). Influence of copigmentation on the stability of spray dried anthocyanins from blackberry. *LWT, 75*, 72-77.

White, B. L., Howard, L. R., and Prior, R. L. (2010). Polyphenolic composition and antioxidant capacity of extruded cranberry pomace. *Journal of Agricultural and Food Chemistry, 58*(7), 4037-4042.

Williams, J. and Myers, K. (2005). Compositions for detecting food spoilage and related methods: Google Patents.

Wrolstad, R.E. (2004). Anthocyanin pigments—Bioactivity and coloring properties. *Journal of Food Science, 69*(5), C419-C425.

Wu, N.N., Li, H.H., Tan, B., Zhang, M., Xiao, Z.G., Tian, X.H., Zhai, X.T., Liu, M., Liu, Y.X., Wang, L.P. and Gao, K. (2018). Free and bound phenolic profiles of the bran from different rice varieties and their antioxidant activity and inhibitory effects on α-amylose and α-glucosidase. *Journal of Cereal Science, 82*, 206-212.

Wu, Y., Han, Y., Tao, Y., Fan, S., Chu, D.T., Ye, X., Ye, M. and Xie, G. (2018). Ultrasound assisted adsorption and desorption of blueberry anthocyanins using macroporous resins. *Ultrasonics Sonochemistry, 48*, 311-320.

Xu, Q., Zhou, Y., Wu, Y., Jia, Q., Gao, G. and Nie, F. (2016). Enzyme-assisted solvent extraction for extraction of blueberry anthocyanins and separation using resin adsorption combined with extraction technologies. *International Journal of Food Science and Technology, 51*(12), 2567-2573.

Yan, Y., Li, Z., and Koffas, M. A. (2008). High-yield anthocyanin biosynthesis in engineered Escherichia coli. *Biotechnol Bioeng, 100*(1), 126-140.

Yan, Y., Chemler, J., Huang, L., Martens, S. and Koffas, M.A. (2005). Metabolic engineering of anthocyanin biosynthesis in Escherichia coli. *Applied and environmental microbiology, 71*(7), 3617-3623.

Yang, Z. and Zhai, W. (2010). Optimization of microwave-assisted extraction of anthocyanins from purple corn (*Zea mays L.*) cob and identification with HPLC–MS. *Innovative Food Science & Emerging Technologies, 11*(3), 470-476.

Yoshida, C.M., Maciel, V.B.V., Mendonça, M.E.D. and Franco, T.T. (2014). Chitosan biobased and intelligent films: Monitoring pH variations. *LWT-Food Science and technology, 55*(1), 83-89.

Yoshida, K., Mori, M., and Kondo, T. (2009). Blue flower color development by anthocyanins: from chemical structure to cell physiology. *Natural product reports, 26*(7), 884-915.

Yuliani, S., Torley, P.J., D'Arcy, B., Nicholson, T. and Bhandari, B. (2006). Extrusion of mixtures of starch and d-limonene encapsulated with β-cyclodextrin: Flavour retention and physical properties. *Food Research International, 39*(3), 318-331.

Zhai, X., Shi, J., Zou, X., Wang, S., Jiang, C., Zhang, J., Huang, X., Zhang, W. and Holmes, M., (2017). Novel colorimetric films based on starch/polyvinyl alcohol incorporated with roselle anthocyanins for fish freshness monitoring. *Food Hydrocolloids, 69*, 308-317.

hang, H.F., Yang, X.H. and Wang, Y. (2011). Microwave assisted extraction of secondary metabolites from plants: Current status and future directions. *Trends in Food Science & Technology, 22*(12), 672-688.

Zhang, L., Mou, D. and Du, Y. (2007). Procyanidins: extraction and micro- encapsulation. *Journal of the Science of Food and Agriculture, 87*(12), 2192-2197.

Zhang, M.W., Zhang, R.F., Zhang, F.X. and Liu, R.H., (2010). Phenolic Profiles and Antioxidant Activity of Black Rice Bran of Different Commercially Available Varieties. *Journal of Agricultural and Food Chemistry, 58*(13), 7580-7587.

Zhang, M., Zheng, B., Yuan, H. and Xiao, D. (2010). A spectrofluorimetric sensor based on grape skin tissue for determination of iron (III). *Bulletin of the Chemical Society of Ethiopia*, *24*(1).

MATERIALS AND METHODS

CHAPTER 2

MATERIALS AND METHODS

This chapter discusses experimental procedures, use of different chemicals and reagents, and operating conditions for the extraction, adsorption/desorption, microencapsulation of anthocyanin, extrusion of rice flour with microencapsulate and indicator fabrication. It includes the estimation of physical, physicochemical and phytochemical properties such as water activity, density, size, solubility, adsorption/desorption, total phenolic content, anthocyanin, antioxidant activity, functional group, and elemental analyses, etc. The chapter also describes the experimental procedure of rheological and morphological properties of the microencapsulated anthocyanin. The fabrication and efficacy study of anthocyanin based pH-sensitive paper indicator is explained in this chapter. The optimization of the process parameters using the rotatable central composite design, followed by response surface methodology (RSM) has also been deliberated in this chapter. At the end of this chapter, artificial neural networks (ANN) and statistical approaches are also discussed.

2.1. Materials and methods

2.1.1. Raw materials

Purple rice (local name *Chakhao poireiton*) and black rice (local name *Chakhao ambu*) (**Fig. 2.1**) are the most endogenous rice variety in India, especially in North east India. The bran of these rice contains a very high amount of phytochemicals, such as tocopherols, tocotrienols, oryzanols, vitamin B complex and phenolic compounds (Min et al., 2011). In addition to that purple and black rice bran contents anthocyanin and pro-anthocyanidin (Paiva et al., 2014). These phytochemicals are known as bioactive compounds, which can improve human health and immunity (Farnsworth, 1966).

Fig. 2.1: Pictorial view of a) purple rice b) black rice

Therefore, in the present study, black and purple rice cultivars were procured from the local market of Imphal, Manipur, India (24.82º North Latitude and 93.95º East Longitude). The rice bran was separated using the polishing machine. The separated bran was passed through the 72BSS sieve and the particle size varied from 49.3-209.8 µm and 35.8-206.7 µm for purple and black rice bran, respectively (In appendix **Fig. 1A1**). The samples were packed in zip lock polyethylene bag and stored at ambient temperature (28 ± 2 ºC).

2.1.2. Chemicals

All the chemicals used in this study were of analytical grades and used without further purification. The chemicals and/or any reagents used for specific applications are detailed below.

Chemical used for the conventional extraction of phenolic content

Chemicals such as β-carotene, caffeic acid, catechin hydrate, chlorogenic acid, coumeric acid, trans-ferulic acid, 4-hydroxybenzoic acid, syringic acid, sinapic acid, vanillic acid, gallic acid, 2, 2-diphenyl-1-picrylhydrazyl (DPPH) and Folin–Ciocalteu reagent were purchased from Sigma–Aldrich (Wicklow, Ireland) and were used without any further purification. C_2H_5OH, H_2O_2, $(CH_3)_2CO$, $K_2Fe(CN)_6$, $NaNO_2$, Na_2CO_3, NaOH, $FeCl_3$, $FeCl_2$ and $AlCl_3$ were purchased from Sisco Research Laboratory Pvt. Ltd. (Mumbai, Maharashtra, India).

Chemical used for the ultrasound assisted extraction of phenolic content and anthocyanin

Chemicals such as β-Carotene, tocopherol, tocotrienol, cyanidin-3-glucoside, peonidin-3-D-glucoside, caffeic acid, catechin hydrate, chlorogenic acid, coumaric acid, trans-ferulic acid, 4-hydroxybenzoic acid, syringic acid, sinapic acid, vanillic acid, gallic acid, 2, 2-diphenyl-1-picrylhydrazyl (DPPH) and folin–ciocalteu reagent were purchased from Sigma–Aldrich (Wicklow, Ireland). Ethanol, methanol and acetonitrile, Na_2CO_3, and NaOH were purchased from Sisco Research Laboratory Pvt. Ltd. (Mumbai, Maharashtra, India).

Chemical used for the adsorption/desorption study of anthocyanin

The phenolic standards, namely, cyanidin-3-glucoside, peonidin-3-glucoside, caffeic acid, catechin hydrate, chlorogenic acid, vanillic acid, syringic acid, sinapic acid and 4-hydroxybenzoic acid were purchased from Sigma–Aldrich (Wicklow, Ireland). The adsorbents

were used in the experiment such as Amberlite XAD2, Amberlite XAD4, Amberlite XAD7, activated charcoal and bentonite reagents were also purchased from Sigma–Aldrich (Wicklow, Ireland). The characteristics of adsorbents are shown in **Table 2.1.** HPLC grade formic acid, ethanol, and methanol were purchased from Sisco Research Laboratories Pvt. Ltd. (Mumbai, Maharashtra, India).

Chemical used for the degradation study of anthocyanin

The cyanidin-3-glucoside and peonidin-3-glucoside were purchased from Sigma–Aldrich (Wicklow, Ireland). The hydrocolloids, such as carboxymethyl cellulose, xanthan gum, and gum acacia were purchased from Sigma–Aldrich (Wicklow, Ireland). Modified starch was prepared from rice starch according to the method described by Hu et al., (2013). Starch (25 g) with the moisture content of 10 % (db) was mixed in 100 mL of anhydrous 1-butanol and then added 1 mL of concentrated (36 % v/v) hydrochloric acid into the mixture to start the reaction. The modification was conducted at 40 °C for 4 h. The reaction was stopped by adding 14 mL of 1M sodium bicarbonate. The solution was cooled in ice bath for 15 min and centrifuged at 3500 g for another 10 min. The precipitate was washed four times with 50 % ethanol and dried in at 45 °C to maintain 10 % (db) of moisture.

Chemical used for the microencapsulation study of anthocyanin

The 2, 2-diphenyl-1-picrylhydrazyl was supplied by Sigma Aldrich (Wicklow, Ireland). Ethanol, and NaOH were purchased from Sisco Research Laboratory Pvt. Ltd. (Mumbai, Maharashtra, India).

Chemical used for the extrudate product development

The 2, 2-diphenyl-1-picrylhydrazyl was purchased from Sigma–Aldrich (Wicklow, Ireland). Lithium chloride, Magnesium chloride, Potassium carbonate, Magnesium nitrate, Potassium iodide, Sodium chloride, Potassium chloride, and Potassium sulfate were purchased from Sisco Research Laboratories Pvt. Ltd, India.

Table 2.1: Characteristics of adsorbents

Adsorbent	Chemical nature	Specific surface area (m^2/g)	Ionic propertie	Structure
XAD2	Hydrophobic crosslinked polystyrene copolymer resin	330	Nonionic	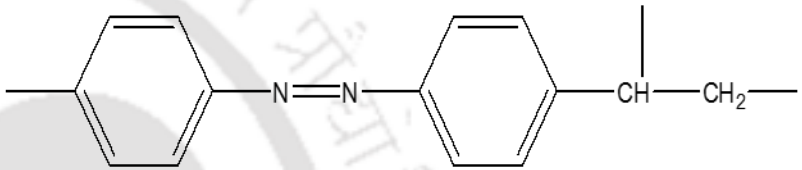
XAD4	Hydrophobic crosslinked polystyrene-divinylbenzene	725	Nonionic	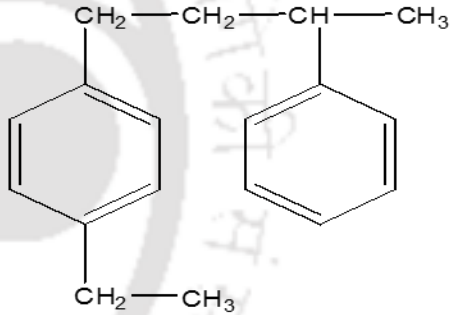
XAD7	Acrylic ester	450	Nonionic	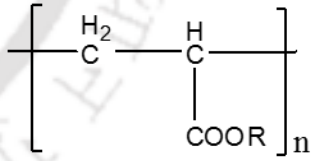
Charcoal	Carbon	500	Nonionic	----------
Bentonite	Hydrophilic Bentonite	750	Hydrophilic	----------

2.1.3. Phytochemical profiling

The phytochemical properties of rice bran extract and microencapsulate were measured in terms of the total phenolics, monomeric anthocyanin, flavonoid and phenolic acids content.

2.1.3.1. Total phenolic contents

The total phenolic contents (TPC) of the rice bran extracts were estimated using Folin–Ciocalteu assay (Moongngarm et al., 2012). The different concentration of gallic acid (0-1000 µg/mL) solution was used for standard curve preparation (**Fig. 2.2**). Initially, 20 µL of each extract was taken in a test tube containing 1.58 mL of distilled water. Then, 100 µL of FC reagent and 300 µL of Sodium carbonate were added within 8 min. The mixture was vortexed and incubated for 30 min at 40 °C. Similarly, the blank samples were prepared where 20 µL of ethanol was used instead of extract. The color of the sample was changed from yellowish to bluish depending upon the concentration of phenolic compounds. The UV-Visible spectrophotometer (Make: Thermo Fisher Scientific, Waltham, Massachusetts, USA; Model: UV-2600) was used to measure the absorbance at 765 nm and the TPC was measured as mg gallic acid equivalent/100 g sample.

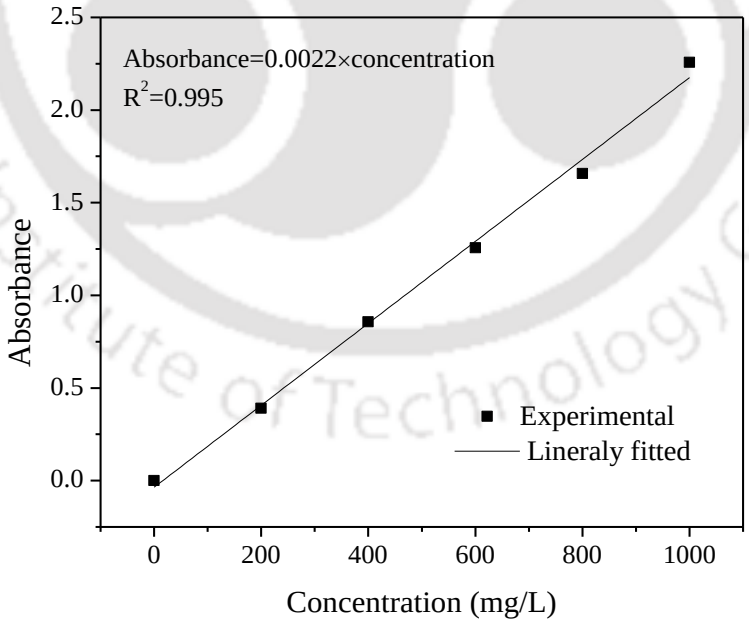

Fig. 2.2: Calibration curve for the determination of total phenolic content

2.1.3.2. Monomeric anthocyanin content

The pH differential method was used to estimate monomeric anthocyanin content in the rice bran extracts (Harakotr et al., 2014). A UV-VIS Spectrophotometer (Make: Thermo Fisher Scientific, Waltham, Massachusetts, USA; Model: UV-2600) was used to measure the absorbance of sample at 515 and 700 nm. Monomeric anthocyanin was expressed as cyanidin-3-glucoside (C3G) equivalent. The molar absorptivity coefficient and molecular weight of C3G is 26,900 and 449.2, respectively.

$$A = (A_{515} - A_{700})_{pH1.0} - (A_{515} - A_{700})_{pH4.5} \quad (2.1)$$

$$\text{Anthocyanin content} \left(\frac{\text{mg}}{\text{L}}\right) = \frac{A \times MW \times DF \times 1000}{\varepsilon \times l} \quad (2.2)$$

Where, DF is dilution factor, MW is molecular weight of C3G, l is path length, and ε is molar absorptivity coefficient.

2.1.3.3. Flavonoid content

Total flavonoid content was measured using the colorimetric assay method adapted as described by Zhishen et al. (1999).

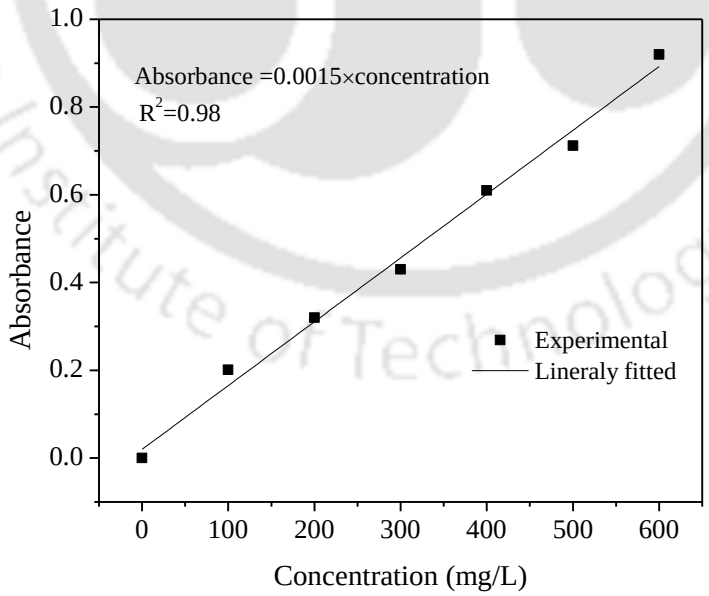

Fig. 2.3: Calibration curve for the determination of flavonoid

Initially, 150 µL of 5 % (w/v) aqueous $NaNO_2$ was added in 2.5 mL of extract. After 5 min, 150 µL of 10 % (w/v) aqueous $AlCl_3$ was added, followed by 1 mL of 1M NaOH. The mixture was allowed to stand for 15 min, and absorbance was measured at 510 nm against the blank (80 % v/v methanol) sample. Total flavonoid was calculated as quercetin equivalent from a standard curve (**Fig. 2.3**) of quercetin (0–600 µg/mL) and expressed as mg of quercetin/g sample.

2.1.3.4. Antioxidant properties

Various antioxidant properties, namely, 2, 2-diphenyl-1-picrylhydrazyl (DPPH) radical-scavenging activity, reducing power, iron chelating power and hydrogen peroxide scavenging activity of the samples were measured.

2.1.3.4.1. 2, 2-diphenyl-1-picrylhydrazyl scavenging activity for liquid

The DPPH scavenging activity of the extract was measured as described by Wojdyło et al. (2007) with modification. For the DPPH radical-scavenging activity, 100 µL of extracts were taken and added to 1.4 mL DPPH methanolic solution (10^{-4} M). After 30 min of incubation, absorbance was taken at 517 nm using a spectrophotometer (Make: Thermo Fisher Scientific, Waltham, Massachusetts, USA; Model: UV-2600) and compared with the blank sample. The DPPH radical-scavenging activity was expressed in percentage.

2.1.3.4.2. 2, 2-diphenyl-1-picrylhydrazyl scavenging activity for powder

The DPPH scavenging activity of powder was measured according to Luo et al. (2009) with some modifications. For analysis, 15 mg of microencapsulated powder was dissolved in 3 mL ethanol: acetic acid: water mixture (50:8:42, v/v). The mixture was filtered through a 0.45 µm filter paper and diluted with methanol. The 100 µL filtrate was taken and added to 1.4 mL DPPH radical methanolic solution (10^{-4} M). The absorbance was measured at 517 nm using a spectrophotometer (Make: Thermo Fisher Scientific, Waltham, Massachusetts, USA; Model: UV-2600). The absorbance of the control was obtained by replacing the sample with ethanol. The DPPH radical scavenging activity of the sample was calculated as follows.

$$\text{Radical scavanging activity} = \frac{A_o - A_s}{A_o} \times 100 \qquad (2.3)$$

Where, A_o is absorbance of control blank, and A_s is absorbance of sample extract.

2.1.3.4.3. Reducing power

For reducing power of the extract, 1 mL sample was mixed with 2.5 mL 0.2 M sodium phosphate buffer (pH 6.6) and 2.5 mL 1 % $K_2Fe(CN)_6$. The mixture was then incubated at 50 °C for 20 min. Then 2.5 mL 10 % trichloroacetic acid was added to the mixture and centrifuged at 2200 g for 5 min. The 2.5 mL of supernatant solution was mixed with 5.0 mL distilled water and 0.5 mL 0.1 % $FeCl_3$. At 700 nm, absorbance was measured using a spectrophotometer (Make: Thermo Fisher Scientific, Waltham, Massachusetts, USA; Model: UV-2600). The reducing power of the extract was expressed in percentage. The mechanism of reducing power as follows (Canabady-Rochelle et al., 2015):

$$2\ Fe(CN)_6^{3-} + C_6H_8O_6 - \rightarrow 2\ Fe(CN)_6^{4-} + C_6H_7O_6 + H^+$$

Ferricyanide Ascorbate Ferrocyanide Dehydroascorbate

$$4\ Fe^{3+} + 3\ Fe(CN)_6^{4-} \rightarrow Fe_4[Fe(CN)_6]_3$$

Ferric ion Ferrocyanide Prussian blue

2.1.3.4.4. Iron chelating power

For iron chelating activity, the rice bran extract (3.7 mL) was incubated with $FeCl_2$ (0.1 mL, 2 mM) for 3 min followed by the addition of a ferrozine solution (0.2 mL, 5 mM). After the mixture reached equilibrium (10 min, room temperature), absorbance was measured spectrophotometrically at 562 nm. The ability of each sample to inhibit the formation of the ferrous iron–ferrozine complex, expressed as its Fe^{2+} chelating activity (%) (Canabady-Rochelle et al., 2015).

$$Fe^{2+} + 3\ Ferrozine^{2-} \rightarrow Fe(Ferrozine)_3^{4-}$$

Chelator Chelator-Fe^{2+}

2.1.3.4.5. Hydrogen peroxide scavenging activity

For hydrogen peroxide scavenging capacity (Ruch et al., 1989), a solution of hydrogen peroxide (40 mM) was prepared in phosphate buffer (pH 7.4). Extracts (100 µg/mL) were added to a hydrogen peroxide solution (0.6 mL, 40 mM) and absorbance of hydrogen peroxide at 230 nm was taken against a blank solution containing the phosphate buffer without hydrogen peroxide. Samples were investigated within the 0–100 µg/mL concentration range and all samples were run in triplicate.

2.1.3.5. GC-MS analysis of extract

The GC-MS analysis of extracts was performed on a Varian Saturn 2200 GC/MS (Make: Agilent, California, United States) fitted with a flame ionization detector (FID) and 30 mm × 0.25 mm WCOT column coated with 0.25 µm thickness film (DB-5). The oven temperature was ranged from 40 °C (hold for 2 min) to 280 °C at a rate of 5 °C/min. The samples were diluted with an appropriate solvent (1/10, v/v) and filtered through 0.2 µm syringe filter. The particle-free diluted 1 µL extracts were taken and injected into the injector. All data were collected after the full-scan mass spectra within the scan range of 35-600 m/z. The percentage composition of the extract constituents was expressed as a percentage peak area. The peak identification was carried out with standards available in mass spectrum libraries.

2.1.3.6. β-Carotene, tocopherol, and tocotrienol

The β-Carotene, tocopherol, and tocotrienol contents were determined using the method described by Laokuldilok et al. (2011). The β-carotene, tocopherol, and tocotrienol were analyzed using Ultimate 3000 Liquid Chromatography Systems (Make: Waltham, Massachusetts, United States) with a UV detector. The C_{18} (5 µm, 120Å) column was used with a size of 4.6 (dia) × 250 (length) mm. The mobile phase was the mixture of methanol and acetonitrile (15:85 v/v) and used with the isocratic mode at a flow rate of 2 mL/min. The injection volume was 20 µL, and the temperature was maintained at 25 °C. The detector was set at 292 nm for the detection of β-carotene, tocopherol, and tocotrienol. The β-carotene, tocopherol, and tocotrienol were identified and quantified on the basis of their peak areas and comparison with a calibration curve obtained with the corresponding standards using chameleon ver. 6.80 software.

2.1.3.7. Cyanidin-3-glucoside and peonidin-3-glucoside

The cyanidin-3-glucoside (C3G) and peonidin-3-glucoside (P3G) were analyzed using the same detector and procedure as described above (section 2.1.3.6). Except for C3G and P3G analysis the mobile phase used was water, methanol, and formic acid (75:20:5 v/v) mixture with isocratic elution at 0.5 mL/min flow rate. The detection was carried out at 530 nm with a sample loop of 20 µL. The standards of C3G and P3G were used to quantify the components in the extract and data was analyzed using chameleon ver. 6.80 software.

2.1.3.8. Phenolic acid

The phenolic acid content was analyzed in terms of caffeic acid, catechin hydrate, chlorogenic acid, vanillic acid, syringic acid, sinapic acid, and 4-hydroxybenzoic acid using HPLC. The phenolic acid analysis was carried out using the detector and procedure same as that used in the analysis of β-carotene, tocopherol, and tocotrienol. For phenolic acid analysis, the mobile phase eluent A was acidified water of pH 2.64 (with the dilute hydrochloric acid), and eluent B was the mixture of acidified water and acetonitrile of 20:80 ratios. The total run time was 30 min at a flow rate of 1.5 mL/min. The phenolic acids were identified and quantified using the various phenolic acids standard.

2.1.4. Physicochemical properties

2.1.4.1. Water activity

The water activity of the samples were measured using a water activity meter (Make: Aqualab Pullman, USA; Model: 4TE).

2.1.4.2. Bulk density

The bulk density of samples were determined using the method described by Gupta and Das (1997). A 500 mL measuring cylindrical was filled with the sample from a height of 150 mm at a constant rate and then weighing the contents.

2.1.4.3. True density

The true density of the extrudate was measured using a gas pycnometer (Model: PYC-100A, Porous Materials Inc, Make: Ithaca, New York, USA). 3 g of sample was placed in the measuring chamber and air at certain pressure was expanded into the chamber, and the pressure was measured. The pressure of the empty chamber was also measured. The difference in the two pressures combined with the known volume of the empty sample chamber allows the volume of the sample to be determined using the gas law.

2.1.4.4. Water solubility index (WSI)

The WSI of the extrudate was determined as described by Holguín-Acuña et al. (2008). A 2.5 g ground sample was mixed with 30 mL of water at 30 °C, in a 50 mL pre-weighed centrifuge tube. The tube was stirred intermittently for 30 min and centrifuged at 3000 rpm (314.1 rad/s) for 10 min. The supernatant liquid was carefully poured into a pre-weighed

evaporating dish. The amount of dried solids recovered by evaporating the supernatant from the water absorption test was expressed as a percentage of dry solids in the 2.5 g sample and defined as the WSI.

2.1.4.5. Porosity

Porosity is the percentage of void space in the bulk sample, which is not occupied by the sample (Mahdavi et al., 2016). Porosity was calculated using the relationship between the bulk density and true density as follows

$$\varepsilon = \frac{\rho_t - \rho_b}{\rho_t} \times 100 \qquad (2.4)$$

Where, ρ_t is true density, ρ_b is bulk density and ε is porosity.

2.1.4.6. Hausner ratio

The Hausner ratio was determined using the standard procedure (Mahdavi et al., 2016) as follows.

$$\text{Hausner ratio (HR)} = \frac{v_t}{v_b} \qquad (2.5)$$

Where, v_t is tap volume and v_b is bulk volume.

Difference ranges for HR in defining the flowability is as below:

(i) 1.0<HR<1.1, free flowing powder

(ii) 1.1<HR<1.25, medium flowing powder

(iii) 1.25<HR<1.4, difficult flowing powder

(iv) HR>1.4, very difficult flowing powder

2.1.4.7. Encapsulation efficiency

The encapsulation efficiency of the sample was measured using the method described by Mahdavi et al. (2016). To estimate the efficiency, total anthocyanin content (TAC) and surface anthocyanin content (SAC) of the microcapsules were measured. For the analysis, 1 mL of distilled water was added to 100 mg of sample and the microencapsulate was crushed in a mortar pestle. Then, the sample was extracted using 10 mL of ethanol. The extraction of surface anthocyanin from the microcapsules was carried out by quickly washing with 10 mL

ethanol in a vortex within 10 s, followed by centrifugation at 3000 rpm (314.1 rad/s) for 3 min at 20 °C. After separation, both the clear supernatants were collected and filtered through 0.45 µm filter paper and used for anthocyanin determination.

$$\text{Encapsulation efficiency (\%)} = \frac{(TAC - SAC)}{TAC} \times 100 \quad (2.6)$$

2.1.4.8. Specific mechanical energy

Specific mechanical energy (SME) was determined by measuring the torque and the screw speed at a constant mass flow rate (Fang et al., 2014). The equation for specific mechanical energy is as follows:

$$\text{Specific mechanical energy (kJ/kg)} = \frac{2\pi \times n \times T}{Mass\ flow\ rate} \quad (2.7)$$

where, n is the screw speed and T is the motor torque.

2.1.4.9. Color

Hunter Colorimeter (Make: HunterLab, Reston, Virginia, Model: ColorLab Ultrascan Vis) was used to measure the color of the sample. The *L*, *a*, and *b* values were recorded as the mean of three replicates. The *L*-value signifies the light and dark color where a low number (0-50) indicates dark and a high number (51-100) indicates light. The *a*-value ranges from red to green, where a positive number indicates red and a negative number indicates green. The *b*-values represents the yellow and blue color, where a positive number indicates yellow and a negative number indicates blue.

2.1.4.10. Cooking yield, cooking loss, and optimal cooking time

The cooking time of the sample was determined using the AACC method 66-50 (AACC, 2000). Briefly, 10 g of sample was cooked in 300 mL of boiling distilled water. Optimum cooking time was determined when the core in the sample was still present but disappeared after squeezing between two plates.

Cooking loss of the sample was determined according to the AACC 66-50 method (AACC, 2000). Drain the cooked sample for 15 min and the weight was measured. The sample was weighed individually before and after cooking. The drained water was then poured in petri-dish of a known weight and dried at 105 °C to obtain the dried sample in the cooking water.

The cooking yield was calculated as follows:

$$\text{Cooking yield (\%)} = \frac{\text{Weight of cooked extrudate}}{\text{Weight of fresh dry extrudate}} \times 100 \quad (2.8)$$

The cooking loss was calculated as follows:

$$\text{Cooking loss (\%)} = \frac{\text{Weight before cooking-Weight after cooking}}{\text{Weight before cooking}} \times 100 \quad (2.9)$$

2.1.4.11. Thermal properties

A Differential scanning calorimetry instrument (Make: NETZSCH, Selb, Germany; Model: DSC 214) was used to determine the thermal properties of the sample. The temperature varied from 30 to 250 °C with 10 °C/min rate. The onset, endset, and peak temperature of the powder were measured and analysed using the DSC instrument's software.

2.1.4.12. X-Ray diffraction

The crystallinity of the microencapsulated powder was studied at 35 kV and 20 mA Cu-Ka radiation in an X-ray diffractometer (Make: Bruker Axs, Karlsruhe, Germany; Model: D8 FOCUS). Data were recorded over an angular range of 2° to 50° (2θ) with a scanning rate of 2° /min.

2.1.4.13. FT-IR analysis

The FT-IR spectra of powders were recorded using a spectrometer (Make: NICOLET, Wisconsin, USA; Model: IMPACT 410). The absorbance spectra of the samples were recorded in the range of 4000 to 400 cm^{-1} with a resolution of 4 cm^{-1}. All the experimental data were analysed using OMNIC E.S.P.5.0 software.

2.1.4.14. Morphological properties

The morphological properties of samples were investigated using scanning electron microscope (Make: JEOL Akishima, Tokyo, Japan; Model: JSM 6390 LVSingapore). The powdered samples were coated with gold after attaching with the tape stubs. The sample were analyzed under 20 kV energy with 5000X magnification.

2.1.4.15. Steady-shear rheology

The effect of microencapsulate incorporation on rheological properties of rice dough was investigated in terms of steady-shear rheology. The flow properties of dough were evaluated using a controlled shear stress rheometer (Make: Antron Paar, Graz, Austria; Model: Physical MCR 72) with a plate and plate attachment having a 50 mm diameter. For the analysis, various amount of microencapsulated powder (5, 10, 15, and 20 % w/w) was incorporated in rice flour dough with a moisture content of 35 % w/w. For the test, the shear rate varied from 0.1 to 100 /s and the temperature was 25 ± 1 °C. The experimental data were fitted with Herschel–Bulkley, and Mizrahi-Berk model as follows,

$$\sigma = k_H \gamma^{\eta_H} + \sigma_{O_H} \quad (2.10)$$

$$\sigma^{0.5} = k_M \gamma^{\eta_M} + \sigma_{O_M} \quad (2.11)$$

Where, σ shear stress, σ_{0_H} and σ_{0_M} are yield stress, k_H and k_M are consistency index, η_H and η_M are flow behavior index, and γ is shear rate.

2.1.4.16. Oscillatory rheological properties

The effect of microencapsulated powder incorporation on rheological properties of rice dough was investigated in terms of oscillatory rheological properties. The oscillatory rheological properties of dough were assessed using a Rotational Rheometer (Make: Antron Paar, Graz, Austria; Model: Physical MCR 72) with a plate and plate geometry of 50 mm diameter. For the analysis, various amount of microencapsulate (5, 10, 15, and 20 % w/w) was incorporated in rice flour dough with a moisture content of 35 % w/w. The dough was placed on the plate and the excess sample was removed carefully by using a sharp razor blade. A thin layer of oil was used on the exposed surface of the sample to prevent drying during testing. Frequency sweep tests from 0.1 to 100 /s were performed at 25 °C. The storage modulus (G'), and loss modulus (G'') were calculated for each dough sample. The data was analysed using Rheoplus version 3.61 software.

2.1.5. Storage study

The storage study of the microencapsulated powder was carried out for 90 days at 4 °C and 25 °C (Weber et al., 2017). An amount of 500 mg of microencapsulated powder was spread in closed petri dishes and subjected to the storage conditions. Samples were stored at 4 °C and

25 °C in a temperature-controlled cabinet without light exposure. Samples were taken after every 10 days and measured the anthocyanin content.

2.1.6. Extraction

2.1.6.1. Conventional extraction

Preliminary experiments were conducted for conventional extraction process in a water bath (Model: OVFU O-SRWB2, Make: OVFU, Kolkata, India) to determine the range of extraction variables, including extraction time (5 to 65 min), extraction temperature (30 to 70 °C), solvent to solid ratio (5:1 to 25:1 mL/g), and (ethanol and acetone) concentration (0 to 100 % v/v) in the extractant solution. The influence of each factor on the extraction yield was studied using "one-factor-at-a-time" method. To investigate the effect of one parameter on extraction yield, remaining other parameters were kept constant (values were: extraction time, 20 min; extraction temperature, 40 °C; solvent-to-solid ratio, 10:1; and ethanol concentration, 50 % v/v). All the experimental runs were carried out in triplicate to access reproducibility, and the average response values are reported here and were considered for analysis.

After the preliminary study, for process optimization, the conventional extraction of total phenolic content from black and purple rice bran was carried out in a time and temperature control water bath (Model: OVFU O-SRWB2, Make: OVFU, Kolkata, India). During conational extraction the variable were extraction time (10 to 60 min), extraction temperature (30 to 60 °C), solvent to solid ratio (5:1 to 20:1 mL/g) and (ethanol and acetone) concentration (25 to 100 % v/v) in the extractant solution. After extraction, the sample was filtrated through Whatman no. 1 filter paper and the filtrate was collected in a volumetric flask for further analysis.

2.1.6.2. Ultrasound-assisted extraction

The Ultrasound-assisted extraction process was performed with an ultrasonic water bath (Model: RK 510 H, 35 kHz, 230 W, Make: Bandelin Sonorex, Missouri, United States) equipped with digital timer and temperature controller. Four extraction variables, namely, temperature (30-60 °C), pH (2-4), Solvent (ethanol) concentration (20-60 % v/v) and time (10-60 min) were considered in this study. The pH of the extractant was maintained using HCl with different concentrations in the extracting solvent. After ultrasonic extraction, the sample was

filtrated through Whatman no. 1 filter paper and the filtrate was collected in a volumetric flask for further analysis.

2.1.7. Adsorption and desorption

2.1.7.1. Pretreatment of adsorbent

The amberlite polymeric adsorbent was purchased as a wet product embedded with sodium chloride and sodium carbonate salt to retard the bacterial growth. This salt must be washed out from the resin prior to use for adsorption. Moreover, for the concentration of hydrophobic compounds, the amberlite resin must be pretreated with a water-miscible organic solvent. Therefore, the amberlite resins were pretreated prior to use to ensure efficient adsorption of anthocyanin from the crude extract. The amberlite resins (XAD2, XAD4, and XAD7) were pretreated by soaking in ethanol for 24 h. After removal from ethanol, the resins were washed with distilled water and soaked in 1M NaOH for 5 h to remove monomers trapped inside the resin pores. The resins were washed with distilled water and kept in an oven at 60 °C for 24 h before use for adsorption (Yang et al., 2016). Activated charcoal was washed with hot water to remove air bubbles from pores to ensure anoxic conditions. However, the presence of oxygen may improve adsorption efficiency, but it also promotes an undesired polymerization reaction (Soto et al., 2008). Bentonite was washed with water repeatedly before use for adsorption.

2.1.7.2. Adsorption and desorption tests

Pretreated adsorbents (1 g) and 25 mL of purple rice bran extract were mixed in 250 mL flasks. Flasks were kept in a shaker at a rate of 45 rpm (4.71 rad/s) for 24 h at room temperature (28 ± 2 °C) (Buran et al., 2014). After adsorption, the adsorbents were separated from the crude extract solution through filtration. For desorption testing, resins were washed with 25 mL distilled water. After washing, the resin was mixed with 50 mL of 95 % ethanol in flasks. The flasks were kept in a shaker at 45 rpm (4.71 rad/s) for 24 h at room temperature (28 ± 2 °C) for desorption. Adsorption/desorption ratio and capacities were calculated using the following equations:

$$\text{Adsorption ratio, } E\ (\%) = \frac{C_o - C_e}{C_o} \times 100 \qquad (2.12)$$

$$\text{Adsorption capacity, } q_e\ (\%) = (C_o - C_e) \times \frac{V_i}{(1-M)W} \quad (2.13)$$

Where, E is the adsorption ratio (%); q_e is the adsorption capacity (mg/g dry resin) at equilibrium, C_o (mg/L) is the initial concentration of anthocyanin in the extract; C_e (mg/L) is the equilibrium concentration of anthocyanin in the extract. After the completion of the adsorption process, the resin was separated from the extract and the anthocyanin content of the extract was measured as equilibrium concentration anthocyanin. V_i (mL) is the volume of the crude extract; W (g) is the mass of the resin and M is the moisture content of the resin (% w/w)

$$\text{Desorption ratio, } D(\%) = \frac{C_d V_d}{(C_o - C_e)V_i} \times 100 \quad (2.14)$$

$$\text{Desorption capacity, } q_d\ (\text{mg/g}) = \frac{C_d V_d}{(1-M)W} \quad (2.15)$$

$$\text{Recovery, } R_{ad}\ (\%) = \frac{C_d V_d}{C_o V_i} \times 100 \quad (2.16)$$

Where, D (%) is the desorption ratio; C_d (mg/L) is the concentration of anthocyanin in the desorption solutions; V_d is the volume of the desorption solution (mL); V_i is the volume of the initial sample solution (mL); C_o and C_e are the same as those defined above, and q_e (mg/g) is the adsorption capacity at adsorption equilibrium. R_{ad} is recovery percentage (%).

2.1.7.3. Adsorption kinetics

Pretreated adsorbent (1 g) was mixed with 25 mL of purple rice bran extract in a flask and placed in a shaker at 45 rpm (4.71 rad/s) at ambient temperature (28 ± 2 °C). Aliquots of 1 mL were drawn from the solution at regular intervals of 30 min, up to 210 min, in order to identify the time at which the adsorption process attains equilibrium. Adsorption kinetics was assessed using the pseudo-first and pseudo-second-order kinetic models, which used to predict the mechanism of adsorption process (Chen et al., 2016)

Pseudo-first order model

$$q_t = q_e - q_e e^{-k_1 t} \quad (2.17)$$

$$\log(q_e - q_t) = \log q_e - \frac{k_1}{2.303} t \quad (2.18)$$

Pseudo-second order model

$$q_t = \frac{k_2 q_e^2 t}{1 + k_2 q_e t} \tag{2.19}$$

$$\frac{t}{q_t} = \frac{t}{q_e} + \frac{1}{k_2 q_e^2} \tag{2.20}$$

Where, k_1 and k_2 are rate constant of the pseudo-first and pseudo-second order models, respectively. q_e (mg/g) is the adsorption capacity of resins at equilibrium; q_t (mg/g) is the concentration of anthocyanin absorbed at time *t*.

2.1.7.4. Adsorption isotherm

Pretreated adsorbent (1 g) was added to 25 mL purple rice bran extract of different concentrations of anthocyanin (15-40 mg/L). Adsorption was conducted at room temperature (28 ± 2 °C) in a shaker at 45 rpm (4.71 rad/s). The equilibrium adsorption isotherms for anthocyanin were determined using various adsorption isotherms models as shown in Table 2.2. The adsorption capacity of adsorbent at various equilibrium conditions (q_e, mg/g) and the equilibrium concentration of anthocyanin (C_e, mg/L) was the input variable.

Table 2.2: Adsorption isotherms models

SL. No.	Model	Nonlinear form	Plot
		Two parameter model	
1	Langmuir	$q_e = \frac{q_m C_e}{K_L + C_e}$	$\frac{C_e}{q_e}$ Vs C_e
2	Freundlich	$q_e = K_f C_e^{1/n}$	$\log q_e$ Vs $\log C_e$
3	Hill	$q_e = \frac{q_m C_e^n}{K_d + C_e^n}$	$\log \frac{q_e}{(q_m - q_e)}$ Vs $\log C_e$
		Three parameter model	
4	Redlich–Peterson	$q_e = \frac{K_r C_e}{1 + A_r C_e^n}$	$\ln\left(K_r \frac{C_e}{q_e} - 1\right)$ Vs $\ln C_e$
5	Toth	$q_e = \frac{K_T C_e}{(a_t + C_e)^{1/n}}$	$\ln\left(\frac{q_e}{K_T}\right)$ Vs $\ln C_e$
6	Koble–Corrigan	$q_e = \frac{A_1 C_e^n}{1 + B C_e^n}$	----------

2.1.7.5. Diffusion model

In the present work, the adsorption mechanisms of anthocyanin were investigated using a model that takes into account the influence of adsorption on solute transport in the adsorbent.

In order to investigate this mechanism of adsorption for anthocyanin on various adsorbents, an intra-particle diffusion model-based mechanism was used. According to a functional relationship of the intra-particle diffusion model, the uptake varies almost proportionately with the half-power of time, $t^{0.5}$, rather than t. The most-widely applied intra-particle diffusion equation for the bio-sorption system is given by Weber. and Morris (1963):

$$q_t = k_t t^{0.5} + \psi \tag{2.21}$$

Where, q_t is the adsorption capacity of adsorbent (mg/g), k_t is the intra-particle diffusion rate constant (g/mg $min^{0.5}$) and ψ is intercept.

2.1.7.6. Thermodynamic parameters of adsorption

The only XAD7 resin was considered for the investigation of adsorption thermodynamics for anthocyanin. Adsorption thermodynamics of resin was found to reflect the in-depth information regarding structural and inherent energy change of adsorbent (Gao et el., 2013). It also provided the mechanisms involved in the adsorption process. During adsorption, the enthalpy change was calculated using the Clausius–Clapeyron equation, which was linearized as:

$$\frac{d(\ln K_L)}{dT} = -\frac{\Delta H}{RT^2} \tag{2.22}$$

$$\ln K_L = -\frac{\Delta H}{RT} + \ln K_o \tag{2.23}$$

The Gibbs free energy change can be calculated as follows:

$$\Delta G = -RT \ln K_L \tag{2.24}$$

The adsorptive entropy was calculated with the following equation

$$\Delta S = \frac{(\Delta H - \Delta G)}{T} \tag{2.25}$$

Where, ΔH (kJ/mol) is enthalpy change; ΔS (J/mol K) is entropy change; ΔG (kJ/mol) is Gibbs free energy change; R (8.314 J/mol K) is the ideal gas constant; T (K) is the temperature; K_L is the equilibrium distribution coefficient, which is the ratio of the amount adsorbed on the solid to the equilibrium concentration in solution; K_o is constant.

2.1.8. Degradation experiment

2.1.8.1. Preparation of samples with hydrocolloids

Few researchers have reported that hydrocolloids, acids, sugars, and salt affect the stability of anthocyanin during processing (Buchweitz et al., 2013). In the present study, the effect of various hydrocolloids on the stability of monomeric anthocyanin, C3G, and P3G was investigated. The separated anthocyanin from purple rice bran extract was mixed with 0.5 % (w/v) of carboxymethyl cellulose, xanthan gum, gum acacia, and modified starch. After stirring for 30 min, the mixture was adjusted to pH 6 using 1M HCl and 1M NaOH for pH based degradation study. All the samples were placed in dark conditions at ambient temperature (28 ± 2 ^{o}C) before further tests within 24 h. To study the thermal degradation, the mixture with and without hydrocolloids were heated at 90 °C for 30 min.

2.1.8.2. Degradation studies

The thermal degradation of monomeric anthocyanin, C3G, and P3G from purple rice bran were studied at 60, 70, 80 and 90 °C. Aliquots of 10 mL anthocyanin were put into a screw-cap test tube and placed in an already equilibrated water bath at 60, 70, 80, and 90°C. At regular time intervals (0, 30, 60, 90, 120, 150 and 180 min), samples were removed from the water bath and rapidly cooled by plunging into an ice water bath. The analysis was conducted immediately and subsequently at regular time intervals. Similarly, the degradation behavior of monomeric anthocyanin, C3G, and P3G at various pH (2, 4, 6, and 8) was investigated.

2.1.8.3. Degradation kinetics of anthocyanin

The thermal degradation of anthocyanin was found to follow a first-order reaction as reported by Sui et al. (2014). Therefore, in the present study, the pH and thermal degradation reaction of monomeric anthocyanin, C3G, and P3G considered to be a first-order reaction (Eq. 2.26).

$$\ln \frac{C}{C_o} = -k \times t \tag{2.26}$$

$$t_{1/2} = -\frac{\ln 0.5}{k} \tag{2.27}$$

Where, C is the concentration of monomeric anthocyanin, C3G or P3G at time t under a constant temperature or pH condition; k is degradation rate constant; C_o is the initial concentration of monomeric anthocyanin, C3G or P3G in samples. The degradation rate constant was described with a 95 % confidence interval.

The temperature-dependence of thermal degradation rate constant was determined by the Arrhenius equation

$$k = k_{ref} \times e^{-\frac{E_a}{RT}} \quad (2.28)$$

Where, k_{ref} is the frequency factor (per min), E_a is the activation energy (kJ/mol), R is the universal gas constant (8.314 J/mol/K) and T is the absolute temperature (K).

2.1.9. Encapsulation

2.1.9.1. Preparation of feed sample

For microencapsulation of anthocyanin, modified starch was used as wall material and anthocyanin as a core material. The modified glutinous rice starch was prepared as mentioned by Hu et al. (2013). The starch dispersion of various concentrations (5-10 % w/v) was prepared in water with the combination of anthocyanin extract (40 mg C3G/L) (core) under magnetic agitation.

2.1.9.2. Encapsulation

The encapsulation of anthocyanin was done using a spray dryer (Model: Lab plant LU 20 lab sprayer; Make: Labultima, Mumbai, India). During spray drying the inlet air temperature was varied from 140 to 180 °C and atomizer pressure ranged from 2.76 to 5.52 MPa.

2.1.10. Extrusion

The extrusion cooking was carried out using a single screw extruder (extruder with L/D ratio 30:1 and 3 mm die diameter, developed in Tezpur University, Assam) as shown in **Fig. 2.4**. Initially, to find out the ranges of extrusion variables such as screw speed (50 to 250 rpm), barrel temperature (50 to 110 °C) and moisture (15 to 35 % w/w), preliminary experiments were conducted. The influence of a variable on the extrudate was studied using the "one-factor-at-a-time" method. To study the effect of one variable on extrudate, remaining other parameters

were kept constant (values were: screw speed 150 rpm (15.7 rad/s); barrel temperature 80 °C; moisture content 25 % (w/w). The experiments were carried out in triplicate.

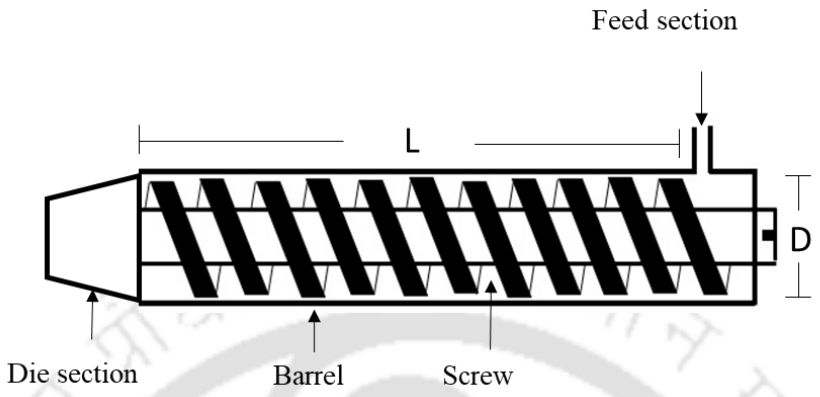

Fig. 2.4: Schematic diagram of extruder

After preliminary study, for optimization, the extrusion cooking was carried out using a single screw extruder (extruder with L/D ratio 30:1 developed in Tezpur University) (**Fig. 2.4**). The extrusion cooking was conducted at a barrel temperature of 60-100 ^{o}C and screw speed 100-200 rpm. The moisture content of the feed material during extrusion was varied from 20-30 % (w/w).

2.1.11. Determination of sorption isotherms

Sorption isotherms behavior for the extruded was determined according to the method of Jena and Das (2012). Eight saturated salt solutions (LiCl, $KC_2H_3O_2$, $MgCl_2.6H_2O$, K_2CO_3, $Mg(NO_3)_2.6H_2O$, NaCl, KCl, and K_2SO_4) with a wide range of relative humidity was used for this investigation as shown in **Table 2.3**. Each solution was transferred to airtight glass desiccators. Extruded samples about 2 g were placed in the desiccators on a petri plate. The desiccators were placed in incubators having a temperature of 25 °C, 30 °C, and 35 °C. The temperatures were selected based on the possible range of temperatures that may be encountered during storage of extrudate. The experiment was completed when less than 1 % change in sample weight was found between two successive readings. No visible mold growth was observed during the experiments.

Table 2.3: Selected salt for moisture sorption isotherms

Salt	RH (%) at temperature		
	25 °C	30 °C	35 °C
Lithium chloride (LiCl)	11.30	11.25	11.16
Magnesium chloride ($MgCl_2$)	32.78	32.05	31.10
Potassium carbonate (K_2CO_3)	43.16	43.17	43.17
Magnesium nitrate ($Mg(NO_3)_2$)	52.89	49.91	46.93
Potassium iodide (KI)	68.86	66.96	65.26
Sodium chloride (NaCl)	75.29	74.87	74.52
Potassium chloride (KCl)	84.34	82.95	81.74
Potassium sulphate (K_2SO_4)	97.30	96.71	96.12

2.1.12. Mathematical modelling of sorption isotherm

In order to obtain a sorption isotherm, the equilibrium moisture content data was fitted with various mathematical models as shown in **Table 2.4**. The constants of the selected models were estimated by non-linear regression analysis. The goodness of fit of each model was assessed with respect to the root mean square error (RMSE), and the maximum R^2.

Table 2.4: Mathematical models for moisture sorption

Sl.No.	Model	Mathematical equation
1	Oswin	$M_W = A(\frac{a_w}{1-a_w})^B$
2	Smith	$M_W = A + B\log(-a_w)$
3	Curie	$M_W = \exp(A + Ba_w)$
4	Modified Halsey	$a_w = \exp(AM_W^{-C})$
5	Lewick 2	$M_W = A\,[(\frac{1}{a_w}) - 1]^{B-1}$
6	Lewicki-3	$M_w = A\,[(\frac{1}{(1-a_w)^B}) - (\frac{1}{(1+a_w^C)})]$
7	Peleg	$M_W = A\,a_w^C + B\,a_w^{D_s}$
8	BET	$M_w = \frac{M_o C a_w}{(1-a_w)[1+(C-1)a_w]}$

2.1.13. Paper indicator

2.1.13.1. Fabrication of pH sensitive paper indicator

The various concentrations of anthocyanin (40, 100, 150, 200, 250, and 300 mg/L) were used as a natural indicator. The round-shaped Whatman no. 1 filter paper was used as a substrate for uniform deposition of anthocyanin. The filter paper was cut with a diameter of 80 mm and dried at 90 °C for 10 min (pre-cooking) before loading the indicator. The dried filter paper was placed on the spin coater and rotated at 4000 rpm (418.9 rad/s) for 4 min in ambient temperature (28 ± 2 °C) for uniform deposition of anthocyanin solution. During loading, 4 mL anthocyanin solution was spread on the paper during rotation. Finally, the filter paper was dried in a vacuum drier at 60 °C for 30 min (post-cooking).

2.1.13.2. Evaluation of indicator in simulated condition

The response of the indicator was assessed in various pH environments. The indicator was put in an aqueous solution of pH values 2, 4, 6, 8 and 10 for analysis of indicator performance and change in color was measured by the Hunter Colorimeter (Make: HunterLab, Reston, Virginia, Model: ColorLabUltrascan Vis).

2.1.13.3. Evaluation of indicator in food system

The indicator was applied to different food systems having a wide range of pH to estimate the efficiency of the indicator. A wide range of pH food materials such as lemon juice (pH 2.3), grapefruit juice (pH 3.4), ketchup (pH 4), aloe vera juice (pH 6.1), and egg white (pH 7.8) was selected to evaluate the efficacy and compatibility of the indicator in the food system. Fully matured and unripe lemon, grape, and aloe vera were purchased from the local market of Tezpur, Assam. The fruits and aloe vera leaves were peeled manually. After peeling, the juice was extracted using a kitchen juicer and passed through Whatman no. 1 filter paper. The developed round shape indicator cut into small pieces of 1 cm × 2.5 cm size and put into the food sample for 20 s, and the change in color of the paper was measured using the Hunter Colorimeter (Make: HunterLab, Reston, Virginia, Model: ColorLabUltrascan Vis).

2.1.13.4. Color stability of indicator

For the color stability study, the indicator was store in 4 and 25 °C for one month. During storage after 5 days interval, the color of the paper was measured using hunter

colorimeter (Make: HunterLab, Reston, Virginia, Model: ColorLab Ultrascan Vis). The *a*-value of the indicator was only considered for stability and further study.

2.1.13.5. Degradation kinetics of color

The degradation kinetics of color (redness "*a*") was investigated using zero and first-order reaction as reported by previous researcher. The following equations (2.29 and 2.30) were used in the present study

Zero-order $$C_a = C_{ao} + kt \quad (2.29)$$

First-order $$\ln \frac{C_a}{C_{ao}} = -kt \quad (2.30)$$

Where, C_a is the redness of indicator at time t under a constant temperature (4 and 25 °C); k is degradation rate constant (1/min); C_{ao} is the initial redness value of indicator. The degradation rate constant was described with a 95 % confidence interval.

2.1.14. Design of experiment

2.1.14.1. Response surface methodology (RSM) for conventional extraction of total phenolic content

RSM is an experimental statistical technique, applied for multiple regression analysis using quantitative data obtained from properly designed experiments. RSM has been used to determine the optimum extraction condition of TPC from black and purple rice bran. On the basis of preliminary study, four potential variables, viz. temperature (X_1), time (X_2), solvent percentage (X_3) and solvent to solid ratio (X_4) (**Table 2.5**) were used as the independent parameters for optimization of TPC extraction from rice bran (Y_1-purple rice bran in acetone, Y_2- purple rice bran in ethanol, Y_3-black rice bran in acetone, and Y_4-black rice bran in ethanol). For each rice bran and solvent, 30 experiments were carried out (In appendix **Table 2A1** and **2A2**). Rotatable central composite design (RCCD) was performed using Design-Expert (version 7, Stat-Ease, Inc. USA) software to determine the effects of factors on the response at 5 % significance level and for analyzing and processing of the data. RCCD is a five-level experimental design that follows second-order polynomial equation.

$$y = \beta_0 + \sum_{j=1}^{n} \beta_j x_j + \sum_{j=1}^{n} \beta_{jj} x_j^2 + \sum \sum_{i<j=2}^{n} \beta_{ij} x_i x_j + \psi \quad (2.31)$$

The coefficient of the polynomial equation were β_0 (constant), β_j (linear effects), β_{jj} (quadratic effects) and β_{ij} (interaction effects). x_i *and* x_j are the coded independent variables. Ψ is constant.

Table 2.5: Independent variables with their coded and actual values

Variable	Unit	Symbol	Level of factor				
			-2	-1	0	+1	+2
Temperature	°C	X_1	30	37.5	45	52.5	60
Time	min	X_2	10	22.50	35	47.5	60
Solvent concentration	% (v/v)	X_3	25	43.75	62.50	81.25	100
Solvent to solid ratio	mL/g	X_4	5	10	12.50	16	20

2.1.14.2. Response surface methodology for ultrasound assisted extraction of TPC and anthocyanin

Four-factor rotatable central composite design (RCCD) was adopted to obtain the optimum extraction conditions to maximize total phenolic and monomeric anthocyanin content for black (Y_5-total phenolic content and Y_6-monomeric anthocyanin content) and purple (Y_7-total phenolic content and Y_8-monomeric anthocyanin content) rice bran. Thirty experiments for each rice bran were conducted including six central points (In appendix **Table 3A1** and **3A2**) to find out the optimum values of extraction parameters. The real and coded values of variables are shown in **Table 2.6**. The quadratic polynomial equation similar to Eq.2.31 was obtained from the experimental data to predict the higher TPC and monomeric anthocyanin.

Table 2.6: Independent variables with their coded and actual values

Variables	Unit	Symbol	Levels				
			-2	**-1**	**0**	**+1**	**+2**
Temperature	°C	X_5	30	37.5	45	52.5	60
pH		X_6	2	2.5	3	3.5	4
Solvent concentration	% (v/v)	X_7	20	30	40	50	60
Time	min	X_8	10	22.5	35	37.5	60

2.1.14.3. Response surface methodology for microencapsulation process

To study the effect of starch concentration (X_9) (5-10 % w/v), atomizer pressure (X_{10}) (2.76-5.52 MPa), and inlet air temperature (X_{11}) (140-180 °C) on microencapsulated anthocyanin during spray drying and to optimize the process parameter, three-factor rotatable central composite design (RCCD) was employed. The optimum spray drying condition for microencapsulated powder was obtained in terms of maximizing encapsulation efficiency (Y_9), anthocyanin content (Y_{10}), DPPH scavenging activity (Y_{11}), true density (Y_{12}) and minimum water activity (Y_{13}). Twenty experiments were conducted, including six central points to find out the optimum values of spray drying parameters (In appendix **Table 4A1**). The real and coded values of independent variables shown in **Table 2.7**.

Table 2.7: Independent variables with their coded and actual values

Variable	Unit	Symbol	Level of factor				
			-2	-1	0	+1	+2
Starch concentration	% (w/v)	X_9	5	6.01	7.5	8.99	10
Pressure	MPa	X_{10}	2.76	3.32	4.14	4.96	5.52
Temperature	°C	X_{11}	140	150	160	170	180

2.1.14.4. Response surface methodology for extrusion cooking

The extrusion cooking was carried out using a single screw extruder (extruder with L/D ratio 30:1 developed in Tezpur University). The extrusion cooking was conducted in varied temperatures, screw speed and feed moisture as shown in **Table 2.8**. The extrusion process was optimized using three-factor rotatable central composite design (RCCD) and twenty experiments were conducted (In appendix **Table 5A1**).

Table 2.8: Independent variables with their coded and actual values

Variable	Unit	Symbol	Level of factor				
			-2	-1	0	+1	+2
Barrel temperature	°C	X_{12}	60	6.01	7.5	8.99	100
Screw speed	RPM	X_{13}	100	481.08	600	718.92	200
Feed moisture	% (w/w)	X_{14}	20	22.5	25	27.5	30

2.1.15. Artificial Neural Networks (ANN)

2.1.15.1. Prediction of TPC for conventional extraction process

Artificial neural network (ANN) is a mathematical tool used to develop a relationship between input and output parameters without any prior knowledge of the relationships between the process parameters. In the present study, a multilayered perceptron was used to build the predictive model with temperature, solvent, time, and solvent to solid ratio as an input, and TPC as an output of the model. In this architecture, a feed-forward back propagation network was used to analyze the data. The neural network was trained using only one hidden layer. RCCD data was used (In appendix **Table 2A1** and **2A2**) to develop the model and all data were normalized in the 0 to 1 range to attain uniform results with less network error. RCCD data was used for training (70 %), testing (15 %), and validating (15 %) of the ANN model to efficiently predict the experimental outcome.

2.1.15.2. Prediction of TPC and anthocyanin for ultrasound assisted extraction process

Four independent variables, i.e., temperature, pH, solvent (ethanol) concentration and time were considered as input layer of ANN. Total phenolic acids (mg/100g) and monomeric anthocyanin content (mg C3G/L) were the output layer. The neural network was trained with only one hidden layer. The neurons number in the hidden layer was varied from 1 to 20. The experimental data of RCCD design (In appendix **Tables 3A1** and **3A2**) was used to train the neural network. A total of 30 data points of each rice variety were distributed into three groups: training (20), validation (5) and test set (5). The best training performance of the neural network was determined based on the highest regression coefficient (R^2). MatLab R2015a (The Mathworks, USA) was used for the ANN tool.

2.1.16. Statistical analysis

For the design of the experiment, Design Expert 7.0.0 (Stat-Ease, Minneapolis, USA) software was used. For prediction and model fitting, the ANN toolbox of MatLab 2015a (Bangalore, India) was used. SPSS 8.0 (Bangalore, India) was used for Duncan's multiple range tests at 5 % significance level.

References

AACC. (2000). Approved methods of the American Association of Cereal Chemists (10th ed.) St. Paul, MN, USA. *American Association of Cereal Chemists*.

Akhavan Mahdavi, S., Jafari, S. M., Assadpoor, E., and Dehnad, D. (2016). Microencapsulation optimization of natural anthocyanins with maltodextrin, gum Arabic and gelatin. *International journal of biological macromolecules, 85*, 379-385.

Buchweitz, M., Speth, M., Kammerer, D.R., and Carle, R. (2013). Impact of pectin type on the storage stability of black currant (*Ribes nigrum L.*) anthocyanins in pectic model solutions. *Food chemistry, 139*(1-4), 1168-1178.

Buran, Timothy J., Sandhu, Amandeep K., Li, Zheng, Rock, Cheryl R., Yang, Weihua W., and Gu, Liwei. (2014). Adsorption/desorption characteristics and separation of anthocyanins and polyphenols from blueberries using macroporous adsorbent resins. *Journal of Food Engineering, 128*, 167-173.

Canabady-Rochelle, L. L., Harscoat-Schiavo, C., Kessler, V., Aymes, A., Fournier, F., and Girardet, J. M. (2015). Determination of reducing power and metal chelating ability of antioxidant peptides: revisited methods. *Food Chemistry, 183*, 129-135.

Chen, Y., Zhang, W., Zhao, T., Li, F., Zhang, M., Li, J., Zou, Y., Wang, W., Cobbina, S.J., Wu, X. and Yang, L., (2016). Adsorption properties of macroporous adsorbent resins for separation of anthocyanins from mulberry. *Food Chemistry, 194*, 712-722.

Fang, Y., Zhang, B. and Wei, Y. (2014). Effects of the specific mechanical energy on the physicochemical properties of texturized soy protein during high-moisture extrusion cooking. *Journal of Food Engineering, 121*(Supplement C), 32-38.

Farnsworth, N. R. (1966). Biological and phytochemical screening of plants. *Journal of Pharmaceutical Sciences, 55*(3), 225-276.

Gao, Z.P., Yu, Z.F., Yue, T.L. and Quek, S.Y. (2013). Adsorption isotherm, thermodynamics and kinetics studies of polyphenols separation from kiwifruit juice using adsorbent resin. *Journal of Food Engineering, 116*(1), 195-201.

Gupta, R.K. and Das, S.K. (1997). Physical properties of sunflower seeds. *Journal of Agricultural Engineering Research, 66*(1), 1-8.

Harakotr, B., Suriharn, B., Tangwongchai, R., Scott, M. P. and Lertrat, K. (2014). Anthocyanin, phenolics and antioxidant activity changes in purple waxy corn as affected by traditional cooking. *Food Chemistry, 164*, 510-517.

Holguín-Acuña, A.L., Carvajal-Millán, E., Santana-Rodríguez, V., Rascón-Chu, A., Márquez-Escalante, J.A., de León-Renova, N.E.P. and Gastelum-Franco, G., (2008). Maize bran/oat flour extruded breakfast cereal: A novel source of complex polysaccharides and an antioxidant. *Food Chemistry, 111*(3), 654-657.

Hu, X., Wei, B., Zhang, B., Li, H., Xu, X., Jin, Z. and Tian, Y. (2013). Interaction between amylose and 1-butanol during 1-butanol-hydrochloric acid hydrolysis of normal rice starch. *International Journal of Biological Macromolecules, 61*, 329-332.

Jena, S. and Das, H. (2012). Moisture sorption studies on vacuum dried coconut presscake. *Journal of food science and technology, 49*(5), 638-642. doi: 10.1007/s13197-011-0306-3

Luo, W., Zhao, M., Yang, B., Shen, G. and Rao, G., (2009). Identification of bioactive compounds in *Phyllenthus emblica L*. fruit and their free radical scavenging activities. *Food Chemistry, 114*(2), 499-504.

Min, B., McClung, A. M. and Chen, M. H. (2011). Phytochemicals and antioxidant capacities in rice brans of different color. *Journal Food Science, 76*(1), C117-126.

Moongngarm, A., Daomukda, N. and Khumpika, S. (2012). Chemical Compositions, Phytochemicals, and Antioxidant Capacity of Rice Bran, Rice Bran Layer, and Rice Germ. *APCBEE Procedia, 2*, 73-79.

Paiva, F.F., Vanier, N.L., Berrios, J.D.J., Pan, J., de Almeida Villanova, F., Takeoka, G. and Elias, M.C. (2014). Physicochemical and nutritional properties of pigmented rice subjected to different degrees of milling. *Journal of Food Composition and Analysis, 35*(1), 10-17.

Ruch, Randall J., Cheng, S., and Klaunig, James E. (1989). Prevention of cytotoxicity and inhibition of intercellular communication by antioxidant catechins isolated from Chinese green tea. *Carcinogenesis, 10*(6), 1003-1008.

Soto, M.L., Moure, A., Domínguez, H. and Parajo, J.C. (2008). Charcoal adsorption of phenolic compounds present in distilled grape pomace. *Journal of Food Engineering, 84*(1), 156-163.

Sui, X., Dong, X. and Zhou, W. (2014). Combined effect of pH and high temperature on the stability and antioxidant capacity of two anthocyanins in aqueous solution. *Food Chemistry, 163*, 163-170.

Weber, F., Boch, K. and Schieber, A. (2017). Influence of copigmentation on the stability of spray dried anthocyanins from blackberry. *LWT, 75*, 72-77.

Weber, W.J. and Morris, J.C. (1963). Kinetics of adsorption on carbon from solution. *Journal of the Sanitary Engineering Division ASCE 89*, 31-59.

Wojdyło, A., Oszmiański, J. and Czemerys, R. (2007). Antioxidant activity and phenolic compounds in 32 selected herbs. *Food Chemistry, 105*(3), 940-949.

Yang, Q., Zhao, M. and Lin, L., (2016). Adsorption and desorption characteristics of adlay bran free phenolics on macroporous resins. *Food Chemistry, 194*, 900-907.

Zhishen, J., Mengcheng, T. and Jianming, W. (1999). The determination of flavonoid contents in mulberry and their scavenging effects on superoxide radicals. *Food Chemistry, 64*(4), 555-559.

TO EVALUATE THE EXTRACTION PROCESSES USING SOLVENT EXTRACTION TECHNIQUE FOR BIOACTIVE PHYTOCONSTITUENTS (ANTHOCYANIN) FROM PURPLE AND BLACK RICE BRAN

Part of this work is published in

- Industrial Crops and Products, 95, 332-341.
- Journal of Food Measurement and Characterization, 12(1), 332-345.

CHAPTER 3

TO EVALUATE THE EXTRACTION PROCESSES USING SOLVENT EXTRACTION TECHNIQUE FOR BIOACTIVE PHYTOCONSTITUENTS (ANTHOCYANIN) FROM PURPLE AND BLACK RICE BRAN

3.1. Overview

The extraction of phenolic content and monomeric anthocyanin from black and purple rice bran were conducted using conventional extraction process followed by ultrasound-assisted extraction. Initially, conventional extraction of phenolic contents from black and purple rice bran in acetone, ethanol, and water, was optimized using the rotatable central composite design (RCCD). Results of the study suggested that ethanol was the most efficient solvent to extract total phenolic content (TPC) from rice bran. The optimal condition for extraction of TPC from purple rice bran was, 43.74 % (v/v) ethanol concentration, 37.5 °C temperature, 22.5 min extraction time and 8.75 (mL/g) solvent to solid ratio. Whereas, for black rice bran, except for solvent to solid ratio (8.8 mL/g), the optimal condition was the same as purple rice bran. TPC was found to be higher in purple rice bran than black rice bran extracts at optimum conditions. RCCD data was successfully used to predict the extraction yield using the artificial neural network. The purple rice bran extract showed a promisingly higher amount of phytochemical content in terms of TPC, flavonoid, anthocyanins and phenolic acid than black rice bran extract. After conventional extraction, to increase the extraction yield ultrasound-assisted extraction (UAE) was employed. The phenolic compounds and monomeric anthocyanin from both the bran were extracted using UAE and the process was optimized using four variables RCCD. The effect of temperature, pH, extraction time and solvent concentration on extraction yield were examined. The comparative analysis of purple and black rice bran at the optimized conditions revealed higher monomeric anthocyanin (34.9 mg C3G/L) and TPC (2232 mg GAE/100 g) in the purple rice bran extracts than black rice (32 mg C3G/L and 1978.8 mg GAE/100 g). Moreover, the extraction yield using UAE for both rice bran was significantly higher than the conventional extraction process. The prediction of extraction yield using Artificial Neural Network (ANN) was carried out successfully. The GC-MS analysis of extracts showed the presence of nine compounds in purple bran extract and four in black bran extract. The HPLC analysis showed that α-Tocopherol (163.5 and 154.7 µg/L),

Cynanidin-3-glucoside (192.6 and 2.8 µg/L), 4-Hydroxybenzoic acid (349 and 347 µg/L) and Vanillic acid (101.7 and 152.8 µg/L) were the predominant compounds in bran extracts.

3.2. Precise background

The black and purple rice bran of the Northeast region of India are potential sources of phenolic compounds. However, both the rice brans are commonly considered as a by-product or waste of the crop. Thereby, to increase the utilization of these brans, the phenolic compounds from rice bran needs to separate and use in terms of natural antioxidants. Therefore, extraction is the first step to recover the phenolic compounds from pigmented rice bran. The recovery of phenolic compounds depends on various processing factors; hence initially conventional extraction process for total phenolic content is discussed in this chapter as an initial screening process. The extraction parameters such as the concentration of the solvent, extraction time, temperature, and solvent-to-solid ratio can affect the extraction efficiency and so, the process needs to optimize. The phenolic compounds are heat sensitive. Thus, in this chapter, the extraction of phenolic compounds especially anthocyanin from the black and purple rice bran using ultrasound-assisted extraction as a non-thermal process have been discussed. The effect of extraction parameters, process optimisation and artificial neural network prediction of the extraction process have been elaborated in detail. The phytochemical properties such as the content of β-carotene, tocopherol, tocotrienol, cyanidin-3-glucoside, peonidin-3-glucoside, caffeic acid, catechin hydrate, chlorogenic acid, coumaric acid, 4-hydroxybenzoic acid, syringic acid, sinapic acid, vanillic acid, and antioxidant activity of bran extracts also elaborated in this chapter.

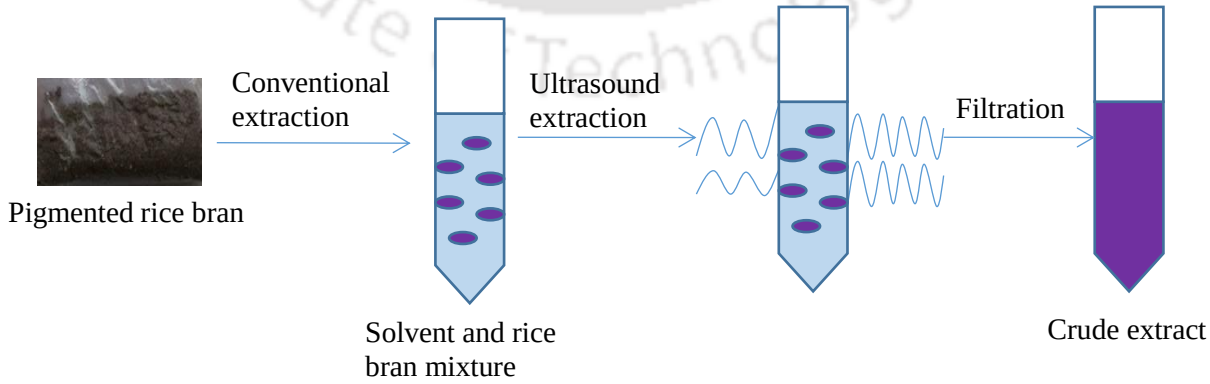

Fig. 3.1: Graphical abstract

3.3. Results and discussion

3.3.1. Preliminary studies

In this study, different solvents were used to extract total phenolic content (TPC) from purple and black rice bran. With the change of solvent in the extraction medium, the recovery of TPC from rice bran was varied significantly (**Figs. 3.2a1** and **3.2a2**). The highest TPC (788.3 and 733.8 mg GAE/100g) in the extracts from both the bran was observed in 50 % (v/v) ethanolic solution. It may be due to the similar polarity of phenolic compounds present in the bran and 50 % (v/v) ethanolic solvent (Spigno and De Faveri, 2009). Whereas, it was observed from **Fig. 3.2a2** that TPC in the acetone extract did not show a promising difference when acetone concentration was varied from 25 to 75 % (v/v). It may be due to the lower polarity of acetone medium than the phenolic compound (Mokrani and Madani, 2016) and unable to extract the high polarity substances from the rice bran hence showed plateau behaviour. While, in water (100 % v/v), the lowest TPC recovery was observed from both the rice bran. The use of only water as a solvent provides an extract with high impurities that could reduce the phenolic quantity in the extracts (Mokrani and Madani, 2016). From the above discussion, ethanol and acetone are found to be efficient for the extraction of TPC from rice bran compared to other solvents. Therefore, for further experimentation purpose, solvent concentration (ethanol and acetone) was varied from 25 to 100 % (v/v).

The effect of temperature on extraction yield in ethanolic (50 % v/v) solution is illustrated in **Fig. 3.2b**. The highest extraction yield in terms of TPC was obtained at 40 °C from purple rice bran. A similar pattern of results was reported by Celli et al. (2015). In their study, the most effective temperature for extraction of TPC from haskap berries was 35 °C. However, for black rice bran, the highest TPC yield was obtained at 50 °C. During extraction, due to the effect of temperature, plant tissue becomes soften; thereby weaken the phenol–protein, and phenol–polysaccharide interactions. Therefore, the weaken interactions may be enhanced polyphenols diffusion into the solvent. Moreover, the variation in the extraction temperature of both the bran may be due to the compositional difference. However, the lowest TPC in the extract was observed at 70 °C for purple (594.6 mg GAE/100g) and black rice bran (657.9 mg GAE/100g). The decrease in TPC at higher temperatures is obvious due to the oxidation and decomposition of phenolic compounds. Therefore, in the present study, the temperature range of 30-60 °C was considered for further experimentation.

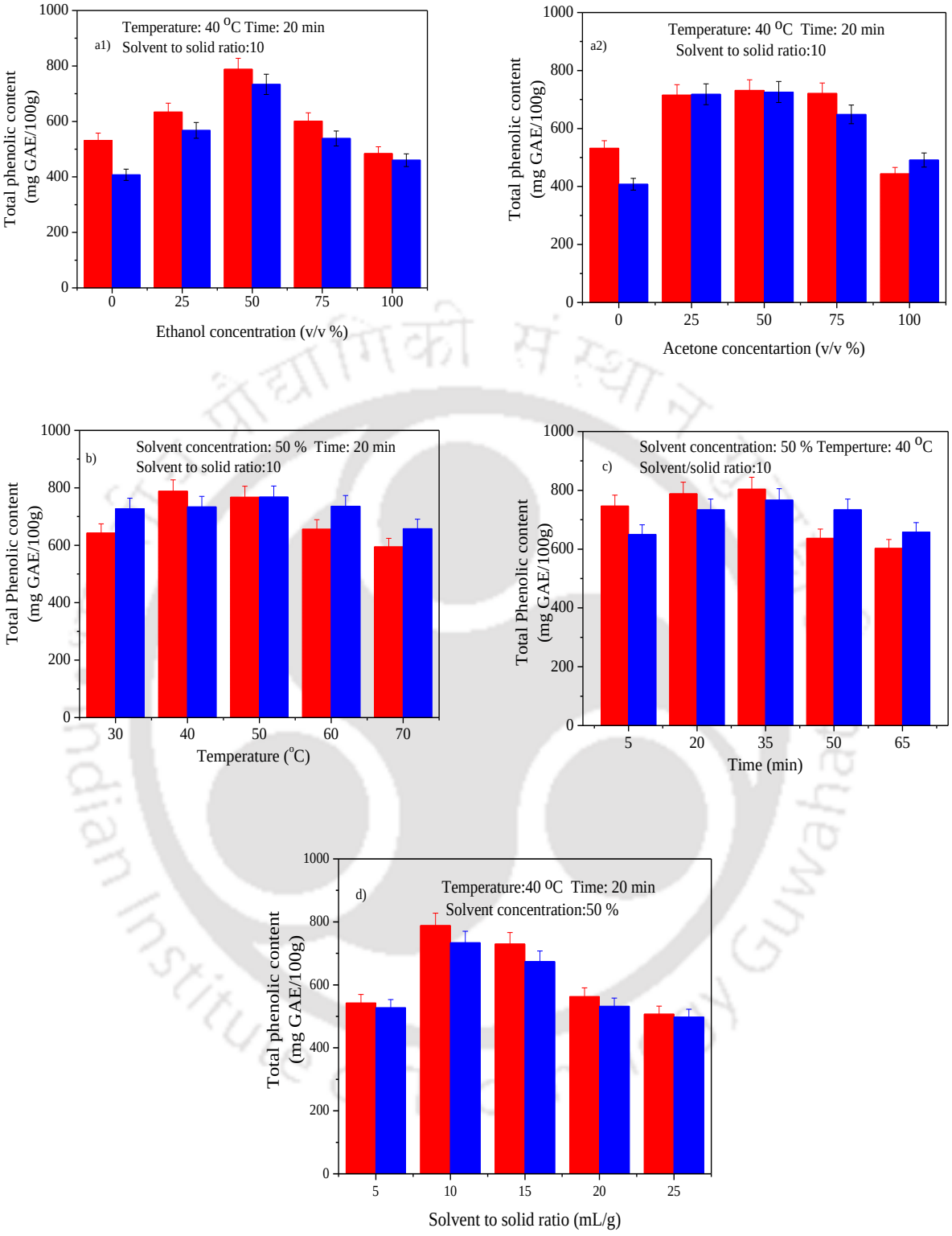

Fig. 3.2: Influence of ethanol concentration a$_1$) acetone concentration a$_2$), temperature b) extraction time c) solvent to solid ratio d) on the extraction yield of TPC for purple rice bran (■) and black rice bran (■)

Extraction time is essential for economizing the energy consumption and expenses of the extraction process. From **Fig. 3.2c**, it can be seen that with an increase in the extraction time from 5 to 35 min, TPC in the extract increases. Further, an increase in the extraction time decreased the TPC. From the results, it was inferred that the extraction of TPC from rice bran almost completes within 35 min by conventional extraction. This phenomenon can be explained by Fick's second law of diffusion. According to it, after a certain time interval concentrations of solute in the solid matrix and bulk solution reaches a final equilibrium and show no further recoveries (Mokrani and Madani, 2016). Furthermore, the observed decrease in TPC for longer extraction time might be due to the oxidation of phenolic compounds (Liu et al., 2013). Hence, for further investigation, the extraction time was varied from 10 to 60 min.

Regarding the influence of solvent to solid ratio, TPC was found to be highest at 10 mL/g solvent to solid ratio for purple (788.3 mg GAE/100g) and black (733.8 mg GAE/100g) rice bran (**Fig. 3.2d**). Further increase in solvent to solid ratio (beyond 10 mL/g), decreased the extraction yield. The increase in TPC in extract for the increase of solvent to solid ratio is reliable with mass transfer principles. During solid-liquid extraction the driving force for mass transfer is the concentration gradient between the solid and liquid. The concentration gradient is greater when a higher solvent-to-solid ratio is used, which enhances the mass transfer (Mokrani and Madani, 2016). However, for the increase of solvent to solid ratio after a certain value, there was a decrease in the extraction yield. Similar kind of results was reported by Santos et al. (2010) during the extraction of antioxidant from Jabuticaba (Santos et al., 2010). It may possible that a higher amount of liquid would not change the driving force anymore as the mass transfer is more confined to the solid interior thereby decrease the TPC recovery (Liu et al., 2013). Therefore, in the present investigation solvent to solid ratio was varied from 5 to 20 (mL/g).

3.3.2. Model and response surface analysis

After preliminary investigation, the selected independent variable namely extraction time, temperature, solvent concentration and solvent to solid ratio with selected levels were used for the experimental design of conventional extraction. The RCCD followed by RSM was used for regression and response surface analysis.

3.3.2.1. Model fitting

To investigate the effect of independent parameters on the extraction of TPC from purple and black rice bran, rotatable central composite design was used. The correlation between independent namely temperature (x_1), extraction time (x_2), solvent percentage (x_3) and solvent to solid ratio (x_4) and dependent variables as TPC (y_1-purple rice bran in acetone, y_2-purple rice bran in ethanol, y_3-black rice bran in acetone and y_4-black rice bran in ethanol) were developed in term of second-order polynomial equation followed by regression analysis. The quadratic polynomial equations of the response surfaces were obtained as follow:

$$y_1 = 990.46 + 30.94x_1 - 61.41x_2 - 24.52x_3 - 23.45x_4 + 1.52x_1x_2 + 16.09x_1x_3 + 37.17x_1x_4 - 7x_2x_3 - 43.43x_2x_4 - 5.81x_2x_4 + 9.35x_1^2 - 44.38x_2^2 + 11.95x_3^2 - 97.98x_4^2 \quad (3.1)$$

$$y_2 = 941.25 + 1909x_1 - 77.31x_2 - 28.41x_3 - 77.93x_4 + 28.94x_1x_2 + 3.16x_1x_3 - 36.88x_1x_4 - 4.40x_2x_3 + 43.58x_2x_4 - 41.60x_3x_4 - 35.22x_1^2 - 97.36x_2^2 - 1.83x_3^2 - 74.28x_4^2 \quad (3.2)$$

$$y_3 = 934.76 + 15.69x_1 - 75.24x_2 - 8.21x_3 - 45.01x_4 - 11.28x_1x_2 - 24.62x_1x_3 - 47.50x_1x_4 - 10.35x_2x_3 + 1.64x_2x_4 - 16.92x_3x_4 - 3.47x_1^2 - 100.11x_2^2 + 10.28x_3^2 - 19.49x_4^2 \quad (3.3)$$

$$y_4 = 944.63 - 8.84x_1 - 56.78x_2 + 22.48x_3 - 48.28x_4 + 20.95x_1x_2 + 12.80x_1x_3 - 4.95x_1x_4 + 0.092x_2x_3 - 12.46x_2x_4 - 51.68x_3x_4 - 6.72x_1^2 - 97.66x_2^2 + 8.80x_3^2 - 49.43x_4^2 \quad (3.4)$$

The analyses of variance (ANOVA) of the response variables for quadratic polynomial models are summarized in **Table 3.1.** The determination of coefficients (R^2) for y_1 (0.97), y_2 (0.97), y_3 (0.97), and y_4 (0.95), indicated that the models could significantly explain all the variations. Higher the R^2 values better the fit of experimental model to the real data. However, the smaller the value of R^2, the less co-relation but can elucidating the behaviour of independent variables (Myers and Montgomery, 1995). The ANOVA for the lack of fit test was insignificant which indicates that the models could adequately fit the experimental data for all response variables (**Table 3.1**).

Table 3.1: Analysis of variance of the regression parameters

Response	Sources	Sum of squares	Degree of freedom	F	P	R^2	Adj R^2
y_1	Regression	5.16×10^5	14	50.7	0.0001	0.97	0.96
	Lack of Fit	6644.45	10	0.8	0.6		
	Pure error	4254.84	5				
y_2	Regression	7.34×10^5	14	46.5	0.0001	0.97	0.95
	Lack of Fit	7683.76	10	0.4	0.9		
	Pure error	9241.60	5				
y_3	Regression	5.18×10^5	14	37.2	0.0002	0.97	0.94
	Lack of Fit	7006.35	10	0.4	0.8		
	Pure error	7907.01	5				
y_4	Regression	4.98×10^5	14	44.8	0.0001	0.95	0.95
	Lack of Fit	5136.57	10	0.4	0.9		
	Pure error	6753.48	5				

3.3.2.2. Analysis of response surfaces

Effect of temperature on total phenolic content

Fig. 3.3 (**a, b, c,** and **d**) shows the effect of temperature on TPC of black and purple rice bran extract in acetone and ethanol solution. Extraction was carried out at different temperatures varied from 30-60 °C. The TPC in acetone solution was gradually increased (718.3-991.2 and 972-1060 mg GAE/100g) with an increase in the temperature from 30-60 °C for black and purple rice bran (**Figs 3.3a** and **3.3c**). From the study, it can be observed that higher the extraction temperature, better the extraction rate. It may be attributed to higher solubility of TPC in acetone at higher extraction temperature. Moreover, it may possible that at higher temperature plant material became soft which enhance the mass transfer of TPC from plant tissue to solvent, thereby it also increases diffusion coefficient hence increases the TPC recovery.

Figs. 3.3b and **3.3d** show a complex interaction between temperature and TPC in bran extract. The TPC extraction in ethanolic solution was affected moderately with the change of temperature. The total phenolic yield was increased with an increase in temperature from 30 to 45 °C. It may be due to the increases in solubility and rate of diffusion of phenolic compounds in ethanol and water mixture (Wang et al., 2013).

However, in ethanolic solution when the temperature was above 45 °C, total phenolic yield decreased to 890.4 and 541.4 mg GAE/100 g for black and purple rice bran, respectively. This may be due to the oxidative degradation and structural decomposition of phenolic compounds in the extract at high temperatures (Wang et al., 2008). A similar type of change was observed by the previous researchers (Spigno et al., 2007; Wang et al., 2008).

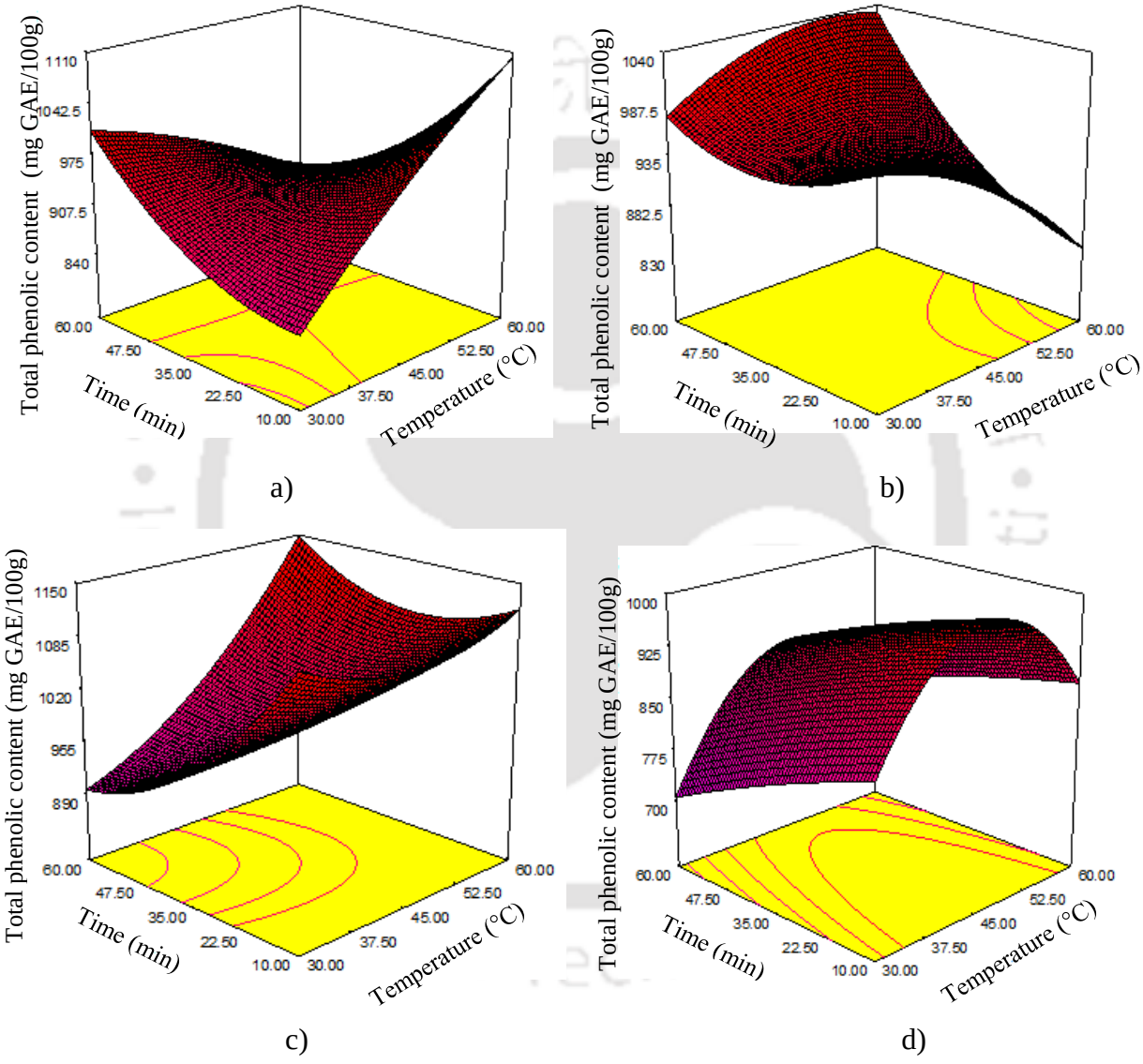

Fig. 3.3: Response surface plots for the effects of time and temperature on total phenolic content in a) acetone from black rice bran b) ethanol from black rice bran c) acetone from purple rice bran d) ethanol from purple rice bran.

Effect of extraction time on total phenolic content

In solvent extraction process, the selection of optimal extraction time is an important parameter, because of the time-dependent thermal degradation of the phenolic compounds. For this reason, a relationship was developed between extraction time and TPC as shown in **Fig. 3.3** (**a, b, c,** and **d**). The effect of extraction time on TPC of rice bran extract in acetone solution is shown in **Figs. 3.3a** and **3.3c**. It was observed from the figure that with an increase in the extraction time, there was a rapid increase in extraction yield from black and purple rice bran. From **Fig. 3.3a**, it was also observed that from black rice bran, the extraction yield of the phenolic compound was increased sharply than purple rice bran. However, in an ethanol solution, the extraction yield has shown (**Figs. 3.3b** and **3.3d**) opposite behaviour for black and purple rice bran with time. For black rice bran the extraction yield was increased after a certain time, but, for purple rice bran, the reverse trend was observed. The increase in TPC of extract with the increase in extraction time can be explained by Fick's law, which predicts the equilibrium condition between the solute and solvent after a certain time. But, the decrease in TPC with an increase in extraction time could be due to the structural changes and decomposition of polyphenols during the prolonged extraction (Liu et al., 2013). Furthermore, the change in extraction yield is due to the composition difference in extracted phenolic compounds from black and purple rice bran.

Effect of solvent concentration on total phenolic content

Fig. 3.4 shows an interaction between solvent concentration and TPC yield. It was observed from **Fig. 3.4** (**a, b, c** and **d**) that in acetone and ethanol solution, the TPC increased with an increase in the solvent concentration up to a certain level (55 % and 62.5 % v/v) and decreases thereafter. This is probably due to the change in solubility of phenolic compounds in the mixture of acetone/ethanol and water which may due to the change in polarity of extractant. As water has a high dielectric constant, which leads to change in the polarities of the mixture with different solvent concentrations (Spigno et al., 2007). This phenomenon might also be attributed to the change of viscosity of extractant, which affect the mass transfer. Water has a higher viscosity than that of acetone and ethanol which enables the solvent to more completely penetrate the bran and thereby increases the TPC recovery (Sahin and Samli, 2013). Moreover, it is reported that water is acted as the plant swelling agent, while ethanol and acetone are believed to disrupt the bonding between solutes and plant matrices, which further can change the recoveries. A similar kind of result

was observed by Sahin and Samli (2013) during the extraction of the phenolic compounds from olive leaf. Hence, a combination of organic solvent with water is more effective in the extraction of phenolic compounds than alcohol alone.

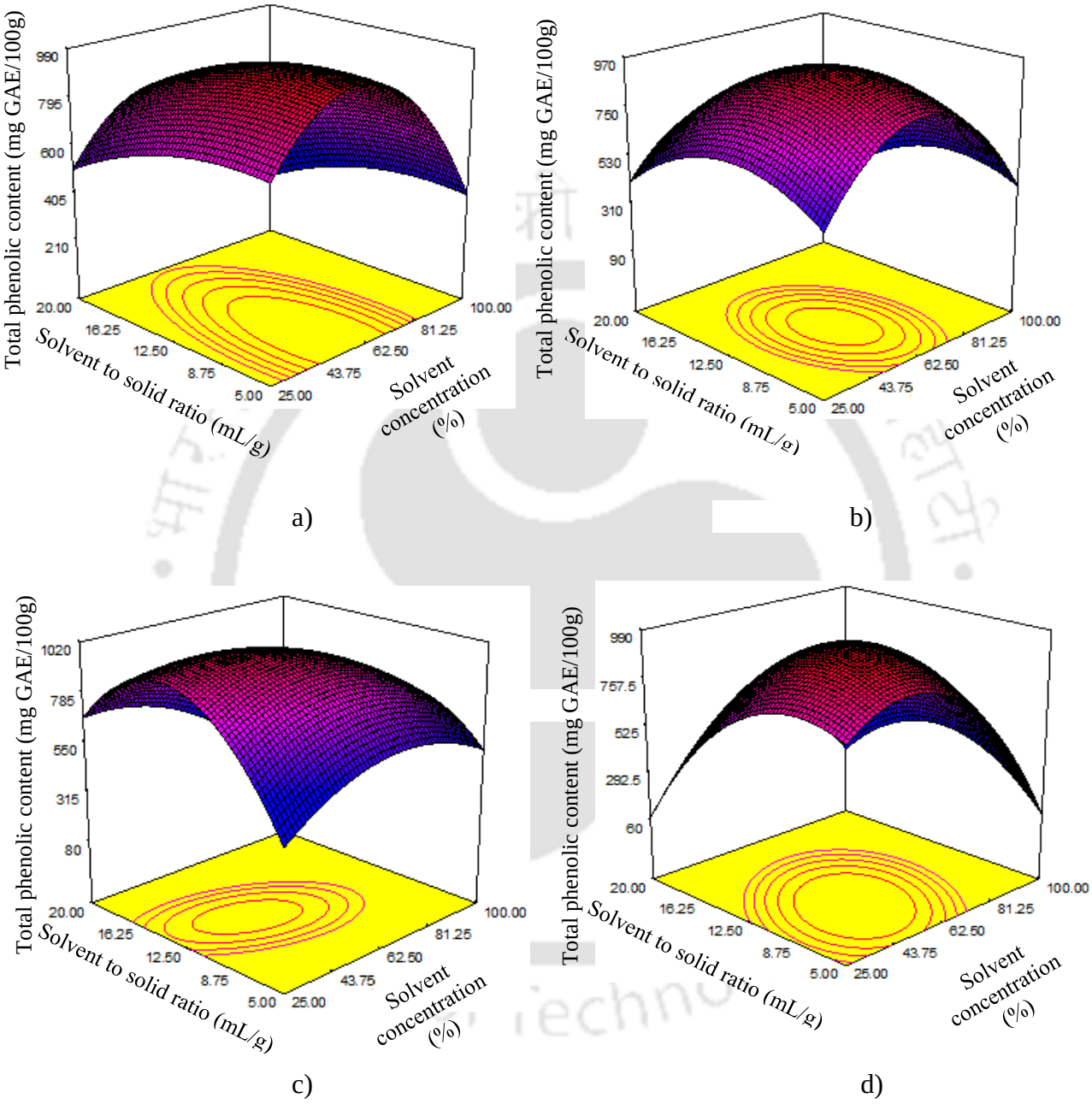

Fig. 3.4: Response surface plots for the effects of solvent composition and solvent to solid ratio on total phenolic content in a) acetone from black rice bran b) ethanol from black rice bran c) acetone from purple rice bran d) ethanol from purple rice bran.

Effect of solvent to solid ratio on total phenolic content

The influence of the solvent to solid ratio on TPC recovery from rice bran was investigated. **Fig. 3.4** shows that initially increase of solvent to solid ratio from 5 to 12 (mL/g), enhances the total phenolic recovery from black and purple rice bran. It is due to the increase of concentration gradient which is the driving force in the solvent extraction process. This is consistent with mass transfer principles since the concentration gradient which is driving force is higher when a higher solvent to solid ratio used, leading to higher diffusion and increase the extraction yield (Mokrani and Madani, 2016). The same tendency of the parameter was also observed by Spigno and De Faveri (2009) for the phenols extraction from tea. However, after a certain ratio of solvent to solid (12 mL/g), there was a decrease in yield with the further increase of solvent to solid ratio. Similar types of the result were observed by a number of researchers (Chen et al., 2015; Chen et al., 2007). It may be attributed that at a high solvent to solid ratio, the high amount of solvent in the extraction system would not change the driving force anymore as the mass transfer is more confined into the solid interior (Zhang et al., 2008) and thereby decrease the recovery of TPC.

3.3.2.3. Optimization and prediction of parameters

The solid-liquid extraction conditions for TPC from pigmented rice brans were optimized. The optimization of phenolic compound extraction conditions from black and purple rice bran was based on maximizing TPC in rice bran extract. Multiple regression analysis was used to achieve the optimum extraction condition. After regression analysis, the extraction process was optimized using predicted models (Equation 3.1, 3.2, 3.3, and 3.4) on the basis of the highest desirability values. All the optimum conditions are shown in **Table 3.2** The highest predicted TPC was observed (**Table 3.2**) in purple rice bran (y_2) as 889.9 mg GAE/100g at 37.5 °C, 43.75 % (v/v) solvent concentration (ethanol), 22.5 min of extraction time and 8.75 (mL/g) solvent to solid ratio. The black rice bran also showed high TPC (857.3 mg GAE/100g) in ethanolic solution (y_4).

3.3.2.4. Validation of optimal condition

The model validation was carried out by performing the experiment at optimized conditions (**Table 3.2**). From **Table 3.2**, it can be seen that the obtained values are in good agreement with the predicted values. No significant difference was found between the experimental and predicted values of TPC for individual models which indicate that the

developed models were significantly efficient to optimize the process. This finding confirmed that the efficiency of the final reduced models was accurately authenticated. However, comparative analysis of y_1, y_2, y_3, and y_4 suggests that y_2 and y_4 give significantly higher TPC in the extract. Hence, to predict the non-linear relationships between the dependent and independent parameters using ANN and to compare with the RSM model only y_2 and y_4 were considered further.

Table 3.2: Predicted and experimental values of TPC obtained under the optimal extraction conditions

Sample	Temperature (°C)	Solvent concen-tration (%)	Time (min)	Solvent to solid ratio (mL/g)	Desirability	TPC (mgGAE/100g)	
						Predicted	Experimental
y_1	37.5	43.76	22.5	8.75	0.93	846.3	865.9
y_2	37.5	43.75	22.5	8.75	0.96	889.9	901.3
y_3	37.5	43.75	22.5	8.77	0.94	825.7	818.9
y_4	37.5	43.75	22.5	8.80	0.99	857.3	852.6

3.3.2.5. Comparison of ANN and RSM models

The data generated from the experimental design (In appendix **Table 2A1** and **Table 2A2**) for purple and black rice bran extract were used to construct the ANN-model. Only the optimum condition of purple (y_2) and black (y_4) rice bran extracts were used for ANN modelling. ANN model was developed using the sigmoidal function. The RCCD data was distributed as training (20), testing (5), and validation (5) to develop the ANN model. The efficacy of the developed ANN model was analysed using the co-efficient of determination (R^2). From the results, it was observed that ANN models with co-efficient of determination (R^2) 0.98 and 0.96 for purple and black rice bran extract indicates the higher ability to predict the experimental outcomes than the RSM models (**Fig. 3.5**). The ANN model predictions lie much closer to the line of "perfect prediction" as compared to the RSM model (**Fig. 3.5**). Thus, the ANN models show a significant and higher generalization capacity than the RSM models.

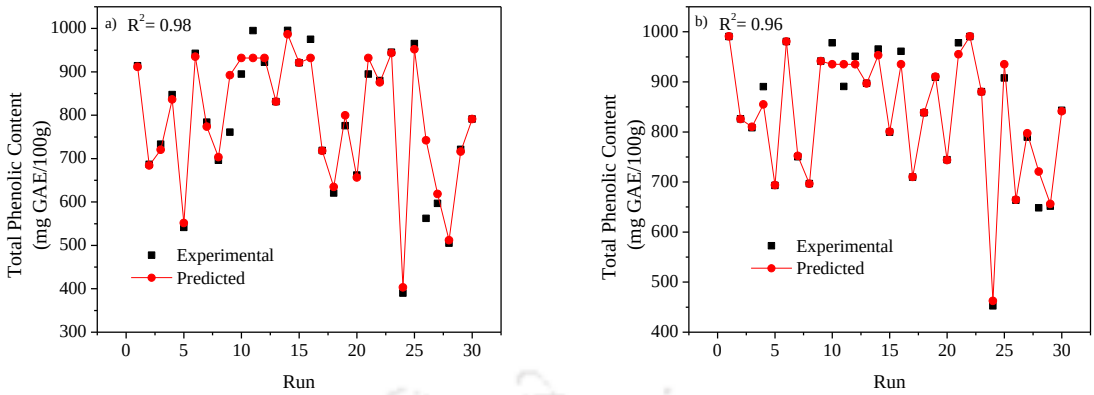

Fig. 3.5: ANN prediction versus experimental total phenolic yield of a) purple (y_2) and b) black (y_4) rice bran in ethanol

3.3.3. Phytochemical properties

3.3.3.1. Total phenolic, anthocyanin, and flavonoid content

The phytochemical constituents of purple (y_2) and black (y_4) rice bran extract are shown in **Table 3.3**. The result of quantitative analysis of bran extract showed the presence of high amount phytochemical such as anthocyanin and flavonoids. The purple rice bran extract contented higher amount of TPC (901.3 mg GAE/100g), anthocyanin (20.2 mg cyanidin-3-glucoside/L) (**Table 3.3**) than black rice bran (18.9 mg cyanidin-3-glucoside/L) extract. Whereas, black rice bran extract contained high amount of flavonoid (17.8 mg quercetin/g) than purple rice bran (16.3 mg quercetin/g) extract as shown in **Table 3.3**.

3.3.3.2. Phenolic acid

The major portion of phenolic acids that existed in rice bran extract is shown in **Table 3.3**. In purple (y_2) and black (y_4) rice bran extract, seven and five numbers of phenolic acids were detected, respectively. The phenolic acids in purple and black rice bran extract was dominated by 4-hydroxybenzoic acid (284.3 and 289.6 µg/L) with lesser amounts of catechin-hydrate (4.2 and 98.1 µg/L), syringic acid (59.9 and 58 µg/L), sinapic acid (20.2 and 13.8 µg/L), and vanillic acid (87.3 and 135.2 µg/L). It was also observed that Caffeic acid (21.6 µg/L) and Chlorogenic acid (56.3 µg/L) were detected in purple rice bran extracts but were not detected in black rice bran extract. Very few studies have reported the occurrence of bound vanillic acid in cereal (Miyazawa et al., 2003). Laokuldilok et al. (2010) reported the detection of six types of phenolic acid in the black, red and white rice bran. These observations was confirmed in the present study.

Table 3.3: Phytochemical content in rice bran extract

Phytochemical	Purple rice bran Extract	Black rice bran extract
TPC (mgGAE/100g)	901.3±8.2	852.6±4.0
Anthocyanin (mg cyanidin-3-glucoside/L)	20.2±1.3	18.9±0.7
Flavonoid (mg quercetin/g)	16.3±1.6	17.8±0.6
Phenol acid (µg/L)		
1. Caffeic acid	21.6±2.0	0
2. Catechin hydrate	4.2±0.8	98.1±1.0
3. Chlorogenic acid	56.3±2.5	0
4. Syringic acid	59.9±3.2	58±0.9
5. Sinapic acid	20.2±1.7	13.8±0.7
6. Vanillic acid	87.3±3.2	135.2±2.3
7. 4-hydroxybenzoic acid	284.3±3.0	289.6±1.8

All the experiments were conducted in triplicate.

3.3.3.3. Antioxidant properties

3.3.3.3.1. DPPH scavenging activity

The DPPH scavenging activity of ethanolic extract of purple (y_2) and black (y_4) rice brans are shown in **Table 3.4**. The scavenging activity was investigated as a function of the concentration of extract. It was observed that for the increase of extract concentration, DPPH scavenging activity increase significantly ($p \leq 0.05$) for both the extract. In maximum concentration, purple and black rice bran extracted showed 91.9 % and 82.2 % DPPH scavenging activity, respectively (**Table 3.4**). Sompong et al. (2011) investigated the scavenging activity of black rice of China, Sri Lanka. According to Sompong et al. (2011), scavenging activity was varied from 13.0 % to 76.4 % which was quite lower than the scavenging activity of Indian purple and black rice variety. It was also illustrated from data that purple rice bran extract had a notable effect on DPPH scavenging activity than black rice bran extract, due to the presence of the high amount of TPC.

3.3.3.3.2. Reducing power

The reducing power of ethanolic purple and black rice bran extract was varied from 0.6 to 2.7 (%) and 0.5 to 2.0 (%) respectively, with the change of concentration. From **Table 3.4**, it was observed that as the concentrations of extract increased, the reducing power also increased significantly ($p \leq 0.05$) for both the rice bran extract. It was also observed that

reducing power of purple rice bran extract was quite higher than black rice bran extract. It may be due to the presence of the high amount of TPC in purple rice bran extract than black rice bran extract, which causes the higher amount reduction of ferric (Fe^{3+}) form to the ferrous (Fe^{2+}) form (Ferreira et al., 2007).

Table 3.4: DPPH scavenging activity, reducing power, chelating activity, and peroxide scavenging activity of extract

Rice Bran	Concentration (%)	Radical scavenging activity (%)	Reducing power (%)	Chelating activity (%)	Peroxide scavenging capacity (%)
Purple	20	68.7 ± 0.8^{a}	0.6 ± 0.03^{a}	20.4 ± 2.0^{a}	0.002
	40	74.5 ± 0.6^{b}	0.9 ± 0.02^{b}	38.3 ± 3.0^{b}	0.004
	60	77 ± 0.8^{c}	1.5 ± 0.04^{c}	54.8 ± 2.0^{c}	0.007
	80	81.1 ± 1.0^{d}	2.1 ± 0.08^{d}	65.3 ± 1.0^{d}	0.011
	100	91.9 ± 2.0^{e}	2.7 ± 0.08^{e}	68.6 ± 1.0^{e}	0.013
Black	20	45.3 ± 2.0^{a}	0.5 ± 0.01^{a}	20.2 ± 1.0^{a}	0.001
	40	54.4 ± 1.0^{b}	0.7 ± 0.01^{b}	28.8 ± 2.0^{b}	0.002
	60	66.3 ± 3.0^{c}	1.0 ± 0.03^{c}	44.7 ± 3.0^{c}	0.004
	80	73.1 ± 1.0^{d}	1.5 ± 0.02^{d}	65.4 ± 1.0^{d}	0.008
	100	82.2 ± 4.0^{e}	2.0 ± 0.04^{e}	66.3 ± 2.0^{d}	0.010

Superscript letters in the same column represent the significant difference in Duncan's multiple range tests at 5% level. All the experiments were conducted in triplicate.

3.3.3.3.3. Iron chelating activity

Purple and black rice bran extracts were assayed for Fe^{2+} chelating activity at different concentrations. The phenolic compounds in rice bran extract could interact with ferric (Fe^{2+}) ion in the mixture and thereby changes the absorbance properties of the mixture. The purple rice bran extracts shown higher chelating activity (20.4-68.6 %) than black rice bran extract (20.2-66.3 %) for ferric (Fe^{2+}) ion at any concentrations level (**Table 3.4**). From the results, it was obvious that there was a significant ($p \leq 0.05$) correlation between the reduction of ferric ion and extract concentration of both the rice bran. It was illustrated from the **Table 3.4** that as the concentration of the sample was increased from 20 to 100 % (v/v), the Iron chelating activity was increased from 20.2 to 66.3 and 20.4 to 68.6 (%) for black and purple rice bran extract, respectively.

3.3.3.3.4. Hydrogen peroxide scavenging capacity

The H_2O_2 scavenging activity is the method for the estimation of reactive oxygen scavenging ability in biological material (Paździoch-Czochra and Wideńska, 2002). It was observed from the present study (**Table 3.4**) that purple rice bran extract had higher potency to scavenge the free superoxide radical produced from hydrogen peroxide than black rice bran extract. Hydrogen peroxide scavenging capacity of purple and black rice bran extracts was also significantly ($p \leq 0.05$) dependent upon the concentration of the extract. As the concentration of the extract in the sample was increased from 20 to 100 % (v/v), the hydrogen peroxide scavenging capacity was varied from 0.001 to 0.010 and 0.002 to 0.013 % for black and purple rice bran extract, respectively.

After conventional extraction, ultrasound was applied to efficiently extract the TPC and anthocyanin from black and purple rice bran. The conventional extraction showed that ethanol is the most effective solvent to extract the TPC. Thereby, for ultrasound-assisted extraction, only ethanol was used as extractant. Moreover, on the basis of optimizing the condition of conventional extraction the solvent to solid ratio was constant for ultrasound-assisted extraction (UAE) as 9.

3.3.4. Modelling of UAE extraction process

In the present study, RCCD was used to optimize the UAE process with the aim to maximize extraction yields for TPC and monomeric anthocyanin content. Thirty experiments were conducted including six center points for each rice bran sample. The data obtained from RCCD were analyzed using response surface regression and developed a second-order polynomial relationship with high correlation coefficient (R^2) values of 0.91 and 0.95 for TPC and monomeric anthocyanin content in black rice bran extract and 0.90 and 0.93 for TPC and monomeric anthocyanin content in purple rice bran extract, respectively (**Table 3.5**).

$$y_5 = 1666.92 - 5.33x_5 - 67.46x_6 - 61.08x_7 - 88.08x_8 + 53.69x_1x_3 + 11.50x_5x_8 + 71.00x_7x_8 - 50.75x_5^2 - 8.62x_6^2 - 32.25x_7^2 - 30.19x_8^2 \quad (3.5)$$

$$y_6 = 22.08 - 0.74x_5 - 1.46x_6 - 1.32x_7 - 1.11x_8 + 1.16x_5x_7 + 0.71x_5x_8 + 0.73x_7x_8 - 0.51x_5^2 - 0.49x_6^2 - 0.43x_7^2 + 0.99x_8^2 \quad (3.6)$$

$$y_7 = 1842.54 - 5.61x_5 - 71.01x_6 - 68.86x_7 - 89.62x_8 + 56.51x_5x_7 + 12.11x_5x_8 + 74.74x_7x_8 - 9.44x_5^2 - 5.10x_6^2 - 23.13x_7^2 - 32.45x_8^2 \quad (3.7)$$

$$y_8 = 27.07 - 0.70x_5 - 1.41x_6 - 1.35x_7 - 0.89x_8 + 1.01x_5x_7 + 0.46x_5x_7 + 0.58x_7x_8 - 0.43x_5^2 - 0.43x_6^2 - 0.38x_7^2 + 0.66x_8^2 \quad (3.8)$$

The developed models were validated by the lack of fit test (**Table 3.5**). Analysis of variance (ANOVA) for the lack of fit test was insignificant for four responses (0.05, 0.27, 0.08 and 0.50) ($p \leq 0.05$) which conferred that the developed relationship was suitable for the experimental data and shown good correlations between variables. The effects, interaction, and significance of four variables were determined and shown in **Table 3.5**.

Table 3.5: Analysis of variance (ANOVA) for the fitted quadratic polynomial model

Source	Black rice bran		Purple rice bran	
	TPC	Anthocyanin	TPC	Anthocyanin
	p-value Prob> F	p-value Prob> F	p-value Prob> F	p-value Prob> F
Model	< 0.0001	< 0.0001	< 0.0001	< 0.0001
x_5 -Temperature	0.70	0.0003	0.68	0.0009
x_6 -pH	0.0001	< 0.0001	< 0.0001	< 0.0001
x_7 -Ethanol concentration	0.0003	< 0.0001	< 0.0001	< 0.0001
x_8 -Time	< 0.0001	< 0.0001	< 0.0001	< 0.0001
x_5x_7	0.004	< 0.0001	0.0028	0.0002
x_5x_8	0.50	0.003	0.47	0.05
x_7x_8	0.0005	0.002	0.0002	0.01
x_5^2	0.0009	0.004	0.0009	0.02
x_6^2	0.51	0.005	0.69	0.02
x_7^2	0.02	0.01	0.08	0.03
x_8^2	0.03	< 0.0001	0.02	0.0008
Lack of Fit	0.06	0.27	0.08	0.50
R^2	0.91	0.95	0.90	0.93

3.3.5. Response surface analysis

3.3.5.1. Response surface analysis of total phenolic content

The effects of extraction parameters such as temperature (°C), pH, extraction time (min) and ethanol concentration (% v/v) on total phenolic content were studied, and their effects are shown in **Fig. 3.6** (**a, b, c** and **d**). **Figs. 3.6a** and **3.6c** illustrated the effect of pH and extraction time on the total phenolic content of rice bran extract. TPC of black and

purple bran extracts was found to be higher at pH 2.5 and then gradually decreases with an increase in the pH up to 4. As reported, at low pH, most of the phenolic form a stable structure, therefore, absorption spectra's of phenols are unchanged. But, at high pH, there is a change in resonance, tautomers, hydrogen-bonding, and hydrated structures, as well as colors of phenolic compounds, are strongly influenced by pH of the solution which makes them vulnerable to oxidative degradation and complex formation (Friedman and Jürgens, 2000).

It has been previously reported that UAE intensifies the extraction efficiency by increasing the yield and reducing the extraction time (Abid et al., 2013; Ramić et al., 2015). In the present study, the extraction process was carried out for 10 to 60 min for both the bran. The effect of sonication time on TPC from black and purple rice bran is shown in **Figs. 3.6a** and **3.6c**. From the study, it was revealed that with an increase in ultrasound time from 10-22.50 min, TPC increased gradually and thereafter decreased with a further increase in the extraction time. A similar type of observation was made by Tiwari et al. (2010) on the extraction of anthocyanin from red grape juice. It may be due to increase in the mass transfer from bran to extractant. Wang et al. (2008) and Ghafoor et al. (2009) reported a detrimental effect on the extracted components due to the prolonged extraction period. During ultrasonication, propagation of ultrasound pressure waves and resulting cavitation caused high shear forces, which enhanced the eddy diffusion and internal diffusion. The increase in the rate of diffusion increases the mass transfer in the extractants (Vilkhu et al., 2008). Whereas, a sharp decrease in the phenolic content for both the bran after 22.5 min of sonication may be due to volatilization of the phenols caused by heat generation during sonication (Tiwari et al., 2010) and some unwanted reactions like enzymatic degradation and oxidation (Vilkhu et al., 2008).

The effect of ethanol concentration on the total phenolic content of black and purple bran is illustrated in **Figs. 3.6b** and **3.6d**. As can be seen from **Figs. 3.6b** and **3.6d**, the total phenolic content in the extract increased with an increase in the solvent concentration up to 30 % (v/v). However, the reversed trend was observed when the ethanol concentration in extractant reached above 30 % (v/v). Based on these experimental results, it was believed that an increase in solubility of phenolic compounds in the liquid phase was because of change in polarity (Feng et al., 2015).

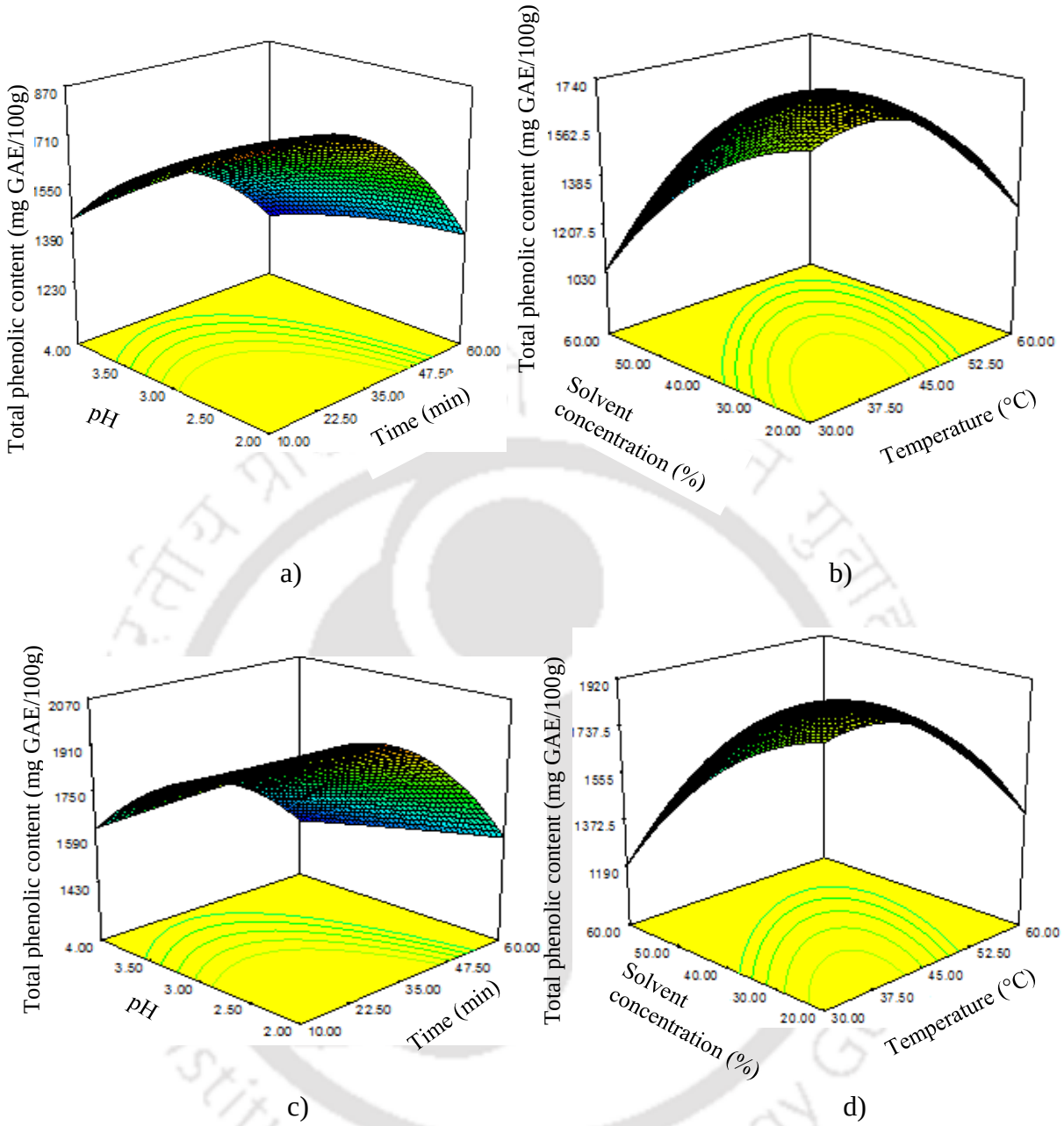

Fig. 3.6: Response surface and contour plots for the effect of independent variables a) pH and extraction time b) solvent concentration and temperature on TPC of black bran extract c) pH and extraction time d) solvent concentration and temperature on TPC of purple rice extract.

Figs. 3.6b and **3.6d** show the effect of temperature on TPC in black and purple rice bran extract. The total phenolics yield was increased with an increase in the temperature from 30 to 37.5 °C. This attribute to the increased solubility of phenolic compounds in ethanol and water mixture. During extraction, heating of the sample might soften the plant tissue and weaken the phenol–protein, and phenol–polysaccharide interactions, leading to

more polyphenols diffusion into the solvent (Tao et al., 2014). However, beyond 37.50 °C, a drastic decrease in total phenolic content was observed. This may be due to the oxidative degradation of phenolic compounds in the extract at high temperatures. A similar type of behavior was observed by other researchers as well (Spigno et al., 2007 and Wang et al., 2008).

3.3.5.2. Response surface analysis of anthocyanin content

Fig. 3.7 (**a, b, c,** and **d**) illustrated the effect of pH, time (min) solvent concentration (%), and temperature (°C) on monomeric anthocyanin content in the black and purple rice bran extract.

Figs. 3.7a and **3.7c** represent the effect of pH and extraction time on anthocyanin content of black and purple rice bran extract. The results of the study showed that a slight increase in the anthocyanin content was observed with an increase in the pH up to 2.5. Further, an increase in the pH beyond 2.5 drastically decreased monomeric anthocyanin content in the rice bran extract. This decrease in anthocyanin content in black and purple rice extract may due to the formation of colorless structures after pH 2.5. At this pH, red flavylium cation hydrated to colorless carbinol (Hurtado et al., 2009). It was also observed from **Figs. 3.7a** and **3.7c** that with an increased in pH from 2-2.5, there was a slight increase in the anthocyanin content. It may be due to the presence of a stable form of the red flavylium cation in the bran extract (Cevallos-Casals and Cisneros-Zevallos, 2004).

Fig. 3.7 (**a** and **c**) it can be seen that UAE up to 22.5 min of sonication showed a significant increase in the monomeric anthocyanin content in the of black rice bran extract and decreased thereafter. Whereas, in the case of purple rice bran, only a slight increase was observed. In the initial stage of extraction, monomeric anthocyanin content was increased, because ultrasound enhanced the release of monomeric anthocyanin into the solvent and also increased the mass transfer in the first 22.50 min (Vilkhu et al., 2008). After 22.5 min, anthocyanin degradation occurred, likely due to various sonochemical reactions including free radicals generation, polymerisation/depolymerisation and some other reactions (Schueller and Yang, 2001) which are responsible for the degradation of anthocyanin in the extract. It was also observed that for the black rice bran extract, the degradation was quite higher than the purple rice bran. It may be attributed to the compositional difference between both the rice bran.

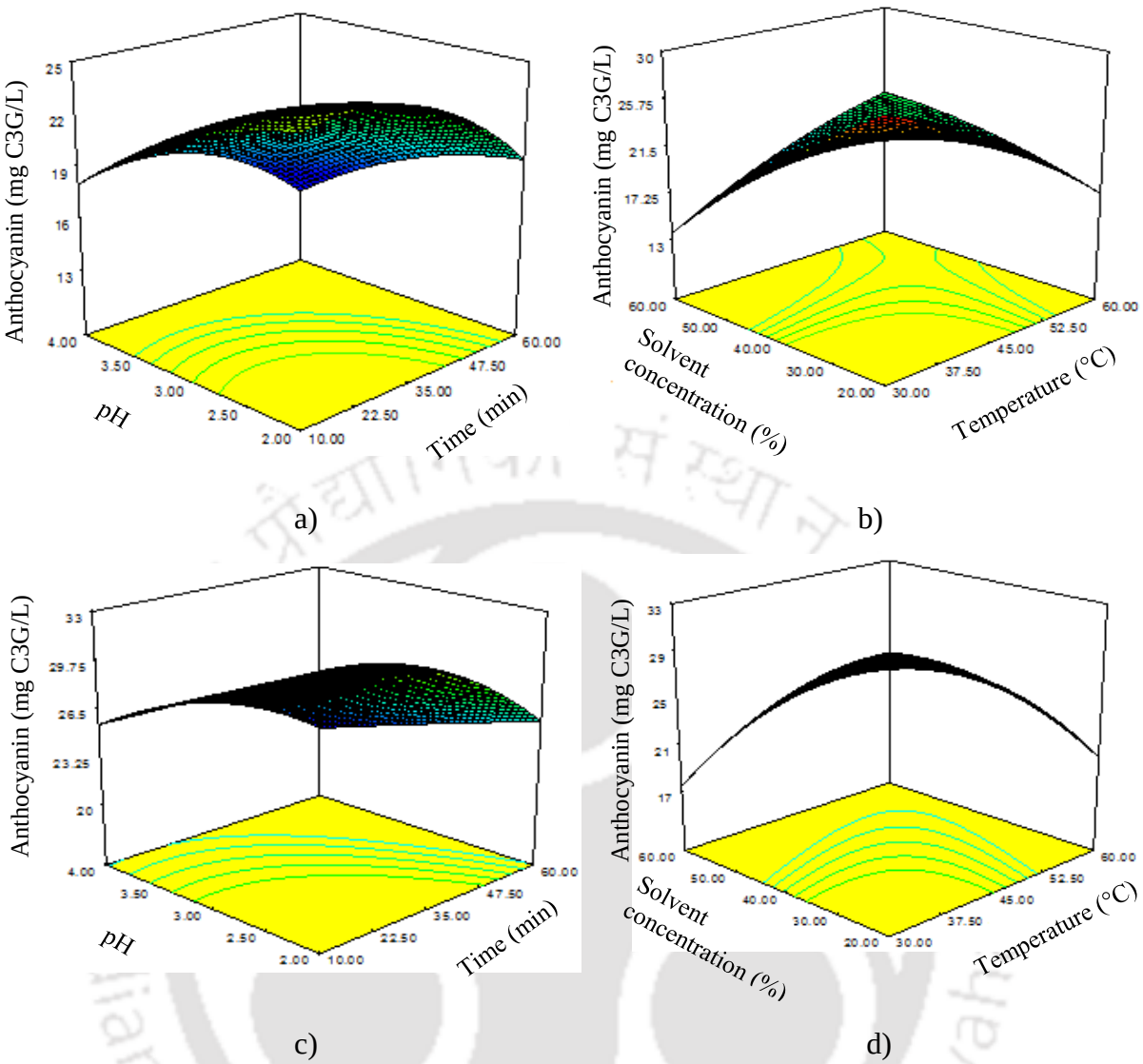

Fig. 3.7: Response surface and contour plots for the effect of independent variables a) pH and extraction time b) solvent concentration and temperature on anthocyanin of black bran extract c) pH and extraction time d) solvent concentration and temperature on anthocyanin of purple rice extract.

The change in solvent concentrations exerted a considerable effect on monomeric anthocyanin content of black and purple rice bran extract. **Figs. 3.7b** and **3.7d** showed the relationship between solvent concentrations with anthocyanin content in rice bran extract. For the increase in ethanol concentration up to 30 % (v/v), there was an increase in monomeric anthocyanin content in the extract. Further, an increase in ethanol concentration beyond this range leads to the reduced monomeric anthocyanin content in the extract similar to TPC. A similar type of behavior was observed by Chen et al. (2015) during the extraction of phenolic compounds, antioxidants, and anthocyanins from sugar beet

molasses. It may be attributed to the change of polarity which affected the diffusivity of the anthocyanin in rice bran and caused less extraction of anthocyanin from the rice bran (Bridgers et al., 2010).

The effect of temperature on extraction yield in ethanolic solution is illustrated in **Figs. 3.7b** and **3.7d**. The highest extraction yield in terms of anthocyanin was obtained at 37.50 °C for purple rice bran, whereas for black rice bran it was at 45 °C. A similar type of result was reported by Celli et al. (2015), in their study the highest anthocyanin content was obtained at 35 °C for haskap extract. The increase in temperature increases the anthocyanin content in the extract, which may be due to the diffusion of more polyphenol into the solvent during heating. Due to heat, the sample becomes soft and weakens the various phenol interactions, thus diffused more polyphenols into the solvent (Tao et al., 2014). However, the increase in the temperature beyond 37.50 °C for purple and 45 °C for black rice decrease the anthocyanin content in the extract. The decrease in anthocyanin at higher temperatures may be ascribed to the oxidation and degradation of anthocyanin (Tiwari et al., 2010).

3.3.6. Optimization and validation of extraction conditions

The objective of this step was to obtain the values of independent variables which would allow to obtain an extract with high total phenolic and monomeric anthocyanin content. From **Table 3.5** it was illustrated that the developed model (Equation no 3.5, 3.6, 3.7 and 3.8) can efficiently predict the value of total phenolic compound and monomeric anthocyanin content in UAE extract for black and purple rice bran (**Fig. 3.8**). Therefore, the developed models were used to optimize the process parameters for the UAE. Optimum conditions were selected using desirability for the maximum amounts of TPC and monomeric anthocyanin content in the extract. The maximum desirability of extraction conditions were 0.98 and 0.99 for black and purple rice bran, respectively. **Table 3.6** shows the optimal condition of the UAE for black and purple rice bran.

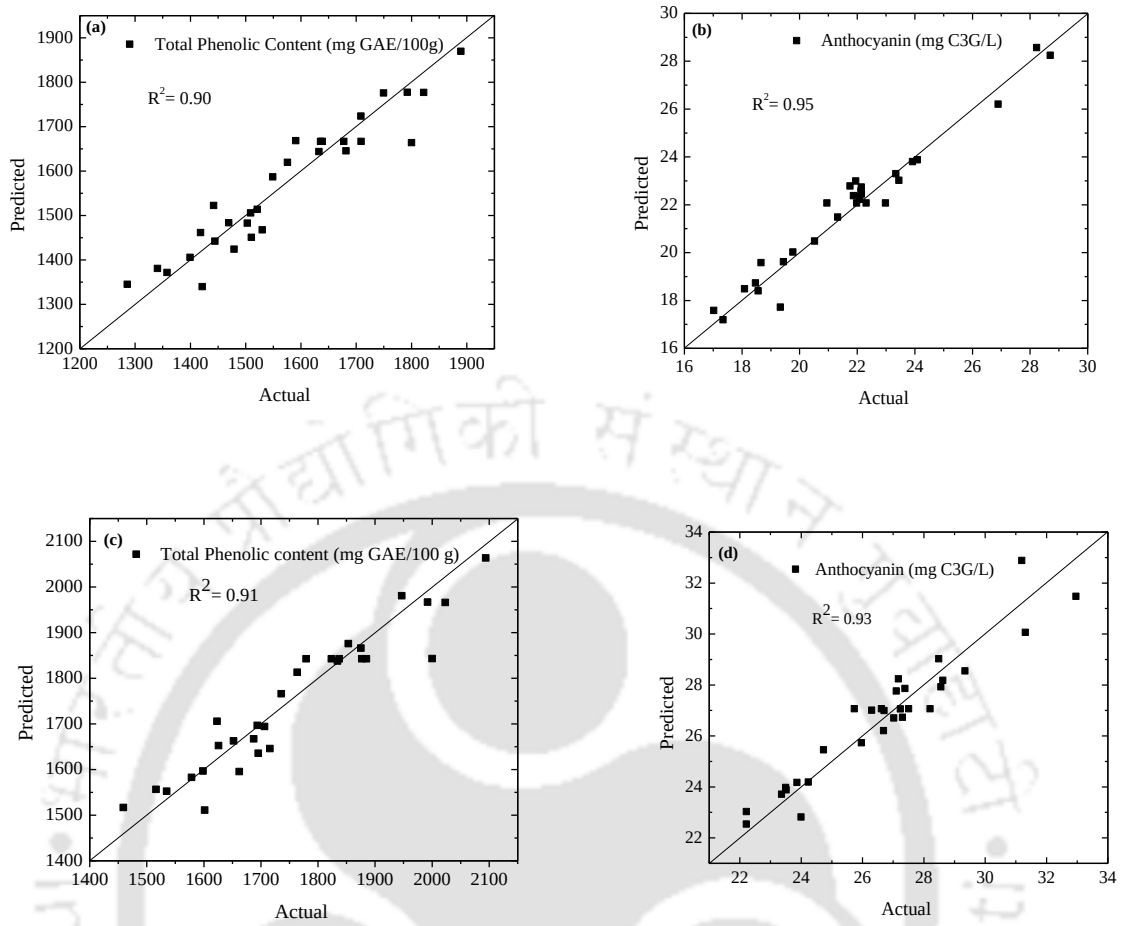

Fig. 3.8: Correlation between actual and predicted value of a) total phenolic b) monomeric anthocyanin content of black bran c) total phenolic d) monomeric anthocyanin content of purple bran extract

In order to verify the predictive capacity of the models, the optimum response variables were tested at the optimum condition by conducting the laboratory experiment. At the optimized condition, total phenolic compounds and monomeric anthocyanin content did not significantly differ from predicted values, (**Table 3.6**) which suggests that the formulated model was believed to be accurate and reliable. Therefore, for further prediction of experimental outcomes using ANN, RCCD data was used.

Table 3.6: Optimum conditions of UAE for black and purple rice bran

Rice bran	Temperature (°C)	pH	Solvent concent-ration (%)	Time (min)	Predicted		Experimental	
					Anthocy-anin (mg C3G/L)	TPC (mg GAE/100 g)	Anthoc-yanin (mg C3G/L)	TPC (mgGAE /100g)
Black	35.97	2.52	23.78	22.89	30.4	1957.4	31.9	1978.7
Purple	31.7	2.39	31.17	15.77	35.6	2125	34.9	2232.9

3.3.7. Comparison with conventional extraction process

The comparative analysis of UAE and conventional extraction process is shown in **Fig. 3.9**. From figure, it was observed that ultrasound significantly increased the TPC (1978.7 and 2232.9 mg GAE/100g) and monomeric anthocyanin (30.4 and 35.6 mg C3G/L) content over the conventional extraction (753.9 and 779 mg GAE/100g of TPC, 18.7 and 21.8 mg C3G/L) for black and purple rice bran, respectively.

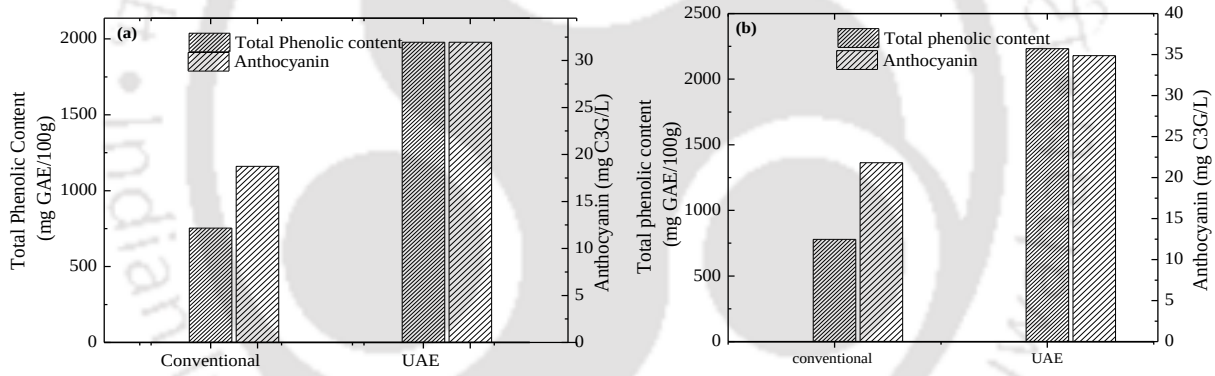

Fig. 3.9: Comparison of UAE and convention extraction process in optimum condition for a) black rice bran b) purple rice bran

In the ultrasound-assisted extraction, yield enhancement has been attributed to the propagation of ultrasound waves and resulting cavitation. The ultrasound wave causes high shear force which increases the mass transfer of TPC and anthocyanin from rice bran. The ultrasound wave also causes particle breakdown which provides more surface area that increases the mass transfer. On the other hand, cavitation bubbles collapse and generate macro-turbulence which caused high-velocity inter-particle collisions and agitation in microporous particles of the bran which accelerates the eddy diffusion and internal diffusion (Tao et al., 2014). Therefore, the UAE process showed a high yield in terms of

TPC and monomeric anthocyanin in black and purple rice bran extract over the conventional extraction process.

3.3.8. Comparison between ANN and RSM models

The RCCD data (In appendix **Tables 3A1** and **3A2**) was used to develop ANN-model for purple and black rice bran extract.

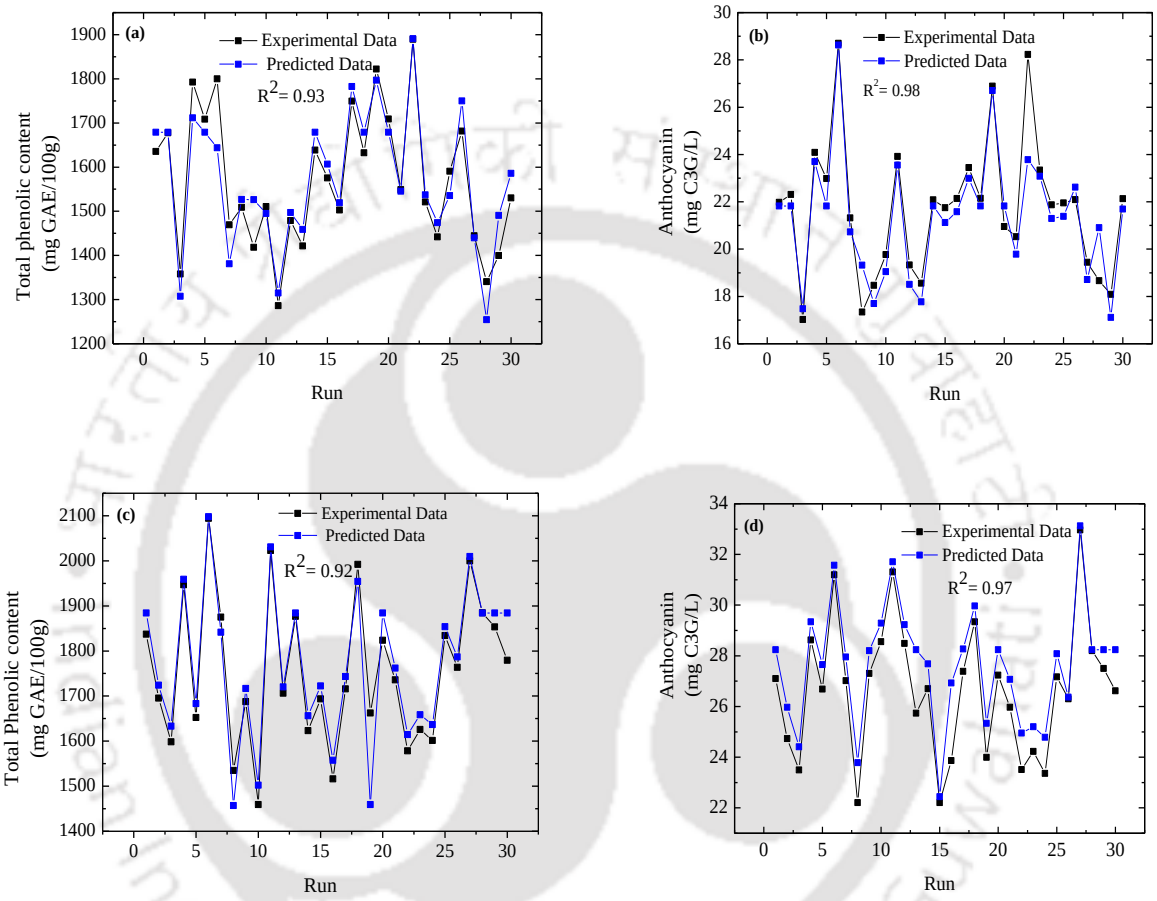

Fig. 3.10: Comparisons between ANN and RSM model for a) TPC b) anthocyanin from black rice bran and c) TPC d) anthocyanin from purple rice bran

The artificial neural network was developed using feed-forward network namely a multilayer perceptron (MLP) model. The performance and predictive capacity of developed ANN were determined using the coefficient of regression (R^2). It was found that ANN models with a high coefficient of regression (R^2) can predict the experimental outcome and the predictive capability of ANN model was higher than the RSM models. The ANN model predictions (R^2) were near to 1 than the RSM model (**Fig. 3.10**). Thus, the ANN model showed a significant and higher prediction capacity of experimental outcomes than the RSM model.

3.3.9. Analysis

3.3.9.1. GC-MS analysis of extract

The GC-MS analysis of black and purple rice bran extract is shown in **Table 3.7**. The component corresponding to each signal peak was identified based on the total ion chromatograms, and the results are shown in **Table 3.7**. In the present study, total of nine compounds were identified in purple rice bran extract, whereas in black rice bran extract only four compounds were detected. Among all these compounds, Hexadecanoic acid showed the highest peak area (1.1 and 1.0 %) for both the rice bran at a retention time of 16.85 min. *P*-tyrosol was also identified at a retention time of 24.22 min in both the rice bran extract. Acetic anhydride and propanoic were identified in purple and black rice bran at 3.59 min retention time with different probability (70.3, 4.3, 2.3, and 0.3 %). Thioacetic acid, pentanoic acid, heptacosanoic acid, quercetin, and vanillin were only identified in purple rice bran at 3.59, 19.65, 24.65 and 25.96 min with varying peak area.

Table 3.7: Compounds identified in the UAE extract of purple rice bran by GC-MS

Peak No	Retention time (min.)	Compounds	m/z	MW	Peak area (%)	
					Black Bran	Purple Bran
1	3.59	Propanoic acid	43	74.07	0.5	0.5
2	3.59	Thioacetic acid	43	76.12	----	0.5
3	3.59	Acetic anhydride	43	102.09	0.5	0.5
4	3.59	Pentanoic acid	43	102.13	----	0.5
5	16.85	Hexadecanoic acid	281.8	256.42	1.0	1.1
6	19.65	Heptacosanoic acid	355.7	270.45	----	0.3
7	24.22	p-tyrosol	153.5	138.16	0.9	0.7
8	24.56	Quercetin	355.2	302.23	---	0.1
9	25.96	Vanillin	73.2	152.15	----	0.2

3.3.9.2. β-Carotene, tocopherol, and tocotrienol

HPLC analysis at 280 nm showed several peaks among which 3, 3.5 and 3.8 min peaks were identified as β-carotene, tocopherol, and tocotrienol, respectively. The amounts of the vitamin in extract corresponding to the three peaks were determined by HPLC as shown in **Table 3.8**. The results revealed that β-carotene (182.5 and 165.4 µg/L), tocopherol (163 and 154.6 µg/L), and tocotrienol (133.2 and 127.5 µg/L) were present in high amount in both the rice bran extract, respectively. Purple rice bran contents quite a

high amount of β-carotene, tocopherol, and tocotrienol than black rice. Laokuldilok et al. (2010) found that black rice bran content high amount of tocopherol, and tocotrienol than other variety which was quite similar to the present study.

3.3.9.3. Cyanidin-3-glucoside and peonidin-3-glucoside

The detection of cyanidin-3-glucoside (C3G), and peonidin-3-glucoside (P3G) present in purple and black rice bran extract was performed using HPLC at 530 nm. The peak with retention time 11 and 13 min was identified as cyanidin-3-glucoside, and peonidin-3-glucoside, respectively. From **Table 3.8**, it was observed that cyanidin-3-glucoside was the major anthocyanin (192.6 µg/L) in purple rice bran extract over peonidin-3-D-glucoside (7.7 µg/L). Whereas, in black rice extract only cyanidin-3-glucoside (2.8 µg/L) was detected and quantified. A similar type of observation was reported by the previous researchers (Abdel-Aal et al., 2006; Celli et al., 2015) for various pigmented rice varieties.

Table 3.8: Values of vitamins and phenolic compounds obtained under the optimal UAE extraction conditions

Compounds	Retention time (minute)	Black bran (µg/L)	Purple bran (µg/L)
Vitamins			
1. β-Carotene	3	165.4	182.5
2. (±)-α-Tocopherol	3.5	154.6	163.5
3. D-α-Tocotrienol	3.8	127.5	133.2
Anthocyanin			
1. Cyanidin-3-glucoside	11	2.8	192.6
2. Peonidin-3-glucoside	13	0	7.7
Phenolic acid			
1. Caffeic acid	14.66	0	32
2. (±) Catechin hydrate	13	141.7	5.7
3. Chlorogenic acid	13.8	0	89.4
4. Vanillic acid	14.96	152.8	101.7
5. Syringic acid	15.06	72.9	74.0
6. Sinapic acid	17.8	15.9	27.9
7. 4-Hydroxybenzoic acid	18.03	347	349

3.3.9.4. Phenolic acids

The phenolic acid contents namely, Caffeic acid, Catechin hydrate, Chlorogenic acid, Coumaric acid, 4-Hydroxybenzoic acid, Syringic acid, Sinapic acid, and Vanillic acid were investigated in the purple and black rice bran extract. Caffeic acid, Catechin hydrate, Chlorogenic acid, 4-Hydroxybenzoic acid, Syringic acid, Sinapic acid, and Vanillic acid were identified and quantified in purple rice bran extract. The phenolic acids in purple and black rice bran extract were dominated by 4-Hydroxybenzoic acid (349 and 347 µg/L) with lesser amounts of Vanillic acid, Catechin hydrate, Syringic acid, and Sinapic acid (**Table 3.8**). Whereas, Caffeic acid and Chlorogenic acid were not detected in black rice bran extract. Very few studies have reported the occurrence of bound Vanillic acid in cereal (Miyazawa et al., 2003). Laokuldilok et al. (2010) reported the detection of six types of phenolic acids in the black, red and white rice bran. These observations were confirmed in the present study.

3.4. Summary

The present study has provided insights of conventional and ultrasound-assisted extraction of TPC and anthocyanin from black and purple rice bran. The conclusions are summarized as follows:

- The rotatable central composite design followed by response surface methodology were successfully applied to optimise solvent extraction process of phenolic content from purple and black rice bran.
- Ethanol was found to be promising solvent to extract the phenolic compound from black and purple rice bran.
- The experimental outcomes of extraction process were also successfully predicted using artificial neural network with higher coefficient (R^2=0.98 and 0.96) than RSM.
- The phytochemical profile of purple rice bran extract showed higher amount of TPC and anthocyanin (20.2 mg cyanidin-3-glucoside/L) content than black rice bran extract.
- The black rice bran extract content higher amount of flavonoid (17.8 mg quercetin/g) than purple rice bran (16.4 mg quercetin/g).
- The ultrasound-assisted extraction process was successfully applied to extract the TPC and anthocyanin from purple and black rice bran.

- The effect of variables on extraction process and optimization the process was done using RCCD followed by response surface methodology (RSM) method.
- The UAE process showed more efficiency than conventional extraction process.
- The phytochemical profile of extract in optimum condition using GC-MS and HPLC showed the presence of vitamin, phenolic compounds, and carboxylic acid.

References

Abdel-Aal, E. S. M., Young, J. C., and Rabalski, I. (2006). Anthocyanin composition in black, blue, pink, purple, and red cereal grains. *Journal of agricultural and food chemistry, 54*(13), 4696-4704.

Abid, M., Jabbar, S., Wu, T., Hashim, M.M., Hu, B., Lei, S., Zhang, X. and Zeng, X. (2013). Effect of ultrasound on different quality parameters of apple juice. *Ultrasonics Sonochemistry, 20*(5), 1182-1187.

Bridgers, E.N., Chinn, M.S. and Truong, V.D. (2010). Extraction of anthocyanins from industrial purple-fleshed sweetpotatoes and enzymatic hydrolysis of residues for fermentable sugars. *Industrial Crops and Products, 32*(3), 613-620.

Celli, G. B., Ghanem, A., and Brooks, M. S. (2015). Optimization of ultrasound-assisted extraction of anthocyanins from haskap berries (Lonicera caerulea L.) using Response Surface Methodology. *Ultrasonics Sonochemistry, 27*, 449-455.

Cevallos-Casals, B.A. and Cisneros-Zevallos, L. (2004). Stability of anthocyanin-based aqueous extracts of Andean purple corn and red-fleshed sweet potato compared to synthetic and natural colorants. *Food Chemistry, 86*(1), 69-77.

Chen, M., Zhao, Y., & Yu, S. (2015). Optimisation of ultrasonic-assisted extraction of phenolic compounds, antioxidants, and anthocyanins from sugar beet molasses. *Food Chemistry*, *172*, 543-550.

Chen, Y., Xie, M.Y. and Gong, X.F. (2007). Microwave-assisted extraction used for the isolation of total triterpenoid saponins from Ganoderma atrum. *Journal of Food Engineering*, *81*(1), 162-170.

Feng, S., Luo, Z., Tao, B. and Chen, C., (2015). Ultrasonic-assisted extraction and purification of phenolic compounds from sugarcane (*Saccharum officinarum L.*) rinds. *LWT - Food Science and Technology*, *60*(2, Part 1), 970-976.

Ferreira, I.C., Baptista, P., Vilas-Boas, M. and Barros, L. (2007). Free-radical scavenging capacity and reducing power of wild edible mushrooms from northeast Portugal: Individual cap and stipe activity. *Food Chemistry*, *100*(4), 1511-1516.

Friedman, M. and Jürgens, H. S. (2000). Effect of pH on the Stability of Plant Phenolic Compounds. *Journal of Agricultural and Food Chemistry*, *48*(6), 2101-2110.

Ghafoor, K., Choi, Y. H., Jeon, J. Y., and Jo, I. H. (2009). Optimization of ultrasound-assisted extraction of phenolic compounds, antioxidants, and anthocyanins from grape (*Vitis vinifera*) seeds. *Journal of Agricultural and Food Chemistry*, *57*(11), 4988-4994.

Hurtado, N.H., Morales, A.L., González-Miret, M.L., Escudero-Gilete, M.L. and Heredia, F.J., (2009). Colour, pH stability and antioxidant activity of anthocyanin rutinosides isolated from tamarillo fruit (*Solanum betaceum Cav*.). *Food Chemistry, 117*(1), 88-93.

Laokuldilok, T., Shoemaker, C.F., Jongkaewwattana, S. and Tulyathan, V., (2010). Antioxidants and antioxidant activity of several pigmented rice brans. *Journal of Agricultural and Food Chemistry*, *59*(1), 193-199.

Liu, Y., Wei, S. and Liao, M., (2013). Optimization of ultrasonic extraction of phenolic compounds from Euryale ferox seed shells using response surface methodology. *Industrial Crops and Products, 49*, 837-843.

Miyazawa, M., Oshima, T., Koshio, K., Itsuzaki, Y., and Anzai, J. (2003). Tyrosinase inhibitor from black rice bran. *Journal of Agricultural and Food Chemistry*, *51*(24), 6953-6956.

Miyazawa, M., Oshima, T., Koshio, K., Itsuzaki, Y. and Anzai, J. (2003). Tyrosinase inhibitor from black rice bran. *Journal of Agricultural and Food Chemistry*, *51*(24), 6953-6956.

Mokrani, A. and Madani, K. (2016). Effect of solvent, time and temperature on the extraction of phenolic compounds and antioxidant capacity of peach (*Prunus persica L.*) fruit. *Separation and Purification Technology, 162*, 68-76.

Myers, R.H. and Montgomery, D. C. (1995). *Response surface methodology: process and product optimization using designed experiments* (Vol. 4): Wiley New York.

Paździoch-Czochra, M. and Wideńska, A. (2002). Spectrofluorimetric determination of hydrogen peroxide scavenging activity. *Analytica Chimica Acta, 452*(2), 177-184.

Ramić, M., Vidović, S., Zeković, Z., Vladić, J., Cvejin, A. and Pavlić, B. (2015). Modeling and optimization of ultrasound-assisted extraction of polyphenolic compounds from Aronia melanocarpa by-products from filter-tea factory. *Ultrasonics Sonochemistry, 23*, 360-368.

Sahin, S., and Samli, R. (2013). Optimization of olive leaf extract obtained by ultrasound-assisted extraction with response surface methodology. *Ultrasonics Sonochemistry, 20*(1), 595-602.

Santos, Diego T., Veggi, Priscilla C., and Meireles, M. Angela A. (2010). Extraction of antioxidant compounds from Jabuticaba (*Myrciaria cauliflora*) skins: Yield, composition and economical evaluation. *Journal of Food Engineering, 101*(1), 23-31.

Schueller, Brandon S., and Yang, Ralph T. (2001). Ultrasound Enhanced Adsorption and Desorption of Phenol on Activated Carbon and Polymeric Resin. *Industrial & Engineering Chemistry Research, 40*(22), 4912-4918.

Sompong, R., Siebenhandl-Ehn, S., Linsberger-Martin, G. and Berghofer, E. (2011). Physicochemical and antioxidative properties of red and black rice varieties from Thailand, China and Sri Lanka. *Food Chemistry, 124*(1), 132-140.

Spigno, G., and De Faveri, D. M. (2009). Microwave-assisted extraction of tea phenols: A phenomenological study. *Journal of Food Engineering, 93*(2), 210-217.

Spigno, G., Tramelli, L., and De Faveri, D. M. (2007). Effects of extraction time, temperature and solvent on concentration and antioxidant activity of grape marc phenolics. *Journal of Food Engineering, 81*(1), 200-208.

Tao, Y., Wu, D., Zhang, Q.A. and Sun, D.W. (2014). Ultrasound-assisted extraction of phenolics from wine lees: Modeling, optimization and stability of extracts during storage. *Ultrasonics Sonochemistry, 21*(2), 706-715.

Tiwari, B. K., Patras, A., Brunton, N., Cullen, P. J., and O'Donnell, C. P. (2010). Effect of ultrasound processing on anthocyanins and color of red grape juice. *Ultrasonics Sonochemistry, 17*(3), 598-604.

Vilkhu, K., Mawson, R., Simons, L. and Bates, D. (2008). Applications and opportunities for ultrasound assisted extraction in the food industry — A review. *Innovative Food Science & Emerging Technologies, 9*(2), 161-169.

Wang, J., Sun, B., Cao, Y., Tian, Y. and Li, X. (2008). Optimisation of ultrasound-assisted extraction of phenolic compounds from wheat bran. *Food Chemistry, 106*(2), 804-810.

Wang, X., Wu, Y., Chen, G., Yue, W., Liang, Q., and Wu, Q. (2013). Optimisation of ultrasound assisted extraction of phenolic compounds from Sparganii rhizoma with response surface methodology. *Ultrasonics Sonochemistry, 20*(3), 846-854.

Zhang, Z.S., Wang, L.J., Li, D., Jiao, S.S., Chen, X.D. and Mao, Z.H., (2008). Ultrasound-assisted extraction of oil from flaxseed. *Separation and Purification Technology, 62*(1), 192-198.

TO STUDY THE ADSORPTION AND DESORPTION CHARACTERISTICS OF ANTHOCYANIN EXTRACTED FROM PURPLE RICE BRAN AND ITS DEGRADATION KINETICS

Part of the work is published in

- Journal of Food Process Engineering, 41(6), e12834.
- Journal of Food Process Engineering, DOI:10.1111/jfpe.13360

CHAPTER 4

TO STUDY THE ADSORPTION AND DESORPTION CHARACTERISTICS OF ANTHOCYANIN EXTRACTED FROM PURPLE RICE BRAN AND ITS DEGRADATION KINETICS

4.1. Overview

The adsorption and desorption behavior of anthocyanin in the aqueous solution of crude purple rice bran extract was investigated using various adsorbents such as amberlite XAD2, XAD4, XAD7, activated charcoal, and bentonite. Amberlite XAD7 showed higher adsorption/desorption capacities and recovery of anthocyanin from bran extract over other adsorbents. The recovery of anthocyanin from XAD7 was 41.5 % while adsorption and desorption capacities were 1.9 mg/g and 1.8 mg/g, respectively. The adsorption behavior of anthocyanin indicated that the process was better explained by pseudo-first order kinetics than pseudo-second order kinetics model. Adsorption isotherm behavior of anthocyanin on adsorbents was found to be homogeneous and more suitable for Langmuir (two parameters), and Redlich–Peterson (three parameters) isotherm model. The adsorption mechanisms of adsorbents were well explained by the intra-particle diffusion model and indicated that XAD7 has a higher diffusion rate than the other adsorbents. The phytochemical profiling of the separated and concentrated bran extract was investigated in terms of anthocyanins, cyanidin-3-glucoside (C3G), peonidin-3-glucoside (P3G) and phenolic acid content. After adsorption/desorption, the degradation kinetics of anthocyanin, C3G, and P3G has been investigated at various pH and temperature conditions. The effect of hydrocolloids on the stability of anthocyanins was also determined. At pH 2, the total anthocyanin, C3G, and P3G showed the lowest degradation rate. During thermal degradation, the lowest rate of degradation for total anthocyanin (3.5×10^{-4} /min), C3G (1.8×10^{-4} /min), and P3G (2×10^{-4} /min) was observed at 60 °C. The highest degradation rate of total anthocyanin, C3G, and P3G, was obtained at 6 pH and 90 °C. The effect of carboxymethyl cellulose, xanthan gum, modified starch, and gum arabic on the stability of anthocyanin, C3G, and P3G was significant ($p \leq 0.05$). The modified starch system showed the highest stability of anthocyanins and antioxidant activity in the aqueous medium. The degradation kinetics of anthocyanins in

modified starch medium revealed a lower degradation rate than without a hydrocolloid sample.

4.2. Precise background

After extraction of anthocyanin from purple rice bran, it needs to be separated and concentrated for further enhancement of its activity. Anthocyanins are sensitive to many environmental factors, such as temperature, oxygen, light, and pH, these factors are detrimental to the color and nutritional properties of anthocyanins, thus restricting their applications in foods. Therefore, there is a need to concentrate more specifically using non-thermal processing. Membrane filtration, supercritical fluid extraction, vacuum evaporation, and adsorption are used for the concentration of bioactive compounds from the plant sources. However, except for adsorption, all the above-mentioned processes are sophisticated, complex with a high amount of energy requirement and high maintenance costs. Whereas, adsorption is a single step non-thermal way to concentrate bioactive compounds, namely, anthocyanin from the crude extract of plant sources with low energy and fewer maintenance costs. Moreover, in order to predict the changes in the quality of anthocyanins during storage and processing, degradation behavior is a matter of great concern. Additionally, to develop a stable anthocyanin, there is a need to study the influence of various types of food-grade hydrocolloids on anthocyanin. Thereby, this chapter includes the adsorption/desorption, diffusion, and thermodynamic properties of anthocyanin. The degradation behavior of the anthocyanin at various conditions as well as stability effect of hydrocolloids are also discussed.

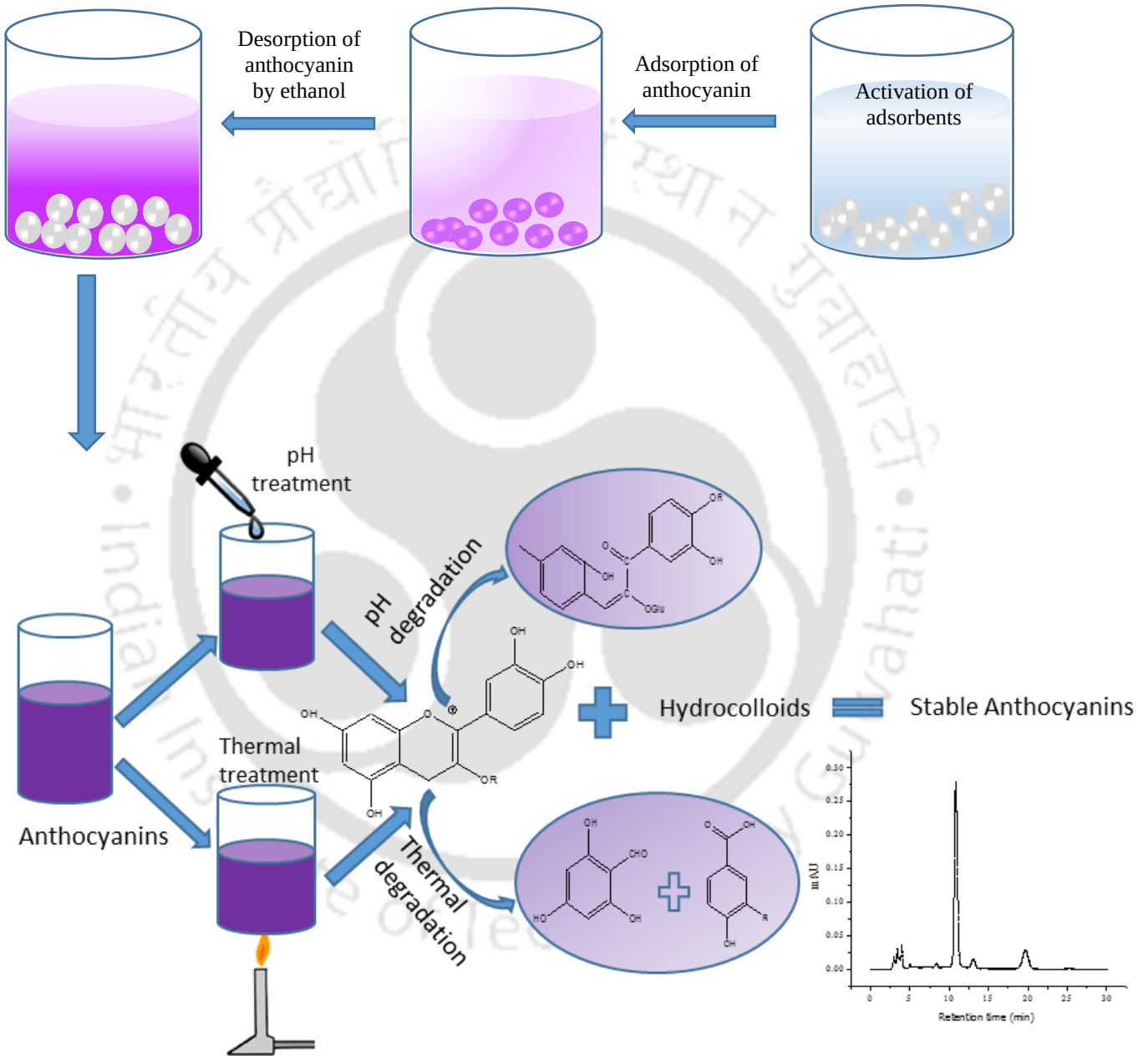

Fig. 4.1: Graphical abstract

4.3. Results and discussion

4.3.1. Adsorption and desorption of anthocyanin

Adsorption and desorption behavior of anthocyanin from purple rice bran extract on various absorbents are shown in **Fig. 4.2** (**a**, **b**, and **c**). The figure shows higher adsorption ratio for bentonite (68.9 %), amberlite XAD2 (52.2 %), and XAD7 (43.3 %), followed by charcoal (32.2 %) and XAD4 (16.5 %). Whereas, the higher adsorption capacity was observed for XAD7 as 1.9 mg/g than XAD2 (0.7 mg/g) and XAD4 (0.6 mg/g). The lower adsorption capacity was observed for bentonite (0.2 mg/g) and charcoal (0.1 mg/g).

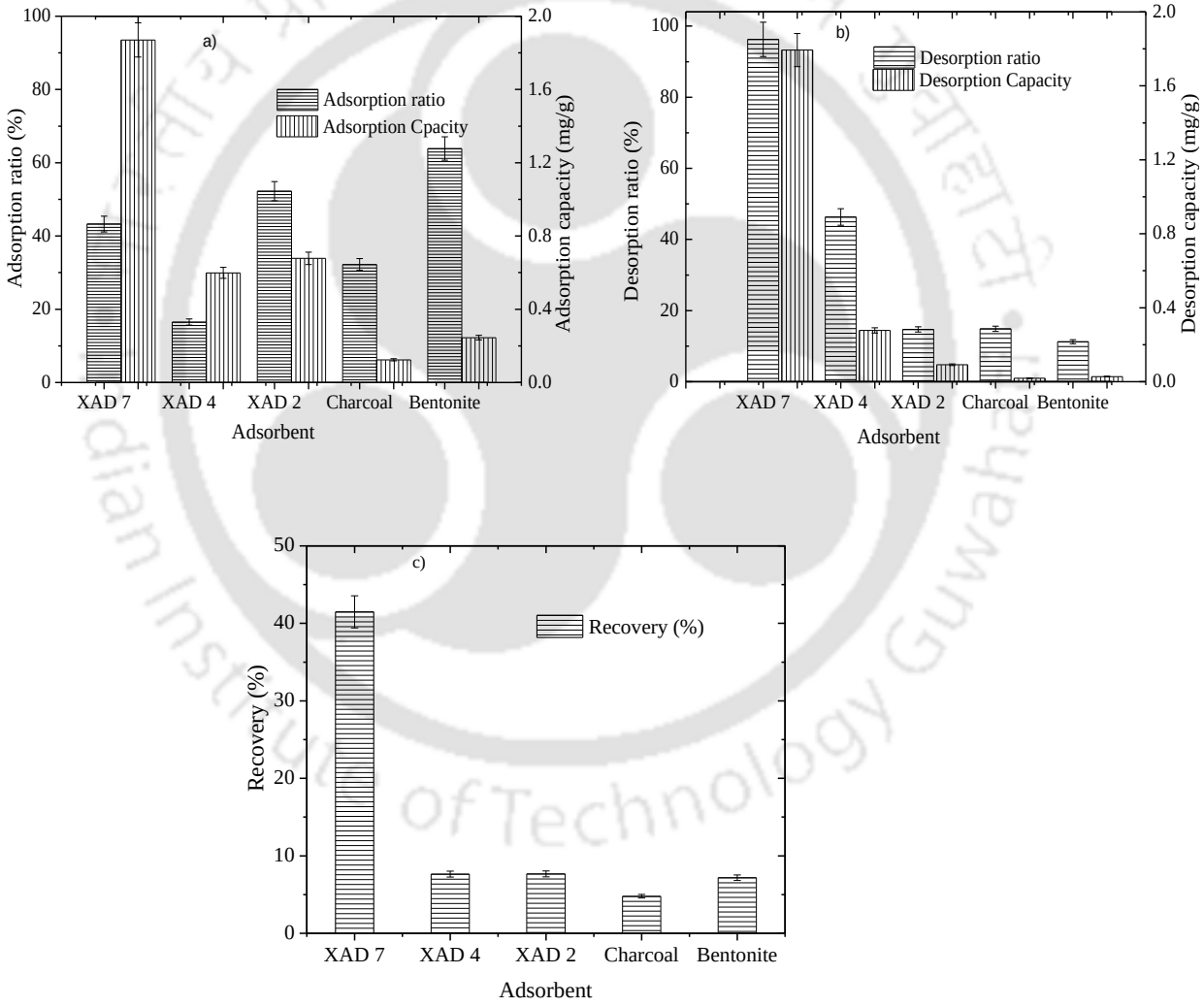

Fig. 4.2: a) Adsorption capacity and adsorption ratio b) desorption capacity and desorption ratio and c) recovery behavior of anthocyanin on various adsorbents

The adsorption of anthocyanin on various adsorbent is a physical phenomenon through van der Waals force or hydrogen bonding between the adsorbent, adsorbate, and solvent (Yang et al., 2016). In the present study, amberlite XAD7 showed highest adsorption capacity followed by XAD2 and XAD4. It may be attributed to similar polarity of XAD7 with the anthocyanin than the other adsorbents (Gao et al., 2013), though the specific surface area of XAD7 is lower than XAD4 but higher than XAD2. It was reported that when the polarity of adsorbent is similar to the polarity of adsorbate a better adsorption ability could be observed (Jampani et al., 2014). It was suggested that as the adsorbent polarity increases the solvent-adsorbent interacts more with a concomitant reduction in the adsorbate-adsorbent interaction (Koresh et al., 1985). However, higher adsorption ratio for bentonite could be due to the presence of negative charge on its surface (Var et al., 2008) which attracts more flavylium cation on the surface. It was reported that all the anthocyanin contain flavylium cation (Castañeda-Ovando et al., 2009). However, the anthocyanin from rice bran was also found to contain flavylium cation within the wide pH range (Jia et al., 2017).

From **Fig. 4.2b**, it was observed that desorption ratio and desorption capacity of amberlite XAD7 (96.3 % and 1.8 mg/g) was significantly higher than XAD2 (14.7 % and 0.09 mg/g), XAD4 (46.3 % and 0.3 mg/g), charcoal (14.9 % and 0.02 mg/g) and bentonite (11.2 % and 0.03 mg/g) for anthocyanin from purple rice bran extract. Zhang et al. (2008) observed the similar type of results during separation of anthocyanin from mulberry. The higher desorption ratio and capacity of XAD7, may be due to the higher pore volume (Buran et al., 2014), which tend to increase the mass transfer rate and allow more material to be transferred from the resin, thereby increasing the desorption ratio and capacity, which indirectly increase the recovery of anthocyanin (Foo and Hameed, 2010). It was observed from the **Fig. 4.2c** that XAD7 has exhibited the highest recovery (41.5 %) of anthocyanin than XAD2 (7.7 %), XAD4 (7.6 %), bentonite (7.2 %), and charcoal (4.8 %) which is in agreement with the desorption behavior.

4.3.2. Adsorption kinetics

The adsorption kinetics of anthocyanin on XAD2, XAD4, XAD7, and bentonite are shown in **Table 4.1**. The anthocyanin recovery from activated charcoal was very less; therefore, activated charcoal was not considered for adsorption kinetics study. The adsorption kinetics was investigated with the pseudo-first-order (Lagergren, 1898) and pseudo-second-

order (Ho and McKay, 1999) kinetics model. In general, the pseudo-first order model is applicable in the initial stage of the adsorption process, while the pseudo-second order model is applicable over the whole range of adsorption process (Chen et al., 2016). The experimental result of anthocyanin uptake (q_t) by resin versus time (t) was fitted to the above-mentioned models by nonlinear regression method. In order to assess the applicability of pseudo-first order model for anthocyanin adsorption process, a linear plot of $\log(q_e–q_t)$ Vs t was obtained as shown in **Fig. 4.3a**. **Fig. 4.3b** shows the linear plot of t/q_t Vs t for pseudo-second order kinetic study. The equilibrium adsorption capacity (q_e) and rate constant (k_1) were determined from the slope and intercept of **Fig. 4.3a** and presented in **Table 4.1**. It was revealed from **Table 4.1** that the pseudo-first order model agreed well with the adsorption data and provided higher coefficients of determination (R^2). It was inferred from the result that the adsorption of anthocyanin on adsorbents was diffusion controlled (Yuh-Shan, 2004). Moreover, it can also be concluded that adsorption process is not dependent on the concentrations of both reactants (physical exchange), therefore the adsorption process of anthocyanin onto adsorbents was physisorption (Fierro et al., 2008). The pseudo-first-order model for anthocyanin on XAD7 showed the highest q_e value (1.9 mg/g) with k_1 (0.03 1/min). It can be seen from the **Table 4.1** that the q_e values of anthocyanin from the pseudo-first-order kinetic model were close to the experimental data. Therefore, it can be concluded that pseudo-first order kinetic model can efficiently predict the anthocyanin adsorption capacity of adsorbents at equilibrium condition. Similar types of results were observed by the previous researcher during the separation of anthocyanins from mulberry using macro porous adsorbent resins (Chen et al., 2016).

From **Table 4.1**, it can be observed that the adsorption of anthocyanin onto the adsorbent was more suitable for pseudo-first order than the pseudo-second order kinetics, due its diffusion controlled behavior and physic-sorption characteristic. In the pseudo-second order kinetics study, XAD7 showed the highest coefficients of determination (R^2) value than other adsorbents. The equilibrium adsorption capacity (q_e) and rate constant (k_2) determined from the slope and intercept of the plot (**Fig. 4.3b**) are presented in **Table 4.1**. It can be seen from **Table 4.1** that the adsorption capacity (q_e) obtained from the model was much higher than the experimental value which elucidates that pseudo-second order kinetic model is not suitable to describe the adsorption behavior and unable to predict the equilibrium adsorption capacity of anthocyanin on adsorbents.

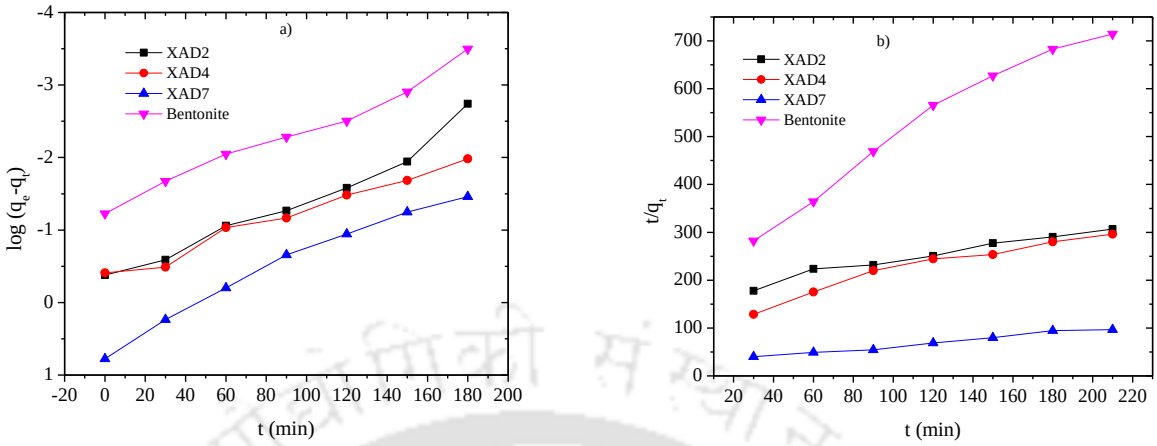

Fig. 4.3: Modelling of the kinetics data using a) pseudo-first-order kinetics, and b) pseudo-second-order kinetics model

It was suggested that pseudo-second order kinetics signifies the rate-limiting step for chemical sorption involving valence forces through sharing or exchange of electrons between sorbent and sorbate (Ho and McKay, 1999). Therefore, from the present study, it can be inferred that pseudo-first order model can efficiently explain the adsorption kinetics behavior of anthocyanin from purple rice bran extract using XAD2, XAD4, XAD7 and bentonite than pseudo-second order kinetics model.

Table 4.1: Pseudo first and pseudo second order kinetics model parameters

Pseudo first order	q_e **(mg/g)**	k_1 **(1/min)**	R^2
XAD2	0.8	0.03	0.96
XAD4	0.7	0.02	0.97
XAD7	1.9	0.03	0.97
Bentonite	0.3	0.03	0.98
Pseudo second order	q_e **(mg/g)**	k_2 **(g/mg min)**	R^2
XAD2	1.5	0.002	0.96
XAD4	1.1	0.006	0.94
XAD7	2.9	0.004	0.97
Bentonite	0.4	0.026	0.97

4.3.3. Adsorption isotherms

In general, an adsorption isotherm describes the mobility of a substance from the liquid environment to a solid-phase in a certain condition (Foo and Hameed, 2010). The adsorption process takes place until an equilibrium is established between an amount of solid-bound sorbate pieces and its portion remaining in solution (Zhou et al., 2001). In the present study, the adsorption isotherms of anthocyanin from purple rice bran extract on XAD2, XAD4, XAD7, and bentonite were studied using various adsorption isotherm models as shown in **Table 4.2**.

4.3.3.1. Two parameter isotherms

Langmuir isotherm model

The Langmuir isotherm model describes monolayer adsorption onto a homogeneous surface with no interaction between adjacent adsorbed molecules (Gao et al., 2013). The constants of Langmuir equations were calculated from the slope and intercepts of the plots shown in **Fig. 4.4a** and presented in **Table 4.2**. The highest value of coefficients of determination (R^2) for the Langmuir model was observed for XAD4 (0.99) followed by XAD2 (0.99), XAD7 (0.99) and bentonite (0.99). The K_L value of Langmuir model is known as affinity constant (Buran et al., 2014) and from the **Table 4.2**, it can be observed that bentonite (195.4 L/mg) has the highest affinity than XAD7, XAD2, and XAD4, respectively. From **Table 4.2**, it was observed that the coefficients of determination (R^2) of various absorbents for the Langmuir model were quite higher than Freundlich model, thereby it can be concluded that the adsorption behavior of anthocyanin from purple rice bran extract was quite favorable for Langmuir isotherm (Buran et al., 2014; Chandrasekhar et al., 2012; Foo and Hameed, 2010).

Freundlich isotherm model

According to the Freundlich model, the surface of the adsorbent is heterogeneous and it describes the adsorption behavior of a mono and multi-molecular layer (Buran et al., 2014). The constants of Freundlich equations were calculated from the slope, intercepts of **Fig. 4.4b**, and tabulated in **Table 4.2**. This table shows that except Bentonite, all the adsorbents have coefficients of determination (R^2) lower than the Langmuir isotherm model, which revealed that adsorption data of XAD7, XAD2, and XAD4 were better fitted with Langmuir isotherm model than the Freundlich isotherm model. A similar type of result was observed by Buran et

al. (2014) during separation of anthocyanin from blueberries using macro-porous adsorbent resins. From the **Table 4.2**, it can be observed that the coefficients of determination of XAD7 (0.99) and XAD4 (0.99) resin are higher than XAD2 (0.99) for Freundlich model. It is observed from **Table 4.2** that the *n* values of XAD2 (1.6), XAD4 (1.8), XAD7 (2.0), and bentonite (1.1) are higher than one and thereby it can be inferred that the adsorption of anthocyanin was homogeneous in nature, which implies that the adsorption of anthocyanin on the selected adsorbent surface cannot be explained efficiently with the Freundlich isotherm model.

Table 4.2: Adsorption isotherm model constants for anthocyanin on various adsorbents

Model	**Adsorbent**			
Langmuir	**XAD2**	**XAD4**	**XAD7**	**Bentonite**
q_m (mg/g)	1.3	1.3	2.7	1.8
K_L (L/mg)	41.3	35.04	23.3	195.4
R^2	0.99	0.99	0.99	0.99
Freundlich				
K_F (L/g)	0.3	0.3	0.6	0.1
N	1.6	1.8	2.0	1.1
R^2	0.99	0.99	0.99	0.99
Hill				
q_m (mg/g)	1.5	8.02	1.8	13.8
K_d (L/g)	1.2	8.8	5.9	0.8
N	0.6	0.6	0.5	14.0
R^2	0.99	0.99	0.99	0.99
Redlich–Peterson				
K_r (L/mg)	0.2	0.4	0.2	0.7
A_t (1/mg)	0.2	0.5	0.4	0.8
N	0.9	0.9	0.9	1.1
R^2	0.99	0.99	0.99	0.98
Toth				
K_t (mg/g)	0.8	0.6	8.2	0.9
a_t (L/mg)	42.0	35.0	23.2	175.3
N	0.6	0.5	4.7	0.6
R^2	0.99	0.99	0.99	0.99
Koble–Corrigan				
A (L mg/g)	0.02	0.07	0.07	0.08
B (L/mg)	0..09	0.01	0.2	0.06
N	0.6	0.5	0.5	0.9
R^2	0.99	0.99	0.99	0.99

However, for bentonite, the coefficients of determination (0.99) are higher for Freundlich model than Langmuir isotherm model, thus it can be inferred that adsorption of anthocyanin onto bentonite was heterogeneous in nature.

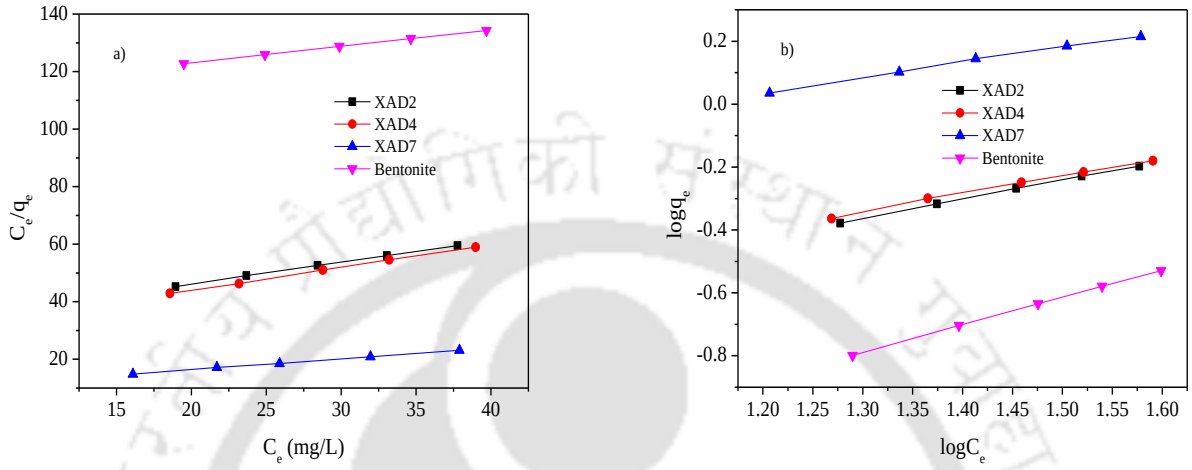

Fig. 4.4: a) Langmuir isotherm plot (C_e/q_e Vs C_e) and b) Freundlich isotherm plot (log q_e Vs log C_e) for adsorption of anthocyanins

Hill isotherm model

Hill equation was used to describe the adsorption of substance on the homogeneous surface. According to Hill model, the adsorption is assumed to be a cooperative phenomenon (Foo and Hameed, 2010). It can be observed from the **Table 4.2** that the coefficients of determination (R^2) of Hill model for anthocyanin adsorption onto adsorbents were quite lower than Langmuir isotherm model. Hence, it was evidenced that the adsorption data of XAD7, XAD4, XAD2, and Bentonite were not fitted well with the Hill isotherm model and thereby Hill model may not explain properly the adsorption isotherm of anthocyanin from purple rice bran extract on the adsorbent surface.

4.3.3.2. Three parameter isotherms

Redlich–Peterson isotherm model

Redlich–Peterson isotherm is a combination of Langmuir and Freundlich isotherms (Foo and Hameed, 2010), with three parameters empirical equation. It has a linear part in the numerator and an exponential part in the denominator that can be applied either in homogeneous or heterogeneous systems. It was observed that for Redlich–Peterson isotherm

model, XAD4 (0.99) had the higher coefficients of determination (R^2) than XAD2 (0.99), XAD7 (0.99), and bentonite (0.98). According to Redlich–Peterson isotherm, an adsorption process will be a heterogeneous non-ideal isotherm, when *n* greater than 1 and a homogeneous isotherm, when *n* less than 1 (Gao et al., 2013). In the present study, XAD2, XAD4, and XAD7 showed *n* values lower than one, which elucidated the homogeneous nature of adsorption (**Table 4.2**), which was quite similar to Langmuir isotherm behavior. However, the *n* value of bentonite was greater than 1, which implies that the adsorption behavior of anthocyanin on bentonite was heterogeneous in nature, similar to Freundlich model.

Toth isotherm model

Toth isotherm model is used to improve Langmuir isotherm fittings and to describe the heterogeneous adsorption (Hamdaoui and Naffrechoux, 2007). From **Table 4.2**, it can be seen that the coefficients of determination (R^2) of Toth model for all the adsorbents was quite higher and was similar to Langmuir isotherm model. Moreover, the *n* values of adsorbents were quite higher which revealed the homogeneous adsorption of anthocyanin on the adsorbents. A similar type of observation was reported by Hamdaoui and Naffrechoux (2007) during their study on modeling of adsorption isotherms of phenol and chlorophenols.

Koble–Corrigan isotherm model

Koble–Corrigan isotherm is a three-parameter equation, which is the combination of Langmuir and Freundlich isotherm models (Foo and Hameed, 2010). From the **Table 4.2**, it was observed that the coefficients of determination (R^2) of XAD2 (0.99), XAD4 (0.99), XAD7 (0.99) and bentonite (0.99) were quite higher, that implied the adsorption of anthocyanin on adsorbents could be correlated using Koble-Corrigan isotherm model.

4.3.4. Diffusion model

The adsorption mechanism of anthocyanin from purple rice bran extract on adsorbents was investigated using the Weber and Morris intra-particle diffusion model. The mechanism of adsorption is generally considered to involve three steps: (1) mass transfer of adsorbate from boundary film to the surface of adsorbent (film diffusion); (2) mass transport of adsorbate molecules within the pores of adsorbent (intra-particle diffusion); and (3) adsorption of the adsorbate molecules on the interior surface of adsorbent (Gao et al., 2013). In the present study, the plots of q_t Vs $t^{0.5}$ (**Fig. 4.5**) for various adsorbents, shows multi-linearity which indicates

that the adsorption of anthocyanin from purple rice bran extract might have various adsorption steps of mass transfer on various adsorbents. Moreover, Gao et al. (2013) suggested that if the plot gives a straight line and pass through the origin, then the adsorption process of anthocyanin is controlled only by the intra-particle diffusion. On the other hand, if the plot shows multi-linear characteristic and does not pass through the origin, the adsorption process is controlled by two or more diffusion mechanisms. Therefore, from the **Fig. 4.5**, it can be inferred that intra-particle diffusion is not the sole adsorption mechanism for anthocyanin from purple rice bran extract onto the adsorbents. Moreover, the last part of the **Fig. 4.5** (3rd stage) illustrated the final equilibrium stage at which the diffusion rate decreases due to lower anthocyanin concentration in solution. In the present study, diffusion mechanism was investigated using Weber and Morris intra-particle diffusion model for single and multi-stage diffusion systems as shown in **Table 4.3**.

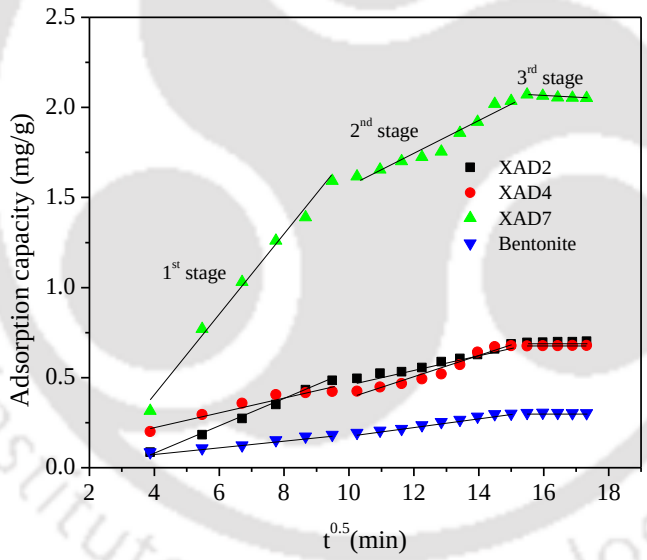

Fig. 4.5: Intra-particle diffusion modelling of anthocyanin on various adsorbents

From the single stage (**Table 4.3**), it was observed that the rate of diffusion was highest for XAD7 (0.1 g/mg $min^{0.5}$). However, in the single stage, bentonite showed the highest coefficients of determination (R^2=0.98), but it also showed the lowest rate of diffusion (0.02 g/mg $min^{0.5}$) as shown in **Table 4.3**. In case of multi-stage (**Table 4.3**), it was observed that the rate of diffusion for the first stage was quite higher than the second and third stage for all

the adsorbents, which indicates that both film diffusion and intra-particle diffusion play an important role in the adsorption of anthocyanin on the adsorbents.

Table 4.3: Intra-particle diffusion model parameter of adsorbent

Adsorbent	Single Stage		Three Stage		
	K_i (g/mg min$^{0.5}$)	R^2	Stage	K_i (g/mg min$^{0.5}$)	R^2
XAD2	0.04	0.95	1st	0.07	0.99
			2nd	0.04	0.98
			3rd	0.003	0.95
XAD4	0.03	0.95	1st	0.04	0.94
			2nd	0.06	0.95
			3rd	0.001	0.99
XAD7	0.11	0.90	1st	0.22	0.99
			2nd	0.09	0.95
			3rd	-0.01	0.89
Bentonite	0.02	0.97	1st	0.02	0.98
			2nd	0.02	0.99
			3rd	-0.001	0.92

4.3.5. Thermodynamics parameters of adsorption

Table 4.4 shows the thermodynamic parameters for adsorption of anthocyanin from purple rice bran extract on XAD7 resin. The enthalpy (ΔH) of the adsorption process was calculated using Eq. 2.22 and showed in **Table 4.4.** The negative values of ΔH (-40.3 kJ/mol) implied the exothermic nature of the anthocyanin adsorption onto the XAD7 resin. Thus, it can be inferred that the adsorption process of anthocyanin on XAD7 can be performed at 28 °C. The magnitude of enthalpy (ΔH) also provides an idea about the type of sorption. Gökmen and Serpen (2002) showed that if the ΔH value is less than 43 kJ/mol, the adsorption is a physical process rather than the chemical process. The entropy change (ΔS) of anthocyanin adsorption on XAD7 showed negative values (**Table 4.4**). The results implied that there was an increase in the randomness of solute adsorption at the solid-liquid interface, which may due to the replacement of water or anthocyanin molecules by subsequent water or anthocyanin on the resin surface. Eventually, the amount of adsorbate on the adsorbent surface was decreased. The change of Gibbs free energy (ΔG) for the adsorption increasing with increases in temperature, indicating that the adsorption was more favorable at a lower temperature. Therefore, from the

results, it can be implied that due to increase in temperature, the adsorption of anthocyanin on XAD7 decreased and was consistent with the results of the adsorption equilibrium study.

Table 4.4: Thermodynamic parameters for the adsorption process of anthocyanins on XAD7

Temperature (K)	ΔH (kJ/mol)	ΔS (J/mol K)	ΔG (kJ/mol)	R^2
298		-0.1361	0.25	
303	-40.3	-0.1362	0.95	0.98
308		-0.1363	1.67	

4.3.6. Anthocyanin and phenolic acid analysis

A comparative analysis of crude anthocyanin extract, and concentrated anthocyanin for monomeric anthocyanin, cyanidin-3-glucoside, peonidin-3-glucoside, and phenolic acids are shown in **Table 4.5**. Monomeric anthocyanin, cyanidin-3-glucoside, and peonidin-3-glucoside contents were higher in concentrated anthocyanin sample than fresh extract.

Table 4.5: Anthocyanin and phenolic acids analysis of extract

Compounds	Retention time (min)	Fresh purple rice bran extract	Concentrated purple rice bran extract
1. Monomeric anthocyanin (mg/L)		35.6	196.8
Anthocyanin (µg/L)			
1. Cyanidin-3-glucoside	11	192.6	1280
2. Peonidin-3-glucoside	13	7.7	68.9
Phenolic acid (µg/L)			
1. Caffeic acid	14.66	32	205.4
2. (±) Catechin hydrate	13	5.7	48.6
3. Chlorogenic acid	13.8	89.4	562.5
4. Vanillic acid	14.96	101.7	538.6
5. Syringic acid	15.06	74.01	361.9
6. Sinapic acid	17.8	27.9	164.6
7. 4-Hydroxybenzoic acid	18.03	349	1021.7

Concentrated anthocyanin sample contents 196.8 mg/L anthocyanin, 1280 µg/L cyanidin-3-glucoside, and 68.9 µg/L peonidin-3-glucoside whereas fresh extract contented 28.8 mg/L anthocyanin, 192.6 µg/L cyanidin-3-glucoside, and 7.7 µg/L peonidin-3-glucoside. **Table 4.5** also showed the phenolic acids content in crude extract and concentrated extract of purple rice bran. It was observed from the **Table 4.5** that separated sample content very high amount of phenolic acid than the fresh extract.

4.4. Degradation of anthocyanins

Degradation of monomeric anthocyanin, C3G, and P3G were studied at various pH (2, 4, 6, and 8) and temperatures (60 °C, 70 °C, 80 °C, and 90 °C) condition. The logarithmic of monomeric anthocyanin, C3G, and P3G content in aqueous medium were plotted as a function of time. The values of reaction rate constant (k) and half-life ($t_{1/2}$) of monomeric anthocyanin, C3G, and P3G are shown in **Table 4.6**.

4.4.1. Effect of pH

The degradation behavior of monomeric anthocyanin, C3G, and P3G from purple rice bran at various pH conditions was investigated and plotted as a function of time as shown in **Figs. 4.6a, 4.6b,** and **4.6c**. Figure illustrated that pH based degradation of monomeric anthocyanin, C3G, and P3G from purple rice bran followed the first-order reaction kinetics. The previous researchers also reported the similar type of observations (Kırca et al., 2007; Martynenko and Chen, 2016; Sui et al., 2014). The goodness of fit for first-order kinetics was only assessed by the coefficient of determination (R^2). The pH based degradation for total anthocyanin, C3G, and P3G showed the quite high coefficient of determination (R^2>0.99) which elucidated that the degradation behavior at various pH efficiently explains using the first-order kinetic model (**Table 4.6**). It is noticed that the degradation of monomeric anthocyanin, C3G, and P3G was increased with an increase in pH up to 6. In pH 2, monomeric anthocyanin, C3G, and P3G showed the highest stability in term of half-life ($t_{1/2}$) (3140.7 min, 4783.6 min, and 5055.8 min) (**Table 4.6**). From **Table 4.6**, it was also observed that at low pH, the degradation reaction rate constant (k) was lower and increased with pH up to 6. After 6 pH, for further increase in pH to 8, there was a decrease in reaction rate constant (k). As reported in the literature, the change of pH influences the chemical structure of C3G and P3G due to the transfer of a proton from Flavylium ion which increases the stability of anthocyanins (Zhang et al., 2008). At pH 2, C3G and P3G both exist as the flavylium cation with having dark red color in the aqueous medium and showed the highest stability (In appendix **Fig. 6A1a** and **6A1b**) (McGhie and Walton, 2007). As the pH of the medium increased from 2 to 4 pH, there is a rapid loss of a proton from the flavylium cation and generate a violet color quinonoidal-base structure which is stable but lower than flavylium cation (McGhie and Walton, 2007). For the further increase in pH to 6, there is a deprotonation of quinonoidal-base structure and formed a colorless carbinol pseudo-base (In appendix **Fig. 6A1a** and **6A1b**)

which is very unstable, thereby at 6 pH the rate of degradation was high. For these phenomena, the highest degradation rate constant for monomeric anthocyanin, C3G and P3G (11×10^{-4} /min, 5×10^{-4} /min, and 3.8×10^{-4} /min) was observed at 6 pH and the lowest value (2.2×10^{-4} /min, 1.4×10^{-4} /min, and 1.4×10^{-4} /min) was observed at pH 2. For the increasing trend of degradation rate constant (k) with increase in pH (up to 6 pH) indicates that anthocyanins was stable at lower pH and unstable at higher pH conditions, especially at 6 pH. A few researchers reported similar types of observation (Ekici et al., 2014; Sui et al., 2014). For the further increase in pH from 6 to 8 the degradation rate constant of monomeric anthocyanin, C3G, and P3G (6.7×10^{-4} /min, 4.4×10^{-4} /min, and 2.6×10^{-4} /min) decreases. At pH 8, the carbinol pseudo-base further generate the blue color ionic anhydrous base structure (In appendix **Fig. 6A1a** and **6A1b**) which has higher stability than colorless carbinol pseudo-base thereby, at 8 pH anthocyanins showed higher stability than 6 pH.

Table 4.6: Degradation kinetics parameters for anthocyanin, C3G, and P3G

Parameter	**Anthocyanin**			**C3G**			**P3G**		
	$k\times10^4$ min	R^2	$t_{1/2}$ (min)	$k\times10^4$ /min	R^2	$t_{1/2}$ (min)	$k\times10^4$ /min	R^2	$t_{1/2}$ (min)
pH									
2	2.2	0.98	3140.7	1.4	0.99	4783.6	1.4	0.99	5055.8
4	3.3	0.99	2082.1	1.9	0.99	3511.4	2.6	0.99	2649.6
6	11	0.99	630.1	4.9	0.99	1387.7	3.8	0.99	1828.9
8	6.7	0.99	1033	4.4	0.99	1580.4	2.6	0.98	2660.8
Temperature									
60	3.4	0.99	2005.0	1.7	0.99	3967.6	1.9	0.99	3474.4
70	5.4	0.99	1292.2	2.9	0.99	2377.9	3.4	0.99	2020.8
80	6.4	0.99	1085.6	4.5	0.99	1535.9	5.1	0.99	1363.9
90	12.8	0.99	541.5	5.8	0.99	1191.9	6.0	0.99	1150.3

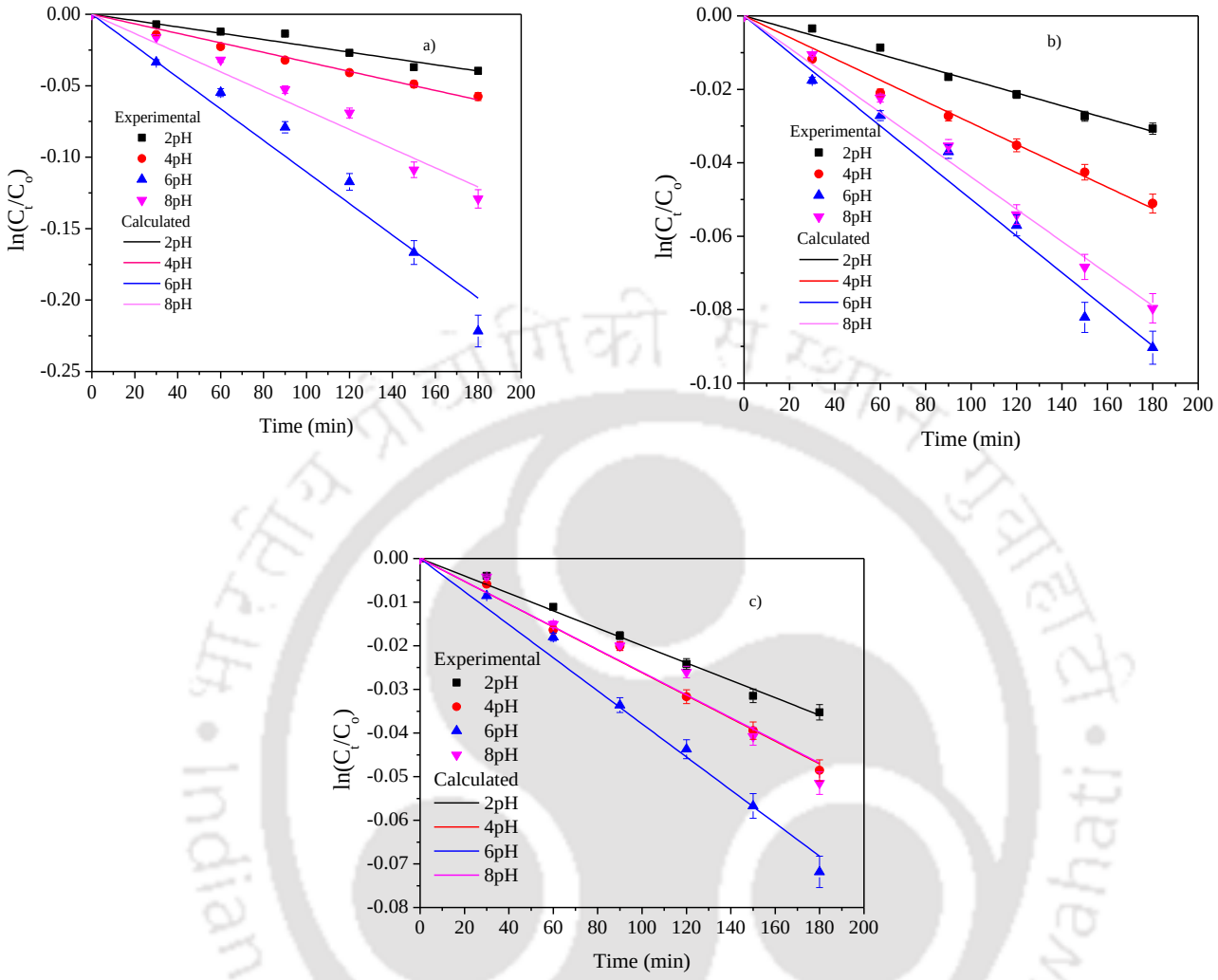

Fig. 4.6: Data plot for First-order kinetics for the degradation of a) anthocyanin b) C3G and c) P3G at different pH

4.4.2. Effect of different temperature

The thermal degradation behavior of monomeric anthocyanin, C3G, and P3G content of purple rice bran extract was plotted as a function of time and shown in **Fig. 4.7** (**a, b,** and **c**). The reaction rate constant (*k*) was determined from the slope of the curve. The degradation data of anthocyanin during thermal treatment follows first-order reaction kinetics (**Fig. 4.7**). The higher coefficient of determination (R^2) was also illustrated that the degradation behavior at various temperatures, suitable for the first-order kinetics model (**Table 4.6**). The previous

researcher reported a similar type of observation (Martynenko and Chen, 2016; Zhao et al., 2013). It was observed that for the increase in temperature the degradation rate constant (*k*) of anthocyanins was increased. At 60 °C the *k* value of anthocyanins was lower than the 70, 80 and 90 °C, which elucidated that the stability of total anthocyanin, C3G, and P3G was higher at low temperatures. Moreover, the half-life ($t_{1/2}$) was high at low temperature and decreased with an increase in temperature. At 60 °C, the half-life ($t_{1/2}$) of total anthocyanin, C3G and P3G were 2005, 3967.6 and 3474.4 min, respectively whereas at 90 °C the half-life ($t_{1/2}$) was 541.5, 1191.9 and 1150.3 min, respectively. The previous researchers reported similar types of results (Martynenko and Chen, 2016; Sui et al., 2014). For the increase of temperature, the rate of degradation increased due to the modification and degradation of chemical structure of C3G, and P3G. During thermal treatment, the modification of chemical structure of C3G and P3G took place depending upon the severity and nature of heating. It was reported (In appendix **Fig. 6A2a** and **6A2b**) that during heating in the aqueous medium, the C3G and P3G initially undergo glucose hydrolysis which separates the glucose moiety from C3G and P3G, as a results there was a formation of cyanidin, peonidin, and glucose (In appendix **Fig. 6A2a** and **6A2b**) (Adams, 1973). For the further thermal treatment in the aqueous medium, heterocyclic ring of cyanidin and peonidin were hydrolyzed and subsequently formed phloroglucin aldehyde and phenolic acid (In appendix **Fig. 6A2a** and **6A2b**) (Sadilova et al., 2007; Tiwari et al., 2010). The 4-hydroxybenzoic acid was produced from C3G and vanillic acid produced from P3G, respectively (In appendix **Fig. 6A2a** and **6A2b**). Form the **Table 4.6**, it was also illustrated that C3G had higher stability than P3G during thermal treatment. The stability may be due to the presence of OCH_3 which has higher resonance effect than OH group.

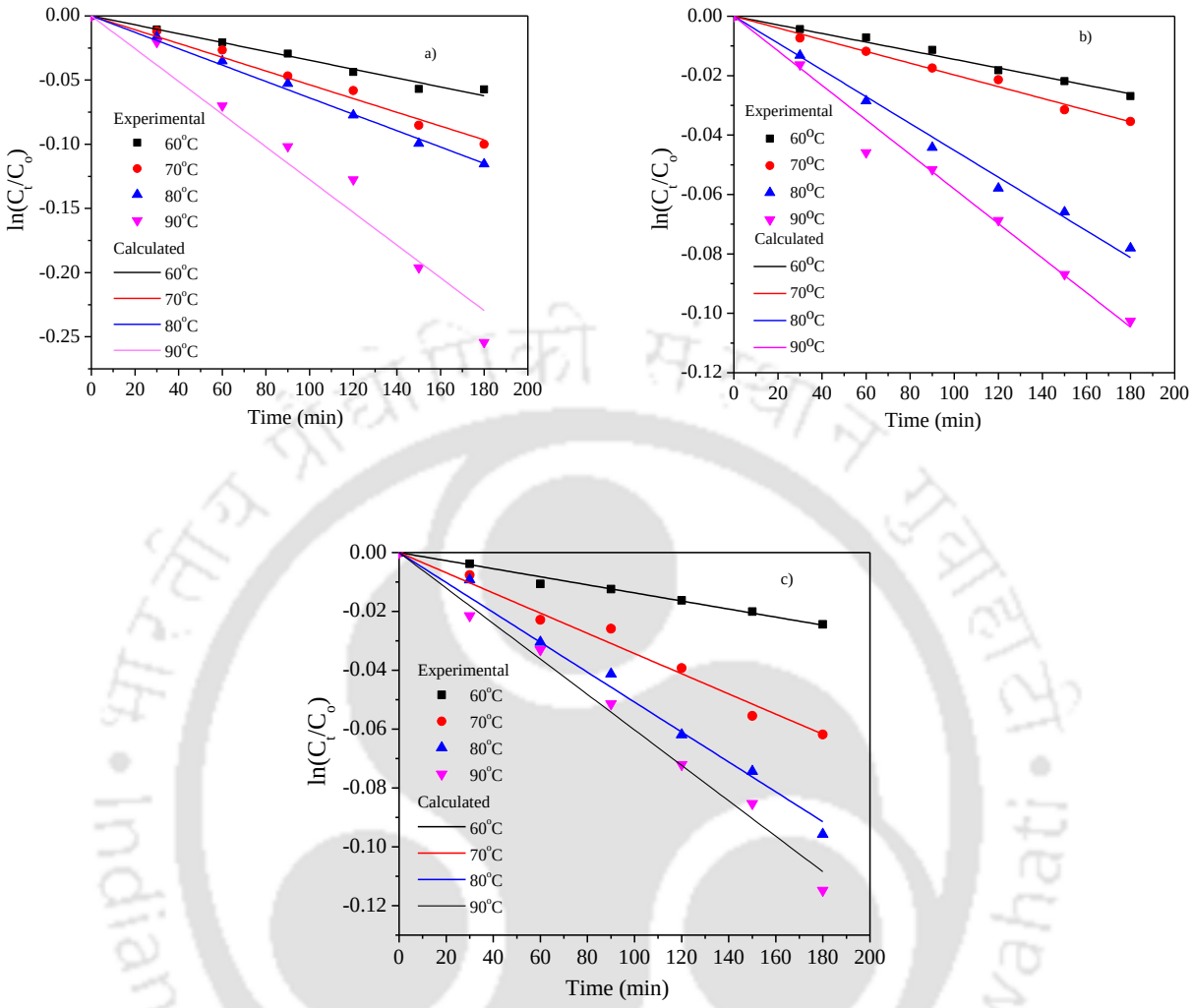

Fig. 4.7: Data plot for First-order kinetics for the degradation of a) anthocyanin b) C3G, and c) P3G at different temperatures

To determine the effect of temperature on the rate constant, the rate constants obtained from Eq. (2.26) for anthocyanin, C3G and P3G were fitted to the Arrhenius-type equation (Eq. 2.28). The calculated activation energy (E_a) for anthocyanin, C3G, and P3G was 41.1, 40.7 and 37.6 kJ/mol, respectively. The E_a of anthocyanin was highest, which indicated that anthocyanin was most stable during thermal treatment. The k_{ref} of thermal degradation was 911.7, 444.8, and 169.2 per min for anthocyanin, C3G, and P3G, respectively.

4.4.3. Effect of degradation on color change

At the end of the degradation study, the color of each sample was measured using Hunter Colorimeter. At various pH, anthocyanin showed a distinct color, and similar behavior was noticed for the pH degradation study. After degradation at 2 pH, the sample showed a high *a*-value (39.6) which signifies the dark red color due to the presence of flavylium cation in anthocyanin structure. At 4 pH, the degraded sample showed *a*-value of 31.5 with light violet color due to the presence of quinonoidal-base structure. The sample degraded at 6 pH showed high brightness and low redness as shown in **Table 4.7**. The color at 6 pH is due to the presence of colorless carbinol pseudo-base in anthocyanin structure. The sample degraded in alkaline condition (8 pH) showed negative *b*-value, which signifies the blue color due to the presence of an ionic anhydrous base. On the other hand, after the thermal degradation, the color of the sample did not change; however, the brightness of the sample increased, and redness of the sample decreased as shown in **Table 4.7**.

Table 4.7: *L*, *a*, and *b* value of anthocyanin at various pH and temperature

pH	*L*	*a*	*B*	Temperature	*L*	*A*	*b*
2	42.6 ± 0.1^{a}	39.6 ± 0.2^{d}	0.59 ± 0.02^{a}	60 °C	47.4 ± 0.1^{a}	35.3 ± 0.2^{c}	0.55 ± 0.01^{a}
4	50.7 ± 0.2^{b}	31.5 ± 0.4^{c}	0.79 ± 0.02^{a}	70 °C	54.6 ± 0.2^{b}	29.6 ± 0.2^{b}	0.72 ± 0.01^{a}
6	61.5 ± 0.3^{d}	10.8 ± 0.2^{b}	-8.5 ± 0.3^{b}	80 °C	61.4 ± 0.3^{c}	24.5 ± 0.1^{a}	0.59 ± 0.03^{b}
8	52.1 ± 0.7^{c}	5.7 ± 0.2^{a}	-29.6 ± 0.4^{c}	90 °C	66.3 ± 0.1^{d}	18.7 ± 0.2^{a}	-0.66 ± 0.02^{c}

Superscript different letters in the same column represent the significant difference in Duncan's multiple range tests at 5% level ($p \leq 0.05$).

4.4.4. Effect of hydrocolloids on anthocyanins and antioxidant activity during pH based degradation

The effect of hydrocolloids on the stability of monomeric anthocyanin, C3G and P3G in pH 6 at ambient conditions (28 ± 2 ^{o}C) were investigated and shown in **Table 4.8**. In order to determine the effect of various hydrocolloids on the stability of monomeric anthocyanin, C3G, and P3G in pH 6, dispersions of 0.5 % (w/v) carboxymethyl cellulose, xanthan gum, gum arabic, and modified starch were used with aqueous anthocyanins from purple rice bran. **Table 4.8** showed that the all the hydrocolloids had a significant ($p \leq 0.05$) stabilizing effect on monomeric anthocyanin, C3G, and P3G during pH based degradation. It can be noticed that at 6pH, modified starch had the higher protective effect on monomeric anthocyanin (33.0

mg/L), C3G (201.6 µg/L), and P3G (15.6 µg/L) than carboxymethyl cellulose (31.2 mg/L, 198.2, and 13.5 µg/L), xanthan gum (31.8 mg/L, 198.1, and 13.2 µg/L) and gum arabic (30.2 mg/L, 196.2, and 13.1 µg/L). A similar type of stabilizing the effect of pectin and gum arabic on anthocyanin was reported by the previous researcher (Buchweitz et al., 2013; Guan and Zhong, 2015). Buchweitz et al. (2013) reported that at pH 3, low esterified amidated methoxylated citrus pectins exhibited best stabilization of anthocyanin from black currant. Guan and Zhong (2015) observed that gum arabic significantly improved the stability of anthocyanins at pH 5.0 during thermal treatment at 80 and 126 °C. They suggested that the functional groups of colloids might protect the positively charged flavylium ion from nucleophilic water attack and subsequent degradation of anthocyanin (Buchweitz et al., 2013). At 6 pH the degradation of monomeric anthocyanin, C3G, and P3G was mainly due to the deprotonation of the flavylium cation, followed by formation of colorless carbinol pseudo-base (Brouillard and Delaporte, 1977). Therefore, it may be due to the presence of hydrocolloids in the aqueous system, the deprotonation of flavylium cation was inhibited (Buchweitz et al., 2013). The stabilizing effect of hydrocolloids may be based on electrostatic interactions between the flavylium cation of anthocyanins and the dissociated groups of the colloids (Buchweitz et al., 2013). Due to this association of C3G and P3G, deprotonation may be inhibited, which leads to the stabilization of C3G and P3G in the aqueous system at 6 pH. The interaction between anthocyanins and colloidal substances has already been elicited in flower petals (Robinson and Robinson, 1939). The hydrocolloids can also protect monomeric anthocyanin, C3G, and P3G due to the steric hindrance, developed by the colloids, which can protect or slow down the nucleophilic attacks of water on flavylium cation (Kopjar and Piližota, 2011). Brouillard and Delaporte (1977) suggested that for the presence of hydrocolloids in the aqueous medium, water activity of the medium decrease which might also reduce the extent of the hydration reaction and increase the stability of flavylium cation. The modified starch showed the highest stability of anthocyanins in 6 pH than other colloids. It may be due to the presence of highly branched amylopectin molecule. Lewis et al. (1995) suggested that amylopectin is a highly branched molecule and can easily form helical structures within the unbranched straight chains and therefore restricted the degradation of anthocyanin. The antioxidant activity of the anthocyanin after pH based degradation showed a significant ($p \leq 0.05$) effect of hydrocolloids (**Table 4.8**). Hydrocolloids were retained the antioxidant

activity of anthocyanin after pH treatment. In general, the antioxidant activity is directly proportion with anthocyanin contain which was in accordance with the above observation.

4.4.5. Effect of hydrocolloids on anthocyanins and antioxidant activity during thermal degradation

Table 4.8 showed, the effect of carboxymethyl cellulose, xanthan gum, gum arabic, and modified starch on the stability of monomeric anthocyanin, C3G, and P3G during thermal degradation. It can be noticed from **Table 4.8** that modified starch had significantly ($p \leq 0.05$) higher protective activity than other hydrocolloids. After thermal treatment of anthocyanin at 90 °C for 30 min in 2pH, the control sample (without hydrocolloids) showed 27.1 mg/L monomeric anthocyanin, 178.6 µg/L C3G, and 11.8 µg/L P3G, whereas the sample with modified starch showed 31.7 mg/L, 202.01 µg/L and 14.1 µg/L of monomeric anthocyanin, C3G, and P3G, respectively. Guan and Zhong (2015) reported quite similar kind of effect of gum arabic during the thermal treatment of anthocyanin at 80 and 126 °C in pH 5.0 medium. The thermal degradation of anthocyanins is mainly due to the formation of aglycon from hydrolysis of the 3-glycoside linkage and a hydrolytic opening of the pyrylium ring to form a substituted chalcone (Sadilova et al., 2007). Therefore, during thermal treatment, due to the presence of hydrocolloids, two degradation mechanisms of anthocyanins may be suppressed. Guan and Zhong (2015) suggested that during thermal treatment for the formation of complexes with gum arabic, the degradation of anthocyanin inhibited. Mazza and Brouillard (1990) also suggested that for the presence of hydrocolloids, the flavylium cation is stabilized by its interaction with the colloids as co-pigment which prevents the hydration reaction. Moreover, the presence of hydrocolloids in the aqueous medium reduce the water activity which may also reduce the extent of the hydration reaction and increase the stability of flavylium cation (Brouillard and Delaporte, 1977) during thermal treatment. In general, the antioxidant activity is directly related to the anthocyanin content of medium. Therefore, it was observed that the antioxidant activity of the colloid system was varied according to anthocyanin content (**Table 4.8**). The hydrocolloids significantly ($p \leq 0.05$) increase the retention of antioxidant activity of the anthocyanin after thermal treatment. Guan and Zhong (2015) reported a similar kind of observation during the thermal treatment of anthocyanin at 80 and 126 °C with gum arabic. It may due to the reduced thermal breakdown of anthocyanins due to the complex formation with hydrocolloids (Guan and Zhong, 2015).

Table 4.8: Effect of hydrocolloids on anthocyanin, C3G, and P3G

Sample	pH treatment (6 pH)				Temperature treatment (90 °C)			
	Anthocyanin (mg/L)	C3G (µg/L)	P3G (µg/L)	Antioxidant activity (%)	Anthocyanin (mg/L)	C3G (µg/L)	P3G (µg/L)	Antioxidant activity (%)
Control	29.3±0.1^{a}	191.5±1^{a}	11.9±1^{a}	82.6±0.3^{a}	27.1±0.08^{a}	178.6±1^{a}	11.8±1^{a}	80.3±0.5^{a}
CMC	31.2±0.1^{bc}	198.2±0.3^{b}	13.5±0.4^{b}	86.2±0.1^{bc}	30.3±0.1^{c}	198.3±0.4^{cd}	13.3±0.3^{b}	85.6±0.6^{c}
Arabic	30.2±0.1^{ab}	196.2±0.2^{b}	13.1±0.3^{b}	85.2±0.9^{b}	28.8±0.1^{ab}	193.5±0.1^{b}	13.1±0.7^{b}	83.5±0.4^{b}
Xanthan	31.9±0.3^{cd}	198.1±0.8^{b}	13.2±0.5^{b}	89.8±0.9^{c}	29.4±0.2^{bc}	196.6±0.2^{bc}	13.1±0.6^{b}	87.3±0.9^{d}
Starch	33.0±0.6^{d}	201.6±0.6^{c}	15.6±1^{c}	92.2±0.7^{d}	31.7±0.7^{c}	202.01±0.1^{d}	14.1±1^{c}	90.5±0.5^{e}

Superscript letters in the same column represent the significant difference in Duncan's multiple range tests at 5% level.

4.4.6. Effect of modified starch on degradation kinetics of anthocyanin

The modified starch showed the highest retention of anthocyanin and antioxidant activity in pH and thermal degradation. Therefore, pH (6 pH) and thermal (90 °C) degradation kinetic of anthocyanin with modified starch was investigated and compared with the sample without hydrocolloid. **Fig. 4.8** showed that pH and thermal degradation of anthocyanin, C3G, and P3G in modified starch system followed the first-order reaction kinetics. The determination of coefficient (R^2) of pH and thermal degradation of total anthocyanin (0.99 and 0.99), C3G (0.98 and 0.99), and P3G (0.99 and 0.99) were high, which elucidated that the degradation behavior in 6 pH and 90 °C efficiently explains using the first-order kinetic model.

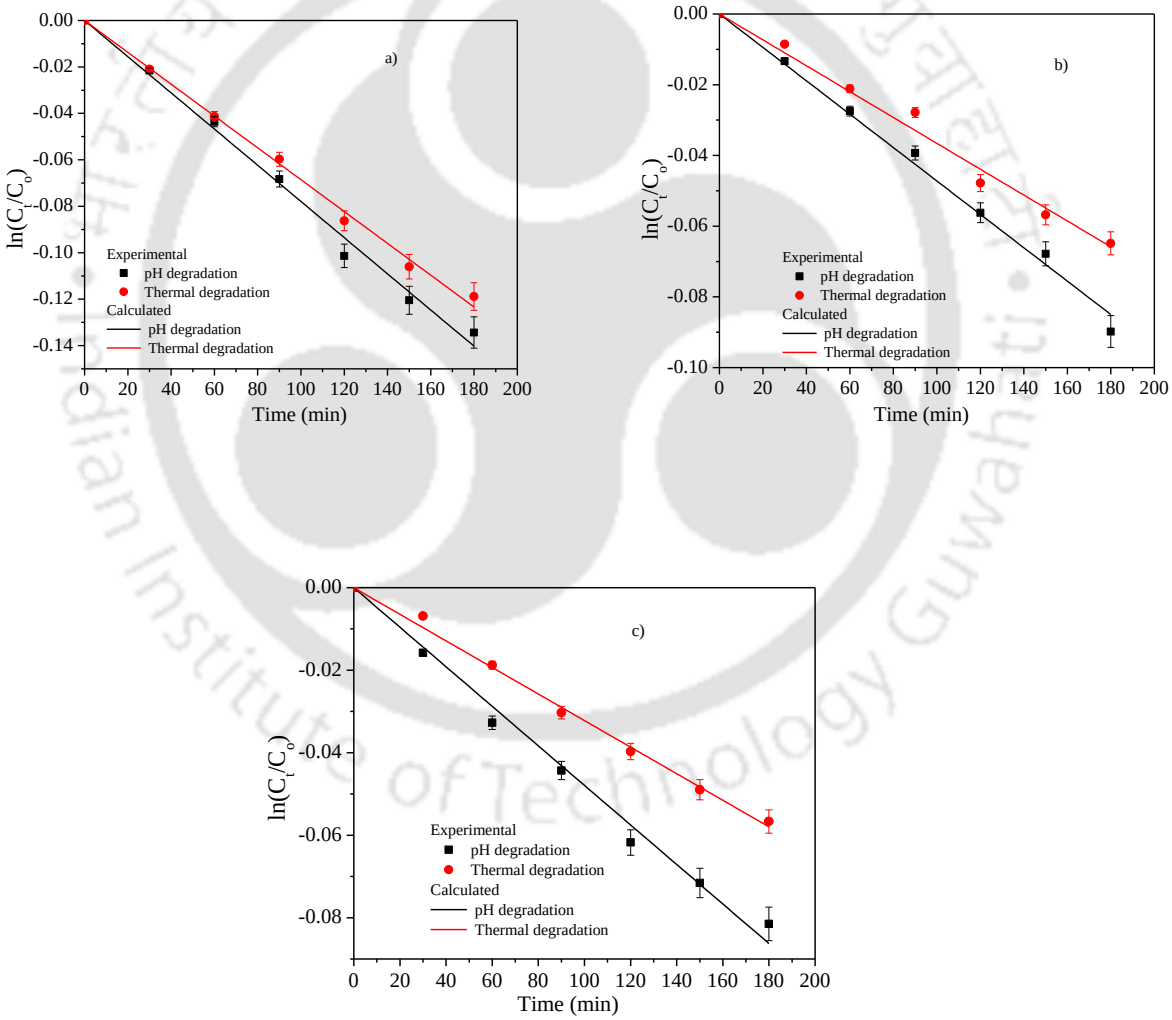

Fig. 4.8: Degradation kinetics of a) anthocyanin b) C3G, and c) P3G in modified starch medium at 6 pH and 90 °C

At 6 pH, the degradation rate constant of total anthocyanin (6.9×10^{-4} /min), C3G (3.7×10^{-4} /min), and P3G (3.2×10^{-4} /min) in the modified starch medium was lower than without hydrocolloid sample (**Table 4.6**). Similar pattern was observed for the thermal degradation of anthocyanin (7.8×10^{-4} /min), C3G (4.7×10^{-4} /min) and P3G (4.8×10^{-4} /min) in starch medium. The half-life of anthocyanin during pH and thermal degradation in the modified starch medium was higher than the half-life of without hydrocolloid sample (**Table 4.6**). The higher stability of anthocyanin in the modified starch medium may be due to the formation of complex with highly branched amylopectin in starch (Lewis et al., 1995) and reduction of the water activity of the medium.

4.5. Summary

The present study has provided insights of adsorption, desorption and diffusion characteristics of anthocyanin from purple rice bran extract using XAD2, XAD4, XAD7, activated charcoal and bentonite as adsorbents. The conclusions are summarized as follows:

- The amberlite XAD7 resin showed higher adsorption (1.9 mg/g) and desorption (1.8 mg/g) capacities than the other adsorbents. The amberlite XAD7 also showed the highest recovery (41.5 %) of anthocyanin from purple rice bran extract than other adsorbents.
- The adsorption of anthocyanin was homogeneous in nature. The two parameter Langmuir isotherm and three-parameter Redlich–Peterson isotherm model can efficiently describe the adsorption isotherm behavior of anthocyanin on various adsorbents.
- The adsorption kinetics of anthocyanin was best fitted with pseudo-first order kinetic model than pseudo-second order kinetic model. The XAD7 showed the highest reaction rate constant (0.02 /min) than other adsorbents.
- The diffusion study revealed that intra-particle diffusion is not the sole mechanisms of anthocyanin adsorption process onto adsorbents as shown by the Weber and Morris intra-particle diffusion model.
- The thermodynamic properties of anthocyanin adsorption process onto XAD7 was successfully investigated. From the ΔH values (-40.3 kJ/mol), it was implied that the adsorption of anthocyanin onto the XAD7 resin was exothermic in nature.

- The concentrated sample showed a higher amount of cyanidin-3-glucoside (1279.9 µg/L), peonidin-3-glucoside (68.9 µg/L) and phenolic acids than crude extract.
- The degradation behavior of anthocyanins was followed the first-order kinetics model. The highest rate of degradation for the monomeric anthocyanin, C3G and P3G were observed at 6 pH (11×10^{-4} /min, 4.9×10^{-4} /min, and 3.8×10^{-4} /min) and 90°C (12.8×10^{-4} /min, 5.8×10^{-4} /min, and 6×10^{-4} /min).
- The hydrocolloids showed a significant effect of the stability on monomeric anthocyanin, C3G, and P3G in various pH and temperature condition.
- Modified rice starch showed a promising effect on the stability of anthocyanins and antioxidant activity than the other hydrocolloids. Moreover, in modified starch medium total anthocyanin, C3G, and P3G showed the lower degradation rate constant and higher half-life as compared to without hydrocolloid sample.

References

Adams, J.B. (1973). Thermal degradation of anthocyanins with particular reference to the 3-glycosides of cyanidin. I. In acidified aqueous solution at 100° C. *Journal of the Science of Food and Agriculture*, *24*(7), 747-762.

Brouillard, R. and Delaporte, B. (1977). Chemistry of anthocyanin pigments. 2. Kinetic and thermodynamic study of proton transfer, hydration, and tautomeric reactions of malvidin 3-glucoside. *Journal of the American Chemical Society*, *99*(26), 8461-8468.

Buchweitz, M., Speth, M., Kammerer, D.R., and Carle, R. (2013). Impact of pectin type on the storage stability of black currant (*Ribes nigrum L.*) anthocyanins in pectic model solutions. *Food chemistry*, *139*(1-4), 1168-1178.

Buran, T. J., Sandhu, A. K., Li, Zheng, Rock, Cheryl R., Yang, Weihua W., and Gu, L. (2014). Adsorption/desorption characteristics and separation of anthocyanins and polyphenols from blueberries using macroporous adsorbent resins. *Journal of Food Engineering*, *128*, 167-173.

Castaneda-Ovando, A., de Lourdes Pacheco-Hernández, M., Páez-Hernández, M.E., Rodríguez, J.A. and Galán-Vidal, C.A., (2009). Chemical studies of anthocyanins: A review. *Food Chemistry*, *113*(4), 859-871.

Chandrasekhar, J., Madhusudhan, M. C. and Raghavarao, K. S. M. S. (2012). Extraction of anthocyanins from red cabbage and purification using adsorption. *Food and Bioproducts Processing*, *90*(4), 615-623.

Chen, Y., Zhang, W., Zhao, T., Li, F., Zhang, M., Li, J., Zou, Y., Wang, W., Cobbina, S.J., Wu, X. and Yang, L. (2016). Adsorption properties of macroporous adsorbent resins for separation of anthocyanins from mulberry. *Food Chemistry*, *194*, 712-722.

Ekici, L., Simsek, Z., Ozturk, I., Sagdic, O. and Yetim, H. (2014). Effects of temperature, time, and pH on the stability of anthocyanin extracts: Prediction of total anthocyanin content using nonlinear models. *Food Analytical Methods*, *7*(6), 1328-1336.

Fierro, V., Torné-Fernández, V., Montané, D., and Celzard, A. (2008). Adsorption of phenol onto activated carbons having different textural and surface properties. *Microporous and Mesoporous Materials*, *111*(1), 276-284.

Fleschhut, J., Kratzer, F., Rechkemmer, G., and Kulling, S. E. (2006). Stability and biotransformation of various dietary anthocyanins in vitro. *European journal of nutrition*, *45*(1), 7-18.

Foo, K. Y., and Hameed, B. H. (2010). Insights into the modeling of adsorption isotherm systems. *Chemical Engineering Journal*, *156*(1), 2-10.

Gao, Z.P., Yu, Z.F., Yue, T.L. and Quek, S.Y. (2013). Adsorption isotherm, thermodynamics and kinetics studies of polyphenols separation from kiwifruit juice using adsorbent resin. *Journal of Food Engineering*, *116*(1), 195-201.

Gökmen, V. and Serpen, A. (2002). Equilibrium and kinetic studies on the adsorption of dark colored compounds from apple juice using adsorbent resin. *Journal of Food Engineering*, *53*(3), 221-227.

Guan, Y. and Zhong, Q. (2015). The improved thermal stability of anthocyanins at pH 5.0 by gum arabic. *LWT-Food Science and Technology*, *64*(2), 706-712.

Hamdaoui, O. and Naffrechoux, E. (2007). Modeling of adsorption isotherms of phenol and chlorophenols onto granular activated carbon: Part II. Models with more than two parameters. *Journal of Hazardous Materials*, *147*(1), 401-411.

Ho, Y. S., and McKay, G. (1999). Pseudo-second order model for sorption processes. *Process Biochemistry*, *34*(5), 451-465.

Jampani, C., Naik, A. and Raghavarao, K. S. M. S. (2014). Purification of anthocyanins from jamun (*Syzygium cumini L.*) employing adsorption. *Separation and Purification Technology*, *125*, 170-178.

Jia, Y., Jiang, H., Liu, Z. and Wang, R.. (2017). An innovative approach to the preparation of coloured and multifunctional silk material with the natural extracts from chestnut shell and black rice bran. *Coloration Technology*, *133*(3), 262-270.

Kırca, A., Özkan, M. and Cemeroğlu, B. (2007). Effects of temperature, solid content and pH on the stability of black carrot anthocyanins. *Food chemistry, 101*(1), 212-218.

Kopjar, M. and Piližota, V. (2011). Prevention of thermal degradation of anthocyanins in blackberry juice with addition of different sugars Prevención de degradación termal de antocianinas en zumo de mora con adición de diferentes azúcares. *CyTA-Journal of Food, 9*(3), 237-242.

Koresh, J. E., Soffer, A. and Tobias, H. (1985). The effect of surface polarity and pore dimension on the adsorption of polar molecules on activated carbon cloth. *Carbon, 23*(5), 571-577.

Lagergren, S.K. (1898). About the theory of so-called adsorption of soluble substances. *Sven. Vetenskapsakad. Handingarl, 24*, 1-39.

Lewis, C. E., Walker, John R. L., and Lancaster, J. E. (1995). Effect of polysaccharides on the colour of anthocyanins. *Food Chemistry, 54*(3), 315-319.

Martynenko, A. and Chen, Y. (2016). Degradation kinetics of total anthocyanins and formation of polymeric color in blueberry hydrothermodynamic (HTD) processing. *Journal of Food Engineering, 171*, 44-51.

Mazza, G., and Brouillard, R. (1990). The mechanism of co-pigmentation of anthocyanins in aqueous solutions. *Phytochemistry, 29*(4), 1097-1102.

McGhie, T. K. and Walton, M. C. (2007). The bioavailability and absorption of anthocyanins: towards a better understanding. *Molecular Nutrition and Food Research, 51*(6), 702-713.

Robinson, R. and Robinson, G. M. (1939). The colloid chemistry of leaf and flower pigments and the precursors of the anthocyanins. *Journal of the American Chemical Society, 61*(6), 1605-1606.

Sadilova, E., Carle, R. and Stintzing, F. C. (2007). Thermal degradation of anthocyanins and its impact on color and in vitro antioxidant capacity. *Molecular Nutrition and Food Research, 51*(12), 1461-1471.

Sui, X., Dong, Xin. and Zhou, W. (2014). Combined effect of pH and high temperature on the stability and antioxidant capacity of two anthocyanins in aqueous solution. *Food Chemistry, 163*, 163-170.

Tiwari, B.K., Patras, A., Brunton, N., Cullen, P.J. and O'donnell, C.P. (2010). Effect of ultrasound processing on anthocyanins and color of red grape juice. *Ultrasonics Sonochemistry, 17*(3), 598-604.

Var, I., Kabak, B. and Erginkaya, Z. (2008). Reduction in ochratoxin A levels in white wine, following treatment with activated carbon and sodium bentonite. *Food Control, 19*(6), 592-598.

Yang, Q., Zhao, M. and Lin, L. (2016). Adsorption and desorption characteristics of adlay bran free phenolics on macroporous resins. *Food chemistry, 194*, 900-907.

Yuh-Shan, H. (2004). Citation review of Lagergren kinetic rate equation on adsorption reactions. *Scientometrics, 59*(1), 171-177.

Zhang, Y., Liao, X., Chen, F., Wu, J. and Hu, X. (2008). Isolation, identification, and color characterization of cyanidin-3-glucoside and cyanidin-3-sophoroside from red raspberry. *European Food Research and Technology, 226*(3), 395-403.

Zhao, M., Luo, Y., Li, Y., Liu, X., Wu, J., Liao, X. and Chen, F. (2013). The identification of degradation products and degradation pathway of malvidin-3-glucoside and malvidin-3, 5-diglucoside under microwave treatment. *Food chemistry, 141*(3), 3260-3267.

Zhou, L., Zhang, J. & Zhou, Y. (2001). A simple isotherm equation for modeling the adsorption equilibria on porous solids over wide temperature ranges. *Langmuir, 17*(18), 5503-5507.

TO EVALUATE THE MICROENCAPSULATION PROCESS OF ANTHOCYANIN AND ITS EFFECT ON RICE DOUGH RHEOLOGY

Part of the work is published in

- International Journal of Biological Macromolecules, 124, 573-581.

CHAPTER 5

TO EVALUATE THE MICROENCAPSULATION PROCESS OF ANTHOCYANIN AND ITS EFFECT ON RICE DOUGH RHEOLOGY

5.1. Overview

This investigation aims to microencapsulate anthocyanin from purple rice bran with modified glutinous rice starch to provide stable anthocyanin powder. The modified glutinous rice starch was used as wall material while anthocyanin was a core material for microencapsulation. The microencapsulation was carried out in a spray dryer, and the process was optimized using a rotatable central composite design. The effect of independent parameters, viz., starch concentration, inlet air temperature, and atomizer pressure, on the dependent parameters, such as encapsulation efficiency, anthocyanin content, 2, 2-diphenyl-1-picrylhydrazyl scavenging activity, true density and water activity were investigated. The optimum values of spray drying process parameters were 6 % (w/v) of starch concentration, 168.8 °C inlet air temperature, and 4.9 MPa atomizer pressure. The physical characteristics of spray-dried powders were investigated in term of water activity (0.5), solubility (51.8 % w/w), bulk density (1.4 g/cm^3), porosity (0.2), and diameter (6.4 µm) and the Hausner ratio (1.02). The thermal properties, crystallinity and surface morphology of the microencapsulated particles were also comprehensively studied using DSC, XRD, FTIR, and SEM. The storage stability of microencapsulated anthocyanin showed more stability at 4 °C than at 25 °C for 90 days. The microencapsulated particles also have an effect on the steady-shear and dynamic rheology of the rice dough.

5.2. Precise background

The stability of anthocyanin is a major challenge for the food industry. The stability of anthocyanin depends on various environmental factors, such as, pH, light, temperature, oxygen, and enzymatic activities. For the low stability in various conditions during processing and storage, application of anthocyanin as an ingredient in foods is now quite challenging. To obtain a stable and usable food ingredient from anthocyanin, several approaches such as encapsulation, emulsion, and freeze-drying have been considered. For anthocyanin, encapsulation method is commonly used and accepted. The most commonly used encapsulation process is microencapsulation. Microencapsulation is an efficient way to enhance the

bioavailability and stability of the products. Moreover, microencapsulation helps to control the release of active agent. There are various types of microencapsulation techniques, such as, vibrational nozzle, centrifugal extrusion, spray drying, and co-crystallization. The most commonly used technique is spray drying due to its continuous operation, low cost, less time, and can produce particles with good quality. Therefore, this chapter deals with microencapsulation of anthocyanin using spray drying technique. It also includes the effect of microencapsulate anthocyanin on the rheological properties of rice dough.

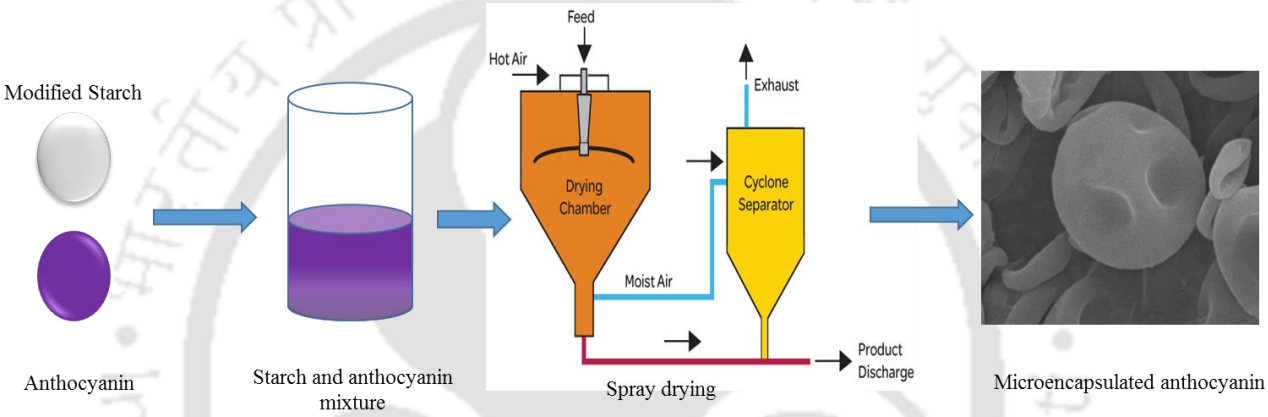

Fig. 5.1: Graphical abstract

5.3. Results and discussion

5.3.1. Analysis of variance

For microencapsulation of anthocyanin extract, the effects of independent parameters on encapsulation efficiency, anthocyanin content, DPPH scavenging activity, water activity and true density of microencapsulated anthocyanin was investigated using RCCD and twenty experiment were conducted (In appendix **Table 5A1**). The results were investigated and fitted to the second-order polynomial equations (Eqs. 5.1 to 5.5) with a high coefficient of determination (R^2) values (**Table 5.1**). ANOVA was carried out for the significance test of the model coefficients (**Table 5.1**).

$$\text{Encapsulation Efficiency} = 90.21 - 4.17x_9 + 1.15x_{10} - 0.41x_{11} - 1.14x_9x_{10} + 2.47x_{10}x_{11} + 0.60x_{10}x_{11} - 0.46x_9^2 + 1.34x_{10}^2 - 0.50x_{11}^2 \quad (5.1)$$

$$\text{Anthocyanin content} = 2.81 - 0.30x_9 + 0.039x_{10} - 0.21x_{11} - 0.20x_9x_{10} + 0.039x_9x_{11} + 0.25x_{10}x_{11} - 0.28x_9^2 - 0.069x_{10}^2 - 0.15x_{11}^2 \quad (5.2)$$

$$\text{DPPH Scavenging Activity} = 52.02 - 4.35x_9 + 0.52x_{10} - 2.09x_{11} - 3.55x_9x_{10} + 1.85x_9x_{11} - 0.42x_{10}x_{11} - 1.70x_9^2 + 0.22x_{10}^2 - 2.06x_{11}^2 \quad (5.3)$$

$$\text{True density} = 1.83 - 0.045x_9 - 1.09\times10^{-4}x_{10} - 0.062x_{11} - 9.5\times10^{-3}x_9x_{10} + 0.022x_9x_{10} - 0.060x_{10}x_{11} - 0.028x_9^2 - 0.053x_{10}^2 + 9.85\times10^{-3}x_{11}^2 \quad (5.4)$$

$$\text{Water Activity} = 0.52 - 0.011x_9 + 3.56\times10^{-3}x_{10} - 0.013x_{11} - 5.7\times10^{-3}x_9x_{10} + 7.77\times10^{-3}x_9x_{11} - 0.011x_{10}x_{11} - 5.032\times10^{-3}x_9^2 - 7.20\times10^{-3}x_{10}^2 + 2.83\times10^{-3}x_{11}^2 \quad (5.5)$$

The lack of fit of five responses was insignificant (0.8, 0.27, 0.45, 0.31, and 0.73) ($p \leq 0.05$) which conferred that the developed relationships were suitable for the experimental data. From the ANOVA analysis, it can be inferred that the developed models can be efficiently used for the optimization of the microencapsulation process.

Table 5.1: Analysis of variance for the fitted quadratic polynomial model

Terms	Encapsulation Efficiency	Anthocyanin Content	DPPH Scavenging Activity	True density	Water Activity
Model	< 0.0001	<0.0001	< 0.0001	< 0.0001	< 0.0001
x_9	< 0.0001	< 0.0001	< 0.0001	0.0008	0.0002
x_{10}	0.01	0.03	0.03	0.009	0.105
x_{11}	0.03	0.001	0.001	< 0.0001	< 0.0001
x_9x_{10}	0.04	0.01	0.0002	0.4	0.05
x_9x_{11}	0.0006	0.5	0.01	0.1	0.01
$x_{10}x_{11}$	0.2	0.002	0.5	0.0007	0.001
x_9^2	0.2	0.0001	0.004	0.01	0.02
x_{10}^2	0.004	0.1	0.7	0.0002	0.004
x_{11}^2	0.2	0.009	0.001	0.3	0.2
Lack of Fit	0.8	0.3	0.5	0.7	0.3
R^2	0.9	0.9	0.9	0.9	0.9
Adj-R^2	0.9	0.9	0.9	0.9	0.9

5.3.2. Response surface analysis

Fig. 5.2 (**a** and **b**) shows the relationship between encapsulation efficiency and the spray drying process parameters. As the inlet air temperature increased, the encapsulation efficiency increased significantly ($p \leq 0.05$). During spray drying, as the inlet air temperature increases the drying rate of droplets accelerated and hence there is a quick formation of particle crust which prevents leaching of anthocyanin and penetration heat in the droplet. **Fig. 5.2a** and **5.2b** show that for the increase of atomizer pressure the encapsulation efficiency increases significantly ($p \leq 0.05$), whereas, for the increase in starch concentration as wall material after a certain concentration (7 % w/v) there was drastically decreased in the encapsulation efficiency. In this regards, Jafari et al. (2008) suggested that retention of core material significantly depends upon the viscosity of the initial emulsion. For the increase of solid concentration, there is an increase in viscosity which may be resulting eventual cracking on the particles which increase the diffusion of the anthocyanin from core to the wall, hence decrease the encapsulation efficiency (Bhandari et al., 1992).

Fig. 5.2 (**c** and **e**) illustrated that for the increase of inlet air temperature; anthocyanin content decreases and DPPH scavenging activity of microencapsulated powder, due to the thermal sensitivity of anthocyanin. For the increase in starch concentration up to 7 % (w/v) the anthocyanin content and DPPH scavenging activity of powder was increased, beyond that both decreases. The increase in starch concentration increases the emulsion viscosity that suppresses the internal circulations and enhances the anthocyanin and DPPH scavenging activity of microencapsulate (Bhandari et al., 1992). However at high starch concentration, due to the cracking on the particles wall, the core anthocyanin leached out to the surface and degraded (Bhandari et al., 1992). **Fig. 5.2** (**d** and **f**) illustrated that higher atomizer pressure enhances the anthocyanin content and DPPH scavenging activity of particles. For the increase of atomizer pressure, the momentum of atomized droplets increases into the spray stream (Jafari et al., 2008) and rapid development of the film around the droplet, which reduces the anthocyanin diffusion and enhances the anthocyanin retention and DPPH scavenging activity in microencapsulates.

The water activity of microencapsulates was varied between 0.49 to 0.56 and showed a significant ($p \leq 0.05$) effect of independent variables during processing as shown in **Fig. 5.2** (**g** and **h**). At high inlet air temperatures, the atomized feed and drying air has a high temperature gradient thereby, the water activity of microencapsulate was gradually decreased. It can be observed from **Fig. 5.2g**, that water activity decreased with increases in starch concentration as wall material. The higher solids contents in feed reduce the total available moisture and decrease the water activity of powder (Tuyen et al., 2010). The water activity of the powders was increased with increase in atomizer pressure (**Fig. 5.2h**). At high atomization pressure the retention time of particles in the drying chamber reduces, and hence the water activity of finished particles increased.

From the **Fig. 5.2i**, it was illustrated that for the increase in inlet air temperature, true density decreased. At very high temperatures, a high rate of drying implies a lower shrinkage of the droplets, and thereby a lower true density microencapsulated powder was obtained (Bhandari et al., 1992). For the increase in starch concentration, a slight decrease in true density was noticed. For the increase in starch concentration the viscosity of the droplet increases and cause cracking on the particles surface which reduces the true density of particle

(Bhandari et al., 1992). It is observed that for the increase of atomization pressure up to 4.1 MPa there was an increase in true density beyond that there was a decrease in true density of microencapsulate.

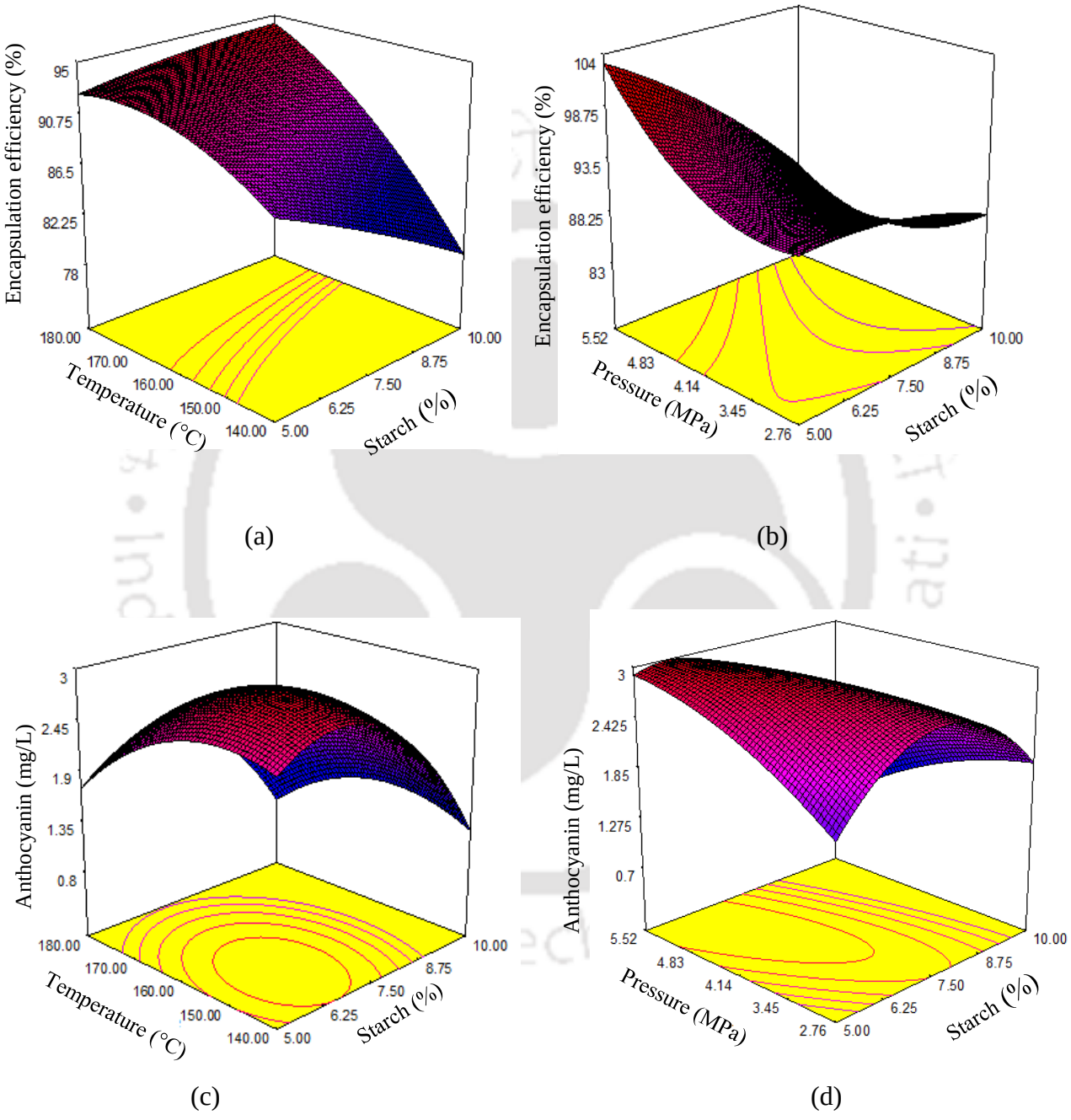

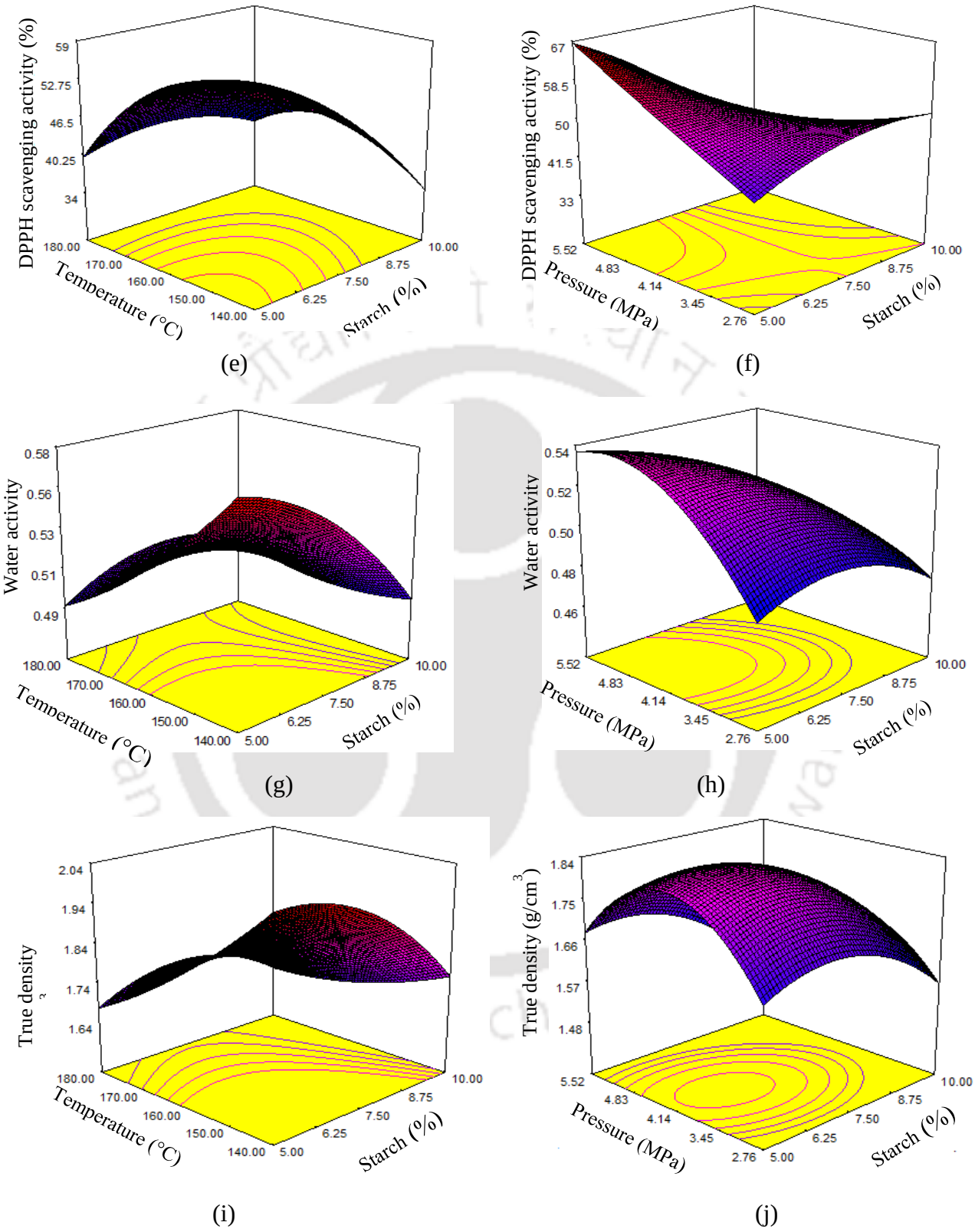

Fig. 5.2: Effect of temperature, starch concentration, and atomizer pressure on microencapsulate

5.3.3. Optimization and validation

The section was aimed to find out the values of spray drying process parameters, which would allow getting a microencapsulated powder with high encapsulation efficiency, anthocyanin content, DPPH scavenging activity, true density, and low water activity. Thereby during the optimization, the targets of dependent parameter were maximum encapsulation efficiency, maximum anthocyanin content, maximum DPPH scavenging activity, maximum true density, and minimum water activity. Optimum conditions were selected based on the highest desirability value. The developed models (Eqs. 5.1 to 5.5) were used for optimization of spray drying process parameters. The maximum desirability of spray drying conditions was 0.88. The optimal condition of spray drying was 6 % (w/v) modified starch, 4.9 MPa atomizer pressure, and 168.7 °C inlet air temperature. In the optimum condition, the predicted values of the dependent variables were, encapsulation efficiency 94.2 %, DPPH scavenging activity 54.6 %, anthocyanin content 2.9 mg/L, true density 1.7 g/cm^3, and water activity 0.5. For the validation of optimized condition, the experiment was conducted in optimum condition. At the optimized condition, encapsulation efficiency, anthocyanin content, DPPH activity, true density, and water activity of powder did not significantly ($p \leq 0.05$) varied from predicted values, hence the developed model was reliable.

5.3.4. Physicochemical properties of powder

The physicochemical properties of microencapsulated anthocyanin powder were investigated in term of true density, Hausner ratio, bulk density, porosity, diameter, water activity and solubility. It was observed that the true density was 1.7 (g/cm^3), Hausner ratio (HR) 1.02, bulk density 1.4 (g/cm^3), porosity 0.2, solubility 51.8 % (w/w), diameter 6.4 (µm), and water activity was 0.5 of the developed powder.

5.3.5. Gelatinization properties

Gelatinization properties of the microencapsulated anthocyanin powder were analyzed through DSC and compared with both the starch samples. As shown in **Fig. 5.3** the microencapsulated anthocyanin powder, as well as modified starch showed higher onset and peak temperature than native starch. The onset, peak, and endset temperature signify the initiation of gelatinization, maximum gelatinization, and end of the gelatinization of the sample, respectively. There were distinct differences in the peak of melting temperatures of

the native, modified starch and encapsulated powder. The onset, peak and endset temperature of native rice starch were 74, 73.2 and 77.2 °C, respectively (**Fig. 5.3**).

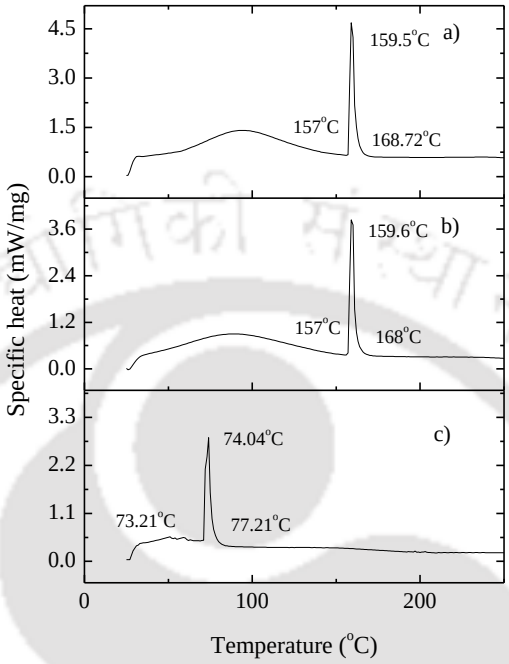

Fig. 5.3: Thermogram of a) microencapsulated powder, b) modified starch, and c) native starch

From the **Fig. 5.3**, it can be observed that the onset temperature of microencapsulated particles and modified starch were significantly changed. It may be due to the formation of various complexes with amylose for the hydrolysis of starch, especially amorphous regions and affect the thermal properties. A similar observation was reported by the previous researcher (Pereira et al., 2015). The onset temperature of the samples was increased from 73.2 ºC to 157 ºC, may be due to the formation of amylose-phenolic compounds long chain complex, which needed a higher temperature to break. This increase could also be due to high number of longer amylopectin double helices resulting from modification than in unhydrolyzed amylopectin molecule, because branch points in unhydrolyzed amylopectin may reduce the length of helix-forming side chains. From the result, it can be inferred that the developed powder is heat stable.

5.3.6. X-ray diffraction patterns

Fig. 5.4 shows the X-ray diffraction pattern of microencapsulated anthocyanin powder, native and modified starch. As shown in **Fig. 5.4**, a strong diffraction peak was observed around 15° which indicates A-type crystallinity of starch, a doublet at 17°, and 23° (2θ) (Zhu et al., 2011). After microencapsulation, the typical starch peaks disappeared and the loaded microencapsulated powders demonstrated an amorphous nature. The **Fig. 5.4** illustrated that for microencapsulated anthocyanin powder, a sharp peak at 19.18° was observed which may be due to the formation of the biopolymer with an amorphous structure (Kumar et al., 2014). It may possible that there is formation of V-amylose with other bioactive compounds present in anthocyanin extract, which is responsible for the distinct peak (Rezaei et al., 2019). In addition to that, the effect of spray drying process may also responsible for the distinct peak of microencapsulated anthocyanin powder.

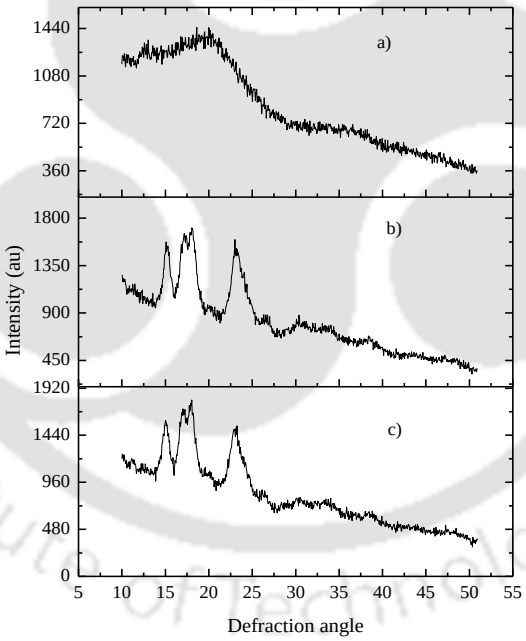

Fig. 5.4: XRD of a) microencapsulated powder b) native, and c) modified starch

5.3.7. FT-IR analysis

The FT-IR spectrum of anthocyanin extract, starch, modified starch and encapsulated powder shown in **Fig. 5.5**. The infrared spectra of the samples were characterized with the help of previous investigations (Chen et al., 2016; Pereira Jr et al., 2015). The spectrum of native,

modified starches and microencapsulated anthocyanin powder were having quite similar stretches and functional groups. The peaks were observed in the regions between 800 to 1,500 cm^{-1} (the fingerprint region), the region between 1500 to 2000 cm^{-1} (C-H stretch region), and finally the region between 2500 and 3500 cm^{-1} (O-H stretch region). The peaks between 1000 to 1250 cm^{-1} may be due to the C–O–C bond, which illustrated that the three samples were carbohydrate in nature. From **Fig. 5.5**, a band was observed at 1022 cm^{-1} which is responsible for more amorphous samples, while the bands at 1000 and 1047 cm^{-1} defined the more crystalline samples (Warren et al., 2016). The predominant peaks located at 1636 cm^{-1} is also associated with ring stretching of C=C. From **Fig. 5.5,** it was observed that at 2950 cm^{-1} there is a sharp peak which may be due to the C-H stretching vibration. The FT-IR spectrum for the anthocyanin extract shows a strong absorption band at 1032 cm^{-1} assigned to aromatic ring C-H deformation and 3489 cm^{-1} for OH. The absorption band between 1500 and 3000 cm^{-1} corresponding to the stretching of C–H, C=C asymmetric deformation in $–OCH_3$, CH_2 in pyran ring, typical of flavonoid compounds (Pereira Jr et al., 2015).

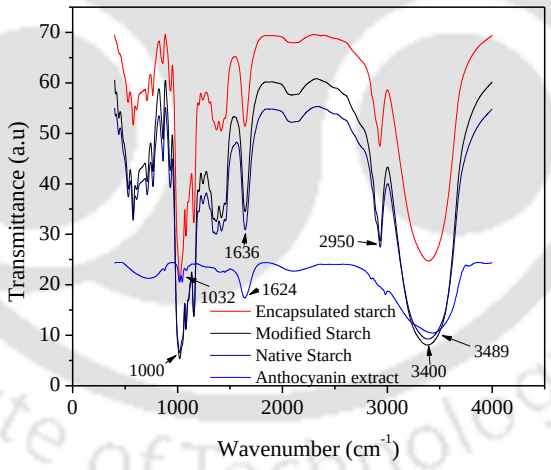

Fig. 5.5: FT-IR spectrum of native starch, modified starch, microencapsulated powder, and anthocyanin

5.3.8. Surface morphology

The microencapsulated powder obtained under optimum spray drying conditions (6 % (w/v) modified starch, 4.96 MPa atomizer pressure, and 168.8 °C inlet air temperature) was characterized using SEM technique and compared with native starch and modified starch. As

shown in **Fig. 5.6**, the surface morphology of spray dried microcapsule was more uniform and smooth than native starch and modified starch surface. Moreover, no particle aggregation was observed in the microencapsulated anthocyanin powder (Almeida et al., 2013). Kanakdande et al. (2007) suggested that the microencapsulated powder should have a uniform and smooth surface having slightly spherical shape with minimum cracks and collapses on walls. Few broken microcapsules can be observed from **Fig. 5.6**, it indicates quite inefficient encapsulating properties of the carrier materials. This result was in agreement with earlier reports (Kanakdande et al., 2007).

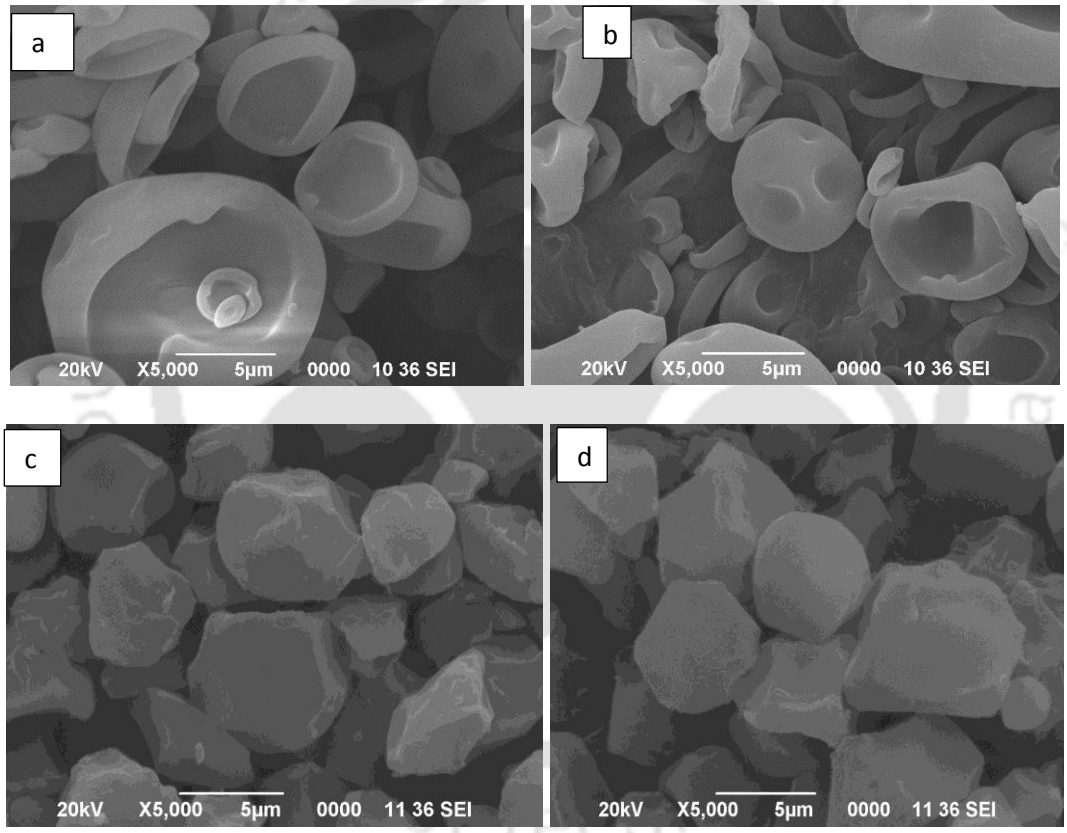

Fig. 5.6: Scanning electron microscope of a) and b) microencapsulated powder, c) native, and d) modified rice starch

5.3.9. Storage study

The storage stability of microencapsulated anthocyanin powder was studied for 90 days at 25 and 4 °C. In both, the temperatures, a decrease in anthocyanin content was observed as shown in **Fig. 5.7**. This phenomenon illustrated that after the microencapsulation; there can

also be a significant decrease in the anthocyanin content. The degradation of anthocyanin in microencapsulated powder was higher at 25 °C than 4 °C. A similar types of observation were reported by the previous researcher (Weber et al., 2017). Degradation of anthocyanin, during storage, may occur due to various reaction mechanisms, such as condensation reactions, oxidation, and cleavage of a covalent bond. During high-temperature storage, the reaction rate of these reactions is high, which enhance anthocyanin degradation. However, the exact mechanism for anthocyanin degradation during storage is difficult to establish (Patras et al., 2010).

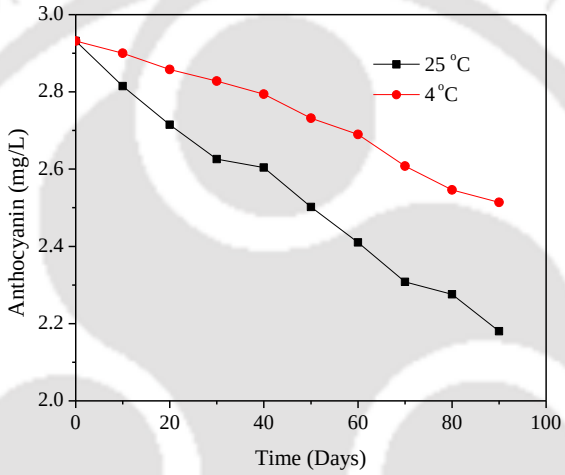

Fig. 5.7: Storage stability of anthocyanin in microencapsulate powder at 25 °C and 4 °C

5.3.10. Anthocyanin release

Fig. 5.8 illustrated the release profile of anthocyanin in simulated condition. It was noticed that the anthocyanin concentration in the medium reached to a maximum value within the 20 and 30 min at pH 2 and pH 7, indicative of complete release. Afterward release of anthocyanin reached a plateau and remains stable. At low pH, the release of anthocyanin was higher than neutral pH. It may be due to the hydrolysis of starch, which enhance the release of anthocyanin. Moreover, anthocyanin is most stable in acidic pH, hence high anthocyanin was observed in medium (Wang et al., 2013). **Fig. 5.8** showed the lowest anthocyanins released from microencapsulate in simulated fluid during incubation at higher pH. It may be due to the degradation of anthocyanin at neutral pH conditions. It was also observed that the graph was not from the origin, which indicated that anthocyanins at the surfaces of microcapsule released

earlier than those in their inner core and matrix, respectively. Similar kind of observation was reported by Oidtmann et al. (2012).

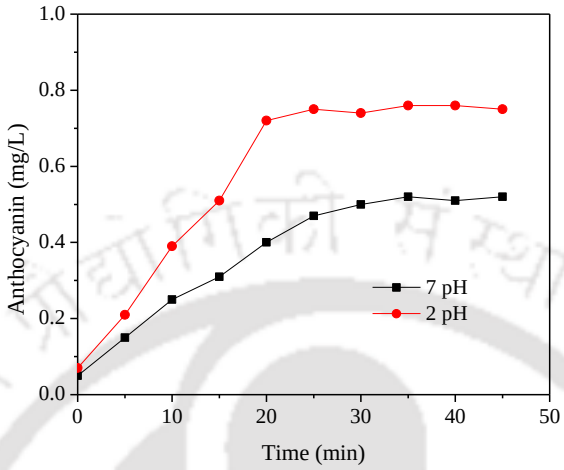

Fig. 5.8: Release profile of anthocyanin from microcapsule

5.3.11. Steady-shear rheology

The effect of microencapsulated powder on the steady-shear rheology of rice dough was determined and presented in **Table 5.2**. The Herschel–Bulkley, and Mizrahi-Berk model were applied for the investigation. The flow behavior index (η_H and η_M) of the samples was less than 1, which depicted the shear thinning behavior. Moreover, as the proportion of microencapsulated powder increased in dough, the flow behavior index increased for both the model.

Table 5.2: Steady shear rheological parameters

Sample	Herschel–Bulkley				Mizrahi-Berk			
	***k* (*Pa s*^{n})**	η_H	σ	R^2	***k* (*Pa s*^{n})**	η_M	Σ	R^2
Control	834	0.4	0.9	0.82	335	0.2	0.7	0.83
C_5	1096	0.5	156.9	0.89	524	0.6	12.3	0.89
C_{10}	1370	0.5	98.9	0.84	890	0.6	3.8	0.84
C_{15}	1469	0.7	40.9	0.88	681	0.7	5.6	0.88
C_{20}	1460	0.7	89.2	0.97	724	0.9	8.6	0.97

This indicated that the microencapsulated powder decreases the pseudo-plasticity of the dough samples. It may be due to the formation of new networks in the rice dough in the presence of microencapsulated powder. For the increase of microencapsulated powder in rice dough, resulted in a very sticky and cohesive dough, which required a high force for shearing as compared to only rice dough and enhance the consistence of the dough. The Herschel–Bulkley model showed the higher coefficient of determination (R^2) than Mizrahi-Berk model, hence it can be inferred that Herschel–Bulkley model can efficiently predict the effect of microencapsulated powder on the steady-shear rheology of rice dough.

5.3.12. Dynamic oscillatory rheology

The effect of microencapsulated anthocyanin powder incorporation in rice dough rheology shown in **Fig. 5.9**. The G′ and G″ modulus of rice flour without microencapsulated anthocyanin powder and with microencapsulated anthocyanin powder was plotted against angular frequency (ω) and shown in **Fig. 5.9**. The incorporation of microencapsulated powder significantly change the oscillatory rheological behaviors of rice dough. Storage and loss moduli of the rice dough were investigated at an angular frequency range from 0.1 to 100 rad/s. The value of storage and loss moduli increased linearly with an increase in frequency for both the rice flour dough. The previous researcher reported a similar type of result (Demirkesen et al., 2010; Sivaramakrishnan et al., 2004).

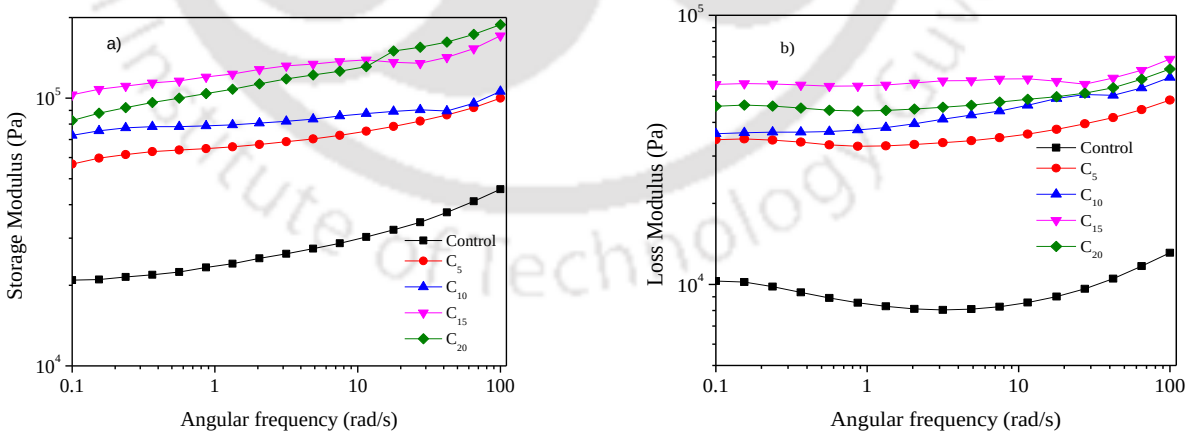

Fig. 5.9: Effect of microencapsulated powder on a) storage modulus b) loss modulus of rice dough

The linear viscoelastic behavior of dough illustrated the less frequency dependence of moduli and more rigid system than fluid. The moduli were higher for microencapsulated anthocyanin powder incorporated rice dough than that for only rice flour dough. Moreover, for the increase in microencapsulated powder concentration from 5 to 20 % (w/w), there was a sharp increase in moduli value as shown in **Fig. 5.9**. This increase in moduli suggested that rearrangement of internal structure took place during the oscillatory test, and thereby dough became more rigid. It may be due to the formation of three-dimensional (3D) gel network by starch, present in flour and reinforced by microencapsulated anthocyanin powder.

5.4. Summary

The present study has provided details of microencapsulation process for anthocyanin, storage stability and effect on rice dough rheology. The conclusions are summarized as follows:

- The process was optimized using RCCD followed by RSM and the optimum process condition for microencapsulation was 6 % (w/v) of starch concentration, 168.8 °C drying temperature and 4.9 MPa nozzle pressure.
- Microencapsulate showed higher onset (157.0 °C) and peak temperature (168.8 °C).
- The morphological properties of microencapsulate showed that the surface of microcapsules was more uniform and smooth surfaces than the native and modified starch.
- The storage study of microencapsulated powder illustrated that at low-temperature storage the anthocyanin degradation in particles was less than high-temperature storage.
- The maximum amount of anthocyanin from microcapsule was released in low pH within 20 min in simulated condition.
- The microencapsulated particles affect the steady-shear rheology of rice dough. The increase in microencapsulated powder concentration from 5 to 20 % in rice dough, decrease the pseudo-plasticity of dough.
- The value of storage and loss moduli increased with increase in microencapsulated anthocyanin concentration in dough.

References

Al Almeida, A.P., Rodríguez-Rojo, S., Serra, A.T., Vila-Real, H., Simplicio, A.L., Delgadilho, I., da Costa, S.B., da Costa, L.B., Nogueira, I.D. and Duarte, C.M. (2013). Microencapsulation of oregano essential oil in starch-based materials using supercritical fluid technology. *Innovative Food Science and Emerging Technologies, 20,* 140-145.

Bhandari, B.R., Dumoulin, E.D., Richard, H.M.J., Noleau, I. and Lebert, A.M. (1992). Flavor encapsulation by spray drying: application to citral and linalyl acetate. *Journal of Food Science*, *57*(1), 217-221.

Chen, Y., Zhang, W., Zhao, T., Li, F., Zhang, M., Li, J., Zou, Y., Wang, W., Cobbina, S.J., Wu, X. and Yang, L. (2016). Adsorption properties of macroporous adsorbent resins for separation of anthocyanins from mulberry. *Food Chemistry, 194*, 712-722.

Demirkesen, I., Mert, B., Sumnu, G., and Sahin, S. (2010). Rheological properties of gluten-free bread formulations. *Journal of Food Engineering, 96*(2), 295-303.

Jafari, S.M., Assadpoor, E., He, Y. and Bhandari, B. (2008). Encapsulation efficiency of food flavours and oils during spray drying. *Drying Technology, 26*(7), 816-835.

Kanakdande, D., Bhosale, R. and Singhal, R.S. (2007). Stability of cumin oleoresin microencapsulated in different combination of gum arabic, maltodextrin and modified starch. *Carbohydrate Polymers, 67*(4), 536-541.

Kumar, P., Senthamilselvi, S. and Govindaraju, M. (2014). Phloroglucinol-encapsulated starch biopolymer: preparation, antioxidant and cytotoxic effects on HepG2 liver cancer cell lines. *RSC Advances, 4*(51), 26787-26795.

Oidtmann, J., Schantz, M., Mäder, K., Baum, M., Berg, S., Betz, M., Kulozik, U., Leick, S., Rehage, H., Schwarz, K. and Richling, E. (2012). Preparation and Comparative Release Characteristics of Three Anthocyanin Encapsulation Systems. *Journal of Agricultural and Food Chemistry, 60*(3), 844-851.

Patras, A., Brunton, N.P., O'Donnell, C. and Tiwari, B.K. (2010). Effect of thermal processing on anthocyanin stability in foods; mechanisms and kinetics of degradation. *Trends in Food Science and Technology, 21*(1), 3-11.

Pereira Jr, V.A., de Arruda, I.N.Q. and Stefani, R., (2015). Active chitosan/PVA films with anthocyanins from Brassica oleraceae (Red Cabbage) as time–temperature indicators for application in intelligent food packaging. *Food Hydrocolloids, 43*, 180-188.

Rezaei, A., Fathi, M. and Jafari, Seid M. (2019). Nanoencapsulation of hydrophobic and low-soluble food bioactive compounds within different nanocarriers. *Food Hydrocolloids, 88*, 146-162.

Sivaramakrishnan, Hema P., Senge, B., and Chattopadhyay, P. K. (2004). Rheological properties of rice dough for making rice bread. *Journal of Food Engineering, 62*(1), 37-45.

Tuyen, C.K., Nguyen, M.H. and Roach, P.D. (2010). Effects of spray drying conditions on the physicochemical and antioxidant properties of the Gac (*Momordica cochinchinensis*) fruit aril powder. *Journal of Food Engineering, 98*(3), 385-392.

Wang, Z., Li, Y., Chen, L., Xin, X., and Yuan, Q. (2013). A study of controlled uptake and release of anthocyanins by oxidized starch microgels. *Journal of Agricultural and Food Chemistry, 61*(24), 5880-5887.

Warren, F. J., Gidley, M. J. and Flanagan, B. M. (2016). Infrared spectroscopy as a tool to characterise starch ordered structure-a joint FTIR-ATR, NMR, XRD and DSC study. *Carbohydrate Polymers, 139*, 35-42.

Weber, F., Boch, K. and Schieber, A. (2017). Influence of copigmentation on the stability of spray dried anthocyanins from blackberry. *LWT-Food Science and Technology, 75*, 72-77.

Zhu, L.J., Liu, Q.Q., Wilson, J.D., Gu, M.H. and Shi, Y.C. (2011). Digestibility and physicochemical properties of rice (*Oryza sativa L.*) flours and starches differing in amylose content. *Carbohydrate Polymers, 86*(4), 1751-1759.

TO DEVELOP FUNCTIONAL FOOD AND PAPER BASED INDICATOR FROM ANTHOCYANIN

Part of the work is under review in

- Journal of Packaging Technology and Research
- Journal of food science and biotechnology

CHAPTER 6

TO DEVELOP FUNCTIONAL FOOD AND PAPER BASED INDICATOR FROM ANTHOCYANIN

6.1. Overview

The application of anthocyanin as an ingredient in extrudate food and paper based pH indicator were carried out. The effect of extrusion cooking on the quality of rice extrudate with microencapsulated anthocyanin was determined. The moisture sorption isotherm behavior of the extrudate was also investigated in the present study. The RCCD was used to optimize the extrusion process and the optimized conditions were: screw speed, 121 rpm (12.7 rad/s); barrel temperature, 91.9 °C; and moisture content, 22.03 % (w/w). The extrudate having anthocyanin content, 0.2 mg/L; true density, 1.5 g/cc; water activity 0.5, water solubility index, 7.5 % (w/w); and specific mechanical energy, 31.4 kJ/kg. The antioxidant activity, solubility, and cooking properties of the extrudate were also determined and compared with control extrudate. The storage study of the extrudate was determined in terms of moisture sorption isotherm and found to follow type III isotherm behavior according to the BET classification. The sorption isotherm was analyzed using several models among the studeid models Caurie and Peleg models found to show good agreement with the extrudate isotherm data. Apart from that, anthocyanin was also used as pH indicator. A portable filter paper based pH indicator has been developed using anthocyanin for rapid food quality monitoring. The efficiency of the indicator was studied with different buffer solutions of pH range from 2 to 10. The indicator made with 150 mg/L anthocyanin concentration showed a distinct L, a, and b values of color. Further, the indicator was tested in different liquid foods and indicated a distinct color with respect to pH values. The degradation behavior of a-value (redness) of the indicator showed first-order kinetics behavior. At high-temperature storage conditions, the degradation rate constant of a-value was higher than the low-temperature storage condition. The process provides a green route of monitoring of liquid food quality using low cost, flexible and highly sensitive pH indicator with high L sensitivity.

6.2. Precise background

For the busy daily work schedules and on-the-go consumption habits, in the global market there is a growth of ready-to-eat food products. For that, food industries have increased the production of ready-to-eat products using several processes namely extrusion, freeze-drying and many more. Among these processes, extrusion is a well-established industrial technology, which is characterized by continuous cooking, mixing and forming process and produces direct expanded materials with high quality at high temperatures in a short time. Recently, consumers have developed a growing understanding of how the composition of food products can impact the nutritional quality of the foods. Therefore, in order to develop the ready-to-eat functional food products, bioactive ingredients are to be added with the extruded mixtures. The majority of these compounds are lost during processing due to their sensitivity towards processing conditions such as temperature, pressure, and pH. Thereby, in this chapter, microencapsulated anthocyanin incorporated extrudate was developed and the extrusion process optimized. It includes the storage study and sorption isotherm behavior of the extrudate. The discussion on anthocyanin based paper indicator is also included in this chapter.

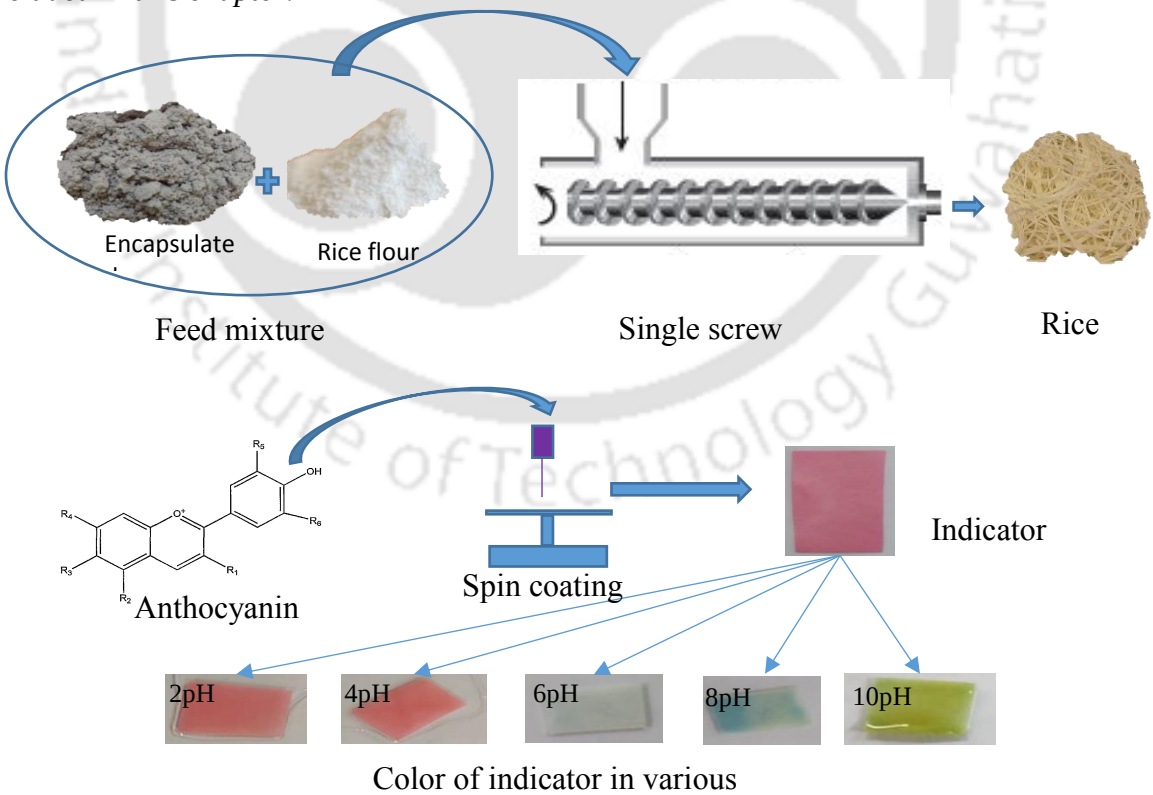

Fig. 6.1: Graphical abstract

6.3. Results and disscussion

6.3.1. Prelimeniery study for extrusion cooking

In the preliminary study, the effects of extrusion variables on water solubility index (WSI) and cooking loss of the extrudate was investigated. The water solubility index of the extrudate significantly ($p \leq 0.05$) effected by the screw speed when the other parameters were constant (**Fig. 6.2a**). The WSI of the extrudate was increased with screw speed upto 150 RPM (15.7 rad/s) (8.6 % w/v) and then decrease with incrasesing screw speed (**Fig. 6.2a**). The WSI generally use as an indicator of molecular degradation of biopolymer after extrusion (Ding et al., 2006). Thereby, upto 150 RPM (15.7 rad/s), due to the damage of starch for gelatinization and extrusion-induced fragmentation, WSI of extrudate increased (Sharma et al., 2017). However, at high screw speed the residence time of the feed in the extruder was less, hence the degradation of the biopolymer is less and thereby less WSI is observed. **Fig. 6.2a** illustrated that for the increase of screw speed upto 150 RPM (15.7 rad/s), the cooking loss (10.5 % w/w) of the extrudate decreases and increase with further increase in screw speed. Therefore, for furthere study the screw speed was varied from 100 (10.5 rad/s) to 200 RPM (20.9 rad/s).

From the **Fig. 6.2b**, it was observed that for the increase of extrusion cooking temperature, the WSI of the extrudate increased rapidly (2.1-12.5 % w/w). The increase in WSI of extrudate may due to the disintegration of starch granules and formation of low molecular compounds during extrusion cooking, thereby increase the WSI (Sharma et al., 2017). **Fig. 6.2b** illustrated that for the increase of barrel temperature from 50 °C to 80 °C, the cooking loss of the extrude decrease from 19.2 to 10.5 % (w/w). Whereas, after 80 °C a reverse trend was observed for the cooking loss of the extrudate (**Fig. 6.2b**). At low temperature, due to improper gelatinization, a weak starch network may be formed which enhance the loss of bioplymer during cooking of extrudate. However, for the increase of extrusion temperature cooking loss of extrudate decreases (**Fig. 6.2b**), due to the proper gelatinization and formation of the strong starch network. At very high extrusion temperature (≥80 °C), the degradation of starch such that it can't form a proper network and enhance the cooking loss (**Fig. 6.2b**). On the basis of this observation, for further study, the extrusion cooking temperature range varied from 60 to 100 °C.

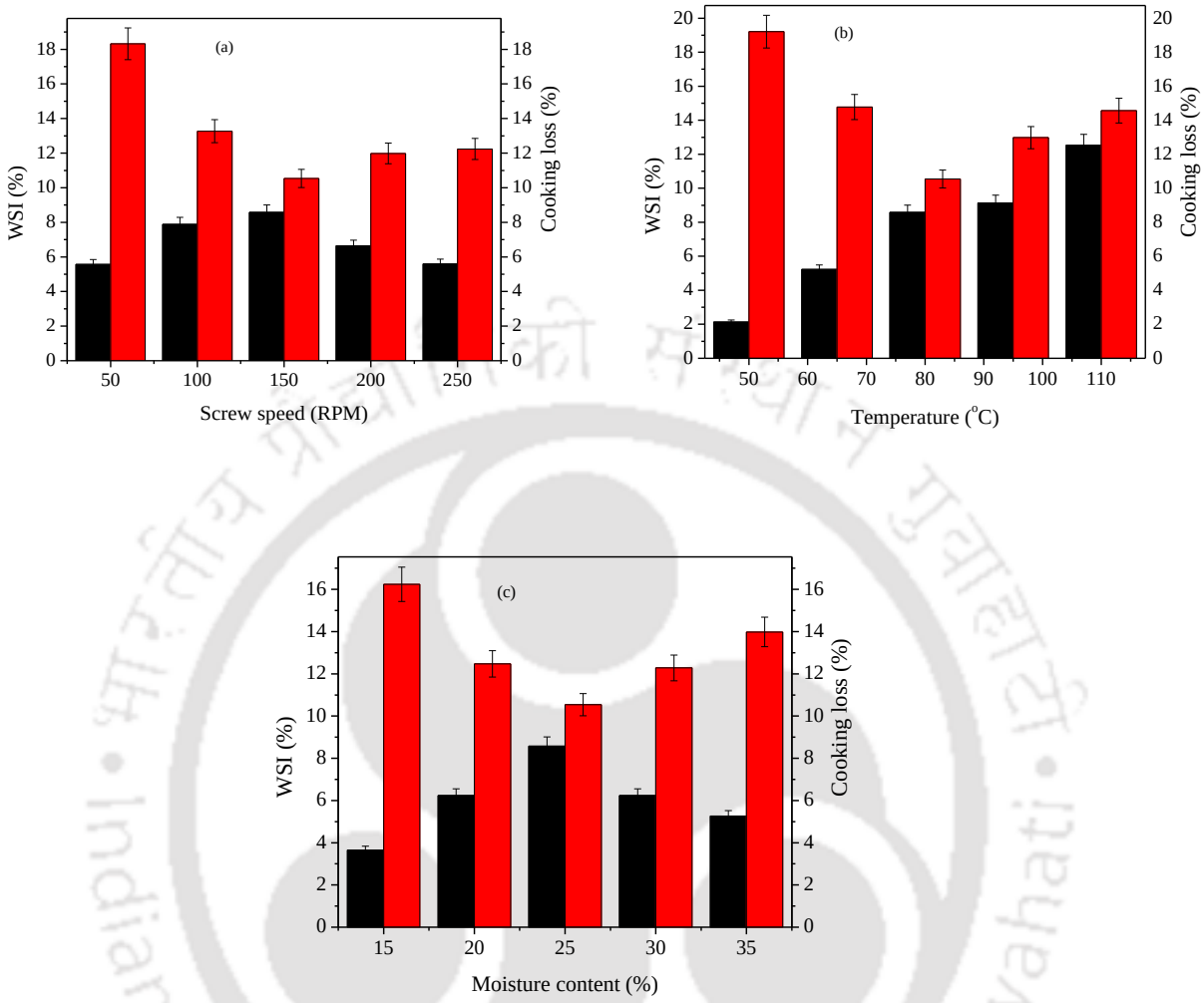

Fig. 6.2: Effect of a) screw speed, b) temperature, and c) moisture content on WSI (■) and cooking loss (■)

Feed moisture had a significant ($p \leq 0.05$) effect on the WSI of the extrudate (**Fig. 6.2c**). At low feed moisture, the extrudate showed a low level of WSI and increases with feed moisture content upto 25 % (w/w) (**Fig. 6.2c**). However, excessive moisture showed a decrease in WSI of the extrudate. At low feed moisture, due to partial gelatinization and hydrolysis of starch, extrudate showed a low WSI. Whereas at high feed moisture level, due to complete gelatinization and hydrolysis of starch, WSI of the extrudate increased (Ding et al., 2006). However, excess moisture increases the slippage of feed material in the extruder and inhibit the gelatinization, thereby reduce the WSI of the extrudate (Sharma et al., 2017). The feed

moisture also showed a significant ($p \leq 0.05$) effect on the cooking loss of the extrudate. At low feed moisture, the cooking loss of the etrudate was very high, due to improper gelatinization and segregated product structure. However, it decreased upto 25 % (w/v) of moisture content (**Fig. 6.2c**). When the moisture content was higher than 25 % (w/v), the cooking loss increases again, due to the formation of a weak starch network. Therefore, in the further investigation, feed moisture varied from 20 to 30 % (w/v).

6.3.2. Regression analysis

After the prilimenary investigation, the selected ranges of independent parameters were used in the RCCD to developed the relationship of independent parametres with dependent parameters and to optimize the extrusion cooking process.

Effects of three independent parameters such as barrel temperature (x_{12}), screw speed (x_{13}) and feed moisture content (x_{14}) on the anthocyanin content, true density, water activity, water solubility index and specific mechanical energy of extrusion cooking were determined. The relationship between dependent and independent parameters of rice extrudate was described using second-order polynomial models and analysed using analysis of variance (ANOVA) as shown in **Table 6.1**. The result of ANOVA for dependent parameters showed that the model, linear, quadratic and interaction terms were significant ($p \leq 0.05$). The *p*-value of lack of fit for anthocyanin content, true density, water activity, water solubility index and specific mechanical energy were not significant ($p \leq 0.05$). Hence developed relationship was suitable for the experimental data. All the developed second-order polynomial models showed the high cofficient of determination (R^2) which implied that the development model can efficently explain the variable relationships and can be used for the optimization of the process parameter.

$$\begin{aligned}\text{Anthocyanin (mg/L)} = {} & 0.16 - 0.029x_{12} - 0.11x_{13} + 0.029x_{14} + 0.021x_{12}x_{13} + 3.04\times10^{-3}x_{12}x_{14} \\ & - 0.038x_{13}x_{14} + 0.020x_{12}^2 + 0.049x_{13}^2 + 0.074x_{14}^2\end{aligned} \quad (6.1)$$

$$\begin{aligned}\text{True density (g/cc)} = {} & 1.64 - 0.068x_{12} - 0.11x_{13} + 0.063x_{14} + 0.016x_{12}x_{13} - 0.043x_{12}x_{14} \\ & + 0.052x_{13}x_{14} - 3.37\times10^{-3}x_{12}^2 - 0.053x_{13}^2 + 0.11x_{14}^2\end{aligned} \quad (6.2)$$

$$\begin{aligned}\text{Water activity} = {} & 0.53 - 0.022x_{12} - 0.057x_{13} + 0.029x_{14} - 0.021x_{12}x_{13} - 0.021x_{12}x_{14} \\ & + 9.37\times10^{-4}x_{13}x_{14} + 0.011x_{12}^2 + 0.023x_{13}^2 + 0.021x_{14}^2\end{aligned} \quad (6.3)$$

$$\text{Water soubility index (\%)} = 26.35 - 1.77x_{12} + 3.99x_{13} - 4.31x_{14} + 2.89x_{12}x_{13} - 1.25x_{12}x_{14} - 4.56x_{13}x_{14} - 6.25x_{12}^2 - 2.71x_{13}^2 - 5.63x_{14}^2 \quad (6.4)$$

$$\text{Specific mechnical energy (kJ/kg)} = 4097 + 696x_{12} + 156x_{13} - 285x_{14} - 113x_{12}x_{13} - 152x_{12}x_{14} - 053x_{13}x_{14} + 133x_{12}^2 - 432x_{13}^2 - 423x_{14}^2 \quad (6.5)$$

Table 6.1: Analysis of variance of the model

Source	Anthocyanin content (mg C3G/L)	True density (g/cc)	Water activity	Water solubility index (%)	Specific mechanical energy (kJ/kg)
Model	< 0.0001	0.0001	0.0001	< 0.0001	< 0.0001
x_{12}	0.04	0.003	0.009	0.05	< 0.0001
x_{13}	< 0.0001	0.0001	< 0.0001	0.0005	0.04
x_{14}	0.05	0.005	0.001	0.0003	0.001
$x_{12}x_{13}$	0.2	0.5	0.04	0.01	0.2
$x_{12}x_{14}$	0.8	0.09	0.04	0.25	0.1
$x_{13}x_{14}$	0.04	0.05	0.9	0.001	0.6
x_{12}^2	0.1	0.8	0.1	< 0.0001	0.07
x_{13}^2	0.002	0.01	0.007	0.005	< 0.0001
x_{14}^2	0.0001	< 0.0001	0.01	< 0.0001	< 0.0001
Lack of Fit	0.1	0.86	0.45	0.26	0.07
R^2	0.93	0.93	0.92	0.95	0.95
Adj-R^2	0.87	0.86	0.86	0.91	0.91

6.3.3. Response surface analysis

6.3.3.1. Effect of process variable on anthocyanin content

The effect of extrusion cooking on microencapsulated anthocyanin retention in the extrudate is depicted in **Fig. 6.3** (**a** and **b**). For the increase of barrel temperature during extrusion cooking, anthocyanin content in the extrudate decreased (**Fig. 6.3a**). Similar type of result was reported by Hirth et al. (2014) and Camire et al. (2002) during the extrusion of bilberry and blueberry anthocyanins in starch-based food. The significant loss of anthocyanins during extrusion cooking is mainly due to the degradation of anthocyanin in presence of high extrusion temperature. For the increase of screw speed, anthocyanin content in extrudate

product decreased significantly ($p \leq 0.05$) (**Fig. 6.3a**). Hirth et al. (2014) and Khanal et al. (2009) reported similar kind of observation during the extrusion of bilberry anthocyanins in starch-based food and blueberry pomace, respectively. For the increase of screw speed, there is an increase in friction and hence high heat dissipation in feed material, which cause the higher degradation of anthocyanin. Khanal et al. (2009) also suggested that due to the influence of thermo-mechanical energy during extrusion cooking, there was a change in molecular structure and reactions of starch-based materials and phytochemicals, thereby degrade the anthocyanin. It is observed that at a higher level of moisture content, the anthocyanin retention in the extrudate product was high (In appendix **Fig. 5A1**). High moisture content acts as a lubricant during extrusion cooking and decrease the effect of thermo-mechanical energy on microencapsulated anthocyanin and thereby enhance the retention of anthocyanin in the extrudate.

6.3.3.2. Effect of process parameter on true density

True density determines the average density of the particulate solid in a specific medium. **Fig. 6.3c** showed that for the increases of barrel temperature, the true density of the extrudate decreased. It is obvious that for the increase of extrusion cooking temperature the moisture content of the finished product decreased, resulting in the decrease in true density of the finished product. For the increase of screw speed up to 150 rpm (15.7 rad/s), there is a moderate increase in true density of the product beyond that a reverse trend can be observed (**Fig. 6.3b**). At lower screw speed, due to the less heat dissipation in the feed material and less pressure drop in the die, the bubble formation in the product is less, which increase the true density of the product. At high screw speed, a higher amount of heat dissipation is occurred in the feed material that resulted in a higher degree of superheated water in the feed material during cooking, encouraging the formation of bubble and decrease in melt viscosity, thus leading to reduce true density (Gui et al., 2012). The increase of moisture content up to 25 % (db) decreases the true density beyond that a reverse trend was observed (**Fig. 6.3d**). At lower feed moisture, the rice flour and microencapsulated anthocyanin powder produce a high viscous material with high bubble holding capacity resulted reduces in true density. Excess moisture in the feed, results incomplete starch gelatinization and hence, high moisture results in a higher true density of extrudate (Akdogan, 1999). Also, higher the moisture content,

lower the viscosity, and dough temperature, which might have resulted in an incomplete texturization (Lin et al., 2000) and a higher density.

6.3.3.3. Effect of process parameter on water activity

Fig. 6.3e illustrated the effect of various extrusion parameters on the water activity of microencapsulated anthocyanin incorporated extrudate product. **Fig. 6.3e**, showed that for the increase of barrel temperature the water activity of the product decreased. This phenomenon is in agreement with drying behavior of food material. For the increase of barrel temperature, the vapor pressure difference between the core of the product and surface of the product increased, causing the outward movement of more moisture and thereby decrease the water activity of the product. For the increase in screw speed, there was a slight increase in water activity (**Fig. 6.3f**). Similar type of observation was reported by Chevanan et al. (2008) during the extrusion of three isocaloric ingredient blends. It may be due to less residence time of the feed material in the barrel thereby increases the moisture content and water activity. For the increase of moisture content in the feed material, there is an increase in the water activity of the extrudate (**Fig. 6.3f**). It is obvious that if the feed moisture increase there should be an increase in water activity of the finished extrudate product.

6.3.3.4. Effect of process parameter on water solubility index

The WSI indicates the solubility of extrudates product in water, which generally caused by starch conversion during extrusion cooking. The effect of independent variables on the WSI of extrudate product shown in **Fig. 6.3g** and the figure showed WSI increased with the increase of barrel temperature. This could be due to starch degradation and disintegration at high temperature during extrusion cooking and thereby increase the solubility of the finished product. It was also suggested that the fiber and protein present in the feed material also affect the WSI of finish product (Jones et al., 2000). Similar type of observation was reported by previous researcher (Singh et al., 2007). For the increase of screw speed up to 150 rpm (15.7 rad/s) there is an increase in WSI of the extrudates, beyond that there is a reverse trend is observed (**Fig. 6.3g**). The increase in WSI may be due to the mechanical and thermal breakdown of biopolymers during extrusion cooking and increase the solubility. However, beyond certain screw speed, the WSI of the finished product decreases may due to the less residence time of feed material in the extruder. For the increase of moisture content in the feed

material up to 25 % (w/w), WSI increase (**Fig. 6.3h**), may be due to higher degradation of the polymer at lower feed moisture level (Singh et al., 2007). However, the excess water in the feed material may act as a lubricant, which reduce the shear rate and degradation of feed material during extrusion cooking, thereby decrease the solubility.

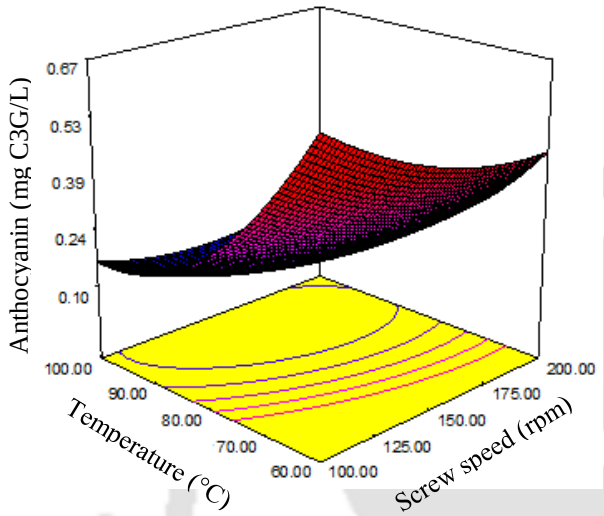

a)

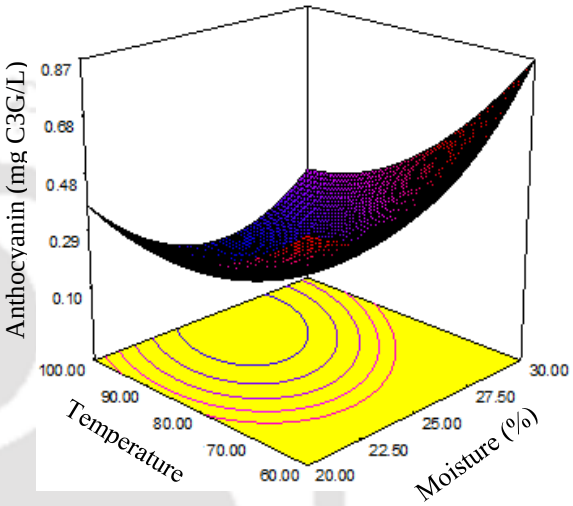

b)

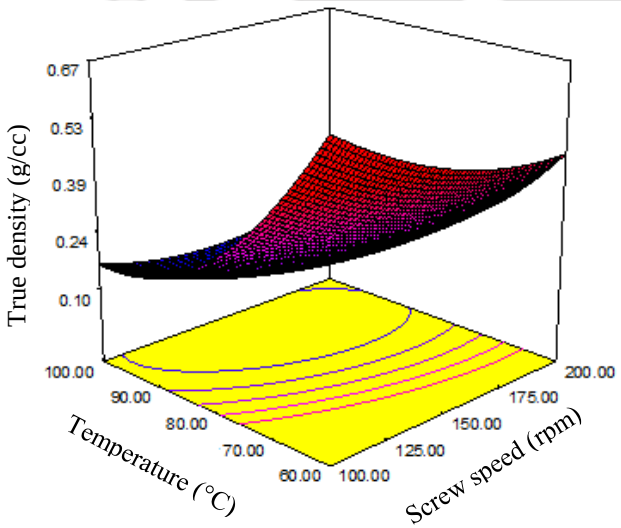

c)

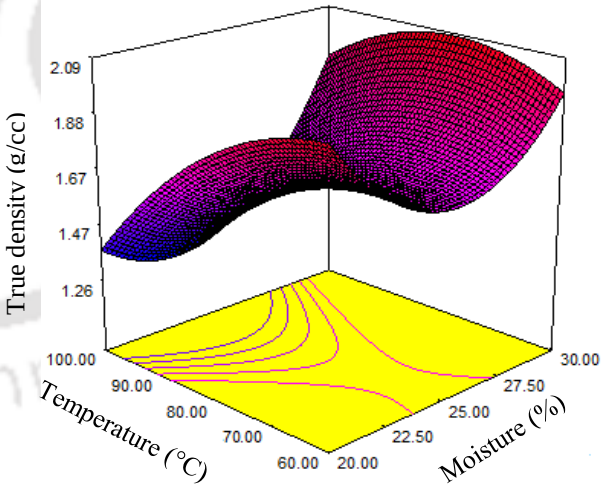

d)

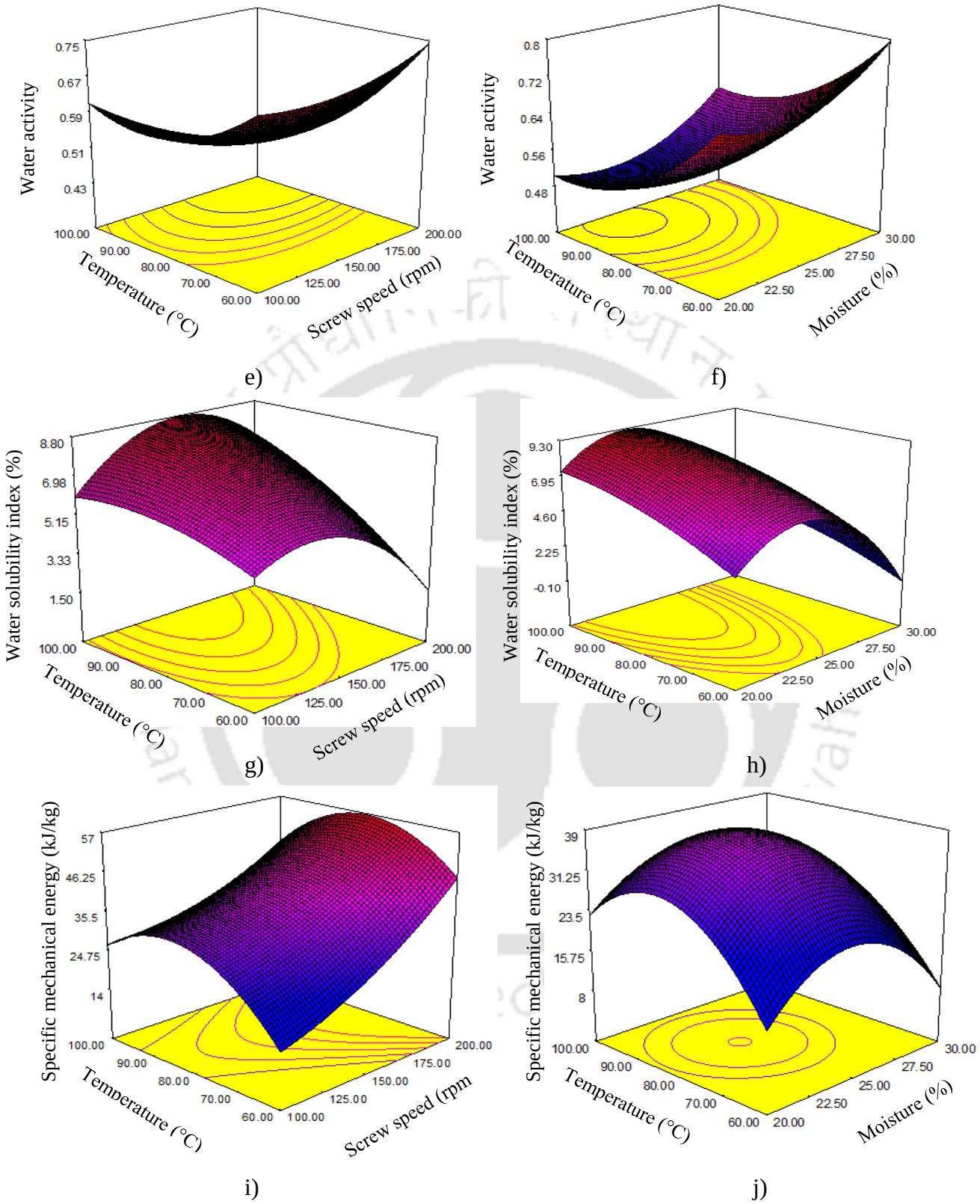

Fig. 6.3: Effect of independent parameters on dependent parameters during extrusion

6.3.3.5. Effect of process parameter on specific mechanical energy

Fig. 6.3i illustrated the effect of temperature, screw speed and moisture on specific mechanical energy (SME) during extrusion of microencapsulated anthocyanin incorporated extrudate. SME is the amount of mechanical energy degenerate as heat inside the feed (unit mass) (Chang et al., 1999). It can be observed (**Fig. 6.3i**) that for the increase of extrusion temperature up to 80 °C there was a sharp increase in the SME, beyond that there was a slight decrease in SME. The increase in the SME for an increase of temperature during extrusion may be due to the molecular breakdown or degradation of starch and protein up to a certain limit that forms a strong network hence increases the viscosity. It was suggested that for the increase of viscosity there was an increase in SME during extrusion (Osen et al., 2014). On the other hand, in the presence of high temperature in extrusion cooking, the breakdown of feed material was increased. The size reduction of macromolecules such that it could not form a strong network and decreases the SME (Altan et al., 2009; Camacho-Hernández et al., 2014). A similar type of result was reported by Chang et al. (1999) during the extrusion of corn-meal. **Fig. 6.3i** illustrated that for the increase in screw speed, SME increases. It is obvious that for the increase of screw speed; there is a proportional increase in energy input thereby there is a sharp increase in SME. For the increase of feed moisture content up to 25 % (w/w), the specific mechanical energy was increased significantly ($p \leq 0.05$) (**Fig. 6.3j**). For the increase in water content up to a certain limit in the feed, the heat dissipation on feed material from the barrel increased. Therefore, the viscosity, shear, and friction was increased during extrusion cooking, thereby increases the SME. Further increase in the moisture content in feed material, showed a decrease in the SME. In general, higher moisture content in the feed lowers the SME, due to the reduction in the force required to drag the feed material through the die.

6.3.4. Optimization and validation

In this step, optimum values of independent parameters were obtained which would allow to obtain an extrudate with high anthocyanin content, water solubility index, true density, low water activity, and low SME. From **Table 6.1** it was observed that the developed models (Eqs. 6.1, 6.2, 6.3, 6.4, and 6.5) can efficiently optimized that extrusion process parameters. In the maximum desirability value, the extrusion conditions were screw speed 121 rpm (12.7 rad/s), barrel temperature 91.9 °C and moisture content 22.03 %. The predicted values of dependent parameters were anthocyanin content 0.2 (mg/L), true density 1.5 (g/cc), water

activity 0.5, water solubility index 7.5 (% w/w), and specific mechanical energy 31.4 (kJ/kg). In the optimum condition, the experiment was conducted and found out that there was no significant ($p \leq 0.05$) difference between predicted and experimental values of the independent parameters.

6.3.5. Comparison of physico-chemical properties

The physico-chemical properties of the extrudate with anthocyanin was investigated in terms of DPPH scavenging activity, solubility, moisture content, and bulk density. The physico-chemical properties were also compared with native rice extrudate. The DPPH scavenging activity of the extrudate was 24 %, solubility 7.5 % (w/w), and moisture content 10.3 % (w/w). The cooking properties, such as, cooking time, cooking yield of the extrudate were investigated according to the standard AACC method. It was found that the developed extrudate had the cooking yield of 201.4 % (w/w), cooking loss of 9.5 % (w/w) and optimal cooking time of 6.7 min. However, the native rice extrudate showed low DPPH scavenging activity (5.2 %) and solubility (4.3 % w/w). Although, the moisture content was not varied significantly. The cooking yield, cooking loss and cooking time of native rice extrudate were 209.2 % (w/w), 6.9 % (w/w) and 9.6 min, respectively.

6.3.6. Storage study

The storage study of the developed extrudate was conducted in term of moisture sorption isotherm. The understanding of the change in EMC of extrudate food is indicative of the storage conditions and stability of the extrudate. The moisture sorption isotherms of optimized rice extrudate shown in **Fig. 6.4**. It was illustrated that water adsorption trends followed the nonlinear growth patterns and it was clearly shown that the sorption behavior of the extrudate was temperature dependent. The equilibrium moisture content of extrudate increased exponentially with increasing water activity at a constant temperature. This behavior can be attributed to the hydrophilic nature of the starch, protein and other carbohydrates present in the rice flour as well as in microcapsules. Moreover, in **Fig. 6.4**, there is no flat portion, which indicates that there was no monolayer formation during storage. The sorption behavior of extrudate corresponding to the classification Type III isotherm according to the BET classification (Panjagari et al., 2015). A similar type of observation was reported by Włodarczyk-Stasiak and Jamroz (2008) for starch–protein extrudate. From the Figure, it was

also observed that for the increase in storage temperature there was a decrease in equilibrium moisture content (EMC). Due to the higher storage temperature, the number of active water binding reduction in extrudate and hence the EMC was reduced (Yağcı and Göğüş, 2008). It was revealed that at high temperatures, some water molecules were activated and break away from their binding sites, thus decreasing the EMC and indicated that at higher temperatures, the extrudate became less hygroscopic.

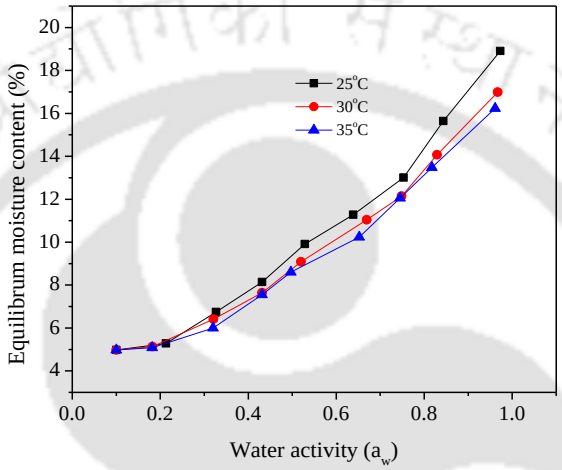

Fig. 6.4: Moisture sorption isotherm of extrudate

The EMC values of the extrudate obtained from experiment data at a different water activity (a_w) (0.11–0.97), with three different temperatures (25, 30, and 35 °C), were fitted with eight isotherm models. The models with two parameters, three parameter and four parameters as shown in **Table 6.2**, were fitted with experimental EMC data. From **Table 6.2**, it is noticed that for all the conditions, Curie and Peleg model are the most suitable to explain the sorption isotherm behavior of the extrudate. Both the model showed the high coefficient of determination (R^2) with lower RSME. This suggests that Curie and Peleg sorption models could efficiently illustrate the sorption isotherm behavior of extrudate. For **Table 6.2**, it can be observed that BET constant (C) is very less than one (0.001) which confirmed that type III sorption behaviors of the extrudate.

Table 6.2: Sorption model parameters for optimized extrudate product

Temperature	Model	*A*	*B*	*C*	*D*	R^2	RSME
	Oswin	9.2	0.2	--	--	0.92	1.4
	Smith	5.9	-4.1	--	--	0.90	1.6
	Curie	1.4	1.6	--	--	0.99	0.3
25 °C	Modified Halsey	2.9	-0.4	--	--	0.97	0.8
	Lewick 2	9.2	0.8	--	--	0.92	1.4
	Lewicki 3	7.1	0.3	-24.5	--	0.83	2.2
	Peleg	5.3	0.06	14.1	1.9	0.99	0.4
	BET	0.001	--	--	--	0.92	1.4
	Oswin	8.8	0.2	--	--	0.92	1.2
	Smith	5.6	-3.8	--	--	0.91	1.3
	Curie	1.4	1.5	--	--	0.99	0.2
30 °C	Modified Halsey	2.8	-0.4	--	--	0.97	0.7
	Lewick 2	9.7	-0.2	--	--	0.93	0.9
	Lewicki-3	20	0.09	0.6	--	0.97	0.8
	Peleg	4.6	-0.002	13	1.8	0.99	0.9
	BET	0.0003	--	--	--	0.88	1.5
	Oswin	8.5	0.2	--	--	0.93	1.09
	Smith	5.4	-3.8	--	--	0.91	1.2
	Curie	1.4	1.5	--	--	0.99	0.2
35 °C	Modified Halsey	2.8	-0.4	--	--	0.96	0.8
	Lewick 2	9.5	-0.2	--	--	0.93	1.04
	Lewicki-3	19.07	0.09	0.6	--	0.96	0.9
	Peleg	13.9	1.5	3.09	-0.2	0.99	0.2
	BET	0.0001	--	--	--	0.86	1.5

6.3.7. Paper indicator

6.3.7.1. Sensitivity of color value

Fig. 6.5 shows that *L*-value of the indicator increased significantly ($p \leq 0.05$) for the increase in anthocyanin concentration up to 150 mg/L deposited on the indicator. However, at 8 pH, a reverse trend was observed (**Fig. 6.5**). With the increase of concentration beyond 150 mg/L for the deposition on the indicator, there was no significant increase or decrease in the *L*-value of the indicator, representing the brightness of the paper indicator (Rauf et al., 2018). In various pH, anthocyanin present in the indicator shows various colors such as red for 2 pH, pink for 4 pH, white for 6 pH, blue for 8 pH and yellow for 10 pH (**Fig. 6.5**). The color of the indicator directly affects the brightness of the paper. Thereby, due to the white appearance at pH of value 6 and blue appearance at pH of value 8, the indicator shows the high (68.3) and low (45.04) brightness, respectively. This is due to the interaction of deposited anthocyanin on the indicator surface with the buffer solution of the above mention pH. The brightness of the indicator was not increased after 150 mg/L anthocyanin concentration, which may be due to the saturation of adsorption and holding capacity of the paper for anthocyanin. The filter paper was made up of cellulose, which has certain adsorption and holding capacity of particles. Thus, after a certain concentration of anthocyanin, there was no further increase in the brightness of the indicator. Therefore, in further study, the indicator coated with 150 mg/L anthocyanin was used.

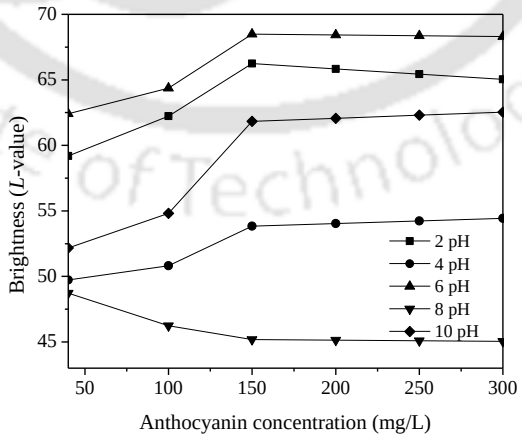

Fig. 6.5: Effect of anthocyanin concentration on *L*-value

6.3.7.2. Color sensitivity in simulated condition

The color sensing capacity of the indicator was investigated in the simulated condition. Various pH (2, 4, 6, 8, and 10 pH) buffer solution was used to simulate the food systems. It was observed that the *L*, *a*, and *b* values of the indicator was varied significantly ($p \leq 0.05$) with the change in pH (**Table 6.3**). At 2 pH, the appearance of the indicator was red; thereby, the *a*-value was positive (25.3); hence *b*-value was very negligible (**Fig. 6.6a**). At pH 2, due to the presence of flavylium cation in anthocyanin, the indicator exhibited a dark red color (McGhie and Walton, 2007), hence exhibited high *a*-value. In the 4 pH, although the *a*-value was positive and lower than 2 pH value, the redness of the indicator was predominated (**Fig. 6.6b**). The similar kind result was noticed from **Table 6.3** that the brightness (*L*-value) of the indicator was lower at 4 pH than that at 2 pH. This is due to the formation of the red color quinonoidal-base structure of anthocyanin on the indicator due to the rapid loss of a proton from the flavylium cation at 4 pH (McGhie and Walton, 2007) and shows moderate redness. At 6 pH, the *a*-value and *b*-value were very less, which complied that the indicator was nearly white in color and obviously the brightness (*L*-value) of the indicator was higher (**Fig. 6.6c**). It is due to the deprotonation of the quinonoidal-base structure of anthocyanin and formed a colorless carbinol pseudo-base structure on the indicator. When the indicator was exposed to the alkaline (pH 8) buffer, it shows negative *b*-value (-12.6) with a dark blue color and consequently less brightness (**Fig. 6.6d**). For a further increase in alkalinity (10 pH) the *b*-value of the indicator became positive (25.3) (**Fig. 6.6e**) and showed yellow color. At higher pH, due to the tautomerism of carbinol pseudo-base through the opening of the C-ring of anthocyanin structure, a yellow color chalcone structure was formed on the indicator. Hence, the *b*-value and *L*-value (56.9) of the indicator was enhanced.

Table 6.3: *L*, *a*, and *b* value of indicator at various pH

pH	*L*	*a*	*b*
2	62.2 ± 0.4^{d}	25.3 ± 0.1^{c}	0.7 ± 0.01^{a}
4	55.8 ± 0.1^{b}	20.8 ± 0.2^{b}	0.8 ± 0.02^{a}
6	68.4 ± 0.2^{e}	0.7 ± 0.1^{a}	-3.5 ± 0.1^{b}
8	43.1 ± 0.4^{a}	$0.9\pm.01^{a}$	-12.6 ± 0.2^{c}
10	56.9 ± 0.1^{c}	0.8 ± 0.02^{a}	25.3 ± 0.3^{d}

Superscript different letters in the same column represent the significant difference in Duncan's multiple range tests at 5 % level ($p \leq 0.05$).

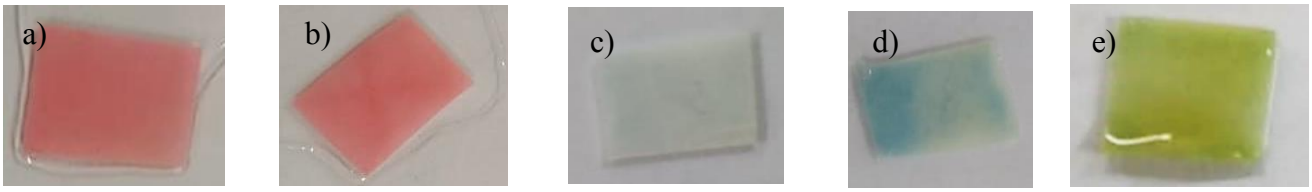

Fig. 6.6: Color of indicator at a) 2, b) 4, c) 6, d) 8 and e) 10 pH conditions

6.3.7.3. Color measurement in food system

The indicator (150 mg/L) was used in the food systems with a wide range of pH to evaluate sensing efficiency. It was noticed that the indicator exhibited a different appearance in the food system with various pH. **Table 6.4** illustrates that as the indicator was put into the lemon juice (pH 2.3), it exhibited a red (21.3) appearance with high brightness (57.2). The pH of fresh lemon juice was 2.3 due to the presence of citric acid. Thereby, in contact with lemon juice, the indicator showed red color, due to the presence of flavylium cation (Zhang et al., 2009) as per the following reaction.

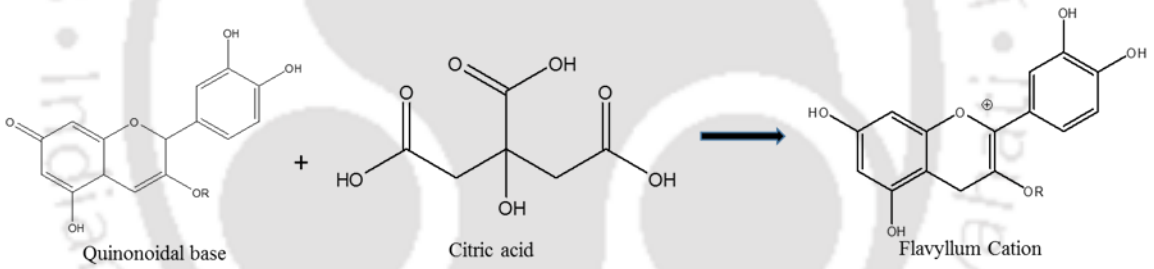

It was observed that when the pH of the food system was increased from 3.4 to 4 (grapefruit juice to ketchup) the redness of the indicator was decreased (16.8 to 13.6) as well as brightness was decreased from 53.8 to 51.8. Graph juice is considered as an acid food and pH was 3.4 due to the presence of ascorbic acid. The ascorbic acid in grape juice enhances the deprotonation of flavylium cation in the indicator and formed a violet color quinonoidal base as shown in reaction. The pH of ketchup was 4 due to the acetic acid. However, there was a slight change in pH with respect to grape juice but there was no change in quinonoidal base structure and the indicator appear to be light violet color.

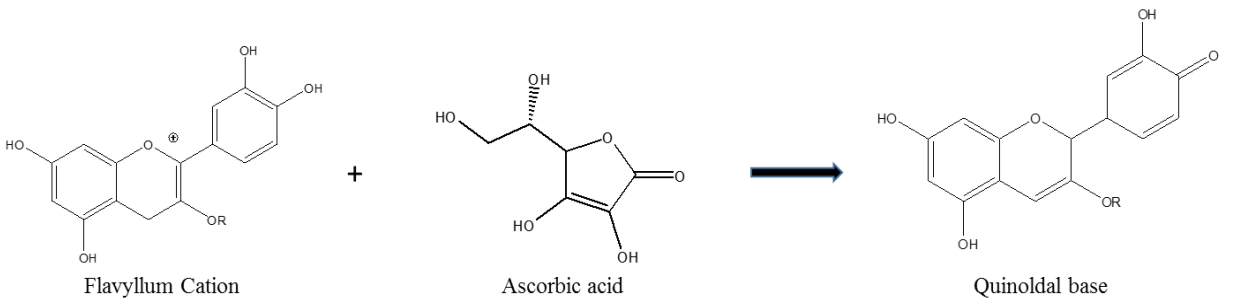

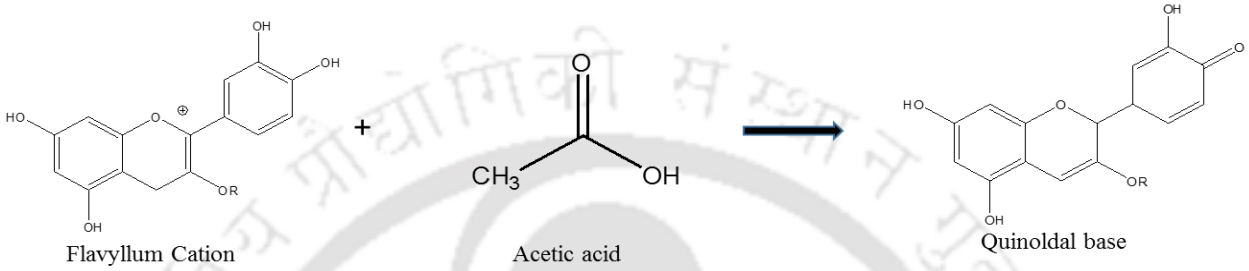

Due to the presence of a high amount of water (96 %) aloe vera juice shows neutral (6.1 pH) pH. In contact with aloe vera juice, the indicator showed a high *L*-value of 62.47 with low *a* and *b*-value which signifies a colorless appearance. In neutral pH the flavylium cation of anthocyanin in the indicator converted to a colorless chromenol compound due to the deprotonation of flavylium cation as per the following reaction (McGhie and Walton 2007) and thus indicator showed a white appearance.

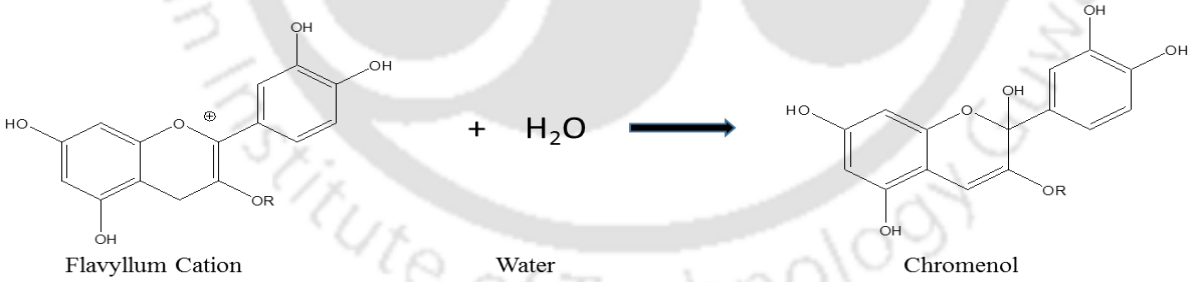

On the other hand, egg white generally considered as alkaline (7.8 pH) food product due to the release of CO_2 during storage. In contact with egg white, the indicator showed low *L*-value (48.14) and negative a-value (-13.39) Thereby, in the contact of egg white the flavylium cation in the indicator converted to a blue color ionic anhydro base as shown in the following reaction.

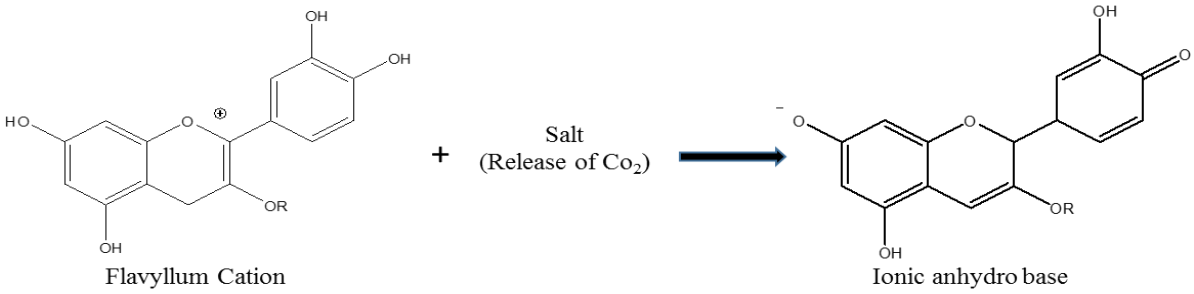

Table 6.4: *L*, *a*, and *b* value of indicator at various food system

Food Item	pH	*L*	*A*	*b*
Lemon Juice	2.3	57.2 ± 0.3^{d}	21.3 ± 0.1^{d}	0.8 ± 0.05^{a}
Grapefruit Juice	3.4	53.8 ± 0.2^{c}	16.8 ± 0.1^{c}	0.6 ± 0.1^{a}
Ketchup	4	51.8 ± 0.1^{b}	13.6 ± 0.2^{b}	0.6 ± 0.6^{a}
Aloe vera juice	6.1	62.5 ± 0.2^{e}	0.7 ± 0.06^{a}	-4.3 ± 0.3^{b}
Egg white	7.8	48.1 ± 0.2^{a}	0.9 ± 0.1^{a}	-13.4 ± 0.2^{c}

Superscript different letters in the same column represent the significant difference in Duncan's multiple range tests at 5 % level ($p \leq 0.05$).

6.3.7.4. Color stability

The stability of *a*-value (redness) of the indicator was investigated at 4 and 25 °C for 30 days. The higher stability of redness was observed at 4 °C than that at 25 °C (**Fig. 6.7**). The redness of the indicator is due to the presence of anthocyanin. Thereby, degradation of anthocyanin decreases the *a*-value of the indicator. The degradation is primarily caused due to oxidation, cleavage of covalent bonds, and enhanced oxidation reactions that take place during thermal processing. However, the exact mechanism for anthocyanin degradation in the paper indicator during storage is also difficult to mention (Patras et al., 2010).

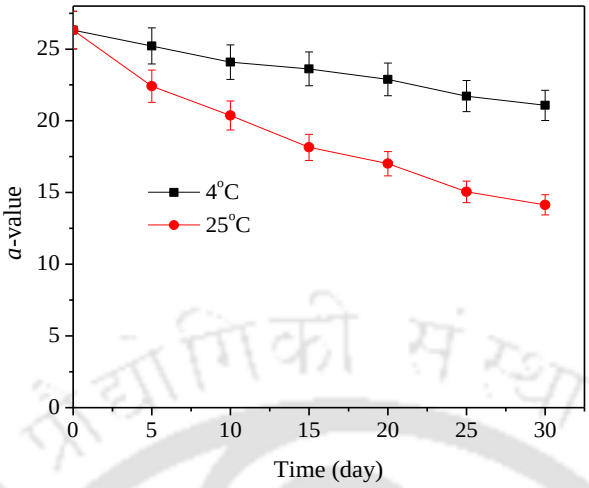

Fig. 6.7: *a*-value of paper indicator during storage in 4 and 25 °C

6.3.7.5. Degradation kinetics

Degradation kinetics of stored samples was investigated in term of stability of redness (*a*-value) in the indicator. The storage study was carried out at 4 °C and 25 °C. The degradation behavior of color was plotted as a function of time and shown in **Fig. 6.8(a)** and **(b)**.The reaction rate constant (*k*) was determined from the slope of the curve. It can be observed (**Fig. 6.8**) that the degradation behavior of color was suitable for the first-order reaction kinetics than zero-order. The higher value of the correlation coefficient (R^2) represents the degradation behavior of color (*a*-value) at various temperatures as it was suitable for the first-order kinetics model (**Table 6.5**). The previous researcher reported similar types of observations for Chinese bayberry (Zhu et al., 2016) and plum puree (Ahmed et al., 2004). However, the observation of Suh et al. (2003) was contradicted with the present observation. This difference is because of the different sources of anthocyanin as mulberry was used as an anthocyanin source.

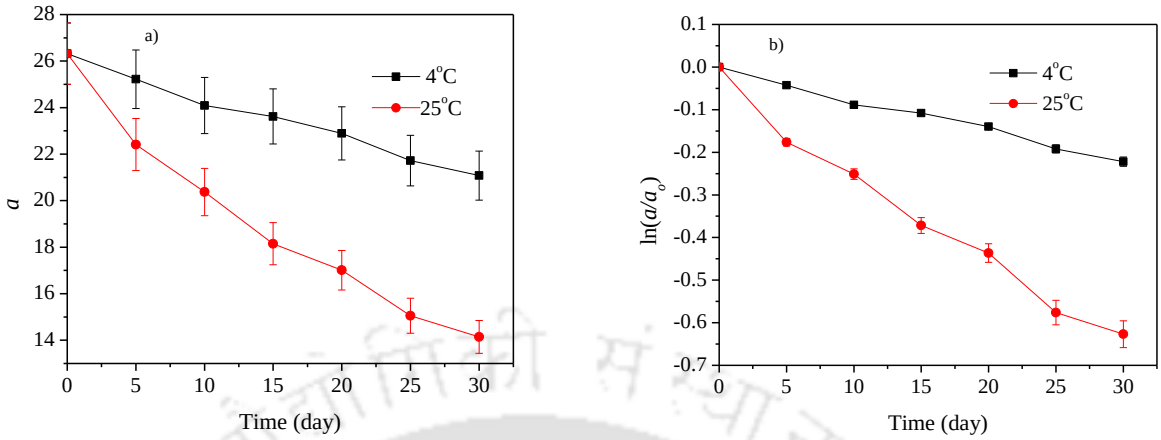

Fig. 6.8: a) Zero-order and b) First-order degradation kinetics of redness (*a*-value) of the indicator

At 25 °C, the degradation rate constant (k) of *a*-value was higher than that at 4 °C. Moreover, the half-life ($t_{1/2}$) was high at low temperatures and decreased with an increase in temperature. The redness (*a*-value) of the indicator was due to the surface deposition of anthocyanin. Thereby, changes in redness of the indicator directly depend on the deposited anthocyanin. As anthocyanin is heat-sensitive, with the increase of temperature, the rate of degradation of *a*-value is increased due to the modification and degradation of the anthocyanin structure (Patras et al., 2010). Hence, the indicator stored at high temperatures (24 °C) showed higher degradation than low temperatures. The degradation and modification of anthocyanin structure depend upon the severity and condition of storage heating.

Table 6.5: Degradation kinetics parameters for indicator color

Temperature (°C)	Zero-order			First-order		
	$k\times10^{-3}$ /day	R^2	$t_{1/2}$ (min)	$k\times10^{-3}$ /day	R^2	$t_{1/2}$ (day)
4	170	0.99	4.07	7.5	0.99	92.4
25	390	0.96	1.7	22.4	0.97	30.9

6.3.7.6. Comparison of sensitivity with literature

The present observation on the indicator was compared with the observation of previous researchers (Choi et al., 2017; Yoshida et al., 2014). The average *L*, *a*, and *b* sensitivity were estimated using the equations as shown in **Table 6.6** and compared with previous work (Choi et al., 2017; Yoshida et al., 2014) where Choi et al. (2017) developed a

colorimetric pH indicator film using agar/potato starch for food quality monitoring. Yoshida et al. (2014) developed a chitosan-based pH sensitive film for food quality control. The purple potato and grape were used as sources of anthocyanin to make the above pH indicators. In the present investigation, purple rice waste bran was used for the extraction of anthocyanin for the deposition of the filter paper of the indicator. It indicates this indicator considered to be cost-effective.

Table 6.6: Sensitivity of *L*, *a*, and *b* value

Sources	**Average L sensitivity=** $\frac{1}{4}\sum_{i=2,4,6,8}\frac{\lvert L_{i+2}-L_i\rvert}{2}$	**Average a sensitivity=** $\frac{1}{4}\sum_{i=2,4,6,8}\frac{\lvert a_{i+2}-a_i\rvert}{2}$	**Average b sensitivity=** $\frac{1}{4}\sum_{i=2,4,6,8}\frac{\lvert b_{i+2}-b_i\rvert}{2}$
This work	7.2	3.1	6.4
Choi et al. (2017)	0.5	3.7	0.7
Yoshida et al. (2014)	2.5	2.2	2.5

where L_i and L_{i+2} are the L-value of the pH sensitive indicator at pH value i and i+2, respectively (i=2, 4, 6, 8)

a_i and a_{i+2} are the a-value of the pH sensitive indicator at pH value i and i+2, respectively (i=2, 4, 6, 8)

b_i and b_{i+2} are the b-value of the pH sensitive indicator at pH value i and i+2,respectively (i=2, 4, 6, 8)

Table 6.6 shows that the average *L* sensitivity of this pH indicator was 13.7 times more than that of pH indicator using agar/potato starch and 2.9 times more than chitosan-based pH indicator films. The average *b* sensitivity of this work is 9.3 times more than that of pH indicator film composed of agar/potato starch and 2.5 times more than chitosan-based pH indicator films whereas average a-sensitivity is almost close to that of Choi et al. (2017) and are slightly more than that of Yoshida et al. (2014). The higher sensitivity of the present investigation was achieved due to the use of slightly opaque white filter paper whereas starch and chitosan used in Choi et al. (2017) and Yoshida et al. (2014) are nearly transparent white providing lower sensitivity. Moreover, the time required for colorimetric measurement (20s) using our filter paper pH indicator was lower than that of previous works (Choi et al., 2017; Yoshida et al., 2014).

6.4. Summary

In the present study, the microencapsulated anthocyanin incorporated rice based extrudate was developed and optimized. The conclusions are summarized as follows:

- The extrusion process was optimized using RCCD and the optimum condition was screw speed 121 rpm (12.7 rad/s), barrel temperature 91.9 °C and moisture content 22.03 % (w/w).
- At the optimum condition sample has anthocyanin content 0.2 (mg/L), true density 1.5 (g/cc), water activity 0.5, water solubility index 22.4 (% w/w), and specific mechanical energy 31.4 (kJ/kg).
- The cooking characteristic of the extrudate was investigated in term of the cooking yield of the product is 201.4 %, cooking losses is 9.5 % and cooking time is 6.7 min.
- The moisture sorption isotherm of the extrudate showed the Type-III isotherm behavior.
- The Caurie and Peleg were found best to represent the experimental data throughout the entire range of water activity in various temperature.
- The anthocyanin with the concentration of 150 mg/L showed highest color value after deposition on the filter paper.
- The degradation kinetics of L and a-value of the indicator was investigated at 4 and 25 °C. The first-order kinetics for degradation of color was suitable for the *L* and *a*-value degradation.

References

Ahmed, J., Shivhare, U. S., and Raghavan, G. S. V. (2004). Thermal degradation kinetics of anthocyanin and visual colour of plum puree. *European Food Research and Technology, 218*(6), 525-528.

Akdogan, H. (1999). High moisture food extrusion. *International Journal of Food Science & Technology, 34*(3), 195-207.

Altan, A., McCarthy, K. L., and Maskan, M. (2009). Effect of screw configuration and raw material on some properties of barley extrudates. *Journal of Food Engineering, 92*(4), 377-382.

Camacho-Hernández, I.L., Zazueta-Morales, J.J., Gallegos-Infante, J.A., Aguilar-Palazuelos, E., Rocha-Guzmán, N.E., Navarro-Cortez, R.O., Jacobo-Valenzuela, N. and Gómez-Aldapa, C.A. (2014). Effect of extrusion conditions on physicochemical characteristics and anthocyanin content of blue corn third-generation snacks. *CyTA - Journal of Food, 12*(4), 320-330.

Camire, M.E., Chaovanalikit, A., Dougherty, M.P. and Briggs, J. (2002). Blueberry and grape anthocyanins as breakfast cereal colorants. *Journal of Food Science, 67*(1), 438-441.

Chang, YK, Martinez-Bustos, F, Park, TS, & Kokini, JL. (1999). The influence of specific mechanical energy on cornmeal viscosity measured by an on-line system during twin-screw extrusion. *Brazilian Journal of Chemical Engineering, 16*(3), 285-295.

Chevanan, N., Rosentrater, Kurt A. and Muthukumarappan, K. (2008). Effect of DDGS, Moisture Content, and Screw Speed on Physical Properties of Extrudates in Single-Screw Extrusion. *Cereal Chemistry, 85*(2), 132-139.

Choi, I., Lee, J. Y., Lacroix, M., and Han, J. (2017). Intelligent pH indicator film composed of agar/potato starch and anthocyanin extracts from purple sweet potato. *Food Chemistry, 218*, 122-128.

Ding, Q.B., Ainsworth, P., Plunkett, A., Tucker, G. and Marson, H. (2006). The effect of extrusion conditions on the functional and physical properties of wheat-based expanded snacks. *Journal of Food Engineering, 73*(2), 142-148.

Gui, Y., Gil, S.K. and Ryu, G.H. (2012). Effects of extrusion conditions on the physicochemical properties of extruded red ginseng. *Preventive Nutrition and Food Science*, *17*(3), 203.

Hirth, M., Leiter, A., Beck, S.M. and Schuchmann, H.P. (2014). Effect of extrusion cooking process parameters on the retention of bilberry anthocyanins in starch based food. *Journal of Food Engineering*, *125*, 139-146.

Jones, D., Chinnaswamy, R., Tan, Y. and Hanna, M. (2000). Physiochemical properties of ready-to-eat breakfast cereals. *Cereal Foods World*, *45*(4), 164-168.

Khanal, R.C., Howard, L.R., Brownmiller, C.R. and Prior, R.L. (2009). Influence of extrusion processing on procyanidin composition and total anthocyanin contents of blueberry pomace. *Journal of Food Science*, *74*(2), H52-H58.

Lin, S, Huff, H.E. and Hsieh, F. (2000). Texture and chemical characteristics of soy protein meat analog extruded at high moisture. *Journal of Food Science*, *65*(2), 264-269.

McGhie, T. K., and Walton, M. C. (2007). The bioavailability and absorption of anthocyanins: towards a better understanding. *Molecular Nutrition and Food Research*, *51*(6), 702-713.

Osen, R., Toelstede, S., Wild, F., Eisner, P. and Schweiggert-Weisz, U. (2014). High moisture extrusion cooking of pea protein isolates: Raw material characteristics, extruder responses, and texture properties. *Journal of Food Engineering*, *127*, 67-74.

Panjagari, N.R., Singh, A.K., Ganguly, S. and Indumati, K.P. (2015). Beta-glucan rich composite flour biscuits: modelling of moisture sorption isotherms and determination of sorption heat. *Journal of Food Science and Technology*, *52*(9), 5497-5509.

Patras, A., Brunton, N.P., O'Donnell, C. and Tiwari, B.K. (2010). Effect of thermal processing on anthocyanin stability in foods; mechanisms and kinetics of degradation. *Trends in Food Science and Technology*, *21*(1), 3-11.

Rauf, S., Ali, Y., Hussain, S., Ullah, F. and Hayat, A. (2018). Design of a novel filter paper based construct for rapid analysis of acetone. *PloS one*, *13*(7), e0199978.

Sharma, C., Singh, B., Hussain, S. Z. and Sharma, S. (2017). Investigation of process and product parameters for physicochemical properties of rice and mung bean (Vigna radiata) flour based extruded snacks. *Journal of Food Science and Technology, 54*(6), 1711-1720.

Singh, B., Sekhon, K.S, and Singh, N. (2007). Effects of moisture, temperature and level of pea grits on extrusion behaviour and product characteristics of rice. *Food Chemistry, 100*(1), 198-202.

Suh, H.J., Noh, D.O., Kang, C.S., Kim, J.M. and Lee, S.W. (2003). Thermal kinetics of color degradation of mulberry fruit extract. *Food / Nahrung, 47*(2), 132-135.

Włodarczyk-Stasiak, M. and Jamroz, J. (2008). Analysis of sorption properties of starch–protein extrudates with the use of water vapour. *Journal of Food Engineering, 85*(4), 580-589.

Yağcı, S. and Göğüş, F. (2008). Response surface methodology for evaluation of physical and functional properties of extruded snack foods developed from food-by-products. *Journal of Food Engineering, 86*(1), 122-132.

Yoshida, C.M., Maciel, V.B.V., Mendonça, M.E.D. and Franco, T.T. (2014). Chitosan biobased and intelligent films: Monitoring pH variations. *LWT - Food Science and Technology, 55*(1), 83-89.

Zhang, C., Ma, Y., Zhao, X. and Mu, J., (2009). Influence of Copigmentation on Stability of Anthocyanins from Purple Potato Peel in Both Liquid State and Solid State. *Journal of Agricultural and Food Chemistry, 57*(20), 9503-9508.

Su, G., Zhu, S., Xu, M., Ramaswamy, H.S., Lin, Y. and Yu, Y. (2016). Pressure Degradation Kinetics of Anthocyanin Pigment and Visual Color of Chinese Bayberry Juice AU - Su, Guangming. *International Journal of Food Properties, 19*(2), 443-453.

OVERALL CONCLUSIONS AND SCOPE FOR FUTURE RESEARCH

CHAPTER 7

OVERALL CONCLUSIONS AND SCOPE FOR FUTURE RESEARCH

Overall conclusions

The findings on the various issues in the extraction, purification, concentration, microencapsulation and sensor development using anthocyanin from purple rice bran are summarized as follows:

- The black and purple rice bran are a good potential source of anthocyanin. Purple rice contains a higher amount of anthocyanin, cyanidin-3-glucoside, and peonidin-3-glucoside. The ethanol is the most efficient solvent to extract the anthocyanins from black and purple rice bran. The rice bran also contains β-carotene, tocopherol, tocotrienol, caffeic acid, catechin hydrate, chlorogenic acid, coumaric acid, 4-hydroxybenzoic acid, syringic acid, sinapic acid, vanillic acid, and gallic acid. The purple rice bran contains a higher amount of bioactive compounds than black rice.
- The adsorption and desorption is an effective non-thermal process to separate and concentrate anthocyanin. The amberlite XAD7 resin is the efficient adsorbent to separate anthocyanin from the crude mixture. Adsorption isotherm behavior of anthocyanin on adsorbents is homogeneous and more suitable for Langmuir (two parameters), and Redlich–Peterson (three parameters) isotherm model. The monomeric anthocyanin, C3G, and P3G showed the lowest degradation rate at pH 2 and 60 °C. The hydrocolloids, namely, carboxymethyl cellulose, xanthan gum, modified starch, and gum acacia effects the stability of anthocyanin, C3G, and P3G. The modified starch has the highest stability on anthocyanin in the aqueous medium.
- Microencapsulation is an efficient way to develop a stable anthocyanin based functional ingredient. The modified starch is used as wall material and anthocyanin is in the core. The microencapsulate store at low-temperature contains higher anthocyanin than high-temperature storage. The microencapsulated particles affect the steady-shear rheology and dynamic oscillatory rheology of rice dough. The increase in microencapsulate concentration from 5 to 20 % in rice dough, decrease the pseudo-plasticity of dough.

- The microencapsulated anthocyanin incorporated rice-based extrudate to develop functional food. The cooking yield of the extrudate is 201.4 % (w/w), the cooking loss is 9.5 % (w/w) and the cooking time is 6.7 min. The extrudate has the Type-III sorption isotherm behavior. The Caurie and Peleg is the best model to represent the experimental data throughout the entire range of water activity at various temperatures.
- The anthocyanin is used as a pH indicator in the paper base sensor. The anthocyanin with a concentration of 150 mg/L shows the highest color value after deposition on the filter paper. The degradation kinetics of *L* and *a*-value of the sensor shows first-order degradation behavior.

Industrial application and feasibility

Anthocyanins are easily affected by food processing factors, such as pH, oxygen, and thermal treatment. Thereby, selection of process for anthocyanin extraction is a major challenge for the food industry. In the present study, extraction, adsorption, and microencapsulation of anthocyanin from pigmented rice bran was demonstrated. This study could act as a reference to the industry for developing a stable anthocyanin powder from pigmented rice bran. This study illustrated that the extract had a high antioxidant activity which could be an alternative to synthetic antioxidants. The stability of anthocyanin at high temperature processed food, such as extrudate is a challenge for the food industry. The present study manifested a possible standardized way to produce functional extrudate with infused anthocyanin from rice bran. The study will also be helpful for the selection of storage temperature and relative humidity to get the maximum shelf life of the food product. From the application point of view, this work could facilitate the industrial production of anthocyanin from purple rice bran as a natural food colorant using adsorption process. Moreover, the study is helpful in understanding the adsorption of anthocyanin as well as designing the adsorption systems.

Scope for future research

The discussion so far has focused on the extraction, purification, and microencapsulation of anthocyanin from purple rice bran. This study also discussed to develop a rice extrudate and pH-sensitive sensor with anthocyanin.

This section delivers a number of future directions, which would be valuable for further study on the anthocyanin from purple rice bran and microencapsulation. Dome essential areas of recommending research are suggested as an extension of the present study as follows:

- New application of anthocyanin can be carried out by applying new approaches such as the development of biodegradable food packing material using anthocyanin.
- Development of new ready to eat functional food can be developed using the microencapsulated anthocyanin.
- Development of stable anthocyanin, which can sustain the detrimental effect of food processing condition.

Despite the progress recognized until now in this area, further advances must expect for the opening of a new horizon in this field. The probable benefits of such advancement in this field may help the grower for local revenue and large-scale producer to develop innovate and functional food products for society in affordable economic.

APPENDIX 1

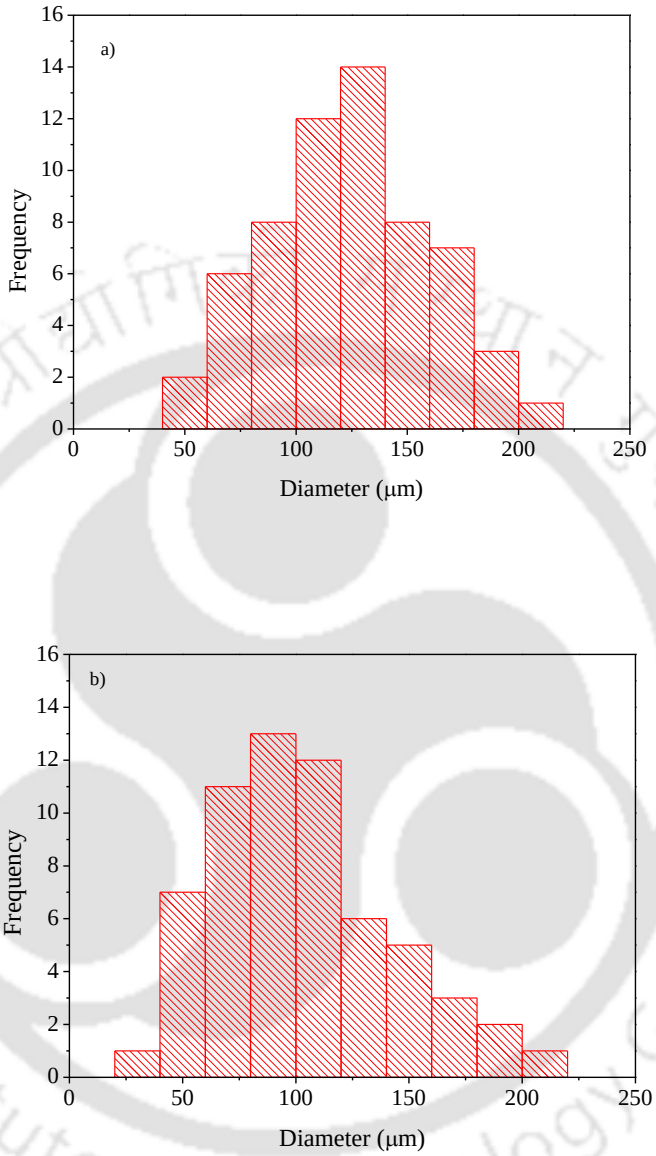

Fig. 1A1: Particle size distribution curve for a) purple rice bran and b) black rice bran

APPENDIX 2

Table 2A1: Coded values of factors with corresponding experimental and predicted responses for purple rice bran.

Run	Temperature (°C)	Solvent concentration (%)	Time (min)	Liquid to solid ratio (mL/g)	Total phenolic content (mg GAE/100g)	
					Predicted	Experimental
1	-1	-1	1	-0.66	764.0	764.0
2	-1	-1	1	0.93	586.8	586.8
3	1	-1	-1	0.93	833.2	833.2
4	2	0	0	0	787.3	787.3
5	1	1	1	0.93	541.4	541.4
6	1	-1	1	-0.66	912.7	912.7
7	1	1	-1	-0.66	794.1	794.1
8	-1	1	-1	0.93	705.9	705.9
9	-2	0	0	0	770.9	771.0
10	0	0	0	0	993.5	1065.0
11	0	0	0	0	993.5	985.0
12	0	0	0	0	993.5	921.9
13	1	1	1	-0.66	871.5	871.4
14	0	0	-2	0	995.4	995.5
15	1	-1	-1	-0.66	1259.6	920.9
16	0	0	0	0	993.5	1065.0
17	1	1	-1	0.93	718.6	718.6
18	-1	1	1	-0.66	630.5	630.5
19	-1	-1	-1	0.93	775.9	775.9
20	-1	1	-1	-0.66	721.8	721.8
21	0	0	0	0	993.5	895.0
22	0	0	2	0	850.0	850.0
23	-1	-1	-1	-0.66	816.9	945.0
24	0	2	0	0	385.1	356.8
25	0	0	0	0	993.5	965.0
26	-1	1	1	0.93	532.3	532.3
27	1	-1	1	0.93	596.8	596.8
28	0	0	0	2	574.6	675.0
29	0	-2	0	0	711.4	711.4
30	0	0	0	-2	651.4	651.4

Table 2A2: Coded values of factors with corresponding experimental and predicted responses for black rice bran.

Run	Temperature (°C)	Solvent concentration (%)	Time (min)	Liquid to solid ratio (mL/g)	Total phenolic content (mg GAE/100g)	
					Predicted	Experimental
1	-1	-1	1	-0.66	920.4	920.4
2	-1	-1	1	0.93	702.3	840
3	1	-1	-1	0.93	748.3	748.3
4	2	0	0	0	890.4	890.4
5	1	1	1	0.93	668.1	662.9
6	1	-1	1	-0.66	980.4	980.4
7	1	1	-1	-0.66	750.4	750.4
8	-1	1	-1	0.93	646.7	646.7
9	-2	0	0	0	941.2	941.2
10	0	0	0	0	917.9	977.9
11	0	0	0	0	917.9	907.9
12	0	0	0	0	917.9	950.9
13	1	1	1	-0.66	755.1	897.1
14	0	0	-2	0	965.4	965.4
15	1	-1	-1	-0.66	789.6	789.6
16	0	0	0	0	917.9	960.9
17	1	1	-1	0.93	729.6	729.6
18	-1	1	1	-0.66	838.3	838.3
19	-1	-1	-1	0.93	809.2	809.2
20	-1	1	-1	-0.66	814.6	814.6
21	0	0	0	0	917.9	977.9
22	0	0	2	0	929.4	980.4
23	-1	-1	-1	-0.66	779.2	880.4
24	0	2	0	0	569.9	352.5
25	0	0	0	0	917.9	807.9
26	-1	1	1	0.93	663.3	663.3
27	1	-1	1	0.93	789.6	789.6
28	0	0	0	2	638.3	638.3
29	0	-2	0	0	681.7	681.7
30	0	0	0	-2	632.9	632.9

APPENDIX 3

Table 3A1: Rotatable central composite design and experimental value of responses for black rice bran

Run	Temperature (°C)	pH	Solvent concentration (%)	Time (min)	TPC (mg GAE/100g)	Anthocyanin (mg C3G/L)
1	0	0	0	0	1635.5	21.9
2	-1	-1	1	1	1677.5	22.3
3	2	0	0	0	1358.0	15.8
4	0	-2	0	0	1792.5	24.1
5	-1	1	-1	1	1708.5	22.9
6	-1	-1	-1	-1	1700.0	22.7
7	1	-1	1	-1	1469.5	20.3
8	-1	1	1	1	1509.0	18.3
9	-2	0	0	0	1418.5	19.9
10	0	0	0	2	1510.5	19.8
11	-1	1	-1	-1	1286.0	16.9
12	-1	-1	-1	1	1479.0	19.3
13	0	0	0	0	1421.5	18.6
14	-1	-1	1	-1	1638.5	22.1
15	0	2	0	0	1575.5	21.7
16	-1	1	1	-1	1503.0	22.1
17	1	-1	-1	1	1749.5	23.4
18	1	-1	-1	-1	1632.5	22.1
19	0	0	2	0	1822.0	26.9
20	0	0	0	0	1709.0	22.9
21	1	1	-1	-1	1549.0	20.5
22	1	1	1	-1	1889.5	29.2
23	1	1	1	1	1521.0	23.3
24	1	1	-1	1	1442.0	21.9
25	0	0	-2	0	1590.5	22.9
26	1	-1	1	1	1681.5	22.1
27	0	0	0	-2	1444.5	19.4
28	0	0	0	0	1340.5	18.2
29	0	0	0	0	1399.5	18.1
30	0	0	0	0	1530.0	22.1

Table 3A2: Rotatable central composite design and the experimental value of responses for purple rice bran

Run	Temperature (°C)	pH	Solvent concentration (%)	Time (min)	TPC (mg GAE/100g)	Anthocyanin (mg C3G/L)
1	0	0	0	0	1837.4	27.1
2	-1	-1	1	1	1695.3	24.7
3	2	0	0	0	1598.4	23.5
4	0	-2	0	0	1946.8	30.6
5	-1	1	-1	1	1652.1	26.7
6	-1	-1	-1	-1	2094.2	35.2
7	1	-1	1	-1	1875.3	27.0
8	-1	1	1	1	1534.7	22.2
9	-2	0	0	0	1687.4	27.3
10	0	0	0	2	1458.9	22.5
11	-1	1	-1	-1	2023.2	31.9
12	-1	-1	-1	1	1706.3	28.5
13	0	0	0	0	1876.8	28.7
14	-1	-1	1	-1	1623.2	26.7
15	0	2	0	0	1693.7	24.2
16	-1	1	1	-1	1516.3	23.9
17	1	-1	-1	1	1715.8	27.4
18	1	-1	-1	-1	1992.1	29.3
19	0	0	2	0	1662.1	23.9
20	0	0	0	0	1823.7	27.2
21	1	1	-1	-1	1735.8	25.9
22	1	1	1	-1	1578.4	23.5
23	1	1	1	1	1625.8	24.2
24	1	1	-1	1	1601.6	23.4
25	0	0	-2	0	1734.2	27.2
26	1	-1	1	1	1763.7	26.3
27	0	0	0	-2	1862.8	28.9
28	0	0	0	0	1884.7	29.2
29	0	0	0	0	1853.2	28.5
30	0	0	0	0	1779.5	26.6

APPENDIX 4

Table 4A1: Experimental design of spray drying of anthocyanin

	Independent parameter			Dependent parameters				
Run	Starch (%)	Pressure (MPa)	Temperature (°C)	Encapsula-tion efficiency (%)	Anthoc-yanin content (mg/L)	DPPH scavenging activity (%)	True density (g/cm^3)	Water activity
1	1	1	-1	80.9	1.5	41.8	1.7	0.49
2	1.68	0	0	84.9	1.8	43.6	1.8	0.51
3	1	-1	-1	88.7	1.6	47.9	1.8	0.51
4	0	0	0	95.4	2.4	51.9	1.7	0.50
5	-1	-1	1	96.7	2.8	52.6	1.8	0.52
6	0	1.68	0	88.5	1.9	44.7	1.8	0.51
7	-1.68	0	0	87.9	1.9	42.6	1.7	0.50
8	0	0	0	95.3	2.9	52.7	1.7	0.51
9	-1	1	1	92.2	2.9	54.9	1.9	0.52
10	0	-1.68	0	89.0	2.1	41.3	1.6	0.49
11	1	-1	1	85.1	2.5	48.1	1.7	0.49
12	0	0	0	99.2	3.0	61.9	1.9	0.56
13	-1	1	-1	90.8	2.9	52.0	1.8	0.51
14	0	0	0	88.6	2.7	47.9	1.9	0.55
15	0	0	0	90.8	2.9	52.0	1.9	0.52
16	0	0	-1.68	95.8	2.4	54.7	1.8	0.52
17	0	0	1.68	87.3	2.6	50.7	1.8	0.52
18	1	1	1	89.3	2.6	49.9	1.8	0.51
19	0	0	0	90.8	2.9	52.9	1.9	0.52
20	-1	-1	-1	91.6	2.7	51.4	1.7	0.50

APPENDIX 5

Table 5A1: Value of dependent and independent variables

	Independent Parameter				Dependent parameter			
Run	Screw speed (RPM)	Temperature (°C)	Moisture content (%)	Anthocyanin (mg/L)	True density (g/cm^3)	Water activity	WSI (%)	Specific mechanical energy
1	1	-1	-1	0.32	1.7	0.64	5.6	43.9
2	0	1.68	0	0.10	1.3	0.47	28.4	31.0
3	-1	-1	-1	0.42	1.8	0.59	11.3	26.4
4	0	0	0	0.15	1.6	0.56	27.4	41.4
5	1.68	0	0	0.14	1.5	0.50	6.2	58.3
6	-1.68	0	0	0.29	1.8	0.59	10.6	28.9
7	0	0	0	0.12	1.7	0.52	27.4	38.4
8	-1	1	-1	0.22	1.4	0.53	21.6	33.1
9	0	-1.68	0	0.49	1.7	0.69	8.3	24.2
10	0	0	-1.68	0.26	1.9	0.51	18.9	33.8
11	0	0	0	0.21	1.7	0.49	27.4	42.2
12	1	1	-1	0.24	1.5	0.50	23.9	44.4
13	0	0	1.68	0.48	2.1	0.64	1.4	21.9
14	0	0	0	0.13	1.7	0.54	27.4	42.0
15	0	0	0	0.17	1.6	0.51	21.4	42.3
16	1	1	1	0.16	1.7	0.50	6.8	36.4
17	-1	1	1	0.17	1.8	0.62	5.8	29.4
18	1	-1.	1	0.43	1.7	0.64	3.1	36.4
19	-1	-1	1	0.48	1.8	0.67	17.4	26.6
20	0	0	0	0.18	1.4	0.51	27.4	39.8

APPENDIX 6

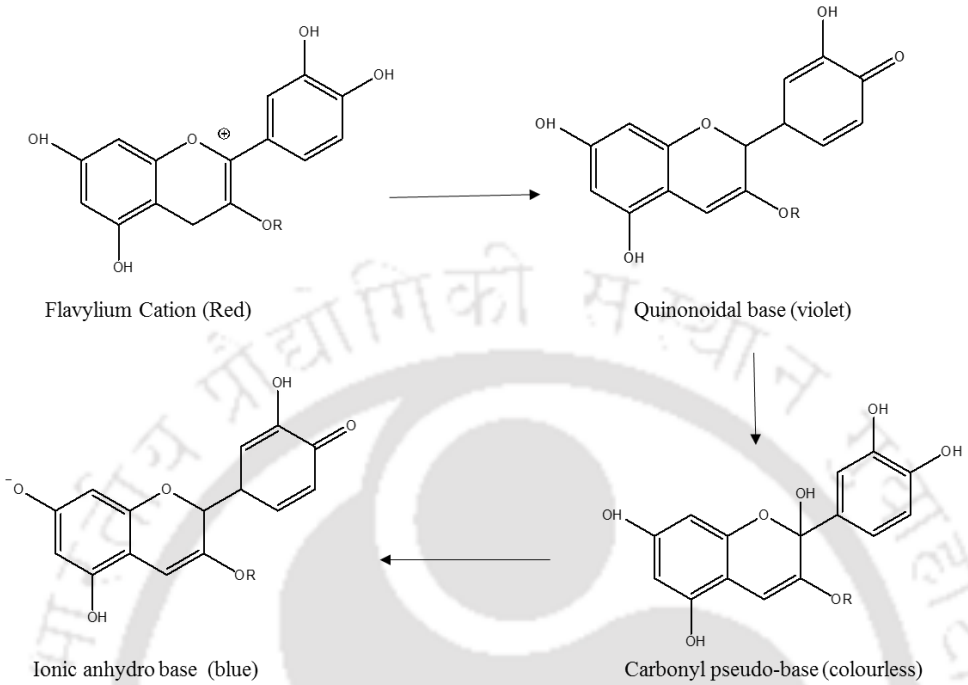

Fig. 6A1a: Non-thermal (pH) degradation of Cyanidin-3-glucoside

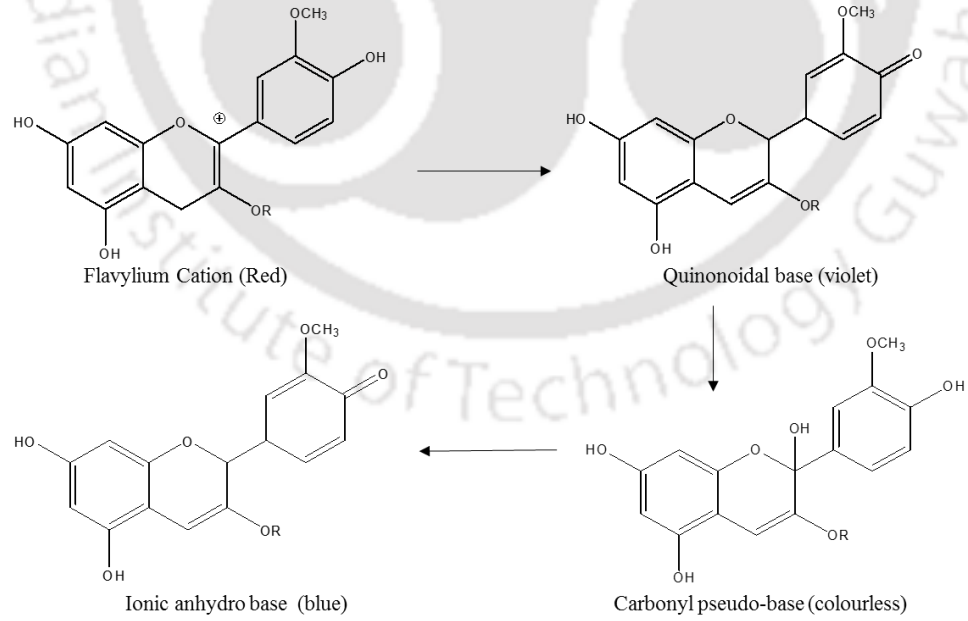

Fig. 6A1b: Non-thermal (pH) degradation of Peonidin-3-glucoside

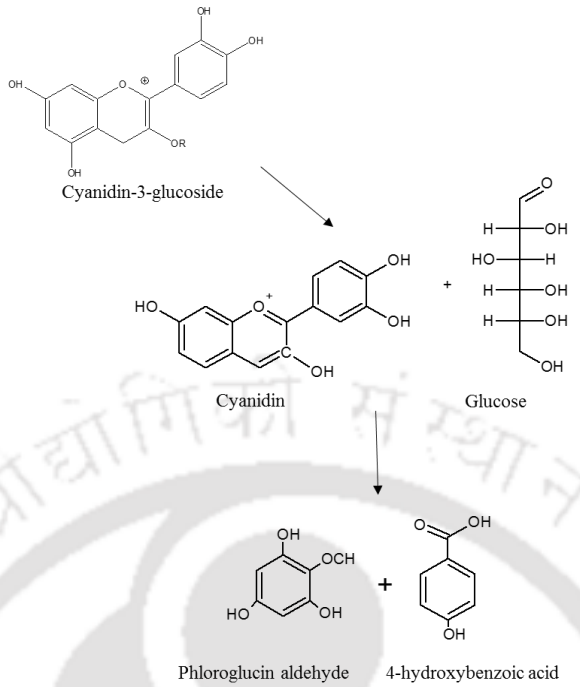

Fig. 6A2a: Thermal degradation of Cyanidin-3-glucoside

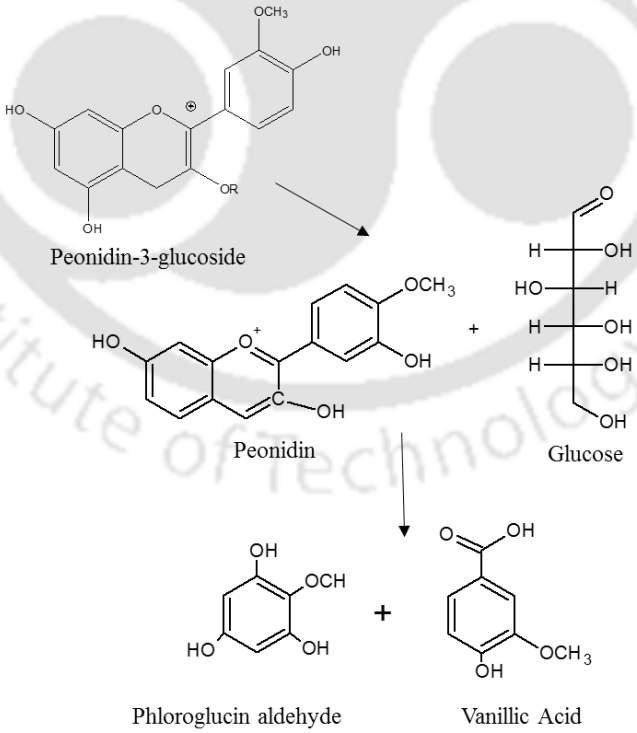

Fig. 6A2b: Thermal degradation of Peonidin-3-glucoside

APPENDIX 7

Error analysis

Step 1: Calculation of sample mean

$$\mu_x = \frac{\sum_{i=1}^{n} x_i}{n} \quad (1)$$

Step 2: calculation of standard deviation

$$s = \sqrt{\frac{\sum_{i=1}^{n} (x_i - \mu_x)^2}{n-1}} \quad (2)$$

Step 3: calculation of standard error (SE)

$$SE = \frac{s}{\sqrt{n}} \quad (3)$$

Sample calculation

Screw speed (RPM)	Water solubility index (%)	Cooking loss (%)
50	5.6	18.3
100	7.9	13.3
150	8.6	10.5
200	6.6	11.9
250	5.6	12.2
Mean	**6.8**	**13.3**
Standard deviation	**1.2**	**2.6**
Standard error	**0.5**	**1.2**

RESEARCH OUTPUT

Published Journal Papers

1. **Das, A. B.,** Goud, V. V. and Das, C. (2017). Extraction of phenolic compounds and anthocyanin from black and purple rice bran (*Oryza sativa L.*) using ultrasound: A comparative analysis and phytochemical profiling. ***Industrial Crops and Products***, 95, 332-341.

2. **Das, A. B.,** Goud, V. V. and Das, C. (2018). Extraction and characterization of phenolic content from purple and black rice (*Oryza sativa L*) bran and its antioxidant activity. ***Journal of Food Measurement and Characterization***, 12(1), 332-345.

3. **Das, A. B.,** Goud, V. V. and Das, C. (2018). Adsorption/desorption, diffusion, and thermodynamic properties of anthocyanin from purple rice bran extract on various adsorbents. ***Journal of Food Process Engineering***, 41(6), e12834.

4. **Das, A. B.,** Goud, V. V. and Das, C. (2019). Microencapsulation of anthocyanin extract from purple rice bran using modified rice starch and its effect on rice dough rheology. ***International Journal of Biological Macromolecules***, 124, 573-581.

5. **Das, A. B.,** Goud, V. V. and Das, C. (2019) Degradation kinetics of anthocyanins from purple rice bran and effect of hydrocolloids on its stability. ***Journal of Food Process Engineering***, DOI:10.1111/jfpe.13360

6. **Das, A. B.,** Goud, V. V. and Das, C. (2020) Extrusion cooking of microencapsulated anthocyanin incorporated rice flour and its sorption isotherm behavior. ***Journal of Food Science and Biotechnology,*** 10.1007/s10068-020-00841-4

Communicated

1. **Das, A. B.,** Goud, V. V. Das, C. and Sahu, P.P. (2019) Calorimetric pH indicator using anthocyanin coated filter paper for rapid liquid food quality monitoring. ***Journal of Packaging Technology and Research*** (Minor revision)

Book Chapter

1. **Das, A. B.,** Goud, V. V. and Das, C. (2019). Phenolic Compounds as Functional Ingredients in Beverages. In Value-Added Ingredients and Enrichments of Beverages (pp. 285-323). Academic Press. Elsevier.

Conferences

1. **Das, A. B.,** Goud, V. V. and Das, C. (2014) Effect of pH on phenolic content and absorbance of black and red rice extract in acetone extract, Annual chemical engineering symposium (REFLUX-1) 29-30th March. Indian Institute of Technology Guwahati, Page No 39.
2. **Das, A. B.,** Goud, V. V. and Das, C. (2015) Ultrasound-assisted extraction of anthocyanin from pigmented rice bran, 68th Annual Session of Indian Institute of Chemical Engineers (CHEMCON), 27-30 December. Indian Institute of Technology Guwahati, India.
3. **Das, A. B.,** Goud, V. V. and Das, C. (2017) Microencapsulation of anthocyanin from purple rice bran using modified starch, Future Perspective of Bioresource Utilization in North -Eastern Region (IJBS-17). Indian Institute of Technology Guwahati, India.

Curriculum vitae

Amit Baran Das

Assistant Professor
Department of Food Engineering & Technology
Tezpur University

Phone: 03712-275714
E-Mail: amit.das@iitg.ac.in
amittu@tezu.ernet.in

Educational Details:

1. **PhD** in **Chemical Engineering** from **Indian Institute of Technology,** Guwahati, Assam, India
2. **M.S in Food Engineering** from **Indian Institute of Technology,** Kharagpur, West Bengal, India
3. **M. Tech.** in **Food Engineering and Technology** from **Sant Longowal Institute Of Engineering And Technology**
4. **B.Tech** in **Food Technology** from **West Bengal University Of Technology**, Kolkata, India

Published in International Journal:

1. **Das, A. B.,** Goud, V. V. and Das, C. (2017). Extraction of phenolic compounds and anthocyanin from black and purple rice bran (*Oryza sativa L.*) using ultrasound: A comparative analysis and phytochemical profiling. ***Industrial Crops and Products***, 95, 332-341.

2. **Das, A. B.,** Goud, V. V. and Das, C. (2018). Extraction and characterization of phenolic content from purple and black rice (*Oryza sativa L*) bran and its antioxidant activity. ***Journal of Food Measurement and Characterization***, 12(1), 332-345.

3. **Das, A. B.,** Goud, V. V. and Das, C. (2018). Adsorption/desorption, diffusion, and thermodynamic properties of anthocyanin from purple rice bran extract on various adsorbents. ***Journal of Food Process Engineering***, 41(6), e12834.

4. **Das, A. B.,** Goud, V. V. and Das, C. (2019). Microencapsulation of anthocyanin extract from purple rice bran using modified rice starch and its effect on rice dough rheology. ***International Journal of Biological Macromolecules***, 124, 573-581.

5. **Das, A. B.,** Goud, V. V. and Das, C. (2019) Degradation kinetics of anthocyanins from purple rice bran and effect of hydrocolloids on its stability. ***Journal of Food Process Engineering***, DOI:10.1111/jfpe.13360

Book Chapter

1. **Das, A. B.,** Goud, V. V. and Das, C. (2019). Phenolic Compounds as Functional Ingredients in Beverages. In Value-Added Ingredients and Enrichments of Beverages (pp. 285-323). Academic Press. Elsevier.

Conferences

1. **Das, A. B.,** Goud, V. V. and Das, C. (2014) Effect of pH on phenolic content and absorbance of black and red rice extract in acetone extract, Annual chemical engineering symposium (REFLUX-1) 29-30th March. Indian Institute of Technology Guwahati, Page No 39.
2. **Das, A. B.,** Goud, V. V. and Das, C. (2015) Ultrasound-assisted extraction of anthocyanin from pigmented rice bran, 68th Annual Session of Indian Institute of Chemical Engineers (CHEMCON), 27-30 December. Indian Institute of Technology Guwahati, India.
3. **Das, A. B.,** Goud, V. V. and Das, C. (2017) Microencapsulation of anthocyanin from purple rice bran using modified starch, Future Perspective of Bioresource Utilization in North -Eastern Region (IJBS-17). Indian Institute of Technology Guwahati, India.